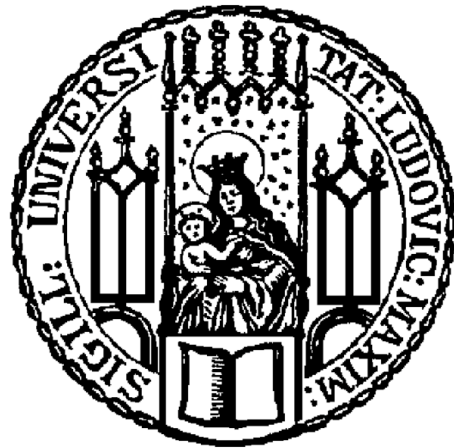


**On the Way to Differentiation:  
Xenopus Suv4-20h Histone Methyltransferases  
Regulate the Transition from the Pluripotent to the  
Ectoderm Cell State**



Dissertation zur Erlangung des akademischen Grades Dr. rer. nat.  
vorgelegt der Fakultät für Biologie der  
Ludwig-Maximilians Universität München

**Dario Nicetto**

München 2012



<b>1. Gutachter:</b>	Prof. Dr. Peter Becker
<b>2. Gutachter:</b>	Prof. Dr. Charles David
<b>Tag der Einteichung:</b>	08 October 2012
<b>Tag der mündlichen Prüfung:</b>	04 December 2012

## **Eidesstattliche Erklärung**

Ich versichere hiermit an Eides statt, dass die vorgelegte Dissertation von mir selbständig und ohne unerlaubte Hilfe angefertigt wurde.

München, den .....

.....  
(Dario Nicetto)

## TABLE OF CONTENTS

<b>1</b>	<b>SUMMARY</b> .....	<b>1</b>
<b>2</b>	<b>INTRODUCTION</b> .....	<b>3</b>
<b>2.1</b>	<b><i>Xenopus</i> as a model organism</b> .....	<b>3</b>
2.1.1	Inductive events during <i>Xenopus</i> development .....	4
2.1.2	<i>Xenopus</i> epidermis and ciliated cells differentiation .....	6
2.1.3	Neural induction and neurogenesis.....	8
2.1.4	Embryonic cell fate specification: from pluripotency to differentiation ....	12
<b>2.2</b>	<b>Epigenetics</b> .....	<b>13</b>
2.2.1	Chromatin structure.....	14
2.2.2	Principal chromatin types .....	16
2.2.3	Chromatin dynamics .....	17
2.2.4	Histone post-translational modifications (PTMs).....	18
2.2.5	Methylation as a key histone PTMs .....	20
2.2.6	The “histone code” hypothesis .....	22
2.2.7	H4K20 methylation states and Suv4-20h histone methyltransferases...	23
<b>2.3</b>	<b>Linking epigenetics to development</b> .....	<b>25</b>
<b>2.4</b>	<b>Objectives</b> .....	<b>28</b>
<b>3</b>	<b>MATERIALS AND METHODS</b> .....	<b>29</b>
<b>3.1</b>	<b>Laboratory Equipment</b> .....	<b>29</b>
<b>3.2</b>	<b>Reagents</b> .....	<b>30</b>
3.2.1	Enzymes and Proteins .....	30
3.2.2	Kits .....	31
<b>3.3</b>	<b>Antibodies</b> .....	<b>31</b>
3.3.1	Primary Antibodies .....	31
3.3.2	Secondary Antibodies .....	32
3.3.2.1	<i>Immunocytochemistry (ICC)</i> .....	32
3.3.2.2	<i>Immunofluorescence (IF)</i> .....	32
3.3.2.3	<i>In Situ hybridization</i> .....	32
3.3.2.4	<i>Western Blot Analysis (WB)</i> .....	32
<b>3.4</b>	<b>Nucleic acids</b> .....	<b>32</b>
3.4.1	Size standard .....	32
3.4.2	Oligonucleotides.....	32
3.4.2.1	<i>Oligonucleotides for endpoint RT-PCR</i> .....	33
3.4.2.2	<i>Oligonucleotides for qRT-PCR</i> .....	33

3.4.2.3	<i>Oligonucleotides for ChIP-PCR</i> .....	34
3.4.2.4	<i>Oligonucleotides for PCR-based mutagenesis</i> .....	35
3.4.2.5	<i>Oligonucleotides for cloning</i> .....	35
3.4.2.6	<i>Morpholino oligonucleotides</i> .....	35
3.4.3	Plasmids.....	36
3.4.3.1	<i>Plasmids used for transfection</i> .....	36
3.4.3.2	<i>Plasmids used for in vitro transcription</i> .....	36
3.4.3.3	<i>Plasmids used for dig-labelled RNA in situ hybridization probes</i> .....	36
<b>3.5</b>	<b>Molecular methods</b> .....	<b>38</b>
3.5.1	Solutions .....	38
3.5.2	Isolation of nucleic acid .....	39
3.5.2.1	<i>DNA isolation</i> .....	39
3.5.2.2	<i>RNA isolation</i> .....	39
3.5.3	Analysis and manipulation of nucleic acids.....	40
3.5.3.1	<i>Cloning methods and bacterial manipulation</i> .....	40
3.5.3.2	<i>Bacterial strains</i> .....	40
3.5.3.3	<i>Gel electrophoresis of nucleic acids</i> .....	40
3.5.3.4	<i>Isolation of DNA fragments from agarose gels</i> .....	40
3.5.4	Polymerase chain reaction (PCR).....	40
3.5.4.1	<i>PCR amplification of fragments for cloning</i> .....	40
3.5.4.2	<i>Endpoint RT-PCR assay</i> .....	41
3.5.4.3	<i>Quantitative Real-Time PCR (qRT-PCR)</i> .....	42
3.5.4.4	<i>Microarray analysis</i> .....	43
3.5.5	In vitro transcription .....	44
3.5.5.1	<i>In vitro transcription for microinjection</i> .....	44
3.5.5.2	<i>In vitro transcription of dig-labelled probes</i> .....	45
3.5.6	RNA In situ hybridization.....	45
<b>3.6</b>	<b>Embryological methods</b> .....	<b>48</b>
3.6.1	Solutions .....	48
3.6.2	Experimental animals.....	49
3.6.3	Superovulation of female frogs .....	49
3.6.4	Testis preparation .....	49
3.6.5	<i>In vitro</i> fertilization of eggs and embryos culture.....	49
3.6.6	Removal of egg jelly coat.....	50
3.6.7	Injection of embryos .....	50
3.6.8	Animal cap explants preparation and culturing .....	51
<b>3.7</b>	<b>Histological methods</b> .....	<b>52</b>

3.7.1	Solutions .....	52
3.7.2	Immunocytochemistry .....	53
3.7.3	Immunohistochemistry of paraffin embedded sections .....	53
3.7.4	Vibratome sections of <i>Xenopus</i> embryos.....	54
3.7.5	X-Gal staining.....	55
<b>3.8</b>	<b>Protein analysis.....</b>	<b>56</b>
3.8.1	Solutions .....	56
3.8.2	Preparation of <i>Xenopus laevis</i> whole embryo lysate for SDS-PAGE.....	56
3.8.3	Histone extraction from nuclei of <i>Xenopus</i> embryos on sucrose cushion for SDS-PAGE .....	57
3.8.4	Myc-tagged fusion protein extraction from embryos .....	57
3.8.5	SDS-PAGE and Western Blot Analysis.....	58
3.8.6	Sample preparation for Mass Spectrometry.....	58
<b>3.9</b>	<b>Chromatin analysis.....</b>	<b>60</b>
3.9.1	Solutions .....	60
3.9.2	Chromatin Immunoprecipitation (ChIP).....	61
<b>4</b>	<b>RESULTS.....</b>	<b>63</b>
<b>4.1</b>	<b>Testing pluripotency by single cell transplantation .....</b>	<b>63</b>
<b>4.2</b>	<b>Identification of <i>Xenopus laevis</i> Suv4-20h enzymes .....</b>	<b>67</b>
<b>4.3</b>	<b>Functional characterization of xSuv4-20h enzymes.....</b>	<b>73</b>
<b>4.4</b>	<b>Developmental functions of xSuv4-20h enzymes.....</b>	<b>78</b>
4.4.1	Loss-of-function analysis.....	79
4.4.2	A functional SET domain is required for proper Suv4-20h enzymes function.....	82
4.4.3	Gain-of-function analysis.....	87
4.4.4	XSuv4-20h depletion misregulates a small group of genes .....	89
4.4.5	XSuv4-20h enzymes are required for ectoderm formation .....	90
4.4.6	XSuv4-20h enzyme depletion affects epidermal ciliogenesis .....	92
4.4.7	XSuv4-20h enzymes are required for neurogenesis .....	95
4.4.8	XSuv4-20h HMTases affect apoptosis and cell proliferation independently from the loss of primary neurons .....	103
4.4.9	XSuv4-20h enzyme depletion triggers the upregulation of the pluripotent gene Oct-25 .....	105
4.4.10	H4K20me3 levels are enriched in the 5'-UTR region of the Oct-25 gene .....	109
4.4.11	Regulation of early neural marker genes by Oct-25.....	111

4.4.12	Downregulation of Oct-25 rescues double-morphant phenotypes .....	113
4.4.13	Suv4-20h enzymes regulate murine Oct-4 expression .....	116
<b>5</b>	<b>DISCUSSION .....</b>	<b>118</b>
<b>5.1</b>	<b>Pluripotent features of single animal pole blastomeres .....</b>	<b>119</b>
<b>5.2</b>	<b><i>Xenopus laevis</i> Suv4-20h HMTases .....</b>	<b>120</b>
5.2.1	Functional analysis of xSuv4-20h HMTases .....	121
5.2.2	Biological analysis of xSuv4-20h HMTases .....	123
5.2.3	XSuv4-20h enzymes contribution to ciliogenesis .....	123
5.2.4	A glimpse on the global role xSuv4-20h HMTases in gene regulation.	125
5.2.5	A germ-layer specific function for xSuv4-20h HMTases .....	126
5.2.6	Apoptosis and proliferation defects in xSuv4-20h morphant embryos .	129
5.2.7	Neurogenesis is controlled by a Suv4-20h/Oct-25 regulatory module .	130
5.2.8	Suv4-20h enzymes regulate Oct4 expression in murine ES cells.....	134
<b>5.3</b>	<b>Conclusion and future directions .....</b>	<b>135</b>
<b>6</b>	<b>ABBREVIATIONS.....</b>	<b>137</b>
<b>7</b>	<b>REFERENCES.....</b>	<b>141</b>
<b>8</b>	<b>APPENDICES .....</b>	<b>148</b>
8.1	Suv4-20h enzymes regulate murine Oct-4 expression.....	148
8.2	Microarray gene lists .....	151
<b>9</b>	<b>ACKNOWLEDGEMENTS.....</b>	<b>188</b>
<b>10</b>	<b>CURRICULUM VITAE .....</b>	<b>189</b>

# 1 SUMMARY

Embryonic development is characterized by a series of morphological and molecular processes caused by and resulting in the spatio-temporal activation and repression of pools of genes. The pluripotent trait, key feature of embryonic stem (ES) cells, is progressively restricted and finally lost as soon as embryonic cells become specified. Cellular differentiation therefore reflects a series of molecular signatures, established by a properly orchestrated network of transcription factors and epigenetic mechanisms. Recent studies have indeed revealed that dynamic changes in chromatin structure and composition represent fundamental processes, which define the “epigenetic landscape” and contribute to fix the identity of cells.

Methylation of histone proteins, and the consequent activation or repression of gene expression, is increasingly considered as an important regulatory layer in development. In particular, repressive histone trimethylation marks are found on conserved lysine residues in position 9 and 27 of histone H3 and in position 20 of histone H4. While H3K9me3 and H3K27me3, as well as the functions of many histone methyltransferases (HMTases) associated with these marks, have been characterized, our knowledge of the function of Suv4-20h1 and Suv4-20h2 enzyme during development is rather limited.

My Ph.D. project was aimed to investigate the function of H4K20 di- and trimethylation during *Xenopus* development by gain and loss of function analysis for the corresponding HMTases xSuv4-20h1 and xSuv4-20h2. Three main insights arose from this work:

1. H4K20me2 and me3 depleted embryos show a specific block in neuroectoderm differentiation and ciliogenesis, with no dramatic effect on formation of the mesoderm and endoderm germ layers.
2. The expression of the pluripotency-associated gene Oct-25 persists in the ectodermal sensorial cell layer of xSuv4-20h depleted embryos, interfering with the transcriptional activation or activities of key regulators of neurogenesis and probably ciliogenesis.
3. Murine Suv4-20h double knockout (DKO) ES cells have higher levels of the POU-V pluripotent gene Oct4 while undifferentiated, and maintain higher levels during differentiation, compared to the wild-type cells. This result

suggests that repression of the POU-V genes through Suv4-20h enzymes might be an evolutionary conserved mechanism.

These results identify Suv4-20h enzymes as novel regulators of ectoderm differentiation and pluripotency associated POU-V gene expression.

## 2 INTRODUCTION

### 2.1 *Xenopus* as a model organism

In the last century the South Africa clawed frog *Xenopus laevis* has been widely used in the field of experimental biology. The ease of maintaining *Xenopus* in captivity, the external fertilization coupled to the high number of eggs produced and the large size of the embryos, which allows easy manipulations and microdissections, represent the main features of this organism. At the same time well-established molecular techniques like RNA *in situ* hybridization, antisense technology and protein overexpression, make it possible to address many questions about how the vertebrate body is patterned and structured. On the other hand, the pseudotetraploid genome and the long generation time, pose a disadvantage for genetic studies. These obstacles may be overcome by the use of *Xenopus tropicalis*, which while retaining many advantages of *laevis*, has a diploid genome (recently sequenced (Hellsten, Harland et al. 2010)), and a considerably shorter generation time. The two closely related species represent amphibian model organisms that are exceptionally useful to combine embryological, cell biological and genetics experiments.

*Xenopus* eggs are characterized by the pigmented upper surface (animal pole) and the non-pigmented lower surface (vegetal pole) enriched in yolk. After fertilization, twelve successive mitotic divisions without G- phases shape the embryo in a ball-like structure known as blastula, consisting of many small cells surrounding the fluid-filled cavity blastocoel, placed above larger yolky cells. Already at this developmental stage, inductive events have occurred and the cells, although still pluripotent (Heasman, Wylie et al. 1984), interacting with each other, become partially specified. At the blastula stage the embryo can be divided in three broad regions: the animal pole, which forms the roof of the blastocoel and will give rise to the ectoderm, the marginal zone, which is the equatorial region of the embryo that will differentiate into mesoderm, and the vegetal pole, which will give rise to the future endoderm (Heasman 2006). A key step in the embryonic development is represented by the activation of the zygotic transcription, known in frogs as mid-blastula transition (MBT). This event, characterized by changes in the chromatin state (active transcription of zygotic genes) as well as in the cell cycle regulation, is a pivotal precondition for the following step, gastrulation. At gastrula stage dramatic rearrangements of embryonic structures occur: the involution of the marginal zone cells, coupled to the convergent extension of the mesoderm and the concomitant

epiboly of the prospective ectoderm, pattern the embryo in a three-dimensional multilayered body plan. The three germ layers (outer ectoderm, inner endoderm and interstitial mesoderm) are thus established. Starting at late blastula and proceeding during early gastrulation, a portion of the dorsal ectoderm is specified to become neural ectoderm. During this process, called neurulation, the neural tube is formed: its anterior-most portion will give rise to the brain, while the posterior region will originate the spinal cord. Neurulation represents one of the first events that characterized the process of organogenesis, during which the number of specialized cells increase to accommodate formation of the different organs. Embryogenesis is completed when the tadpole hatches at an age of three days (NF48) and takes up feeding to prepare to metamorphosis, prior to becoming a sexually mature frog.

### 2.1.1 Inductive events during *Xenopus* development

As mentioned above, the *Xenopus* egg is polarized along the animal-vegetal axis. The original asymmetry refers to the localization of maternally provided mRNAs and proteins. The polarity influences the pattern of the cleavage division. While mRNAs and proteins from housekeeping genes are equally present in the unfertilized egg, the product of some specific developmental regulatory genes are differentially distributed within the egg (Heasman 2006). In particular, the vegetal pole is enriched in factors that exert a pivotal function in the early stages: Veg-T, Vg-1, and Xwnt-11 mRNAs represent crucial transcripts components for the initial inductive events. Among these factors, the T-box protein Veg-T, inherited equally by all vegetal cells, is essential for the correct spatial organization of endoderm and mesoderm. Veg-T activates the expression of pro-endodermal genes like Sox17, GATA factors and Mixer (Heasman 2006), which in turn regulate downstream targets implicated in endoderm formation. Mixer, for example, induces Sox17 while represses the mesodermal genes eomesodermin and fgf8, exerting a key role in the separation of mesoderm and endoderm fates (Heasman 2006). Veg-T also activates the transcription of Nodal related proteins (Xnr1, Xnr2, Xnr4) and Derrière (Kimelman and Griffin 2000). The synergistic interaction with the Wnt pathway effector  $\beta$ -catenin, stabilized in the future dorsal side of the embryo at mid-blastula, induces a higher expression of Xnr genes dorsally than ventrally.

This gradient is critical for mesoderm induction. In the vegetal dorsal most portion of the gradient, where  $\beta$ -catenin, Vg-1 and Veg-T are present and Xnr

proteins concentration is highest, the Nieuwkoop center is formed (Wolpert et al., 1998; (De Robertis and Kuroda 2004) (Fig. 1). One of the main roles of the Nieuwkoop center is to specify the key dorsal signalling center, called Spemann organizer, which is essential for the antero-posterior and dorso-ventral patterning of the embryo. Mesoderm is induced in the marginal zone of the embryo at blastula. Inductive experiments using recombinants of endodermal and ectodermal blastula explants showed that ventral and dorsal endoderm induce ventral (lateral plate, mesenchyme and blood) and dorsal (Spemann organizer) mesoderm tissues, respectively. Mesoderm induction is finally accomplished during gastrulation, when the inductive horizontal signal form the organizer triggers the differentiation of dorsal mesodermal cell types (notochord, somites).

Concomitant to the Nieuwkoop center formation, the dorsal animal pole and marginal zone cells express the Bone Morphogenetic Proteins (BMP) antagonists Chordin and Noggin, under the induction of  $\beta$ -catenin, defining the so called blastula Chordin and Noggin expression center (BCNE) (Kuroda, Wessely et al. 2004). The same factors (Chordin and Noggin), transiently expressed in the prospective neuroectoderm at blastula stage, will be expressed at gastrula in the Spemann organizer mesoderm (Kuroda, Wessely et al. 2004). These two signalling centers formed at blastula stage (Nieuwkoop center and BCNE) under  $\beta$ -catenin control, guarantee the proper establishment of the organizer, which exerts its roles during gastrulation.

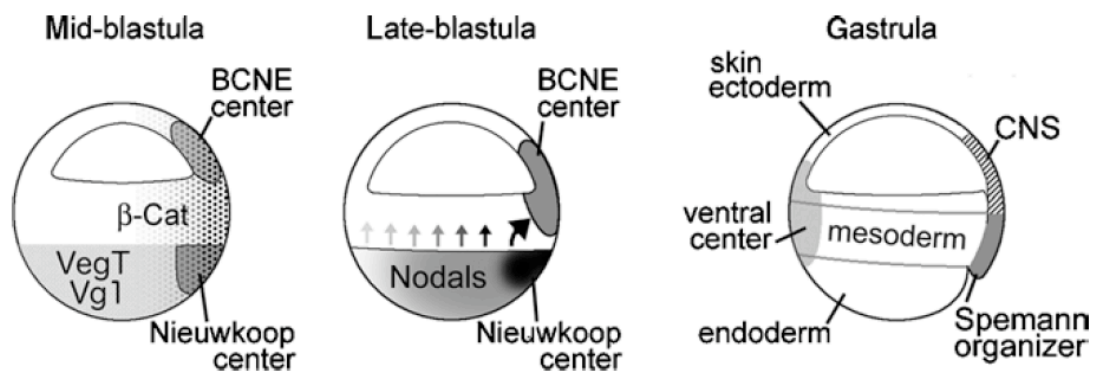


**Fig. 1: Early inductive events in *Xenopus laevis* embryo.** At blastula stage the BCNE center in the animal region and the Nieuwkoop center in the vegetal pole pattern the embryo.  $\beta$ -catenin localization is essential for the centers formation. BNCE center is involved in the establishment of anterior neural tissue, while the Nieuwkoop center induces the Spemann organizer via nodal-related signalling. (From De Robertis and Kuroda 2004).

### 2.1.2 *Xenopus* epidermis and ciliated cells differentiation

Maternal determinants play fundamental role also for specification of the ectodermal layer. Coupling a screening strategy to loss of function experiments, Dupont and colleagues identified and characterized Ectodermin as an essential player for the specification of the ectoderm (Dupont, Zacchigna et al. 2005). This factor, promotes Smad4 degradation via direct binding and ubiquitination, and by this mechanism restricts the mesoderm-inducing activity of TGF- $\beta$  signals, ensuring that ectodermal cells do not adopt a mesodermal fate (Dupont, Zacchigna et al. 2005). Morphologically, during gastrulation the animal cap and the non-involuting marginal zone cells expand by epiboly and cover the entire embryo, forming the surface ectoderm. Vertebrate ectoderm gives rise to three major derivatives: primary epidermis, characterized by the presence of high levels of BMPs; central nervous system (brain and spinal cord), induced by inhibition of BMP signalling by BMP-antagonist (e.g. Noggin, Chordin) and neural crests (which differentiate into peripheral neurons, pigment, facial cartilage, etc.), originating in the border between epidermis and neural plate (Gibert, 2006).

Two types of cells characterize the skin of *Xenopus* embryos. Non-ciliated cells (Fig. 2a), fall in two categories, known as the large secretory goblet cells and the smaller scattered cells, responsible for secretion of mucus and containing electron-dense granules, respectively. The second type of epidermal cells is formed by the multiciliated cells (Fig. 2b) which function in propelling the mucus with coordinated effective and return strokes (Hayes, Kim et al. 2007). Deblandre et al. described a two-step mechanism that governs the differentiation and the generation of the spacing pattern of the ciliated cells (Deblandre, Wettstein et al. 1999). According to this model, at late gastrula stage in the inner ectodermal layer, a subset of cells expresses high levels of Delta-like 1. These cells, through the lateral inhibition mechanism, both generate ciliated-cell precursors, which express the marker alpha tubulin, and prevent neighbour cells to undertake the same differentiation process. At neurula stage, the alpha-tubulin positive cells move and intercalate from the inner into the outer ectodermal layer. Finally, at tadpole stage, ciliated cells differentiate and reach their definitive position in the epithelium (Fig. 2c) (Deblandre, Wettstein et al. 1999).

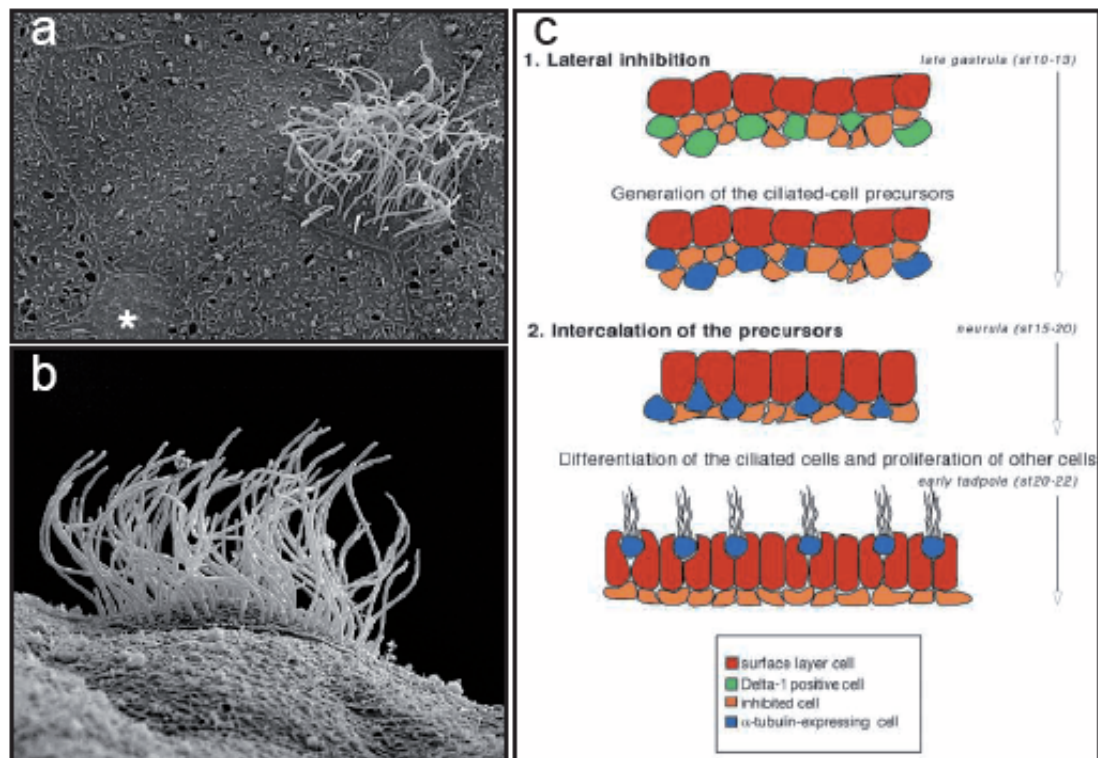


**Fig. 2: *Xenopus* epidermis and ciliated cells generation.** (a) Scan electron microscopy (SEM) picture of mucociliary epithelium including a ciliated cell, small secretory cell (marked by the asterisk) and several large goblet cells. (b) SEM lateral view of a ciliated cell, showing the apical cilia. (c) Schematic representation of the two-step mechanism spacing the ciliated cells (modified after Hayes, Kim et al. 2007 and Deblandre, Wettstein et al. 1999).

It has been shown that the planar cell polarity (PCP) pathway exerts a pivotal role in a variety of vertebrate developmental events (Gray, Abitua et al. 2009; Mitchell, Stubbs et al. 2009; Wallingford 2010). Core PCP components, like Dishevelled, govern a wide range of polarized cellular behaviours, including cell interaction, migration and ciliogenesis (Gray, Abitua et al. 2009). Moreover, studies in mice and frogs, underline the key role of the PCP effectors proteins, which ensure that the proper pattern of ciliated cells is established during development (Park, Haigo et al. 2006; Gray, Abitua et al. 2009). These studies have highlighted the interconnection between cell polarity, morphology, signal transduction and embryonic development, and describe the fundamental role of PCP signalling in cilia development.

### 2.1.3 Neural induction and neurogenesis

Neural induction represents the initial step in the formation of the vertebrate nervous system. In *Xenopus*, neural tissue derives from the dorsal side of the embryonic ectoderm, whereas the ventral side gives rise to epidermis. The first insight into the mechanism of neural induction came from a pioneering experiment of Spemann and Mangold in 1924, in which they showed that the transplantation of the dorsal blastoporal lip of early gastrula embryo (the so called organizer) into the ventral region of a host embryo at same age induced a complete second nervous system in the host (Spemann and Mangold 2001), suggesting a mechanism by which the organizer region acts as a source of inductive signals for neural fate. Five main neural-inductive molecules were identified later: Noggin, Follistatin, Chordin, Xnr3 and Cerberus (for review see (Hemmati-Brivanlou and Melton 1997; Harland 2000)). Following experiments using whole embryos as well as explants of prospective ectoderm, led to the idea that neural fate-inducing molecules act as inhibitors rather than as inducers, antagonizing the epidermal-inducing factors BMPs (Fig. 3a). Important evidence supporting this model came from the result that transient dissociation of ectodermal explants results in a shift from epidermal default differentiation to a neural state, consistent with the presence of inhibitors of neurogenesis – BMPs – in the explants (Grunz and Tacke 1989). All together, these observations, as well as other experiments, led to define the so called “default model”, according to which inhibition of BMP signalling is sufficient to induce neural differentiation: embryonic ectoderm has a natural “default” tendency to differentiate as neural tissue, unless instructed by BMPs to become epidermis (Munoz-Sanjuan and Brivanlou 2002). More recently, experiments in *Xenopus* and in other model systems highlighted the role of FGF signalling in patterning the antero-posterior axis of neural tissues and in reinforcing the antagonism of the BMP pathway (Rogers, Moody et al. 2009). Moreover, additional lines of evidence support the idea that inhibition of Wnt signalling is required for neural induction, describing a complex mechanism for neural fate, involving multiple intercrossing pathways (for review see (Wilson and Edlund 2001)).

Once the presumptive neural ectoderm is established via inductive interactions, a consistent set of transcription factors are expressed in overlapping domains (Fig. 3b). Transcripts of several of these genes (Geminin, Sox3, Sox11 and SoxD) are found in the dorsal ectoderm at the onset of gastrulation (Rogers, Moody et al. 2009). Other mRNAs (FoxD5, Sox2, Zic1, Zic2, Zic3) are expressed in a region close to the blastoporal lip, while *Xenopus* *Iroquois* homologs (Xiro1, Xiro2, Xiro3)

are detected in two dorso-lateral bands close to the blastoporal lip. Although most of these factors, when overexpressed, do not trigger ectopic neural tissue, nevertheless they all expand the neural plate. FoxD5 and Geminin contribute to maintain an undifferentiated neuroectoderm during the early steps of neural plate formation (Kroll, Salic et al. 1998; Yan, Neilson et al. 2009).

Sox genes are Sry-related transcription factors characterized by a high-mobility group (HMG) domain that confers sequence-specific DNA binding activity. Sox2 and Sox3 are pan-neural markers important for neural progenitor maintenance; Sox2, in particular, is induced by dissociation of ectodermal explants in *Xenopus*, (Sasai 1998).

Another important class of neural genes encode Zic-related zinc finger transcription factors. Zic1 and Zic3 have been shown to induce neural and neuronal differentiation in animal cap (AC) experiments in *Xenopus* (Sasai 1998), suggesting an active role in promoting the transition to neural differentiation. On the other hand, Zic2 can counteract the formation of ectopic neurons produced by neurogenin (Xngnr1) mRNA injection, indicating a possible involvement of this factor in maintaining cells in an immature state via neural differentiation repression (Rogers, Moody et al. 2009).

Iroquois genes encode homeodomain proteins involved in the activation of proneural basic helix-loop-helix (bHLH) genes. It was shown that Wnt-dependent activation of Xiro1 mediates the downregulation of BMP4, suggesting a key role of this factor in defining the neural territory and in promoting the expression of bHLH neural differentiation genes (Gomez-Skarmeta, de La Calle-Mustienes et al. 2001).

These observations indicate that the early transcription factors expressed in the newly induced neuroectoderm can be divided into two groups: Geminin, Sox2, Sox3, FoxD5 and Zic2 keep cells of the neuroectoderm in an undifferentiated neural state, while Sox11, Zic1, Zic3 and the Iroquois genes promote the onset of neural differentiation (Rogers, Moody et al. 2009). Gain and loss of function experiments suggested that all these factors define a complex regulatory network (Fig. 4) (for review see (Rogers, Moody et al. 2009)). It is important to note that concomitantly to the stabilization of the neural induction promoted by the aforementioned factors, ventral specific homeobox genes (e.g. Gata1 and Msx1) act as negative regulator of neural differentiation, promoting epidermal differentiation in non-neural ectoderm (Sasai 1998).

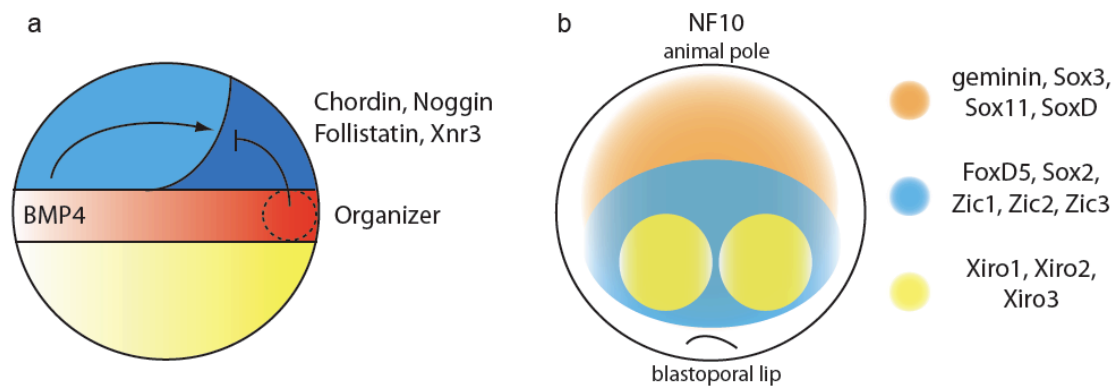


**Fig. 3: Early neural inductive events.** (a) The organizer proteins such as Chordin, Noggin, Follistatin and Xnr3 block the action of the ventralizing factor BMP4. (b) Overlapping expression pattern of neural genes at NF10. At the onset of gastrulation a first class of genes are expressed throughout the dorsal ectoderm (orange domain), a second class of transcription factors is expressed in a broad dorsal band adjacent to the blastoporal lip (blue area), while the Xiro genes are expressed in two posterior-lateral domains (yellow areas). (Pictures modified from Gilbert, 2006 and Rogers, Moody et al. 2009).

Once the neural plate has been established, the next step in neural development aims to define the precise spatio-temporal formation of neurons in the neuroepithelium. Two distinct waves of neuronal differentiation have been described in *Xenopus*: primary neurogenesis occurs at about 13 hours post fertilization (hpf, NF 12) and serves to enable swimming and escape reflexes in the early tadpole. Secondary neurogenesis (NF46) generates the full complements of neurons and it is involved in mediating the more complex behaviour of the late tadpole (Sasai 1998). In *Xenopus* the early step of primary neurogenesis is characterized by the expression of proneural/neurogenic genes. Many of these genes are homologs of the achaete-scute genes of *Drosophila*, and are required for the determination of neural precursors. For example, the bHLH factor Neurogenin related 1a (Ngnr-1a) is present in all the presumptive regions of primary neurogenesis at gastrula stage. Its expression precedes that of Delta-like 1, a cell surface molecule which mediates lateral inhibition. This mechanism represents a cell-cell interaction that acts within the proneural cluster to limit the number of cells that gives rise to neuroblasts (Chitnis 1995): prospective neuroblasts express the Notch ligands Delta or Serrate which, interacting with Notch, trigger the expression of repressors of neuronal differentiation (enhancer of split-hairy family transcription factors) in neighbouring cells. This signalling restricts the expression of Ngnr 1a, Delta-like 1 and finally N-tubulin (differentiated primary neurons marker) to three bilateral longitudinal stripes in the neuroectoderm (medial, intermediate and lateral stripes) (Chitnis 1995; Sasai 1998; Diez del Corral and Storey 2001). Finally, when the neural tube is formed the three

stripes differentiate into motor-, inter- and sensory-neurons. The neuronal subtype specification is then defined according to a precise expression of a combination of transcription factors along the prospective dorso-ventral axis of the forming neural tube (Diez del Corral and Storey 2001).

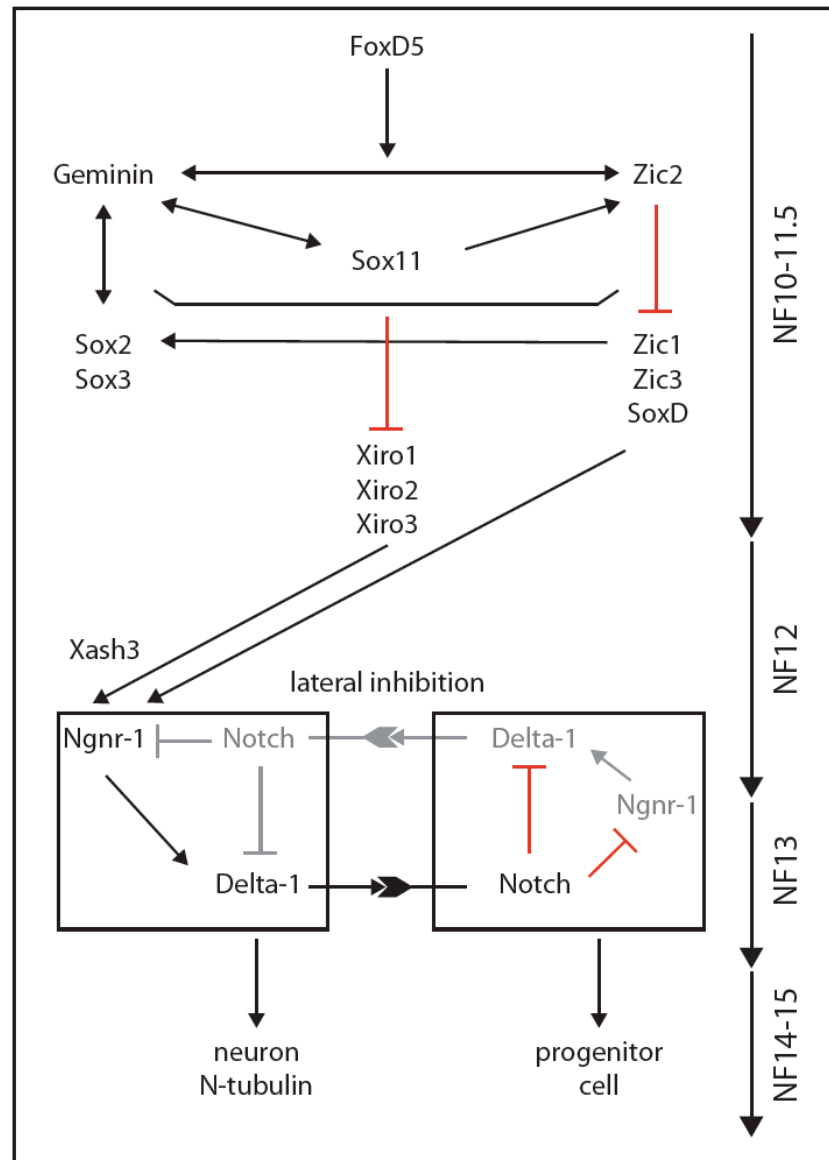


**Fig. 4: Proposed model for early neural differentiation.** According to loss-of-function and gain-of-function experiments, FoxD5 acts at the top of the cascade and regulates Geminin, Sox11 and Zic2. These genes regulate each other and together with Sox2 and Sox3 are thought to maintain neural ectodermal cells in an immature state affecting the expression of the downstream genes. Xiro genes, Zic1, Zic3 and SoxD on the other hand promote the onset of neural differentiation via upregulation of bHLH genes like Ngnr-1, which, in turn, through the lateral inhibition mechanism stimulate Delta-1 expression in future neuron, positive for N-tubulin expression. (Picture modified from Rogers, Moody et al. 2009).

#### 2.1.4 Embryonic cell fate specification: from pluripotency to differentiation

The process leading naïve embryonic cells to a specific cell type is characterized by a series of steps, which restrict the cell behaviour from pluripotent, to committed, to differentiated. Classical transplantation experiments (Spemann and Mangold 2001) highlighted important properties of cell-cell interactions: inductive events rely on the presence of the inducer (the tissue that produces a signal) and of the responder (the tissue which is induced). In this context, the ability of a group of cells to respond to a specific inductive signal is defined as competence, and describes a feature which allows a cell to undertake a particular differentiation pathway if exposed to proper stimuli. This step represents the first important prerequisite for the commitment to a certain fate. A cell is then defined specified, if it is able to differentiate into a particular cell type when placed in a neutral environment. At this stage repressive signals can still compromise cell differentiation. The next step, determination, describes the ability of the cell to differentiate according to its original fate, even when transplanted into a different region of the embryo, and becoming exposed to inhibitory signals. At this stage the cell is irreversibly committed and will eventually express the gene repertoire characteristic of its fully differentiated state (Gilbert, 2006). A series of single-cell transplantation experiments in *Xenopus laevis* showed that when either an animal or a vegetal pole blastomere is transplanted into the blastocoel of a late blastula host embryo, it will give rise to descendants of all the three germ layers. When transplanted from the early gastrula, cells differentiate as they would do if kept in their original position (i.e. ectoderm or endoderm if taken from the animal or vegetal hemisphere respectively), suggesting that the pluripotent character of *Xenopus* embryonic animal and vegetal pole cells is lost at the beginning of gastrulation (Snape, Wylie et al. 1987; Wylie, Snape et al. 1987).

Uncommitted blastula-stage cells are characterized by the expression of the three transcription factors Oct-25, Oct-60 and Oct-91. These genes contain a DNA binding domain referred to as POU domain from the original three members included in this family (the Pituitary-specific Pit-1, the Octamer transcription factors Oct-1, Oct-2 and the *Caenorhabditis elegans* neural transcription factors Unc-86) (Hinkley, Martin et al. 1992). This domain is a 160 aminoacid long bipartite structure, consisting of a specialized homeodomain, which weakly binds DNA and participates in the formation of protein complexes, preceded by a highly conserved POU-specific region, which contributes to the specificity and strength of DNA binding by the POU domain (Hinkley, Martin et al. 1992). The three *Xenopus* genes are expressed during

early embryogenesis: Oct-25 and Oct-60 are maternally expressed, while Oct-91 appears at late blastula. The expression of all the three genes decreases during gastrulation, describing a scenario that resembles the loss of pluripotency assessed by single cell transplantation experiments (Snape, Wylie et al. 1987; Wylie, Snape et al. 1987; Hinkley, Martin et al. 1992). More recently, Morrison and Brickman showed that the *Xenopus* pluripotent genes are functionally homologous to the mammalian Oct3/4 (Morrison and Brickman 2006). Moreover, several lines of evidence support the idea that *Xenopus* POU-V factors are mainly involved in controlling the maintenance of pluripotency, preventing cells from entering terminal differentiation pathways (Cao, Knochel et al. 2004) and regulating competence transition (Snir, Ofir et al. 2006). All these activities allow the three germ layers specification to occur in a proper spatio-temporal manner (Morrison and Brickman 2006; Cao, Siegel et al. 2007).

## 2.2 Epigenetics

The term “epigenetics” defines a panoply of mechanisms that lead to heritable changes in gene function occurring independently of alterations to the DNA sequence (Berger, Kouzarides et al. 2009). The word epigenetics is constantly submitted to re-definitions, underlining the complexity of the processes characterizing this field. Nevertheless it is generally accepted that epigenetic signals are involved in the establishment, maintenance and reversal of transcriptional states in order to provide the cell with a memory of previously experienced stimulation without changes in the genetics information (Bonasio, Tu et al. 2010). The maintenance of a particular cell identity, set up only once at a specific developmental stage, represents a typical example of an inherited cellular memory. All the different epigenetic mechanisms rely on the common feature that DNA exists as complex with highly evolutionary conserved proteins, histones, which together form the so called chromatin (Kornberg 1974). Different lines of evidence in the last decades led to the idea that chromatin is a dynamic structure, existing in many configurations, whose variation modulates the expression of genomic informations. Alterations in chromatin structure include DNA methylation, histone variants, chromatin remodeling (through energy-dependent complexes), covalent histone modifications and non-coding RNAs (for review see (Allis et al., 2007)).

### 2.2.1 Chromatin structure

DNA in chromatin is organized in arrays of nucleosomes (Kornberg 1974). Each nucleosome is composed by an octamer containing two copies of each histone (H2A, H2B, H3, H4) around which ~145-150 bp of left-handed DNA superhelix is wrapped (Luger, Mader et al. 1997). The small and highly basic core histone proteins, forming the octamer, are structured in two main domains: the globular domain, characterized by three alpha helices linked by two loops, and a flexible histone tail, which protrudes from the surface. Amino acid sequence alignments revealed a high degree of conservation among different species, suggesting critical functions for these proteins (Luger, Mader et al. 1997). Histone tails, in particular of H3 and H4, are subjected to post-translational modifications (PTMs) at specific aminoacid residues. These features underline the pivotal role of the nucleosome in gene expression regulation.

Adjacent nucleosomes are separated by a linker DNA region, whose length varies in different cells and among different species. The “beads on a string” chromatin organization, visualized by electron microscopy, describes an 11-nm configuration characterized by regularly spaced nucleosomes. Such a configuration can be modified and turned into higher-order structures (Fig. 5) (for review see (Allis et al., 2007)). The linker histone H1, for example, is known to promote packaging and stabilization of chromatin. The globular domain mediates anchoring of linker histones to the nucleosomes, while the positively charged C-terminal domain binds the DNA between nucleosomes. Recruiting of the linker histone, as well as histone tails modifications and chromatin-associated factors binding, lead to a more compact chromatin structure, 30-nm fiber, which can further be organized into larger looped domains (300-700 nm) as the result of long-range interactions between sequence elements that are distant on linear chromosomes or as consequence of interaction of the genome with anchoring sites within the nucleus, such as the nuclear lamina (van Steensel 2011). This configuration occurs in both interphase and metaphase chromatin. Finally, the most condensed DNA structure is observed during metaphase of mitosis and meiosis, and results from dramatic rearrangements of DNA achieved by hyperphosphorylation of linker H1 and core histone H3 coupled to the concomitant action of cohesin, condensin and topoisomerase II (for review see (Allis et al., 2007)).

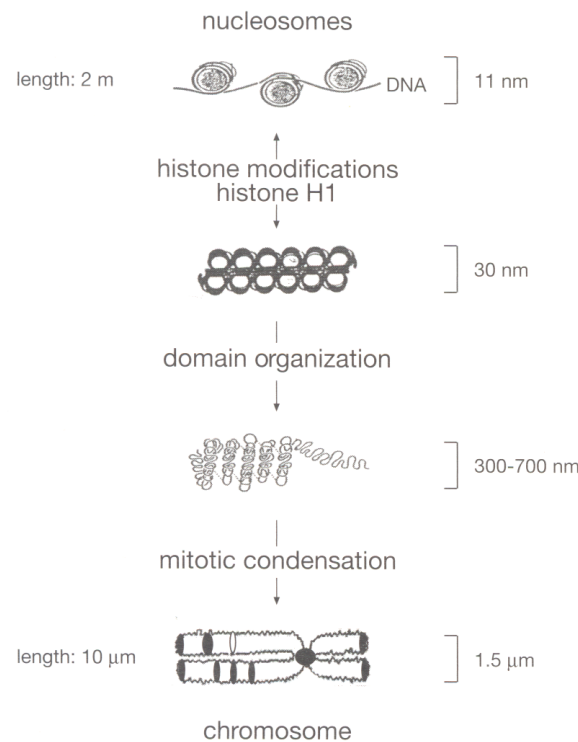


**Fig. 5: Higher-order structures of chromatin – the “historical” textbook view.** DNA wrapped around nucleosomes creates the 11-nm “beads on a string” configuration. Linker histone H1 recruitment leads to the formation of the 30-nm configuration. 300-700-nm fiber represents a further level of compaction present both in interphase and metaphase. The most compacted chromatin configuration is obtained during the metaphase of mitosis or meiosis (From Allis et al., 2007).

While the 11-nm “beads on a string” configuration is commonly accepted, the precise structure of the 30-nm fibre represents an open debate. Recent studies addressed the question whether this chromatin conformation really exists (Maeshima, Hihara et al. 2010; Fussner, Ching et al. 2011). *In vivo* evidence for 30 nm fibres has been collected for certain cell types (i.e. starfish sperm nuclei and chicken erythrocyte nuclei). In these cells electron microscopy (EM) experiments revealed that the 11-nm fibre folds and twists into a structure of approximately 30 nm in width. Nevertheless, interphase nuclei in most higher eukaryote cell type contain no regular 30-nm fibre (Maeshima, Hihara et al. 2010). A new study performed in mitotic HeLa cells demonstrated, in a quantitative manner, that human mitotic chromosomes consist of irregularly folded nucleosome fibres, with no 30-nm configuration (Nishino, Eltsov et al. 2012). Together these data indicate that no periodic structures beyond the 11-nm configuration exist in human mitotic chromosomes. The authors suggest that chromatin condensation is achieved by packing the “beads on a string” fibres in a fractal organization (Fussner, Ching et al.

2011; Nishino, Eltsov et al. 2012). Although it cannot be excluded that the 30-nm structure is present under certain specific conditions, these studies showed that this configuration is not required to achieve large-scale condensation of human mitotic chromosomal DNA (Hansen 2012).

### 2.2.2 Principal chromatin types

Cytological studies led to the idea that chromatin could be categorized in two main types. The first one, called “heterochromatin”, which defines compacted, gene-poor chromatin domains. This silenced chromatin can exist as permanently silent (constitutive) heterochromatin, such as found at centromeric and telomeric regions. Alternatively, gene-silencing can be achieved as a transition from an active to an inactive state (facultative heterochromatin) (for review see (Allis et al., 2007)). The second major type of chromatin is called “euchromatin”, and it identifies relatively uncondensed/open and gene-rich portions of chromatin. This configuration usually characterizes transcriptionally active domains. The oversimplified distinction between euchromatin and heterochromatin reflects a series of features, like nuclease accessibility, histone acetylation, replication timing, that *in toto* indicate opposite roles for the two states. The establishment of euchromatin aims for the transcription of functional RNAs to occur, through dynamic and elaborate interactions of histone modifications, chromatin remodelling complexes and DNA-binding proteins. Heterochromatin, instead, serves an important maintenance function for ensure genome stability (Henikoff 2000).

In a recent study, genome location maps of 53 broadly selected proteins and histone modifications were obtained in *Drosophila melanogaster* and revealed unique combinations of proteins, which may define five principal chromatin types (Filion, van Bommel et al. 2010). According to this annotation, transcriptionally active euchromatin can be subdivided in RED and YELLOW domains. While the overall expression levels are similar between the two groups, a peculiar distinction regards the presence of the transcription elongation-linked histone modification H3K36me3, whose absence defines RED domains. Moreover RED chromatin marks tissue specific genes, while YELLOW chromatin is formed at ubiquitously expressed housekeeping genes (Filion, van Bommel et al. 2010; van Steensel 2011). In contrast, BLUE chromatin is defined by the presence of Polycomb group proteins (PcG) and the histone mark H3K27me3, mainly detectable on genes involved in development. Similarly GREEN chromatin corresponds to classical heterochromatin

marked by Suppressor of Variegation 3-9 (Suv39), the histone modification H3K9me2/me3, heterochromatic protein 1 (HP1) and several HP1-associated proteins. GREEN chromatin is formed mainly at pericentric regions. The 5<sup>th</sup> category, BLACK chromatin, covers ~50% of the genome, thus representing the most prevalent repressing chromatin type. It exhibits extremely low expression levels, is depleted of PcG, HP1 and Suv39 and it is the latest chromatin type to replicate; these features, together with its location at the nuclear periphery, underscore the different character of BLACK chromatin in comparison to other heterochromatic domains (Filion, van Bemmel et al. 2010; van Steensel 2011).

Although these five chromatin types represent the major combinations of proteins among the tested ones, it is still possible that further sub-classifications refine the chromatin structure. Moreover, differences can also emerge comparing different species (van Steensel 2011). This study nevertheless provided for the first time a detailed analysis of chromatin organization, unravelling the complex network of interactions that govern its global architecture.

### **2.2.3 Chromatin dynamics**

The different chromatin types reflect a panel of epigenetic mechanisms which cooperate to establish stable, inheritable chromatin states, which control the transcriptional activity of the genome.

Nucleosome remodelers are a class of multiprotein complexes that alter histone-DNA interactions in an ATP-dependent manner. These perturbations lead to relocation/sliding of the octamers from a particular DNA segment. ATP-dependent nucleosome remodeling factors mediate also chromatin loop formation, chromatin attachment to nuclear structures (like nuclear envelope), and catalyze the transition between relaxed and condensed chromatin fiber (Varga-Weisz and Becker 2006).

The incorporation of histone variants endows nucleosomes with specific features that affect transcription. For instance, the histone H3 variant H3.1 is enriched at inactive genetic elements, whereas the H3.3 variant is present on transcriptionally active genes. Also the processes of DNA damage repair are modulated by histone variants, such as H2A.X, and other chromatin-related processes (Bonisch, Nieratschker et al. 2008). Finally also the linker histone H1 exists in different types. The variants can be divided into maternal and somatic ones.

In *Xenopus*, three somatic variants of linker histones are present (H1A, H1B, H1C); these proteins are not present in the full-grown oocyte and are expressed only in low amount during cleavage stages (Dworkin-Rastl, Kandolf et al. 1994). Until MBT the chromatin is characterized by the oocyte-specific linker histone B4 (also called H1M, maternal histone H1), which becomes progressively replaced by the somatic variants until the end of gastrulation.

DNA methylation represents a repressive modification, particularly enriched at promoter regions and noncoding DNA sequences, wherein cytosines of CpG dinucleotides are converted to 5-methylcytosine by DNA methyltransferases. This modification recruits corepressor complexes to form transcriptionally silenced chromatin structures (Sasai and Defossez 2009).

Increasing lines of evidence assign pivotal roles in transcriptional regulation to noncoding RNAs (ncRNAs). Recent findings indicate that ncRNAs, or their production, create changes in DNA and nucleosome modification, which repress transcription. From an epigenetic point of view, such regulation includes DNA methylation, chromatin remodeling, RNA-associated gene silencing, chromosome inactivation and genomic imprinting (Zhou, Hu et al. 2010).

Covalent post-translational histone modifications, finally, represent another layer of epigenetic mechanisms that affect chromatin architecture. These alterations exert different functions with regard to the type and the position of the modification. In the following chapter this epigenetic mechanism will be further addressed.

#### **2.2.4 Histone post-translational modifications (PTMs)**

The amino-terminal tails of the core histones are subjected to a variety of post-translational modifications occurring at selected amino acidic residues. Extensive evidence documents a collection of post-translational modifications, including the well-studied acetylation, phosphorylation, methylation, ubiquitination, and the less characterized ADP-ribosylation, biotinylation and SUMOylation (Fig. 6). These covalent alterations are involved in a wide range of chromatin-based processes like replication, repair, transcription and genome integrity (Bhaumik, Smith et al. 2007).



2005). These different functions outline a mechanistic complexity linked to this modification.

All core histones but H4 are known to become ubiquitinated. The formation of the isopeptide bond between the ubiquitin moiety and specific lysine residues is promoted via the sequential catalytic action of E1-activating, E2-conjugating enzymes and E3-ligases. Deubiquitinases can reverse the reaction (Bhaumik, Smith et al. 2007). Histone H2A and H2B ubiquitination play critical roles in regulating many processes within the nucleus, including transcription initiation and elongation, silencing and DNA repair (Weake and Workman 2008). It is important to note that the link between transcriptional status and histone ubiquitination are context dependent, involving interaction of this modification with other covalent histone marks.

### 2.2.5 Methylation as a key histone PTMs

Among the main characterized histone PTMs, methylation represents the most complex, for several reasons. First of all this modification occurs both at lysine and arginine residues; second, unlike acetylation and phosphorylation, methylation mediates both activating and repressing effects on transcription. Finally, the possible establishment of different methyl states (mono-, me1; di-, me2; tri-, me3) on the same residue as well as the combinatorial occurrence of this alteration with other PTMs, provides an enormous coding potential for biological readouts (for review see Allis et al., 2007).

Several arginine methyltransferases (PRMTs) have been identified (Zhang and Reinberg 2001). These enzymes catalyze the transfer of methyl groups from S-adenosyl-L-methionine to the arginine residue, which can be either mono- or dimethylated, with the latter in symmetric or asymmetric configurations. It is generally accepted that histone arginine methylation is involved in transcriptional activation, as suggested by the role of PRMT1 in the methylation of histone H4R3, a process that facilitates subsequent acetylation of H4 by p300 (Zhang and Reinberg 2001).

Lysine methylation can occur at residues 4, 9, 27, 36 and 79 on histone H3 and at position 20 of histone H4. Almost all of the histone methyltransferases (HMTases) characterized so far contain a SET domain, named after the initial identification in *Drosophila* position effect variegation (PEV) suppressor S<sub>u</sub>(Var)39, the *Polycomb* group protein Enhancer of zeste (Ezh) and the *Trithorax* group protein

Trithorax (Zhang and Reinberg 2001). Histone lysine methylation has been shown to function in both transcriptional stimulation and repression (Martin and Zhang 2005). Gene activity is mainly linked with methylation at K4, K36 and K79 of histone H3. Genomewide profiling of histone marks by ChIP-chip or ChIP-seq techniques in the human genome indicates that actively transcribed genes are marked with high level of H3K36me3, H3K27me1, H3K9me1, H3K79me1/me2/me3, H4K20me1 and H2BK5me1 (Barski, Cuddapah et al. 2007; Lee and Mahadevan 2009). On the other hand, H3K9me2/me3, H3K27me3 and H4K20me3 are strongly associated with transcriptional repression and heterochromatin (Lee and Mahadevan 2009). Silencing can be detected both at genic and non-genic regions, which are characterized by distinct types of repressive histone modifications (Dambacher, Hahn et al. 2010). H3K27me3 is perhaps the most prominent modification linked to gene repression. This histone mark is placed by the two highly related enzymes Ezh1 and Ezh2, which associate in a mutually exclusive manner with Eed, Suz12 and RbAp46/48 to form polycomb repressive complex 2 (PRC2). The presence of the H3K27me3 mark recruits then a second type of polycomb repressive complex, namely PRC1, which consists of the Ring1a/b, Bmi1, Ph, Cbx subunits. PRC1, in turn, establishes H2A ubiquitylation, a gene-silencing related modification (Martin and Zhang 2005; Dambacher, Hahn et al. 2010). An interesting mechanism involving H3K27me3 concerns embryonic stem (ES) cell, in which this repressive mark coexists in an overlapping manner with H3K4me3 (Azua, Perry et al. 2006). Such regions are called “bivalent domains” and are predominantly present at developmental regulatory genes. It is believed that the concomitant presence of active and repressive marks primes developmentally regulated genes for activation or repression during ES cells differentiation: genes that become active or repressed, in accordance to their transcriptional activities in different cell type, acquire either H3K4me3 or H3K27me3 respectively. This regulatory mechanism suggests a transient character of the bivalent configuration (Azua, Perry et al. 2006).

Large regions of the mammalian genome consist of non-coding DNA sequences, including major satellite and telomeric repeats, mobile elements and interspersed repeats. These regions are marked by H3K9me3 and H4K20me3 (Dambacher, Hahn et al. 2010). H3K9me3 is established by Suv39h1 and Suv39h2 enzymes (Rea, Eisenhaber et al. 2000), while Suv4-20h1 and Suv4-20h2 mediate di- and tri-methylation of H4K20 (Schotta, Lachner et al. 2004). The two heterochromatic signatures are placed at repetitive genomic regions (pericentromeric and telomeric heterochromatin) in a sequential coordinated fashion. The prevalent model predicts

that Setdb1 in complex with CAF1 and HP1 alpha induces H3K9me1, which is converted to H3K9me3. This later modification constitutes a binding platform for HP1 proteins, which in turn recruit Suv4-20h enzymes to establish H4K20me3. Although not completely characterized, interactions with other proteins, such as members of the retinoblastoma (Rb) protein family, as well as DNA methyltransferases, could contribute to the establishment of these modifications (Schotta, Lachner et al. 2004; Dambacher, Hahn et al. 2010). A similar mechanism underlines the formation of heterochromatin at telomeric ends.

### 2.2.6 The “histone code” hypothesis

The large number of PTMs occurring mainly at the histone amino-terminal tails suggests that specific modifications or combinations of different modifications constitute a code that defines actual or potential transcriptional states (Strahl and Allis 2000). A further level of complexity is defined by the fact that these modifications regulate one another, providing regulatory cross-talks (Latham and Dent 2007). A first class of cross-talks is the so-called *in situ* cross-talk, concerning all those residues that can undergo several different forms of PTMs: each modification inhibits subsequent alteration of the same residues. Arginine and lysine residues, for example, are subjected to this kind of cross-talk. Lysine methylation blocks subsequent acetylation, and vice versa, in a process that reflects either possible opposite roles of the different modifications (H3K9ac *versus* H3K9me) or different steps in the same process (H3K36ac presence at promoter regions of transcribed genes and H3K36me occurring within coding regions). The cross-regulation of histone modifications also occurs between modifications of different residues on the same histone tail (*in cis*) or between histones (*in trans*). All these cross-talks define a complex network of interactions that differentially regulate chromatin activity in distinct biological settings (Strahl and Allis 2000). It is important to consider that the histone code represents only one layer of epigenetic information, which involves also DNA methylation, interactions with structural and catalytic proteins and RNAs. Together these layers ensure functionally stable chromatin states, defining a broader and more complex epigenetic code (Turner 2002; Latham and Dent 2007).

### 2.2.7 H4K20 methylation states and Suv4-20h histone methyltransferases

In mammals, only one of the 5 lysines present in the N-terminal tail of histone H4 is methylated, i.e. K20 (Yang and Mizzen 2009). Ten years ago Nishioka and colleagues identified Pr-Set7 (Set8) as a specific H4K20 methyltransferase, which catalyzes the H4K20me1 state (Nishioka, Rice et al. 2002). Mutations in *Drosophila* Pr-Set7 are lethal, indicating an essential role of this enzyme in development and viability. Subsequent studies identified then Suv4-20h1 and Suv4-20h2 as two SET domain HMTases responsible for di- and trimethylation of H4K20 (Schotta, Lachner et al. 2004; (Schotta, Sengupta et al. 2008). As mentioned before, these two enzymes are thought to help establishing pericentric heterochromatin in association with Suv39h HMTases (Schotta, Lachner et al. 2004). A detailed analysis of Suv4-20h mutant mice indicated essential functions of Suv4-20h1 during embryonic and postnatal development. Suv4-20h1<sup>-/-</sup> pups are born at sub-Mendelian ratios, and die perinatally a few hours after birth (Schotta, Sengupta et al. 2008). These features are not present in Suv4-20h2<sup>-/-</sup> mice, but characterized Suv4-20h DKO (double knockout) mice. Together these aspects underline that Suv4-20h1 HMTase exerts an essential function during development.

Mass spectrometry profiles of the H4K20 methylation patterns showed that in cells of diverse species origin, H4K20me2 exceeds the global level of H4K20me1, while H4K20me3 is present at the lowest abundance (Yang and Mizzen 2009). Histone H4K20 methylation appears to be cell-cycle regulated. The majority of newly synthesized H4 that is deposited in chromatin during S phase, is monomethylated by Pr-Set7 at the G2/M transition. Suv4-20h HMTases then convert H4K20me1 mainly in H4K20me2 (whose levels remain high at all the cell cycle stages), while only a small fraction is trimethylated (peak levels of H4K20me3 are detected in early G1 phase) (Yang and Mizzen 2009; Beck, Oda et al. 2012).

From a functional point of view it is important to know, where the K20 methylated histone H4 proteins reside in the genome. Developing *Drosophila* third instar larvae showed H4K20me3 enrichment, together with H3K9me3 and H3K27me3, in the Ultrabithorax (*Ubx*) gene region, when it was repressed (Papp and Muller 2006). On the other hand, histone methylation profiling in human genome via ChIP sequencing failed to detect H4K20me3 enrichment at the corresponding human locus (Barski, Cuddapah et al. 2007). Moreover Mikkelsen et al. showed that H4K20me3 colocalized with H3K9me3 at telomeric, satellite and long terminal repeats sequences (Mikkelsen, Ku et al. 2007). These evidences suggest a

possible involvement of H4K20me3 in the structure and function of constitutive heterochromatin and in the maintenance of genome stability (Schotta, Sengupta et al. 2008).

Similarly, H4K20me2 does not seem to play a direct role in transcriptional regulation. Its abundance argues against the possibility that H4K20me2 is selectively localized to a significant degree (Yang and Mizzen 2009). Interestingly, in *Schizosaccharomyces pombe* a single methyltransferase, Set9, mediates mono-, di-, and trimethylation of H4K20. Loss of Set9 resulted in hypersensitivity to DNA damage (Sanders, Portoso et al. 2004), in a process where Crb2 (or its human homolog p53 binding protein 1 (53BP1)) is recruited to the site of DNA damage and binds H4K20me2, via its tandem tudor domains. The recruitment of 53BP1 to damage-associated foci is reduced in HeLa cells depleted of Suv4-20h1/h2 (Yang and Mizzen 2009).

Monomethylation of H4K20 has been associated with several aspects of DNA metabolism. Immunofluorescence and chromatin immunoprecipitation experiments showed that H4K20me1, together with H3K27me3, are associated with Xist, suggesting that the enrichment of these two marks represent early events in the initiation of X chromosome inactivation (Kohlmaier, Savarese et al. 2004). A more direct evidence of the repressive role of H4K20me1 has been described studying the human lethal 3 malignant brain tumor 1 (L3MBTL1) protein, which preferentially binds to H4K20me1, facilitating chromatin compaction (Trojer, Li et al. 2007). Similarly, characterizing the role of the histone demethylase PHF8, Liu et al. have suggested a repressive role of H4K20 monomethylation (Liu, Tanasa et al. 2010). On the other hand, results from genome-wide ChIP sequencing suggest that H4K20me1 levels are elevated in the gene body of many active genes in human lymphocytes (Barski, Cuddapah et al. 2007). Consistent to this role, a recent study by Li et al. identifies a new function for H4K20me1 in transcriptional activation (Li, Nie et al. 2011). Interestingly, the authors demonstrate that under Wnt stimulation, Pr-Set7 is recruited into the  $\beta$ -catenin/TCF4 (T-cell factor 4) complex, possibly positively regulating the transcription of Wnt-activated genes (Li, Nie et al. 2011).

In summary, the different methylation states and the variety of roles linked to the distinct H4K20 modifications, indicate a highly dynamic function of these modifications in several processes including gene repression and activation, chromatin condensation and DNA damage mechanisms. Finally, although not described at present, the interplay of the multiple forms of H4K20 methylation with

other PTMs might provide an additional complexity levels in regulating chromatin processes.

### 2.3 Linking epigenetics to development

Development, defined as the series of differentiation steps that progressively restrict the totipotent zygote into committed somatic cells, requires an accurate interplay between genetic and epigenetic mechanisms. Waddington's epigenetic landscape (for review see (Slack 2002) describes the divergent developmental paths that a totipotent cell (depicted as a marble at the top of a hill entering a series of furrows) might take as it restricts its fate to a specific cell type. Modern interpretations hypothesize that the cell's trajectory through the valley reflects the pattern of epigenetic states that characterize each differentiation stage (Mohammad and Baylin 2010). The epigenetic dynamics of stem cells and cell lineage commitment have been best studied in mice, where different stem cells lines have been established and derived from the embryo. It is important to note that the epigenetic molecular mechanisms achieved using cell cultures should be treated with caution, since it is unclear to what extent they really reflect developmental properties of whether the culture conditions affect embryonic stem (ES) cells properties (Marks, Kalkan et al. 2012).

The formation of the zygote, and the very early embryonic divisions are characterized by an extensive remodelling of the paternal genome aimed at acquiring an appropriate epigenetic state for further embryonic development (Surani, Hayashi et al. 2007). After fertilization, the sperm nucleus replaces the highly basic non-histone proteins protamines with histones, and undergoes a paternal specific active demethylation of DNA (Hemberger, Dean et al. 2009). Similarly, a genome-wide reprogramming of histones PTMs occurs during this period (Surani, Hayashi et al. 2007). Subsequent rapid cell divisions lead the embryo to the blastocyst stage at which the inner cell mass (ICM) is surrounded by the trophectoderm (TE). In late blasocyst stage, the ICM separates into epiblast or primitive ectoderm (from which embryonic stem – ES – cells are derived) and hypoblast or primitive endoderm (from which extraembryonic endoderm stem –XEN- cells are derived) (Hemberger, Dean et al. 2009). Besides being specifically characterized by the expression of key transcription factors (Oct4, Nanog, Sox2 in the ES cells; Cdx2, Eomesodermin in the TE cells, and Gata4-6, Foxa2 in the XEN cells), the different stem cell lines acquire

distinct epigenetic signatures both at the level of histone modifications and DNA methylation (Surani, Hayashi et al. 2007; Hemberger, Dean et al. 2009; (Rugg-Gunn, Cox et al. 2010; Santos, Pereira et al. 2010). Chromatin immunoprecipitation studies have revealed an unexpected feature of ES cells, not shared by TE and XEN cells: the so called “bivalent domains”. This term describes the presence of genes repressed in ES cells but required for later development, which are marked by both the active H3K4me3 and the inactive H3K27me3 modifications (Azuara, Perry et al. 2006; (Rugg-Gunn, Cox et al. 2010; Santos, Pereira et al. 2010). Upon development the bivalent modification state is resolved into mutual exclusive H3K4me3 or H3K27me3 domains, according to the transcriptional gene activities in different cell types. This event appears to be controlled with the implantation of the blastocyst, a key event during development. Following implantation, epiblast cells start responding to signals from the extraembryonic tissues, and transcriptionally differ from preimplantation primitive ectoderm in the expression of a series of genes, most notably Nanog, whose expression is rapidly downregulated (Surani, Hayashi et al. 2007). Epigenetic mechanisms now acquire a pivotal, active role in development: while preimplantation development relies both on erasure and maintenance of epigenetic alterations, postimplantation development requires the establishment of epigenetic modifications in patterns, which are compatible with the ongoing cellular diversification (Surani, Hayashi et al. 2007). In general the epigenetic contribution to the further development is represented mainly by repressive mechanisms involving histone methyltransferases, transcription repressors, miRNA, and DNA methylation, creating an “epigenetic environment” which, in cooperation with transcription factors networks, creates a cellular memory and thereby a stable cell fate (Hemberger, Dean et al. 2009).

In this regards, model organisms like *Xenopus* and zebrafish have contributed new insights from *in vivo* analysis of embryos, rather than derived embryonic cell lines (Akkers, van Heeringen et al. 2009; Vastenhouw, Zhang et al. 2010; Schneider, Arteaga-Salas et al. 2011). Vastenhouw and colleagues showed that genome activation is coupled to the acquisition of specific H3 trimethylated marks in *Danio rerio*, suggesting that these modifications exert a regulatory function only from and during the maternal-to-zygote transition. Moreover, chromatin immunoprecipitation (ChIP) experiments confirmed the bivalent pattern detected at developmental regulatory genes in murine embryos (Vastenhouw, Zhang et al. 2010). Interestingly, the authors found that many genes are monovalently marked by H3K4me3 but not associated with RNA pol II and thereby inactive, suggesting a scenario in which

H3K4me3 domains poise genes for activation, creating a platform for transcriptional machinery (Vastenhouw, Zhang et al. 2010).

Genome-wide RNA and ChIP sequencing (RNA-Seq and ChIP-Seq respectively) technologies were applied to investigate histone modifications profiles during *Xenopus tropicalis* development (Akkers, van Heeringen et al. 2009). Unlike zebrafish, frog embryos reveal a hierarchy in epigenetic regulation, with specific spatial and temporal aspects. H3K4me3 precedes or coincides with transcriptional activation at MBT; only after the deposition of this mark, H3K27me3 becomes deposited on many transcription factor genes, repressing or spatially restricting gene expression (Akkers, van Heeringen et al. 2009). The epigenetic dynamics of *X.tropicalis* implies that bivalent chromatin domains are largely absent from the embryo, and may quickly resolve in monovalent domains, marked either by H3K4me3 or H3K27me3 only, according to the transcriptional states of genes in different cells and tissues of the embryo. The difference between *Xenopus* and zebrafish may indicate a species-specific difference in gene regulation, although different experimental approaches might have contributed to the contradictory results (Vastenhouw, Zhang et al. 2010).

In an antibody-independent approach, Schneider and colleagues quantified 59 modification states on the core histones H3 and H4 from blastula to tadpole stages in *Xenopus laevis* (Schneider, Arteaga-Salas et al. 2011). The mass spectrometry based histone PTM profiles revealed a stage-specific acquisition of epigenetic signatures during development in accordance to the shift from pluripotency, via germ layer precursors, to committed and finally differentiated cell states (Schneider, Arteaga-Salas et al. 2011). At blastula stage, where the majority of embryonic cells are uncommitted and capable to differentiate in any derivatives of the three germ layers, the H3K4me3 abundance in frog embryos is comparable to that of ES cells; however, H3K27me3 is basically absent from the embryo at this time and several hundreds fold lower than in ES cells. This result confirms the observations of Akkers and colleagues and strengthens the idea that bivalent domains play a much smaller role, if any, in frog embryos. Overall, the analysis highlighted a general decrease in the abundance of active histone PTMs, coupled to a concomitant increase of repressive histone modifications. Although during embryonic development H3K9me3 stays constant at a level lower than 1%, H3K27me3 and H4K20me3 progressively accumulate from blastula to tadpole stage. This result suggests that tri-methylation of K20 on histone H4 behaves as a regulatory modification. The epigenetic state of *Xenopus* embryonic cells changes from an

“active” and “derepressed” conformation at blastula, to a transcriptionally repressed state at tadpole stage, undergoing a general maturation upon differentiation (Schneider, Arteaga-Salas et al. 2011).

*In toto*, the increasing evidences from diverse biological systems highlight the close connection of transcription factors networks and epigenetic processes, which enforces cell fate specification during development. The dissection of the regulatory mechanisms that govern the nature of the epigenomes (i.e. how they are established and orchestrated upon differentiation) represents a fundamental step for the understanding of cell behaviour, development and diseases.

## 2.4 Objectives

Early embryonic development relies on a tightly orchestrated series of events, leading the single-cell zygote to a mature organisms. All these events are characterized by an accurate interplay between transcription factor networks and epigenetics mechanisms. A recent mass spectrometric study in *Xenopus* revealed that post-translational modifications (PTMs) on core histone H3 and H4 are exchanged from transcriptionally active to transcriptionally repressive marks during development (Schneider, Arteaga-Salas et al. 2011). Among these PTMs, bulk H4K20me3 levels considerably increase from blastula stage on, implying a peculiar function of this modification in cell fate establishment. Despite the fact that repressive histone methylation represents a well characterized epigenetic mechanism, little is known about the developmental function of H4K20me2 and H4K20me3.

The main goal of this Ph.D. thesis was to characterize the function of *Xenopus* Suv4-20h histone methyltransferases (HMTases) during development. To this end Gain- and Loss-of-Function approaches were applied. The former relies on microinjection of mRNAs to transiently upregulate the protein levels; the latter employs translation-blocking antisense morpholino oligonucleotides to knock-down endogenous protein levels. Several phenotypes were scored and analysed on the morphological levels and by RNA *in situ* hybridization. This approach, together with other methods (i.e. Immunocytochemistry, qRT-PCR, ChIP, microarray profiling) allowed a comprehensive functional characterization of *Xenopus* Suv4-20h HMTases.

### 3 MATERIALS AND METHODS

#### 3.1 Laboratory Equipment

The following laboratory equipment was used. Companies' name is indicated in brackets.

**Bioruptor™:** Bioruptor Next Gen (Diagenode).

**Camera:** Leica DFC 310FX (Leica).

**Centrifuges:** Eppendorf centrifuge 5417C (Eppendorf); Micro 22R (Hettich Zentrifugen); Sigma 3-18 (Sigma Laborzentrifugen); PicoFuge (Stratagene).

**Developer:** Curix-60 (Agfa).

**Gel documentation System:** G:BOX (Syngene).

**Glass needles:** Glass 1BBL W/FIL 1.0 mm (World Precision Instrument).

**Homogenizer:** Glas-Glas Homogenizer 5 ml (Braun, Melsungen).

**Infrared Imaging System:** Li-Cor (Odyssey).

**Incubators:** Heraeus (GS); Standard-430 (GS).

**MALDI-TOF:** Voyager-DE™STR, BioSpectrometry™ Workstation (Applied Biosystems).

**Microneedle Puller P-87** (Sutter Instrument).

**Micromanipulator** Mm-33 (Science Products); Oxford micromanipulator (Micro Instruments, Oxford, UK).

**Microscopes:** Stereomicroscope Stemi SV11 (Zeiss); Stereo-fluorescence System M205FA (Leica); Optical microscope DM (Leica).

**Pneumatic Micro-Injector** Pli-100 (Digitimer Ltd.).

**Software:** Illustrator CS5 (Adobe); Photoshop CS5 (Adobe); MacVector 11.2 (Oxford Molecular Group); Office 2008 for Mac (Microsoft); Endnote X4 (Thomson); Leica Application Suite V3 3.0 (Leica); Data explorer for MALDI Analysis (Applied

Biosystems); Light Cycler 480 Software Release 1.5.0 SP1 (Roche); Odyssey Application Software Version 3.0 (Odyssey); Gene Snap Image Acquisition Software (Syngene).

**Spectrophotometer:** Nanodrop ND-1000 (PeqLab).

**Thermocycler:** PCR System 2007 (Applied Biosystems); PCR Express (Hybaid); Light Cycler 480 System (Roche).

**Thermo shakers:** Multitron (Infors HT); Thermo Shaker TS-100 (PeqLab).

**Water bath:** Minitherm 2 (Dinkelberg).

**Vibratome:** Vibratome 1000 (Technical Products International, INC.).

## 3.2 Reagents

The subsequent fine- and bio-chemicals were ordered from Fluka, Merck, Sigma or USB.

Agar (Difco); Agarose (Gibco/BRL); Ampicillin, Streptomycin (Difco); Chicken serum, Lamb serum (Gibco/BRL); Human choriongonadotropin Gonasi 5000 (IBSA Farmaceutici Italia); Levamisol (Vectro Laboratories); Glycogen (Fermentas); Triazol® Reagent (Invitrogen).

### 3.2.1 Enzymes and Proteins

The following fine reagents and enzymes were ordered from the companies indicated in brackets: Alkaline phosphatase (Roche); BSA fraction V (Roth); Leupeptin, Pepstatin (Sigma); Protease inhibitor cocktail tablets (Roche); Restriction endonuclease with 10X restriction buffer system (New England Bio Labs, Roche, Fermentas); RNaseA (Sigma); RNasin (Promega); T3, T7, SP6 ploymerases with 5X incubation buffer (Promega); Proteinase K (Sigma); RNase free DNase I (Promega); PeqGOLD Protein marker V (PeqLab); Taq DNA polymerase with 10X PCR buffer (NEB).

### 3.2.2 Kits

QIAquick® Gel extraction kit (Qiagen; DNA extraction from agarose gels); QIAprep® Spin miniprep Kit (Qiagen; DNA plasmid miniprep); QIAquick® PCR purification kit (Qiagen; purification of PCR fragments/products); RNeasy® mini kit (Qiagen; RNA cleaning); Expand High fidelity PCR System (Roche; high fidelity PCR amplification and mutagenesis PCR); F-470L DyNAmo™ cDNA Synthesis Kit (Finnzymes).

## 3.3 Antibodies

### 3.3.1 Primary Antibodies

<b>Antibody</b>	<b>Dilution</b>	<b>Company/Reference</b>
H4K20me1	WB 1:6000 Histological sample 1:5000	Schotta et al, 2008
H4K20me2	WB 1:1000 Histological sample 1:2000	Schotta et al, 2008
H4K20me3	WB 1:500 Histological sample 1:5000	Schotta et al, 2008
Pan-H3	WB 1:25000 Histological sample 1:2000	Abcam
H3K9me3	WB 1:100	IMP Vienna
H3K27me3	WB 1:3000	Diagenode
c-Myc 9E10	WB 1:50	Evan et al, 1985
H3S10p	ICC 1:300	Upstate Biotechnology
Active Caspase-3	ICC 1:500	Promega
Acetylated alpha tubulin	ICC 1:200	Sigma
xbeta-catenin PGDS 7D12	ICC 1:100	Mansperger's thesis 2007
Chicken myosin heavy chain MF20	ICC 1:100	Bader et al, 1982

WB: western blot; IHC: immunohistochemistry; ICC: immunocytochemistry.

\* Developmental Studies Hybridoma Bank.

### 3.3.2 Secondary Antibodies

#### 3.3.2.1 Immunocytochemistry (ICC)

Sheep anti-mouse IgG conjugated with alkaline phosphatase (1:1000, Chemicon); anti-rabbit IgG (Fc) conjugated with alkaline phosphatase (1:1000, Promega).

#### 3.3.2.2 Immunofluorescence (IF)

Alexa Fluor® 488 goat anti-rat IgG (1:500, Molecular Probes); donkey anti-mouse IgG, Cy2 conjugated (1:200, Jackson Immuno Research).

#### 3.3.2.3 In Situ hybridization

Sheep anti-Digoxigenin Fab fragment conjugated with alkaline phosphatase (1:2000, Roche).

#### 3.3.2.4 Western Blot Analysis (WB)

Infrared (IR) 800 goat anti-rabbit (1:5000, Li-Cor Odyssey); Horseradish peroxidase conjugated rabbit anti-mouse (1:3000, Jackson Immunoresearch).

## 3.4 Nucleic acids

### 3.4.1 Size standard

1Kb ladder: GeneRuler™ 1Kb DNA ladder (Fermentas). The DNA ladder yields the following 14 discrete fragments (in base pairs): 10000, 8000, 6000, 5000, 4000, 3500, 3000, 2500, 2000, 1500, 1000, 750, 500, 250.

100bp ladder: GeneRuler™ 100bp DNA ladder plus (Fermentas). The DNA ladder yields the following 14 discrete fragments (in base pairs): 3000, 2000, 1500, 1200, 1000, 900, 800, 700, 600, 500, 400, 300, 200, 100.

### 3.4.2 Oligonucleotides

Oligonucleotides were designed with the program Primer3 (<http://frodo.wi.mit.edu/primer3/>), and ordered from Metabion

(<http://www.metabion.com/>). All oligonucleotides were dissolved in DEPC-H<sub>2</sub>O at a final concentration of 100pmol/μl. and stored at -20°C.

#### 3.4.2.1 Oligonucleotides for endpoint RT-PCR

for= forward/sense; rev= reverse/antisense strand

Random hexamer
RR13: 5'-NNNNNN-3' (N=A, T, C or G)

Xenopus:

<i>odc</i> for	5'-acaagaaacccaaaccaga-3'
<i>odc</i> rev	5'-caaacaacatccagctccaa-3'
<i>suv4-20h1</i> for	5'-gttgcatgaagtgggtg-3'
<i>suv4-20h1</i> rev	5'-gcagacaatcggttccatt-3'
<i>suv4-20h2</i> for	5'-ccggatgttctccagaga-3'
<i>suv4-20h2</i> rev	5'-ccaccaggagtcaatctttc-3'

#### 3.4.2.2 Oligonucleotides for qRT-PCR

Xenopus:

<i>geminin</i> for	5'-tgaagtgctgtgatccag-3'
<i>geminin</i> rev	5'-tcttcgttctctgcaacct-3'
<i>h4</i> for	5'-gaccgcggtcacctacacc-3'
<i>h4</i> rev	5'-ctggcgcttcagaacataca-3'
<i>irx1</i> for	5'-ccataaccaccaccacctc-3'
<i>irx1</i> rev	5'-tgtctgagtgtgggactg-3'
<i>myoD</i> for	5'-aggaaggccgccaactatga-3'
<i>myoD</i> rev	5'-gttgcgaggatctccactt-3'
<i>ngnr 1a</i> for	5'-acctgactctgcgcttgat-3'
<i>ngnr 1a</i> rev	5'-gcgcaaggtctcatcttg-3'
<i>nrp1</i> for	5'-gccatgctgcaaaactctt-3'
<i>nrp1</i> rev	5'-cccacctatagccctccat-3'
<i>n-tubulin</i> for	5'-tgctgatctacgcaaactgg-3'
<i>n-tubulin</i> rev	5'-ctgtcagggctcggtattgt-3'
<i>oct-25</i> for	5'-caggtccaggggtgcag-3'
<i>oct-25</i> rev	5'-gtccttgagggtcaggaag-3'
<i>oct-91</i> for	5'-ggacaacagtcgctgtagca-3'
<i>oct-91</i> rev	5'-cactgctcagccatcacta-3'
<i>sox2</i> for	5'-tgcgtccaacaaccagaata-3'
<i>sox2</i> rev	5'-agttgtcatctggggttc-3'

<i>sox3</i> for	5'-atgaacggctggactaatgg-3'
<i>sox3</i> rev	5'-tacctgtgctggatctgctg-3'
<i>sox11</i> for	5'-cgagaaaatcccctcatca-3'
<i>sox11</i> rev	5'-aggatccactttgggcttttc-3'
<i>sox17 alpha</i> for	5'-tactgcaactaccccagtg-3'
<i>sox17 alpha</i> rev	5'-agagcccgtccttctcaata-3'
<i>xK81</i> for	5'-ccgttggtgtgaacaagt-3'
<i>xK81</i> rev	5'-gcagctcaattccaagctc-3'
<i>zic1</i> for	5'-acagatgaggctgggcttc-3'
<i>zic1</i> rev	5'-cagttggctggaggcataat-3'
<i>zic2</i> for	5'-tcgtaggacggagcaatac-3'
<i>zic2</i> rev	5'-ttcataggggagtactggttg-3'
<i>zic3</i> for	5'-ggtggtgcagcctttaactc-3'
<i>zic3</i> rev	5'-tggcaaaaagtccatgttga-3'

### 3.4.2.3 Oligonucleotides for ChIP-PCR

Xenopus:

<i>gapdh</i> promoter for	5'-ctgtgctactggctttcc-3'
<i>gapdh</i> promoter rev	5'-taagcacaggcagcccttac-3'
<i>oct-25</i> 5'-UTR for	5'-ctccgacttattgggtgga-3'
<i>oct-25</i> 5'-UTR rev	5'-tctaacctggatgggaggtg-3'
<i>oct-25</i> exon 1 for	5'-agagtcccagaacccaaat-3'
<i>oct-25</i> exon 1 rev	5'-aagggctaccagtccatgtg-3'
<i>oct-25</i> intron 1 for	5'-aaagctaccggctgattgg-3'
<i>oct-25</i> intron 1 rev	5'-agcgtgcaggattaggtcat-3'
<i>oct-25</i> exon 4 for	5'-aggggacgctggaaagtac-3'
<i>oct-25</i> exon 4 rev	5'-ccttggctattgcaccatc-3'
<i>msat</i> 3 for	5'-ccaccgttgcgtagacc-3'
<i>msat</i> 3 rev	5'-tgctggggcaattaactg-3'
<i>thibz</i> exon 1 for	5'-gctgtcggaactctcactcc-3'
<i>thibz</i> exon 1 rev	5'-gcgtctcttgcaccagtagc-3'
<i>thra</i> intron 2 for	5'-attgcttcatgccttgct-3'
<i>thra</i> intron 2 rev	5'-tatgaaacggagcgacacaa-3'

#### 3.4.2.4 Oligonucleotides for PCR-based mutagenesis

Mouse:

<i>suvs4-20h1</i> Y299A for	5'-cctggagaagaaattctgttacgcaggagatggctttttggagaaa-3'
<i>suvs4-20h1</i> Y299A rev	5'-tttctcaaaaaagccatctcctgcgtaacaagaaattctctccagg-3'
<i>suvs4-20h2</i> Y217A for	5'-ggatgaagtgactgtctcgcagggtgaggcttcttcgg-3'
<i>suvs4-20h2</i> Y217A rev	5'-ccgaagaagccctcacctgcgaagcaagtcactcatcc-3'
<i>suvs4-20h1</i> N264A for	5'-ggctcggctctgctgcatttatagcccatgattgcagacctaactg-3'
<i>suvs4-20h1</i> N264A rev	5'-cagttaggtctgcaatcatgggctataaatgcagcaggaccgagcc-3'
<i>suvs4-20h2</i> N182A for	5'-ggcccagctgccttcatgcccattgactgcaaacc-3'
<i>suvs4-20h2</i> N182A rev	5'-gggttgcagtcattggcgatgaaggcagctgggcc-3'

#### 3.4.2.5 Oligonucleotides for cloning

Xenopus <i>suvs4-20h1</i> for	5'-ggggacaagttgtacaaaaagcaggcttaactatgaagtggtggcgcaat-3'
Xenopus <i>suvs4-20h1</i> rev	5'-ggggaccactttgtacaagaaagctgggtctgattgagtcttaaggat-3'
Xenopus <i>suvs4-20h2</i> for	5'-ggggacaagttgtacaaaaagcaggcttaactatgggttcaaatcggttga-3'
Xenopus <i>suvs4-20h2</i> rev	5'-ggggaccactttgtacaagaaagctgggtcactggttcttactcagac-3'
Mouse <i>suvs4-20h1</i> for	5'-ggggacaagttgtacaaaaagcaggctacaacatggtggtgaatggcagga-3'
Mouse <i>suvs4-20h1</i> rev	5'-ggggaccactttgtacaagaaagctgggtctgcttgcagcttagaga-3'
Mouse <i>suvs4-20h2</i> for	5'-ggggacaagttgtacaaaaagcaggcttaactatggggcctgatcagatga-3'
Mouse <i>suvs4-20h2</i> rev	5'-ggggaccactttgtacaagaaagctgggtctggctcaccactattgatg-3'

#### 3.4.2.6 Morpholino oligonucleotides

xl, xt <i>suvs4-20h1</i> morpholino	5'-ggattcgccaaccactt <b><u>cat</u></b> gccca-3'
xl <i>suvs4-20h2</i> morpholino	5'-ttgccgtcaaccgattgaacc <b><u>cat</u></b> -3'
xt <i>suvs4-20h2</i> morpholino	5'-ccgtcaagcgattgaacc <b><u>cat</u></b> agt-3'
xl <i>oct-25</i> morpholino	5'-ttgggaagggtgttggtgt <b><u>cat</u></b> -3'
Control morpholino	5'-cctcttacctcagttacaatttata-3'

Underlined and in bold: sequence complementary to the AUG start codon.

Morpholino oligonucleotides were ordered from Gene Tools (<http://www.gene-tools.com/>). "Xl" and "xt" refer to *Xenopus laevis* and *Xenopus tropicalis*. Morpholino oligonucleotides were dissolved in milliQ water to a final concentration of 3mM, aliquoted in 5µl aliquots and stored at -20°C. xSuv4-20h morpholinos were injected from 20 to 40ng/embryo, while standard morpholino was injected from 40 to 80ng/embryo. In cases in which single blastomere at 32-cell stage were injected, the

morpholinos doses were 5ng for Oct-25 morpholino and 1ng for Suv4-20h1 and Suv4-20h2 morpholinos.

### 3.4.3 Plasmids

#### 3.4.3.1 Plasmids used for transfection

Plasmid
pCMV-eGFP xenopus <i>suv4-20h1a</i> wt
pCMV-eGFP xenopus <i>suv4-20h2a</i> wt
pCMV-eGFP mouse <i>suv4-20h1</i> wt
pCMV-eGFP mouse <i>suv4-20h2</i> wt
pCMV-eGFP mouse <i>suv4-20h1</i> N264A, Y299A mutant
pCMV-eGFP mouse <i>suv4-20h2</i> N182A, Y217A mutant

#### 3.4.3.2 Plasmids used for in vitro transcription

Plasmid	Linearization	Polymerase
pCMV-SPORT6 xenopus <i>suv4-20h1a</i> wt	HpaI	SP6
pCMV-SPORT6 xenopus <i>suv4-20h2a</i> wt	HpaI	SP6
pCMV-myc mouse <i>suv4-20h1</i> wt	PvuI	SP6
pCMV-myc mouse <i>suv4-20h2</i> wt	PvuI	SP6
pCMV-myc mouse <i>suv4-20h1</i> N264A, Y299A mutant	PvuI	SP6
pCMV-myc mouse <i>suv4-20h1</i> N182A, Y217A mutant	PvuI	SP6
pCS2 <sup>+</sup> <i>noggin</i>	NotI	T7
pCS2 <sup>+</sup> <i>bcl-2</i>	NotI	SP6
pCS2 <sup>+</sup> myc-VP16- <i>oct-25</i>	NotI	SP6
pCS2 <sup>+</sup> myc-EnR- <i>oct-25</i>	ScaI	SP6

#### 3.4.3.3 cDNA used for dig-labelled RNA in situ hybridization probes

cDNA Name	Linearization	Polymerase
<i>chordin</i>	EcoRI	T7
<i>delta-like 1</i>	XhoI	T7
<i>endodermin</i>	EcoRI	T7
<i>foxD5</i>	XbaI	T7
<i>geminin</i>	EcoRI	T3
<i>goosecoid</i>	EcoRI	T7
<i>irx1</i>	EcoRI	T7

<i>krox20</i>	EcoRI	T7
<i>myoD</i>	EcoRI	T7
<i>n-tubulin</i>	BamHI	T3
<i>ncam</i>	Asp718	SP6
<i>ngnr 1a</i>	BamHI	T3
<i>nodal3</i>	EcoRI	T7
<i>nrp1</i>	BamHI	T3
<i>oct-25</i>	EcoRI	T7
<i>oct-60</i>	BamHI	T7
<i>oct-91</i>	RsaI	T7
<i>otx2</i>	EcoRI	T3
<i>pax-6</i>	NotI	T7
<i>rx-1</i>	BamHI	T7
<i>sox2</i>	EcoRI	T7
<i>sox3</i>	EcoRI	T7
<i>sox11</i>	Sall	T3
<i>sox17 alpha</i>	SmaI	T7
<i>suv4-20h1a</i> (*)	EcoRI	T3
<i>suv4-20h2a</i> (*)	EcoRI	T3
<i>t</i>	HindIII	T7
<i>vegT</i>	HindIII	T3
<i>xK81</i>	EcoRI	SP6
<i>zic1</i>	HindIII	T7
<i>zic2</i>	EcoRI	T7
<i>zic3</i>	BamHI	T3

(\*) For xSuv4-20h1 and h2, fragments of approx. 1675bp and 1600bp, respectively, were subcloned into pBlueScript KS vector via XhoI/EcoRI. These fragments contain the 3'-UTR of the cDNAs

### 3.5 Molecular methods

For each method presented in the Material and Methods section, the solutions and the reagents have been listed *in toto*. This leads to redundant listing of the most common reagents, but it ensures a better overview of all the materials needed for a specific method.

#### 3.5.1 Solutions

**Alkaline Phosphatase (AP) buffer:** 100mM trichlorethane Tris/HCl pH 9.5; 100mM NaCl; 50mM MgCl<sub>2</sub>; 0.1% Tween 20.

**Bleaching solution:** 1% H<sub>2</sub>O<sub>2</sub>; 5% Formamide; 0.5X SSC.

**DEPC-H<sub>2</sub>O:** milliQ water with 0.1% Diethylpyrocarbonate (DEPC), stirred at Room Temperature (RT) overnight (o/n) and autoclaved afterwards.

**DIG NTPs mixture (10mM):** 10mM CTP, GTP, ATP; 6.5mM UTP; 3.5mM Dig-11-UTP (Roche).

**Hybridization Solution:** 5X SSC; 50% formamide; 1% Boeheringer blocking solution; 0.1% Torula RNA; 0.01% Heparin; 0.1% Tween-20; 0.1% CHAPS; 5mM EDTA.

**Lamb Serum:** heat-inactivated lamb serum (30 min at 56°C), stored at -20°C.

**Maleic Acid Buffer (MAB):** 100mM maleic acid; 150mM NaCl, pH 7.5.

**MEMFA:** 0.1M 3-(N-Morpholino)-propanesulfonic acid (MOPS); 2mM EGTA; 1mM MgSO<sub>4</sub>; 3.7% formaldehyde pH 7.4.

**NBT/BCIP solution:** Nitro blue tetrazolium (NBT) 75mg/ml in 70% dimethylformamide; 5-bromo-4-chloro-3-indolyl-phosphate (BCIP) 50mg/ml in 100% dimethylformamide. For staining solution: 4.5µl NBT, 3.5µl BCIP in 1ml AP buffer.

**PBS:** 137mM NaCl; 2.7mM KCl; 8mM Na<sub>2</sub>HPO<sub>4</sub>; 1.7mM KH<sub>2</sub>PO<sub>4</sub>; pH 7.2.

**PBSw:** 1X PBS; 0.1% Tween-20.

**Paraformaldehyde:** 4% paraformaldehyde in PBSw.

**Proteinase K:** 10µg/ml Proteinase K in PBSw.

**SSC (20X):** 3M NaCl; 0.3M sodium citrate; pH 7.0; the solution is stored at RT.

**TE buffer:** 1mM EDTA; 10mM Tris/HCl pH 8.0; the solution is stored at RT.

**TBE buffer:** 100mM Tris/HCl; 83mM borate; 0.1mM EDTA; pH 8.6; the solution is stored at RT.

### 3.5.2 Isolation of nucleic acid

#### 3.5.2.1 DNA isolation

Plasmid DNA preparations were carried out using QIAprep® Spin miniprep Kit (Qiagen). PCR products were purified using QIAquick® PCR purification kit (Qiagen). DNA fragments were purified from agarose gels using QIAquick® Gel extraction kit (Qiagen).

#### 3.5.2.2 RNA isolation

Five embryos or ten dissected tissue explants were collected at the proper developmental stage in 1.5ml Eppendorf tubes. As much buffer as possible was removed. 300µl of Quiazol (Invitrogen) was added. Samples were vortexed for 1-2 min and subsequently stored at -80°C. After thawing on ice, the cell debris were removed by 10min centrifugation at 14000rpm, 4°C. The supernatant from each sample was transferred to a new 1.5ml Eppendorf tube. 60µl chloroform were added. Samples were rotated by hands, kept at RT for 2-3min and subsequently centrifuged for 10min at 14000rpm, 4°C. The upper colourless phase was again transferred in a new 1.5ml tube and the chloroform extraction was repeated. After the second extraction, the upper colourless phase was transferred in a new 1.5ml tube. 4µg/sample of Glycogen (Roche) and 150µl of isopropanol were added in each sample. The samples were vortexed for 2-3min, kept at RT for 10min and subsequently centrifuged 10min at 14000rpm, 4°C. The supernatant was discarded and the pellet was washed with 300µl 75% EtOH by 5min centrifugation at 14000rpm, 4°C. The supernatant was removed and the pellet was briefly air-dried. The RNA was dissolved in RNase free water. RNA was finally cleaned using the RNeasy® mini kit (Qiagen), including the on-column DNA digestion step, according to the manufacturer's protocol. The typical yields were approx. 400ng per tissue explants (animal caps), and 5ng per embryo.

### 3.5.3 Analysis and manipulation of nucleic acids

#### 3.5.3.1 Cloning methods and bacterial manipulation

Preparations of competent cells and transformation have been performed according to standard methods (Sambrook et al., 1989).

#### 3.5.3.2 Bacterial strains

The following E.coli strains were used for transformation:

Stain	Genotype	Company
DH5-alpha	F'proA+B+ lacIqΔ(lacZ)M15 zsf::Tn10 (TetR) / fhuA2Δ (argF-lacZ)U169 phoA glnV44 f80 D(lacZ)M15 gyrA96 recA1 relA1 endA1 thi-1 hsdR17	NEB (*)
XL1 Blue	endA1 gyrA96(nalR) thi-1 recA1 relA1 lac glnV44 F'[::Tn10 proAB+ lacIq Δ(lacZ)M15 Amy CmR] hsdR17(rK- mK+)	Stratagene

(\*) New England BioLabs.

#### 3.5.3.3 Gel electrophoresis of nucleic acids

DNA or in vitro synthesized RNA was electrophorased in horizontal 0.8 – 1.5% TBE agarose gel, depending on the fragments size. 1Kb or 1000bp DNA ladder was used as size standard. Afterwards, the gels were photographed using the Gel documentation System G:BOX (Syngene).

#### 3.5.3.4 Isolation of DNA fragments from agarose gels

To isolate DNA fragments after electrophoresis, the appropriate bands were cut out under UV light. The DNA was extracted using QIAquick® Gel extraction kit (Qiagen), according to the manufacturer's protocol.

### 3.5.4 Polymerase chain reaction (PCR)

#### 3.5.4.1 PCR amplification of fragments for cloning

The reactions were performed in 0.2ml thin-walled PCR tubes (Sarstedt), using the Expand High fidelity PCR System (Roche), following the manufacturer's protocol.

## Thermal Cycling

	Temperature	Time	Cycles
Initial denaturation	94°C	2min	1X
Denaturation	94°C	15sec	
Annealing	45 - 65°C (*)	30sec	30 X
Elongation	72°C	45sec -8 min (**)	
Final Elongation	72°C	7min	1X
Cooling	4°C	unlimited	

(\*) Optimal annealing temperature depends on the melting temperature of the primers and the system used

(\*\*) Elongation time depends on the fragment length: 45sec up to 0.75kb, 1min for 1.5kb, 2min for 3kb, 4min for 6kb, 8min for 10kb.

## 3.5.4.2 Endpoint RT-PCR assay

500ng of isolated total cellular RNA was reverse transcribed using the F-470L DyNAmo™ cDNA Synthesis Kit (Finnzymes), according to the manufacturer's protocol. The desired target cDNAs were amplified using specific primers. Ornithine decarboxylase (ODC) was used as control cDNA. PCRs were carried out in the exponential phase of amplification (estimated by comparing products amount at different cycle numbers) using the Phusion High-Fidelity DNA Polymerase (Finnzymes). 25µl PCR reactions were prepared as following:

Component	25µl reaction
cDNA template	1µl
5X Phusion HF GC Buffer	5µl
10mM dNTPs	0,5µl
0,5µM Primers for and rev	1µl
Phusion DNA Polymerase	0,5µl
H2O	to 25µl

## Thermal cycling

	Temperature	Time	Cycles
Initial denaturation	94°C	30sec	1X
Denaturation	94°C	30sec	
Annealing	55°C	30sec	variable
Elongation	72°C	30sec	
Final Elongation	72°C	7min	1X
Cooling	4°C	unlimited	

PCR samples were loaded side by side in the agarose gel. After electrophoresis, the gels were photographed using the Gel documentation System G:BOX (Syngene).

#### 3.5.4.3 Quantitative Real-Time PCR (qRT-PCR)

For real-time PCRs LightCycler® multi well plates 384/"white" (Roche) were used. 10µl PCR reactions were prepared as following:

Component	10µl reaction
cDNA template	1µl
Fast SYBR Green Master Mix (*)	5µl
3,0µM Primers for and rev	1µl
H2O	3µl

(\*) Applied Biosystem.

Thermal cycling:

	Temperature	Time	Cycles
Initial denaturation	95°C	5min	1X
Denaturation	95°C	10sec	45X
Annealing	60°C	20sec	
Elongation	72°C	10sec	
Melting	95°C	5sec	1X
	65°C	1min	
	97°C		
Cooling	40°C	30sec	1X

#### 3.5.4.4 Microarray analysis

The Affymetrix GeneChip® *Xenopus laevis* Genome 2.0 Array was used for microarray experiments. The array is comprised of more than 32,400 probe sets representing more than 29,900 *Xenopus laevis* transcripts. The Affymetrix GeneChip® *Xenopus laevis* Genome 2.0 Array annotation file was used to identify the different prob-sets. Microarray experiments were performed under the supervision of Dr. Dietmar E. Martin at the Gene Center in Munich. Data analysis was performed by Dr. Tobias Straub (Molecular Biology Department, Adolf Butenandt Institute).

### 3.5.5 In vitro transcription

#### 3.5.5.1 In vitro transcription for microinjection

For the synthesis of capped sense-strand run-off transcripts, plasmid templates were linearized as followed:

---

Component	40µl reaction
plasmid template	10µg
Buffer 10X	4µl
Restriction enzyme 20U/µl	3µl
H2O	to 40 µl

---

The reactions were incubated 60-90min at 37°C. Complete linearization was controlled by loading an aliquot of the digested template side by side with the same amount of unlinearized plasmid from a mock reaction (no restriction enzyme) on 1% agarose gel. Capped mRNAs for microinjection were *in vitro* transcribed with RNA polymerase. Reactions were set up as following:

---

Component	50µl reaction
Linearized DNA plasmid	2µg
5X Transcription buffer (Promega)	10µl
G(5')pppGcap analog (25mM, BioLabs)	5µl
100mM NTPs-Mix (Roche)	10µl
100mM DTT (Promega)	5µl
RNasin 40U/µl (Promega)	0,5µl
RNA-Polymerase (Promega)	2µl
DEPC-H2O	to 50 µl

---

The reactions were incubated 2h at 37°C; afterwards, an additional 1µl of RNA polymerase was added. The reactions were incubated o/n at 37°C. The *in vitro* transcribed mRNA was purified using RNeasy® mini kit (Qiagen) according to manufacturer's protocol. An on-column DNA digestion step was included. mRNA quality was assessed loading 1µg of transcribed mRNA on 1% agarose gel. A successful *in vitro* transcription was considered when a clear band was detected at

the expected molecular size. mRNA concentration was estimated using Nanodrop ND-1000 Spectrophotometer. Samples were aliquoted in volume of 3-5 $\mu$ l and stored at -80°C. mRNA aliquots were subjected to maximum 5 freeze/thaw cycles before being discarded. Synthetic *Xenopus* and mouse Suv4-20h1 and h2 mRNAs were injected in the animal pole of two-cell stage embryos at 2, 3 or 4ng per embryo. Rescue experiments with mouse mRNAs were performed with 3ng of a 1:1 mix of wt or mutated Suv4-20h1 and h2 mRNAs, injected into the animal pole of a single blastomere at two-cell stage. Noggin and xBcl-2 mRNAs were injected at 60pg or 800pg per embryo, respectively. Oct-25-VP16, -EnR mRNAs were injected in the animal pole of two-stage embryos at 100pg per embryo.

### 3.5.5.2 *In vitro* transcription of dig-labelled probes

Plasmids were linearized as described and antisense RNA was generated by *in vitro* transcription. The reactions were set up as following:

Component	50 $\mu$ l reaction
Linearized DNA plasmid	2 $\mu$ g
5X Transcription buffer (Promega)	10 $\mu$ l
Dig-NTPs mix (10mM)	5 $\mu$ l
100mM DTT (Promega)	5 $\mu$ l
RNasin 40U/ $\mu$ l (Promega)	0,5 $\mu$ l
RNA-Polymerase (Promega)	2 $\mu$ l
DEPC-H2O	to 50 $\mu$ l

The reactions were incubated 2h at 37°C; afterwards, an additional 1 $\mu$ l of RNA polymerase was added. The reactions were incubated o/n at 37°C. The *in vitro* transcribed RNA probes were purified using RNeasy® mini kit (Qiagen) according to manufacturer's protocol. An on-column DNA digestion step was included.

### 3.5.6 RNA In situ hybridization

Embryos were fixed in freshly made MEMFA for 1.5-2h at room temperature in 5ml storage vials (Roland Vetter Laborbedarf OHG) on a rotating wheel and then

washed in 1X PBS 3X5min. Explants were fixed in MEMFA for 30min and the processed like embryos. PBS was replaced with absolute ethanol to dehydrate the embryos; vials were kept on the rotator for few minutes and then ethanol was replaced with fresh ethanol. Samples were stored at -20°C at least o/n. Rehydration of the embryos was achieved by serial washes with decreasing ethanol concentrations (75%, 50%, 25%, in 1X PBSw) followed by 3X5min washes in PBSw. To permeabilize the embryos, the solution was then exchanged with PBSw + 10µg/ml Proteinase K for 15min (5min for explants) at room temperature on a rocking table. Embryos were washed twice in PBSw and then refixed for 20min in PBSw containing 4% paraformaldehyde. Embryos were washed 5X5min in PBSw at room temperature. PBSw was replaced with hybridization solution (first wash: 50% PBSw + 50% hybridization solution; second wash: 100% wash with hybridization solution, 3min each step at room temperature). 0.5ml of fresh hybridization solution was added to each vials; samples were then incubated 1h at 65-70°C, in a water-bath, to inactivate endogenous phosphatases. Embryos were subsequently prehybridized for 2-6h at 60°C, to reduce the background staining. 30-50ng of digoxigenin-labelled RNA probe were added to 100µl of hybridization solution, heated at 95°C for 2-5min, cooled down and then added to the 500µl prehybridized solution. Probe hybridization was performed o/n at 60°C in the waterbath. The solution containing the probe was transferred to a new 1.5ml eppendorf tube and stored at -20°C for further experiments (probes were re-used for 3-4 experiments). Embryos were rinsed for 10min at 60°C in fresh hybridization solution and then washed three times in 2X SSC buffer for 20min at 60°C. Embryos were subsequently washed twice for 30min at 60°C in 0.2X SSC, followed by 10min wash in MAB solution. MAB solution was replaced with 1ml of MAB containing 2% BMB blocking solution (Boehringer Mannheim). The vials were placed vertically on a rocking table and agitated 1h at room temperature. MAB + 2% BMB blocking solution was replaced with fresh MAB containing 2% BMB blocking solution and 1/2000 dilution of the affinity-purified antidigoxigenin antibody coupled to alkaline phosphatase. Embryos were rocked vertically for 4h at room temperature. Excess of antibody was removed by washing 6-7 times for 1h the samples in MAB. One wash was performed o/n at 4°C. For the chromogenic reaction embryos were first washed twice for 5min at room temperature in alkaline phosphatase buffer. The solution was then replaced with 0.5ml of fresh alkaline phosphatase buffer containing 4.5µl/ml NBT and 3.5µl/ml BCIP. Samples were incubated in the dark, and the colour reaction was stopped when staining becomes apparent and intense (this process can take 5min to 24h) by washing the

embryos twice for 10min in 1X PBS at room temperature on a rotator. MEMFA fixation was performed at room temperature for at least 90min on a rotator. Embryos were then washed two to three times in 1X PBS containing 75% ethanol for 20-30min to remove chromogenic components and afterwards bleached in bleaching solution on a light box for at least 4h. Samples were finally washed in 1X PBS for three times at room temperature on a rotator and photographed within few days under bright light with Leica DFC 310FX (Leica).

## 3.6 Embryological methods

### 3.6.1 Solutions

**Cysteine (Sigma):** 2% LCysteine in 0.1X MBS (*X. laevis*) or in 1/9 MR (*X. tropicalis*); pH 7.8 (*X. laevis*) or 7.5 (*X. tropicalis*); the solution is kept at RT.

**Human Chorionic Gonadotropin (HCG):** 2000 UI/ml HCG in milliQ water.

**MEMFA:** 0.1M 3-(N-Morpholino)-propanesulfonic acid (MOPS); 2mM EGTA; 1mM MgSO<sub>4</sub>; 3.7% formaldehyde (freshly set up for the use), pH 7.4.

**Modified Barth's saline (MBS, 1X):** 880mM NaCl, 10mM KCl, 24mM NaHCO<sub>3</sub>, 8.2mM MgSO<sub>4</sub>, 3.3mM Ca(NO<sub>3</sub>)<sub>2</sub>, 4.1mM CaCl<sub>2</sub>, 100mM Hepes; pH 7.6. The solution is kept at RT.

**Modified Barth's saline (MBS) high salt (1X):** 1X MBS supplemented with 50mM NaCl.

**0.1X MBS/Gentamycin:** 0.1X MBS supplemented with 10µg/ml Gentamycin.

**0.8X MBS/CS:** 0.8X MBS high salt with 20% chicken serum, 200U Penicillin/ml, 200 µg/ml streptomycin; the solution was stored at -20°C until use.

**1X Modified Ringer Solution (MR):** 0.1M NaCl, 1.8M KCl, 2mM CaCl<sub>2</sub>, 1mM MgCl<sub>2</sub>, 5mM Hepes-NaOH. 1/9 and 1/18 MR solutions were prepared with proper dilution of 1X MR. The solutions are kept at RT.

**1X Ringer's solution:** 116mM NaCl, 2.9mM KCl, 1.8 CaCl<sub>2</sub>, 5mM Hepes. The solution was kept at RT.

**10X Steinberg's Solution (SS):** 580mM NaCl, 6.7mM KCl, 3.4mM CaNO<sub>3</sub>, 8.3mM MgSO<sub>4</sub>, 50mM Tris, 0.1g Kanamycin; pH 7.4; the solution is filtered, autoclaved and kept at RT.

**1X SS/Gentamycin:** 1X SS supplemented with 10µg/ml Gentamycin.

**1X SS/PIF:** 1X SS supplemented with activin supernatant diluted 1:10 (Sokol et al., 1990).

### 3.6.2 Experimental animals

Adult wild type *Xenopus laevis* and *Xenopus tropicalis* frogs were purchased from commercial breeding farms (Xenopus Express, Nasco). Animal work has been conducted in accordance with Deutsches Tierschutzgesetz; experimental use of *Xenopus* embryos has been licensed by the Government of Oberbayern (Projekt/AK ROB: 55.2.1.54-2532.6-3-11). Animal husbandry and use for the work presented here complies to the [Directive 2010/63/EU](#). *Xenopus* frogs were kept in 17-19°C (*X. laevis*) or 21°C (*X. tropicalis*) tap water. The animals were fed three times per week with Pondsticks Premium brittle (Interquell GmbH, Wehringen).

### 3.6.3 Superovulation of female frogs

Ovulation of *Xenopus laevis* females was stimulated by injection of 800 units of HCG into the dorsal lymph sac. In animals maintained at 18-20°C water temperature, egg laying started about 12-16h later.

*Xenopus tropicalis* females were stimulated to lay eggs following a two-step protocol: 12-20h before the main stimulation the females were primed with 10 units of HCG into the dorsal lymph sac. The second stimulation was performed by injecting 200 units of HCG in the dorsal lymph sac.

### 3.6.4 Testis preparation

A male frog was anaesthetized in 0.1% 3-Aminobenzoic acid-ethyl-ester in milliQ water for 30min, cooled down in ice-cold water and killed by decapitation. The two testes were taken from the abdominal cavity by pulling out the fat body through an incision of the skin, to which they are connected. Unless used, the testes from *X. laevis* were kept in MBS/CS at 4°C for a maximum of 6 days. For *X. tropicalis*, the testes were kept in 1X Ringer solution at 4°C for a maximum of 2 days.

### 3.6.5 *In vitro* fertilization of eggs and embryos culture

For *in vitro* fertilization of *X. laevis* eggs a small piece of testis was minced in 1X MBS and subsequently mixed with freshly laid eggs. After 3-4min the eggs were incubated in 0.1X MBS at 16-23°C in 110 mm Petri dish. For *in vitro* fertilization of *X.*

*tropicalis* eggs half a testis was minced in 300 $\mu$ l 1X Ringer solution, and subsequently mixed with freshly laid eggs. After 3-4min eggs were covered with 0.1X MBS and put at 23°C in 110mm Petri dish.

### 3.6.6 Removal of egg jelly coat

Amphibian eggs are encapsulated in a multi-layered protein networks, the jelly coat. Due to its elastic properties, it needs to be removed prior to microinjection.

For *X. laevis* embryos, the jelly coat was routinely removed approx. 60min post-fertilization in order not to interfere with fertilization-associated developmental events, such as cortical rotation. The egg jelly coat was removed by incubating the embryos in 0.1X MBS plus 2% Cysteine solution, pH 7.8 for about 5min with gentle agitation in a glass flask. Embryos were then washed three times with 0.1X MBS and finally cultured in 0.1X MBS/Gentamycin at 16-23°C.

For *X. tropicalis* the egg jelly coat was removed, after 20min post fertilization, by incubating the embryos in 1/9 MR plus 2% Cysteine solution, pH 7.5 for about 10-15min. While in Cysteine solution, embryos were gently mixed. Embryos were then washed 3 times with 0.1X Barth solution and twice with 1/9 MR and subsequently incubated in 1/9 MR at 23°C.

### 3.6.7 Injection of embryos

Injection needles were created from capillaries with the Microneedle Puller (settings: heat: 800; pull: 35; vel: 140; time: 139; Sutter Instrument, model P-87). The needles were placed into the needle holder of the injection equipment (Medical System, model Pi-100). The tip of the needle was broken back carefully with a forceps in order to create an appropriate opening. The injection volume was adjusted by choosing the proper injection pressure (15-30psi) and/or the injection duration (30ms -1s). 2.5 or 5nl drops were injected during the experiments. Embryos were injected at two to eight cell stages into specific animal or vegetal blastomeres. After injection, not more than 50 embryos per dish were incubated in 0.1X MBS/Gentamycin at 16-23°C until the desired developmental stages in a 60mm Petri dish, covered with 1% agarose in 0.1X MBS (for *X. laevis* injections) or in 1/9 MR (for *X. tropicalis* injections). After injections *X. tropicalis* embryos were incubated in 2%

Ficoll in 1/9 MR solution for 1h, then transferred in 1/9 MR solution for 30min; finally embryos were put in 1/18 MR solution and incubated at 23°C. The saline was exchanged every day to increase the survival rates of the embryos. For each experiment uninjected/untreated embryos were cultured in parallel with the injected/treated ones.

### **3.6.8 Animal cap explants preparation and culturing**

Animal cap explants were manually dissected from embryos in 60mm Petri dish covered with 1% agarose in 1X SS and containing 1X SS/Gentamycin. Animal caps were explanted with a pair of forceps and singly transferred into wells of a 96-well plate covered with 90µl of 1% agarose in 1X SS and filled with 150µl of 1X SS/Gentamycin. For neural induction, embryos were injected into the animal pole with Noggin mRNA (60pg per embryo) alone or together with xSuv4-20h1 and h2 morpholinos (40ng each per embryo) at two- to four-cell stage. For mesoderm induction, embryos were injected animally 4 times with 2.5nl of control morpholino (80ng per embryo) or a mix of xSuv4-20h1 and h2 morpholinos (40ng each) at two or four cell stage. Subsequently, animal cap explants were incubated in 1X SS/Gentamycin buffer containing the P388D1-derived inducing factor (PIF) from the mouse macrophage cell line P388D1, previously described as a strong inducers of mesodermal tissues (Sokol, Wong et al. 1990). For Oct-25-VP16 and -EnR overexpression experiments, embryos were injected animally 4 times with 2.5nl of each mRNAs (100pg per embryo). For epistasis experiments on animal caps, embryos were injected 4 times with 2.5nl of xSuv4-20h1 and h2 Morpholinos (40ng each per embryo) and Oct-25 Morpholino (30ng per embryo) at two or four cell stage.

## 3.7 Histological Methods

### 3.7.1 Solutions

**Albumin:** Albumin Fraktion V (Roth).

**Alkaline Phosphatase (AP) buffer:** 100mM trichlorethane Tris/HCl pH 9.5; 100mM NaCl; 50mM MgCl<sub>2</sub>; 0.1% Tween 20; 2mM levamisol was added freshly.

**Bleaching solution:** 1% H<sub>2</sub>O<sub>2</sub>; 5% Formamide; 0.5X SSC.

**Blocking Buffer:** PBT plus 10% heat inactive serum.

**Citrate buffer:** solution A: 0.1M Citric acid mono-hydrate; solution B: 0.1M Tri-sodium citrate di-hydrate; Working solution: 9ml solution A mixed with 41ml solution B, 450ml milliQ water. pH 6.0.

**DAB substrate-chromogen** (Zytomed System).

**Dent's Fixative:** 80% Methanol, 20% dimethyl sulfoxide (DMSO).

**Haemalaun** (Roth).

**Hydrogen Peroxidase 35%** (Roth): working solution: 3% hydrogen peroxidase in 1X PBS and 1/10 methanol.

**MEMFA:** 0.1M 3-(N-Morpholino)-propanesulfonic acid (MOPS); 2mM EGTA; 1mM MgSo<sub>4</sub>; 3.7% formaldehyde (freshly set up for the use), pH 7.4.

**NBT/BCIP solution:** Nitro blue tetrazolium (NBT) 75mg/ml in 70% dimethylformamide; 5-bromo-4-chloro-3-indolyl-phosphate (BCIP) 50mg/ml in 100% dimethylformamide. For staining solution: 4.5µl NBT, 3.5µl BCIP in 1ml AP buffer.

**PBS:** 137mM NaCl; 2.7mM KCl; 8mM Na<sub>2</sub>HPO<sub>4</sub>; 1.7 mM KH<sub>2</sub>PO<sub>4</sub>; the pH 7.2.

**PBSw:** 1X PBS; 0.1% Tween-20.

**PBT:** PBS, 2mg/ml BSA, 0.1% TritonX-100.

**Streptavidin-HRP solution:** (Pierce High Sensitivity Streptavidin-HRP, Thermo Scientific, diluted in blocking solution).

**X-Gal staining solution:** 5mM K<sub>3</sub>Fe(CN)<sub>6</sub>; 5mM K<sub>4</sub>Fe(CN)<sub>6</sub>; 2mM MgCl<sub>2</sub>; 1mg/ml Xgal in 1X PBS.

**X-Gal (5-bromo-4-chloro-3-indolyl-D-Galactosidase):** 40mg/ml X-Gal in 25ml dimethylsulfoxide.

**X-Tra Solv** (Meditate).

**X-Tra Kit** mounting medium (Meditate).

### 3.7.2 Immunocytochemistry

For immunocytochemical staining of embryos, the vitelline membrane was manually removed from the embryos before MEMFA fixation (see “RNA in situ hybridization” chapter 3.5.6). Embryos were rinsed in 1X PBS and then incubated in 100% methanol and left o/n at -20°C. After rehydration (75%, 50%, 25% methanol in 1X PBS) embryos were rinsed in PBT for 15min at room temperature and then incubated for 1h with PBT containing 10% heat inactivated goat serum on an orbital shaker, to reduce non-specific hydrophobic binding of the antibody. Embryos were then incubated o/n at 4°C with PBT containing the primary antibody. Embryos were then washed 5-6 times at room temperature in PBT for 1h each wash. Anti mouse or anti rabbit alkaline phosphatase conjugated antibody were used at 1:1000 dilution (incubation o/n at 4°C). Embryos were again washed 5-6 times at room temperature in PBT for 1h each wash and subsequently incubated in alkaline phosphatase buffer containing Levamisol (0.25mg/ml, Sigma) twice for 30min, to inhibit endogenous alkaline phosphatases. For chromogenic reaction BCIP/NBT (biomol) solution was used. The staining reaction was stopped by rinsing the embryos in PBS. Embryos were fixed in MEMFA and their superficially located pigment granules were bleached to increase stain detection on a light box for at least 4h.

### 3.7.3 Immunohistochemistry of paraffin embedded sections

Embryos were fixed in MEMFA for 1h at room temperature and then transferred into ice-cold Dent's Fixative over night at -20°C. Prior to embedding, embryos were rehydrated for 30min in 100mM NaCl, 100mM Tris/HCl pH 7.4. After secondary dehydration with increasing ethanol concentrations, embryos were incubated for 2h in Xylene. Subsequently embryos were soaked in paraffin at 55°C twice for 2h, followed by proper orientation in moulds, while the paraffin was hardened on cooling plates. Embryos were sectioned to slices of 10µm, which were

dried for 2h at 37°C. Paraffin was removed washing the samples twice with X-tra Solv, decreasing ethanol concentration, and finally 1X PBS. Heat-induced epitope retrieval was performed incubating the slides citrate buffers solutions for 1h at 90°C followed by cooling down to room temperature. Endogenous peroxidase inactivation was inactivats by 10min incubation with 3% peroxidase inactivating solution. Unspecific antibody binding sites were blocked by incubation for 1h with 2% biotin-free albumin in PBS. Primary antibodies, diluted in blocking-solution, were incubated o/n at 4°C. Secondary antibody incubation was preceded by washes in PBSw; subsequently, slices were incubated 1h at room temperature with biotinylated anti-Rabbit secondary. After washes in PBSw slices were incubated 1h in the dark at room temperature in Streptavidin-HRP solution. Detection was achieved incubating the slices for 10min at room temperature in DAB substrate chromogen solution. The reaction was stopped by washing the samples in double distilled water. Haemalaun was used for counterstaining (6min at room temperature in 1:3 haemalaun-solution); slices were then blued with 10min under running tap water. Increasing ethanol concentrations and X-tra Solv were used for dehydration. Finally slides were embedded using X-TRA Kit mounting medium. The immunohistochemical experiments were kindly performed by Alexander Nuber (Laboratory of Professor Schotta, Department of Molecular Biology, Adolf Butenandt Institute, LMU, Munich).

#### **3.7.4 Vibratome sections of *Xenopus* embryos**

Embryos were subjected to whole mount RNA *in situ* hybridization as described above (chapter 3.5.6). After bleaching, embryos were rinsed in gelatine/albumin mixture (2.2g of gelatine dissolved in 500ml 1X PBS subsequently supplemented with 135g of albumin (Roth) and 90g of Sucrose). 100-200µl of 25% glutaraldehyde (Sigma-Aldrich) were added to 2ml of albumin/gelatine mixture. The solution was quickly vortexed and poured in a small plastic tray to create a bottom layer. Embryos were placed and properly oriented on the solidifying layer. A second layer of albumin/gelatine mixture plus 25% glutaraldehyde was prepared and poured onto the embryos. The sample was led to solidify at least for 30min. The gelatinized block with the embryo was cut out under a dissecting microscope. Embedded embryos were properly oriented and glued onto a metal support. 30-50µm sections were created using a Vibratome 1000 (Technical Products International, INC.) according to manufacturer's protocol. Sections were transferred on slides, slightly

dried, covered with X-TRA Kit mounting medium (Medite) and analysed with Leica M205FA Fluorescence Stereomicroscope.

### **3.7.5 X-Gal staining**

For lineage tracing of LacZ injected embryos, samples were fixed 30min in MEMFA at RT, and subsequently washed three times in PBS. 1ml of X-Gal staining solution was added to each sample. The vials were kept in the dark and periodically checked for the appearance of the staining, which usually occurred after 30-40min. The reaction was stopped, at the desired staining intensity, by washing the embryos three times in 1X PBS. The embryos were fixed for 30min in MEMFA at RT and subsequently stored in 100% ethanol at -20°C, until used for RNA *in situ* hybridization.

## 3.8 Protein analysis

### 3.8.1 Solutions

**Loading buffer:** Roti®-Load, stock solution 4X concentrated (Roth).

**Chemiluminescence reagents:** Amersham ECL™ Western Blotting Detection Reagents (GE Healthcare); Amersham ECL Plus™ Western Blotting Detection Reagents (GE Healthcare).

**Coomassie solution:** 0.4g Coomassie brilliant blue G250 dissolved in 200ml of 40% (v/v) methanol in water.

**Destaining solution (v/v ratio):** 10% acidic acid, 30% methanol, 60% milliQ water.

**E1 solution:** 90mM KCl, 50mM Tris, 5mM MgCl, 0.1mM EDTA, 10mM Na-Butyrat, 0.4mM PMSF, 0.025mM Leupeptin, 2mM DTT; pH 7.4; the solution is filtered, aliquoted in 50ml aliquots and stored at -20°C.

**E1 solution/0.25M Sucrose:** E1 solution supplemented with 0.25M Sucrose.

**E1 solution/0.25M Sucrose/0.5% Triton-X/ 0.5% NP-40:** E1 solution supplemented with 0.25M Sucrose, 0.5% Triton-X and NP-40.

**E1 solution/1.25M Sucrose:** E1 solution supplemented with 1.25M Sucrose.

**IP buffer:** 100mM NaCl; 10mM Tris; 0.5% NP-40. The pH was adjusted at 7.5; the solution was stored at 4 °C. Complete IP buffer contains also 1mM NaF, 20mM beta-glycerol, 0.1mM NaV, 1mM PMSF and 1 tablete/25ml solution of complete EDTA free protease inhibitor cocktail tablets (Roche).

### 3.8.2 Preparation of *Xenopus laevis* whole embryo lysates for SDS-PAGE

25 embryos per condition were collected in 15ml Eppendorf tubes. The embryos were lysed in 100µl of complete IP-Buffer (0.25 embryo equivalent/µl). Samples were centrifuged 15min at 14000rpm at 4°C. 90µl of the supernatant (22.5 embryo equivalent) were transferred to a new 1.5ml eppendorf tube and 18µl of loading dye were added to each sample (the solution contained now 0.21 embryo equivalent/µl). Samples were boiled at 95°C for 5min before loading the gels with 20µl (ca. 4.2

embryo equivalent) from each sample. The rest of samples were snap-frozen in liquid nitrogen and stored at  $-80^{\circ}\text{C}$  for repeated use.

### **3.8.3 Histone extraction from nuclei of *Xenopus* embryos on sucrose cushion for SDS-PAGE**

Sixty embryos at NF30 (Morpholino injection) or at NF11.5 (protein overexpression) were harvested and washed with E1 solution/0.25M Sucrose via centrifugation at 600rpm for 1min. Embryos were incubated for 15-20min at room temperature in the same solution and subsequently lysed after homogenization with 20 strokes using a 5ml glass-glass douncer (Braun, Melsungen). Nuclei were prepared by centrifugation at 1000rpm for 10min at  $4^{\circ}\text{C}$ . The supernatant containing the cytoplasmatic fraction was discarded and the nuclear pellets were resuspended in 3ml of E1 solution/0.25M Sucrose/0.5% Triton-X/ 0.5% NP-40. Nuclei were incubated on ice for 20min. The solution was carefully layered on top of a 50ml falcon containing 5ml of E1 solution/1.25M Sucrose, in order to create two separate phases. Samples were centrifuged for 30min at 2000rpm (NF30 embryos) or 1000rpm (NF11.5 embryos) at  $4^{\circ}\text{C}$ ; the solution was discarded and the nuclei were resuspended in 1ml of E1 solution and transferred in 1.5ml Eppendorf tube. Nuclei were centrifuged at 5000rpm for 2min and the pellets were resuspended in the appropriate SDS-loading dye volume ( $2.5\mu\text{l}$  loading dye/embryo). Unless used, the samples were kept at  $-20^{\circ}\text{C}$ . Before loading the gels, the samples were boiled at  $95^{\circ}\text{C}$  for 5min. Samples obtained from NF30 embryos were diluted 1:10 with loading dye in a new 1.5ml eppendorf tube. The samples were boiled again at  $95^{\circ}\text{C}$  for 5min and finally  $15\mu\text{l}$  of each sample (corresponding approx. to 0.6 (NF30) or 6 (NF11.5) embryo equivalents, respectively) were loaded onto the gels.

### **3.8.4 Myc-tagged fusion protein extraction from embryos**

25 embryos per condition were lysed in  $100\mu\text{l}$  of 100mM NaCl, 10mM Tris pH 7.5 buffer supplemented with 1mM NaF, 20mM beta-glycerol, 0.1mM Sodium Vanadate, 10mM Na Butyrate, 0,5% NP-40 and EDTA-free protease inhibitor cocktail tablets (Roche). Embryos were centrifuged 15min at 14,000g at  $4^{\circ}\text{C}$ ; the supernatant was collected and 2X Loading buffer (Roti-Load1; Roth) was added. Samples were subsequently analysed by western blot.

### 3.8.5 SDS-PAGE and Western Blot Analysis

SDS-PAGE (SDS-polyacrylamide gel electrophoresis) and Western Blot analysis were carried out according to standard protocols (Sambrook et al., 1989), with 10% and 15% PAA gels, using Roti PVDF membrane (Roth). The signals were detected with Amersham ECL™, ECL Plus™ Western Blotting Detection Reagents (GE Healthcare) and with the Infrared Imaging System Li-Cor (Odyssey). When ECL detection reagents were used, the membranes were exposed to several Super-RX Fuji medical X-ray films at different exposure times. When the Infrared Imaging System was used, wet membranes were scanned; several scans were recorded, with different sensitivities. Odyssey Application Software Version 3.0 (Odyssey) was used to quantify the western blot bands intensities.

### 3.8.6 Sample preparation for Mass Spectrometry

After SDS-PAGE separation, the gels were incubated o/n at 4 °C with Coomassie solution and destained the following day for 4h with frequent exchange of destaining solution every 30-40min. H3 and H4 bands were excised and cut in small pieces. These samples were washed twice with 200µl of H<sub>2</sub>O on a shaker at 37°C for 5min; neutralization was achieved by incubating the gel pieces with Ammoniumbicarbonate (Ambic) and afterwards a destaining step was performed by incubating the samples with 0.1M Ambic and HPLC-grade Acetonitrile (ACN) on a shaker at 37°C for 30-90min, followed by additional washes with H<sub>2</sub>O. Gel pieces were dehydrated by a further ACN incubation. To convert free amino groups to propionic amides of lysine residues, histones were chemically modified by treatment with propionic anhydride before trypsin digestion (0.2µg/µl in 0.1M Ambic). To purify the samples from salts and acrylamide contaminations, the peptide solution was passed over a tip containing small amounts of C18 reversed phased material (ZipTip, Millipore). The peptides were subsequently eluted in a buffer containing 0.1% trifluoroacetic acid (TFA), 50% ACN (elution buffer) and spotted on a target plate. The target plate was loaded into a Voyager DE STR spectrometer and spectra were analysed using the Data Explorer software and an in-house-developed software Manuelito. Spectra were de-isotoped and calibrated internally using the autoproteolytic peptides of trypsin. For quantification of the different post-translational modifications (PTMs) of the various peptides obtained after digestion, the relative intensities of each PTM were taken into account. The area under the peak, representing relative intensities of the

modification, was used for quantification. The area of all the modifications for each peptide were summarized and the percentage of each modification was then calculated. Sample preparation and PTM quantifications were performed in collaboration with Tobias Schneider (Laboratory of Professor R. Rupp, Department of Molecular Biology, Adolf Butenandt Institute, LMU, Munich).

## 3.9 Chromatin analysis

### 3.9.1 Solutions

**Blocking solution for Protein-G and -A Sepharose Beads Fast Flow 4 (GE Healthcare):** 50 $\mu$ l of beads (25 $\mu$ l ProteinG plus 25 $\mu$ l ProteinA) per sample, blocked in 15ml 5% BSA in PBS at 4°C for at least 1h.

**BSA (fraction V, Roth):** 5% BSA in PBS; the solution was aliquoted in 50ml falcon tubes and stored frozen at -20°C.

**Formaldehyde:** 37% stock (Merck); 1% Formaldehyde in PBS working solution: 676 $\mu$ l formaldehyde in 25ml PBS.

**Glycine** (Merck); 0.125M glycine in PBS (235mg glycine in 25ml 1XPBS).

**PBS:** 137mM NaCl; 2.7mM KCl; 8mM Na<sub>2</sub>HPO<sub>4</sub>; 1.7 mM KH<sub>2</sub>PO<sub>4</sub>; pH 7.2.

**RIPA buffer:** 50mM Tris-HCl, pH 7.4, 1% NP-40, 0.25% Na-Deoxycholate, 150mM NaCl, 1mM EDTA, 0.1% SDS, 0.5mM DTT (to be add freshly), 5mM Na-Butyrate (to be add freshly), Protease inhibitor cocktail (Roche; 1 tablet per 100ml RIPA solution); the solution was kept at 4°C.

**TES buffer:** 50mM Tris-HCl pH 8.0, 10mM EDTA, 1% SDS, 50mM NaHCO<sub>3</sub> (to be added freshly); the solution was kept at RT.

**Wash buffer I:** 20mM Tris-HCl pH 8.0, 0.1% SDS, 1% Triton X-100, 2mM EDTA, 150mM NaCl.

**Wash buffer II:** 20mM Tris-HCl pH 8.0, 0.1% SDS, 1% Triton X-100, 2mM EDTA, 500mM NaCl.

**Wash buffer III:** 10mM Tris-HCl pH 8.0, 0.25M LiCl, 1% NP-40, 1% Na-Deoxycholate, 1mM EDTA.

**Wash buffer IV:** 10mM Tris HCl pH 8.0, 1mM EDTA.

**Proteinase K/Glycogen solution:** 10mg/ml Proteinase K, 20mg/ml Glycogen (Fermentas); mix 10 parts of proteinase K with 2 parts of glycogen.

### 3.9.2 Chromatin Immunoprecipitation (ChIP)

The ChIP protocol was established for *Xenopus* based on a published protocol, with the following modifications (Blythe, Reid et al. 2009). Aliquots of 50 *Xenopus tropicalis* embryos per condition (wildtype or injected) were fixed at NF 14-15 in 5ml 1% formaldehyde in PBS for 5min at 20°C on a rolling wheel. Crosslinking was stopped by a 10min wash with 0.125M glycine/PBS, followed by three washes in PBS. Fixed embryos were transferred in 1.5ml eppendorf tubes, frozen in liquid nitrogen and stocked at -80°C. At experimental day1, embryos were cautiously thawed over 15min on ice.

Two 15ml conical tubes of blocked protein-G and -A beads were prepared by incubating the proper amount of beads with 15ml of 5% BSA in PBS. The tubes were incubated at 4 °C while mixing for at least 1h.

600µl of 4°C RIPA buffer was added to each 50 embryos aliquot. Samples were homogenized with a pellet pestle by gently disrupting the embryos until no large embryo fragments are visible. Embryos were incubated on ice at least 10min and subsequently centrifuged at 14,000rpm for 10min at 4°C. The supernatant was discarded and the wall of the tubes was carefully wiped with a kimwipe to remove any lipid contaminant. 650µl of 4°C RIPA buffer was added to each sample; the pellet was re-homogenized vigorously. Samples were subsequently sonicated using the Bioruptor (Diagenode) for 25 cycles, each composed of a 30sec pulse and 30sec rest. Samples were centrifuged at 14,000rpm for 10min at 4°C. 600µl sheared chromatin from two samples were pooled together (in order to obtain 1.2ml sheared chromatin from 100 fixed embryos) and transferred into a pre-chilled, clean 1.5 microcentrifuge tube. Input samples were prepared as followed: in a clean 1.5ml microcentrifuge 195µl TES buffer were combined with 5µl sheared chromatin. Input samples were snap-frozen in liquid nitrogen and stored at -80°C and processed together with the IP-samples, once they were completed.

One of the two 15ml conical tubes containing the blocked protein-G and -A beads was centrifuged at 1000rpm for 5min at 4°C. Excess of 5% BSA/PBS was removed and the beads were gently resuspended by pipetting. A pre-clearing step was achieved by dispensing 50µl blocked beads to each sample of sheared chromatin and incubating each sample at 4°C with mixing for 1-1.5h. Samples were subsequently centrifuged at 1000rpm for 1min at 4°C. Each 1.2ml sheared chromatin sample was separated into two samples by transferring 580µl of pre-cleared,

sheared chromatin in two new 1.5ml pre-chilled, clean microcentrifuge tubes. Each new tube was filled with RIPA buffer and the immunoprecipitation was begun by adding 5 $\mu$ g of antibody to only one of the two tubes, keeping the second one as negative control. Samples were incubated overnight at 4°C with mixing.

At experimental day 2 the second 15ml conical tube containing the blocked protein-G and -A beads was centrifuged at 1000rpm for 5min at 4°C. Excess 5% BSA/PBS was removed, and the beads were gently resuspended by pipetting. 50 $\mu$ l blocked beads was added to each sample. Samples were incubated at 4°C with mixing for 1.5 hour and afterwards centrifuged at 100rpm for 1min at 4°C. Beads were subsequently washed: each wash consisted of a 1-minute centrifugation at 1000rpm at 4°C to pellet the immunocomplexes; removal of supernatant with a 20-gauge needle; addition of 1ml wash buffer, and final incubation at 4°C on a rotating wheel for 5min. Samples were washed 8 times in total, using 2 washes each with buffers I through IV. Following the washes, the supernatant was aspirated with a 26-gauge needle inserted into the beads to completely removed any residual wash buffer. 200 $\mu$ l TES buffer was added to the beads. Elution was achieved by incubating the samples at 65°C for 1h in a table shaker (1000rpm). During this time the frozen input samples were thawed and vortexed to resuspend any precipitated SDS. All the different samples (input, IP and negative control) were processed in the same manner for the rest of the procedure.

Samples eluted from the beads were centrifuged at 14,000rpm at RT for 1min. 200 $\mu$ l of the eluted supernatant was transferred to a new 1.5ml microcentrifuge tube. RNase treatment was achieved by adding 2 $\mu$ l of 10mg/ml stock RNase A (Quiagen) to each sample and incubation for 45min at 37°C. Subsequently, 12 $\mu$ l of Proteinase K/Glycogen solution was added to each sample. Samples were incubated at 68°C for 4h while shaking (1300rpm) to reverse crosslinks and digest proteins. DNA was purified on column using the QIAquick® PCR purification kit (Qiagen) following the manufacturer's protocol. DNA was eluted in 33 $\mu$ l of EB buffer. qRT-PCR was performed using the Light Cycler 480 System (Roche). Data were analysed using the Light Cycler 480 Software Release 1.5.0 SP1 (Roche).

## **4 RESULTS**

### **4.1 Testing pluripotency by single cell transplantation**

One of the most interesting aspects of developmental biology regards the mechanism of cell fate specification. The timing of commitment for naïve embryonic cells can be tested in *Xenopus* by single cell transplantation. Single animal pole blastomeres, marked by Alexa448, were transplanted into a late blastula host embryos blastocoel (stage NF 9). At stage NF 41-42 normally developed embryos were first examined with a fluorescence stereomicroscope. Embryos containing green cells were then embedded in low melting agarose and analyzed by confocal microscope. This assay allows the analysis of whole-mount transplanted embryos and can be used to test the state of commitment of cells taken from embryos at different stages. Two types of transplantation were performed: 1) homochronic transplantation, i.e. cell donor and host embryos were of the same age; 2) heterochronic transplantation, i.e. transplanted cells differed in their developmental age from the host recipients (Fig. 7). Although the transplanted animal pole cells contribute predominantly to ectoderm during normal embryonic development, upon transplantation, they give rise to progeny detectable in all the three germ layers (Fig. 8, Table 1).

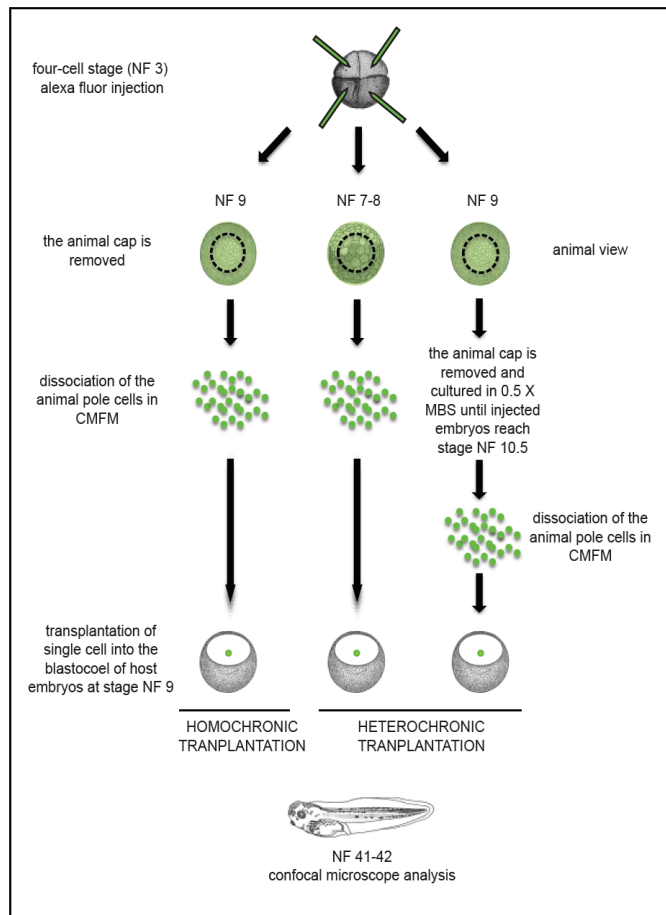


**Fig. 7: Strategy for single cell transplantation in NF9 embryos.** 4-cell stage embryos were injected with green alexa fluor dextran. For homochronic transplantation, NF9 animal cap cells were dissociated in  $\text{Ca}^{2+}$ ,  $\text{Mg}^{2+}$  free medium (CMFM) and injected in the blastocoel of an embryo at the same stage. For heterochronic transplantation NF 7-8 animal pole cells were dissociated in CMFM and transplanted in NF9 embryos. Alternatively, dissociated cells from NF9 embryos were cultured until siblings reached NF10.5, and subsequently injected in NF9 embryos. Analysis of cell derivatives was performed with NF 41-42 transplanted embryos.

Figure 8 displays examples of fluorescent cell progeny, whose differentiated cell type can be identified based on location and morphological features.

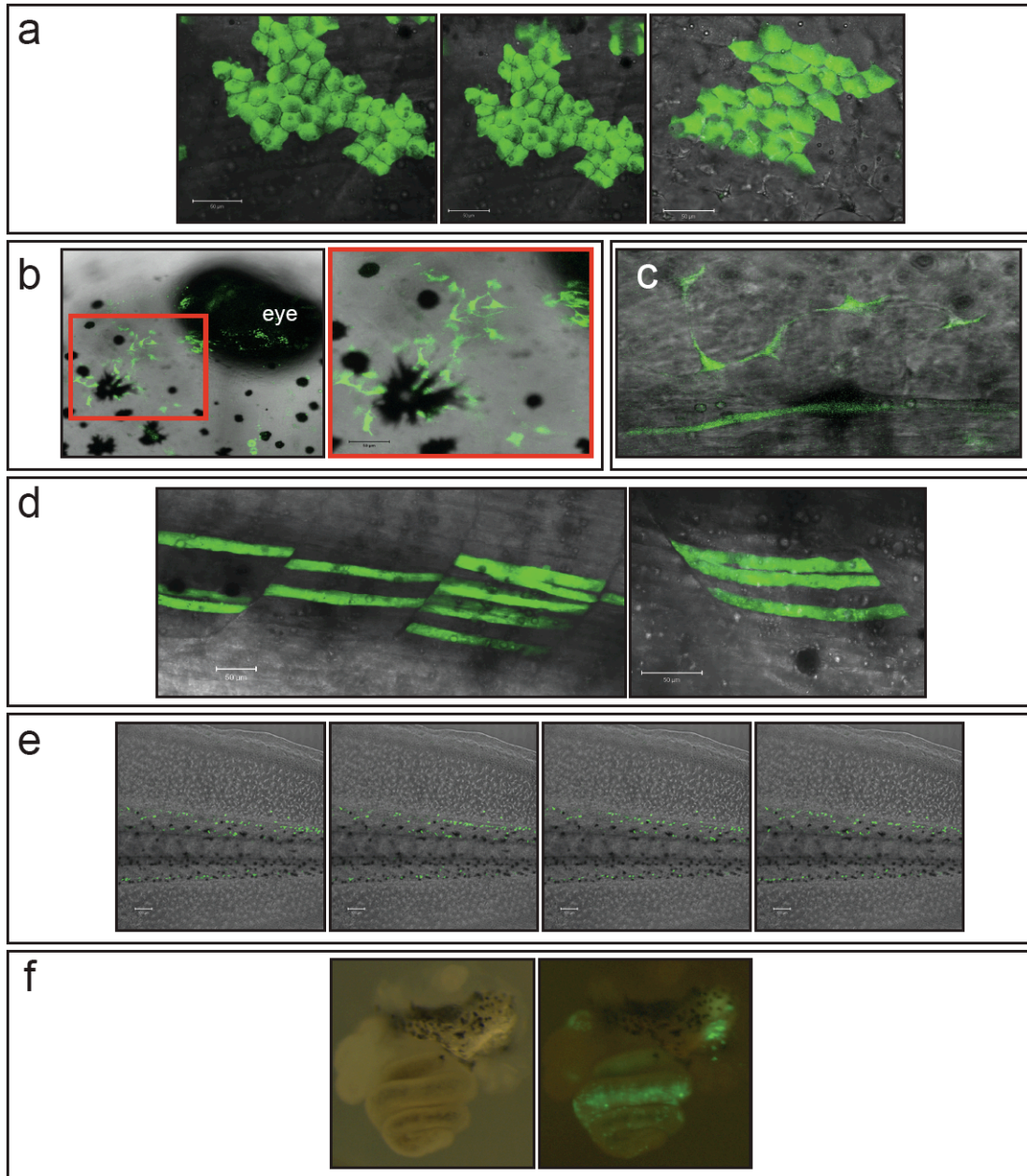


**Fig. 8: Cell progeny detected upon transplantation of single cells.** The figure shows a selection of cell derivatives in the three germ layers. Epidermal cells (a), head neural like structures (b) and dorsal fin sensorial neurons (c) could be detected as ectoderm derivatives. Transplanted cells gave rise also to mesodermal progeny, visible as skeletal myocytes (d) or blood cells (shown a series of sequential frames in e). Endodermal contribution of the transplanted cells could not be visualized at confocal microscope. Panel f shows fluorescence stereomicroscope pictures of cells located in the gut wall of NF46 transplanted embryo.

Table 1 summarizes the statistical analysis of the transplantation experiments.

SINGLE CELL TRANSPLANTATION										
Donor cells stage	Host stage	Transplanted Embryos	Emb with labeled cells	Number and percentage of host embryos containing cells in the following combinations of germ layers						
				ecto	meso	endo	ecto meso	ecto endo	meso endo	ecto meso endo
NF 7-8	NF 9	96	81	–	–	8	6	18	5	45
				–	–	10%	7%	22%	6%	56%
NF 9	NF 9	103	76	7	–	14	3	17	4	31
				9%	–	18%	4%	22%	5%	41%
NF 10.5	NF 9	32	13	3	–	4	–	5	1	–
				23%	–	31%	–	38%	8%	–

**Table 1: Statistical analysis of cell progeny upon homo- and heterochronic single cell transplantation.** The table shows the number and percentage of host embryos containing cells in different combinations of germ layers. With the exception of NF10.5 heterochronic transplantation, which relies only on one experiment, the analysis is based on three independent experiments per condition.

The statistical analysis showed that when younger donor cells (NF 7-8) were transplanted into host embryos, most of the blastomeres (56%) showed pluripotent behaviour, defined as the presence of labelled cells in tissues from at least two, and frequently all three, germ layers within a single embryo. Their cell progeny was found in ectoderm, mesoderm and endoderm. None of the transplanted cell was ectodermally committed. Upon homo- and heterochronic transplantation, late blastula (NF 9) donor cells already showed less pluripotency compared to mid-blastula cells; moreover some of the transplanted blastomeres gave rise to daughter cells restricted to ectoderm only, suggesting that at this stage donor cells start to become committed. Donor cells from stage NF 10.5 were transplanted in a series of heterochronic transplantation experiments into the blastocoel of embryos at stage NF 9; unfortunately the problems of injecting such small cells, and their lower proliferative capacity at this stage, made the transplanted blastomeres difficult to analyze. The result of the single experiment nevertheless highlighted the absence of pluripotency in NF 10.5 transplanted cells. These cells gave rise mainly to derivatives of a single germ layer, showing a higher percentage of ectodermal cells, compared to late blastula donor cells.

## 4.2 Identification of *Xenopus laevis* Suv4-20h enzymes

An increase body of data clearly supports the idea that epigenetic mechanisms play pivotal roles during development (Surani, Hayashi et al. 2007; Akkers, van Heeringen et al. 2009; Vastenhouw, Zhang et al. 2010; Schneider, Arteaga-Salas et al. 2011). In this context, histone post-translational modifications exert a key function during the transition from the pluripotent to the fully differentiated cell states (Azucena, Perry et al. 2006; Rugg-Gunn, Cox et al. 2010; Santos, Pereira et al. 2010). This shift is coupled to the progressive increase in heterochromatin formation, characterized, in addition to several other features, by the presence of the repressive histone methyl marks H3K27me3, H3K9me3 and H4K20me3. While the role of the PRC2, responsible for the deposition of H3K27me3, and of the diverse H3K9-specific HMTases have been characterized in significant depth, little is known about the functions of Suv4-20h1 and Suv4-20h2 enzymes with regard to gene regulation. Because H4K20me3 abundance rises continuously from blastula to tadpole stage (Schneider, Arteaga-Salas et al. 2011), we suspected a regulatory function for this modification, possibly in developmental gene regulation. We therefore decided to characterize the biological functions of the two HMTases during *Xenopus* development.

*Xenopus laevis* Suv4-20h1 and h2 ESTs were initially classified via database mining (Table 2). Because *Xenopus laevis* is an allotetraploid organism, two non-allelic isoforms of each of the two HMTases were identified. Although only partially annotated, the two non-allelic isoforms of each gene could be clearly identified, and nucleotide alignment revealed high sequence similarity identity for each enzymes (data not shown). Mouse and *Xenopus* Suv4-20h1 and h2 protein sequences are well conserved, particularly within the SET domain ( $\geq 88\%$  identity) (Table 3 and Fig. 9). Interestingly, *Xenopus* Suv4-20h2 amino acid sequence appears remarkably longer than the mouse homolog, due to C-terminal insertion.

	EST identification number
xSuv4-20h1a	BC073331
xSuv4-20h1b	BJ070388
xSuv4-20h2a	BC126060
xSuv4-20h2b	BJ623840

**Table 2.** NCBI EST numbers of *Xenopus laevis* Suv4-20h enzymes.

	xSuv4-20h1	xSuv4-20h2	mSuv4-20h1	mSuv4-20h2
xSuv4-20h1	-	83%	98%	81%
xSuv4-20h2	83%	-	83%	88%
mSuv4-20h1	98%	83%	-	75%

**Table 3.** Percentage of amino acid identity of the SET domain between mouse and *Xenopus* proteins.



RNA *in situ* hybridization experiments on *Xenopus* embryos revealed a broad distribution of the two genes during different stages of development: both enzymes were maternally expressed, broadly distributed during gastrula and present in the neural tube at neurula stage. Tailbud stage embryos showed a strong staining in the head, e.g. eye and gills, but also in the trunk, where myocytes and neural tube appear distinctly stained (Fig. 10).

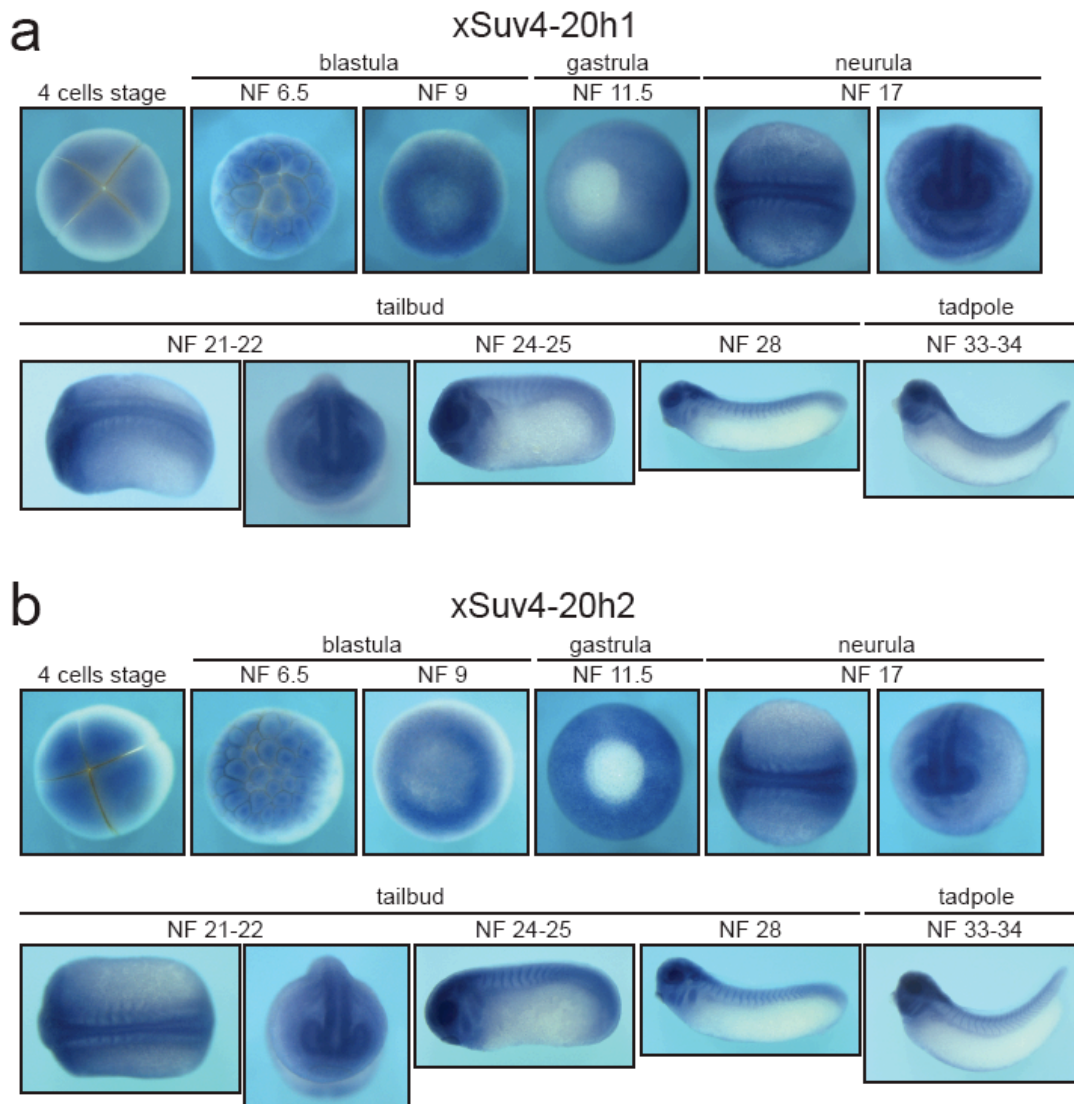


**Fig. 10: *Xenopus laevis* Suv4-20h gene expression during early development.** XSuv4-20h1 (a) and xSuv4-20h2 (b) mRNA expression was detected by RNA *in situ* hybridization at the indicated developmental stages. Both the enzymes were maternally expressed and showed a homogeneous distribution during blastula and gastrula stage. The neural tube is clearly stained at neurula and tailbud stage. Later stages showed a peculiar staining in the head, eye, gills, myocytes and neural tube. The high yolk distribution in the ventro-lateral portion of tadpole embryos partially masked the positive staining of cells present in that area.

Semiquantitative RT-PCR on animal pole (AP), marginal zone (MZ) and vegetal pole (VP) explants at blastula stage showed similar and comparable abundance of Suv4-20h1 and h2 mRNAs (Fig. 11), suggesting a rather homogeneous presence of the mRNAs in the embryo. Since Suv4-20h mRNAs are not known to be subject to post-translational regulation, it may be that also Suv4-20h enzymes are present in most cells.

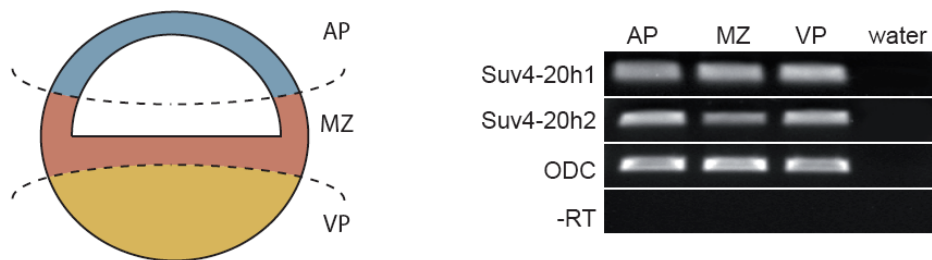


**Fig. 11: xSuv4-20h enzymes mRNA distribution at blastula stage in prospective ectoderm, mesoderm and endoderm.** Total RNA was extracted from animal pole (AP), marginal zone (MZ) and vegetal pole (VP) explants of NF9 embryos; semiquantitative PCR showed levels of xSuv4-20h1 and xSuv4-20h2 transcripts in the three explants. ODC was used as loading control, -RT PCR, performed for ODC, as negative.

On the other hand quantitative RT-PCR analysis showed a different distribution of the two mRNAs during development: while xSuv4-20h1 mRNA abundance decreases throughout the initial stages of development and subsequently rises from mid-gastrula on, at least in part reflecting the maternal-to-zygotic mRNA transition, xSuv4-20h2 mRNA profile is characterized by a constant decrease during development (Fig. 12).

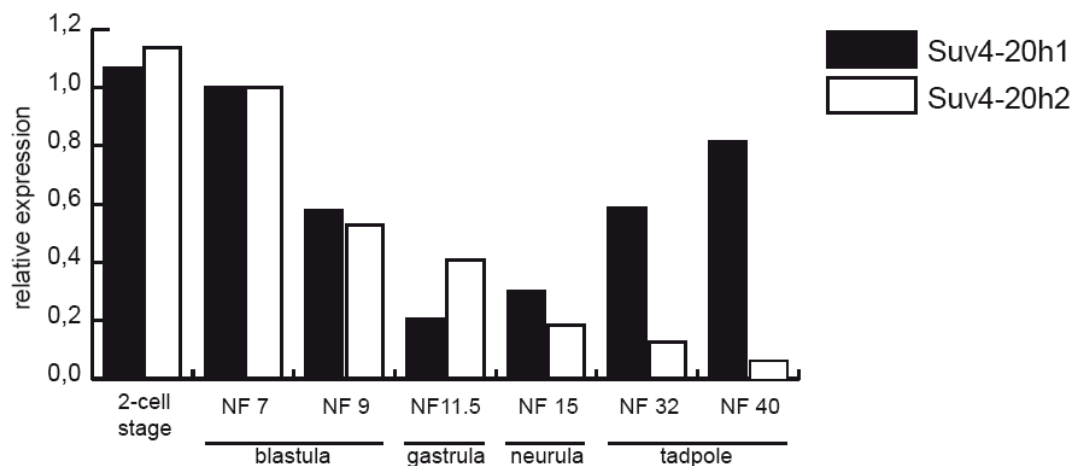


**Fig. 12: xSuv4-20h mRNA profiles during different stages of development.** qRT-PCR profiles of xSuv4-20h enzymes. The chart shows the relative expression of the two enzymes related to ODC at the indicated developmental stages. The shown temporal profiles were confirmed in a second independent experiment.

In order to test whether the presumed *Xenopus* Suv4-20h HMTases were functionally active, we first analyzed their ability to rescue H4K20me3 state in Suv4-20h double knockout (DKO) MEFs (Schotta et al., 2004), lacking the modification. Upon transfection both *Xenopus* enzymes clearly re-established the characteristic H4K20me3 punctuate pattern colocalizing with the chromocenters (DAPI dense foci) in the nuclei (Fig. 13) (Schotta et al., 2004). These results confirm the enzymatic activity of the prospective xSuv4-20h homologs.

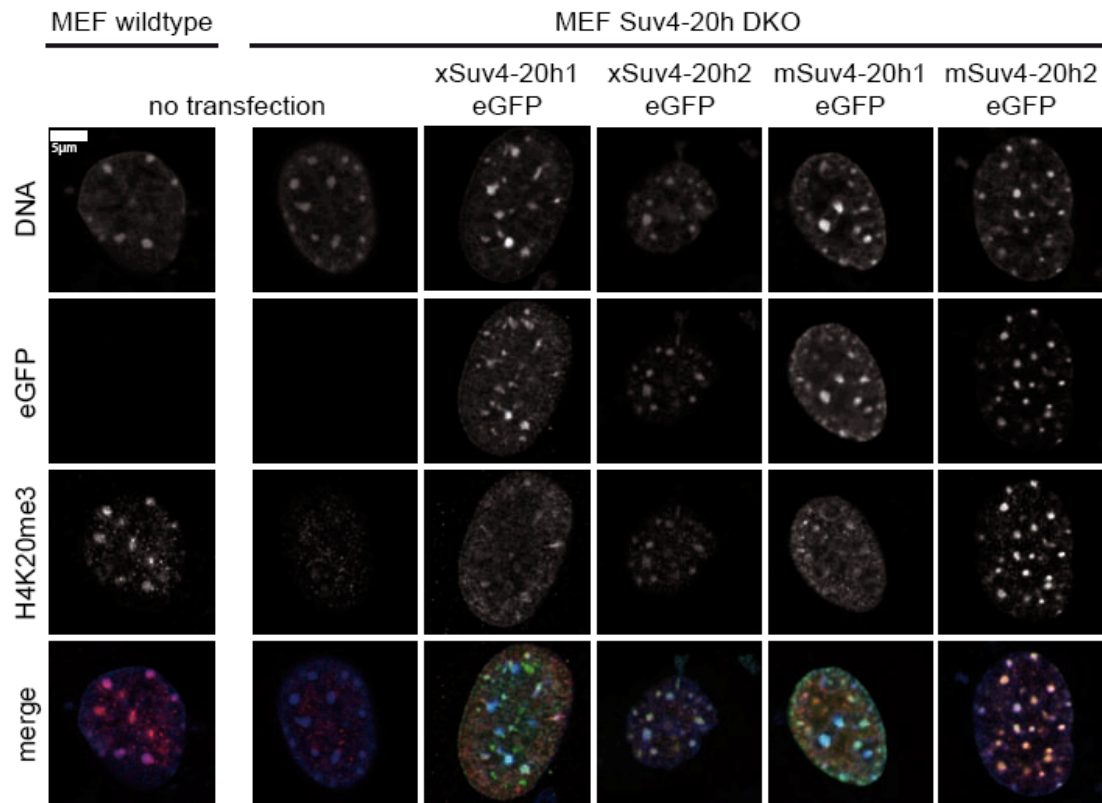


**Fig. 13: Wildtype *Xenopus* and mouse Suv4-20h HMTases re-establish H4K20me3 signals at chromocenters in Suv4-20h1/h2 DKO MEFs.** Transiently transfected eGFP-tagged Suv4-20h1 and h2 enzymes from frog or mouse re-establish H4K20me3 marks in heterochromatic foci of Suv4-20h1/h2 DKO MEFs. (Transfections were performed by Matthias Hahn, Laboratory of Professor Schotta, Department of Molecular Biology, Adolf Butenandt Institute, LMU, Munich).

### 4.3 Functional characterization of xSuv4-20h enzymes

To address the role of the two enzymes during *Xenopus* development we designed specific translation blocking morpholino oligonucleotides against the two paralogues of each gene (Fig. 14 a and b). Since antibodies against the frog enzymes are unavailable, we performed *in vitro* TNT assay to test the ability of the different morpholinos to block translation of the corresponding mRNA. The *in vitro* reaction showed a clear specificity of each morpholino for their cognate templates: incubation of xSuv4-20h1 or h2 morpholinos prevented the synthesis of xSuv4-20h1 or h2 proteins, respectively, while the presence of the control morpholino (ctrl-MO) did not inhibit the reaction (Fig. 14 c).

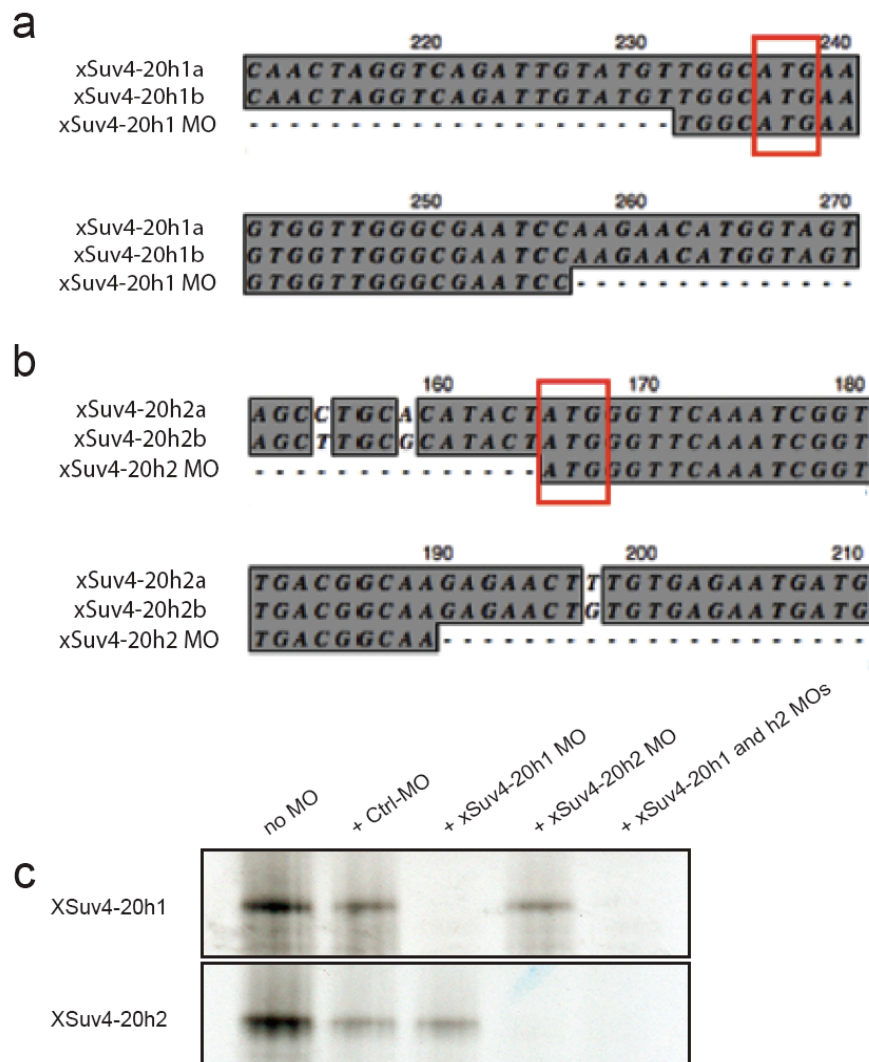


**Fig. 14: Morpholino specificity.** (a) and (b) show sequence alignments of the xSuv4-20h1 and h2 morpholino-targeted regions to the 5'-UTR of the respective ORFs. AUG start codon is boxed in red. (c) *In vitro* TNT assay performed as described in Materials and Methods section. XSuv4-20h1 and h2 MOs specifically inhibited translation of their cognate templates.

To test whether the downregulation of the two enzymes leads to a reduction of H4K20me2 and me3 marks *in vivo*, western blot analysis was performed using specific antibodies against the different modifications on lysine 20 on the histone H4 tail. To avoid possible functional complementation between the xSuv4-20h enzymes *in vivo*, the embryos were injected with a mix of the two morpholinos (double morphants). Compared to uninjected embryos or ctrl-MO injected embryos, the double morphants contained significantly less H4K20me2 ( $p=0.0011$ ) and H4K20me3 ( $p=0.0164$ ). The decrease of the two marks was coupled to an increase in H4K20me1 ( $p=0.0034$ ) (Fig. 15 a and b), suggesting that monomethylation of K20 cannot be converted to the higher methyl states in embryos depleted for xSuv4-20h enzymes.

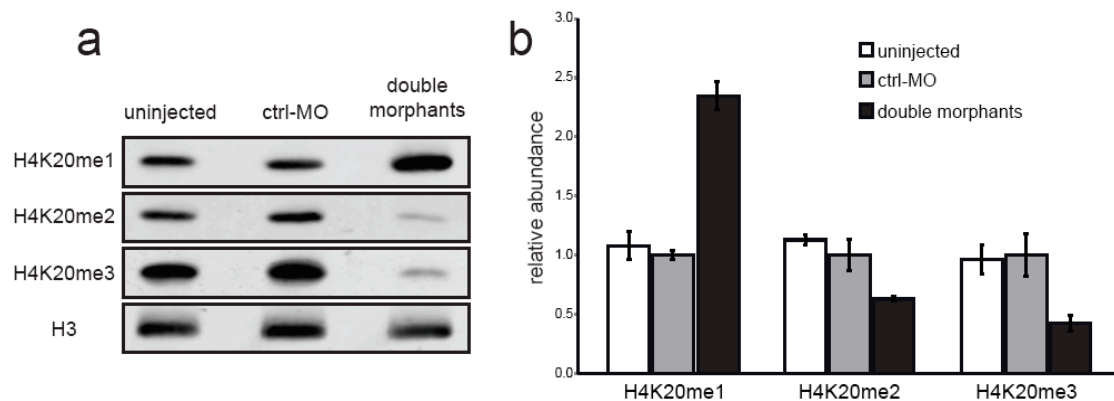


**Fig. 15: xSuv4-20h1, h2 morpholino-mediated downregulation leads to a strong reduction in H4K20me2 and H4K20me3 levels coupled to a concomitant increase in H4K20me1 abundance.** Bulk histones from NF30-33 embryos were isolated and analyzed as described in Materials and Methods section. **(a)** Western Blot analysis of uninjected, control morpholino (ctrl-MO) and xSuv4-20h1, h2 morpholinos (double morphants) injected embryos using antibodies against H4K20 mono-, di- and trimethylation. PanH3 antibody was used as loading control. **(b)** Western Blot quantification of three independent biological experiments described in **(a)**. Data represent mean values, error bars indicate SEM.

This result was confirmed by MALDI-TOF mass spectrometric analysis of the modification states of the tryptic peptide 20-23 from histone H4 (Fig. 16a). MALDI-TOF profiles of peptides 9-17 and 27-40 on histone H3 were considered as control (Fig. 16b and c). Although H4K20me3 identification was not detected in a reproducible manner due to technical problems (Schneider, Arteaga-Salas et al. 2011), nevertheless in double-morphant embryos H4K20me2 levels were 2.5-fold reduced ( $p=0.0153$ ), and H4K20me1 mark was increased 3-fold ( $p=0.0185$ ), while the unmodified peptide abundance remained constant. Notably, the abundance of K9 and K27 methylation was unaffected by the downregulation of xSuv4-20h HMTases

(Fig. 16b and c, compare double morphants with uninjected and Ctrl-MO injected embryos), suggesting that on bulk chromatin these morpholinos trigger a specific alteration of H4K20 marks, without a general effect on other repressive H3 PTMs.

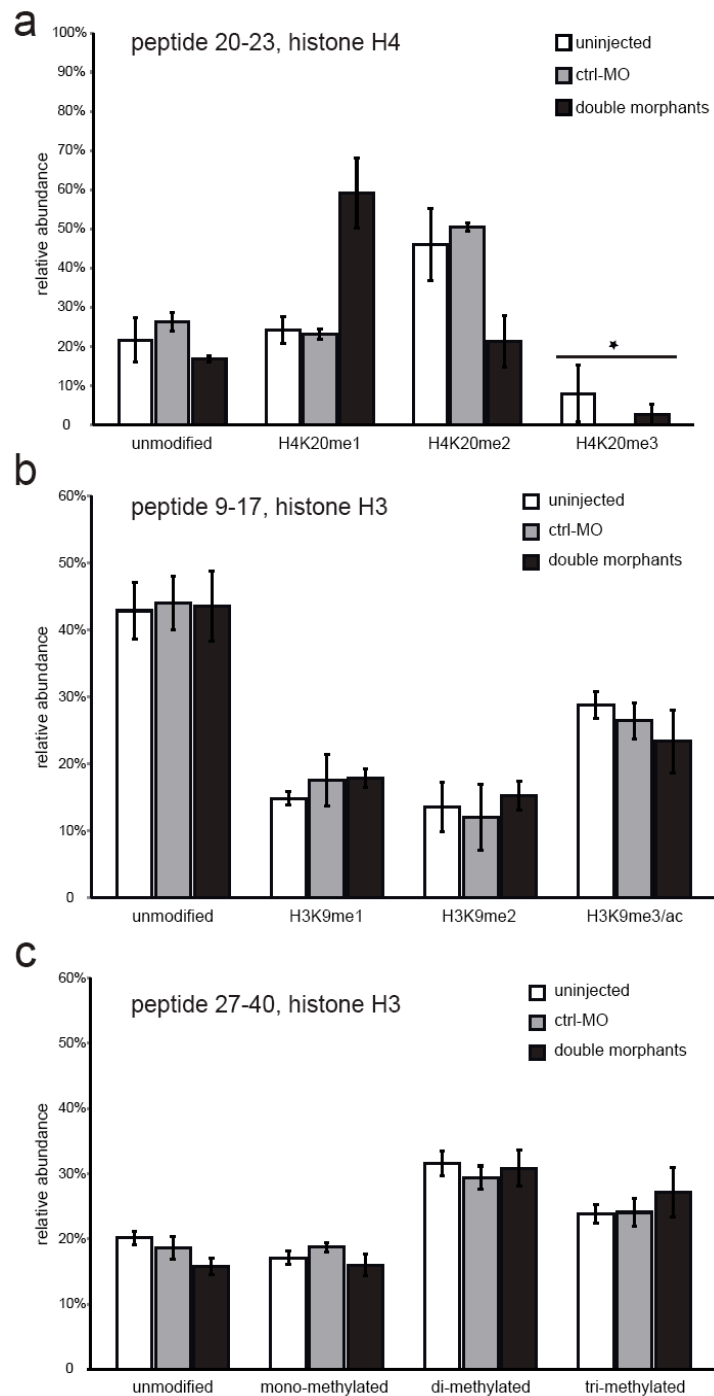


**Fig. 16: Quantification of histone methylation states in xSuv4-20h morphants by MALDI-TOF mass spectrometry.** Bulk histones from NF30-33 embryos were isolated and analysed as described in Materials and Methods. **(a)** H4 peptide 20-23, **(b)** H3 peptide 9-17 and **(c)** H3 peptide 27-40 in uninjected, ctrl-MO and double-morphant embryos. The values represent the relative abundance of the individual modifications states as the mean of three independent experiments; error bars indicate SEM. Star - for technical reasons H4K20me3 mark was quantitated only in some samples.

Furthermore, western blot analysis with antibodies against trimethylated H3K9 and H3K27 showed no difference in the abundance of these two marks between control and xSuv4-20h double-morphant embryos (Fig. 17).

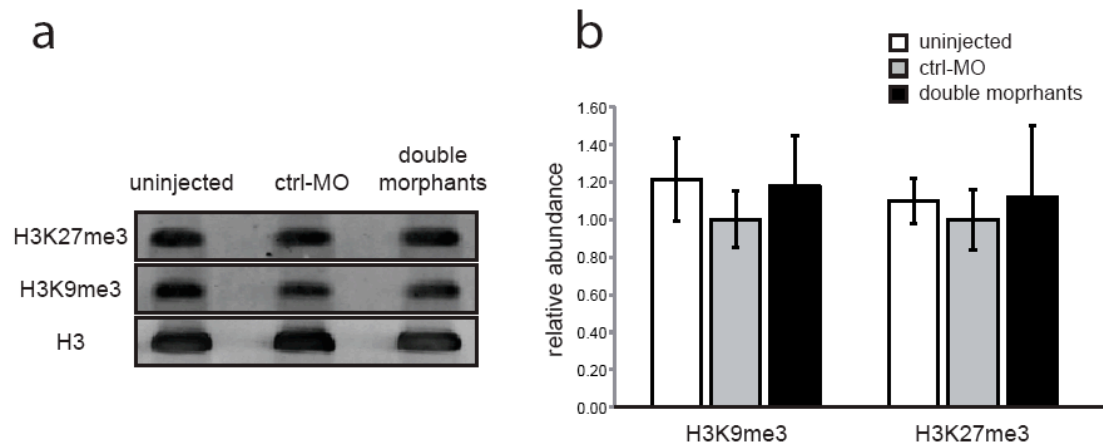


**Fig. 17: xSuv4-20h1, h2 morpholino-mediated downregulation has no effect on H3K9me3 and H3K27me3.** (a) Western Blot analysis of uninjected, control morpholino (ctrl-MO) and xSuv4-20h1, h2 morpholino injected embryos using antibodies against H3K27me3 and H3K9me3. PanH3 antibody was used as loading control. (b) Western Blot quantification of two independent biological experiments described in (a); data represent mean values, error bars indicate SEM.

To further characterize the effects of xSuv4-20h depletion, we performed immunohistochemistry on serial sections from late tailbud embryo injected unilaterally at 2-cell stage with ctrl-MO or xSuv4-20h MOs. Figure 18 details the results for the neural tube, because of its high density of proliferating cells, the clear presence of cells positive for the different H4K20 modifications, and because it represents a tissue where the injected side can be easily distinguished from the uninjected one. While H3 staining was unaffected by Ctrl- and xSuv4-20h morpholinos injections, H4K20me2 and H4K20me3 positive nuclei were reduced on the injected double morphant side of the neural tube. Once again, the reduction in the abundance of di- and tri-methylation was coupled to a compensatory increase in H4K20me1.

Together these results indicate that xSuv4-20h1 and h2 downregulation leads to a specific decrease of H4K20 di- and trimethyl marks in the embryo.

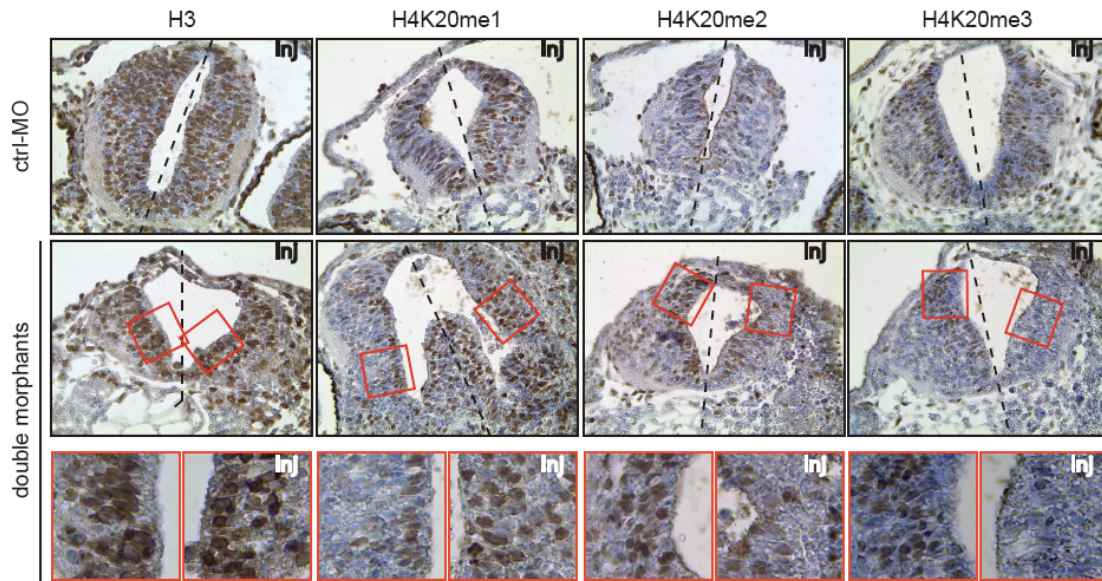


**Fig. 18: Immunohistochemistry on NF 30-33 ctrl-MO and double-morphant embryos.** Immunohistochemistry on ctrl-MO and xSuv4-20h double-morphant tadpoles. Panels show representative cross-sections of neural tubes stained with antibodies against the histone epitopes indicated on top. Dashed lines indicate embryonic mid-line. Squares on double-morphant sections represent the cropped pictures shown in the bottom row. Inj – injected side.

RNA-based overexpression of xSuv4-20h HMTases had the opposite effect in bulk chromatin. Compared to the loss-of-function experiments, western blot analysis showed that, when injected singly, *Xenopus* Suv4-20h1 and h2 mRNAs caused, in a dose-dependent manner, a significant upregulation of H4K20me2 and H4K20me3, while H4K20me1 levels were slightly reduced (Fig. 19a). Interestingly, overexpression of mouse h1 or h2 mRNA altered the H4K20 methyl states to an extent comparable with the *Xenopus* h1 or h2 mRNA injections (Fig. 19b). Individual knockout of murine Suv4-20h HMTases suggest a functional sub-specialization, with Suv4-20h1 being responsible of H4K20me2 and Suv4-20h2 for H4K20me3 (Schotta, Lachner et al. 2004). Remarkably, when injected in *Xenopus* embryos, mouse Suv4-20h HMTases do not show any specificity for either H4K20me2 or H4K20me3, suggesting that the preferential involvement of h1 in directing the di-methylation and h2 in establishing the tri-methylation of K20 can be possibly due to interactions of the enzymes with other factors in the mouse, or to protein domains, that are not conserved in *Xenopus*.

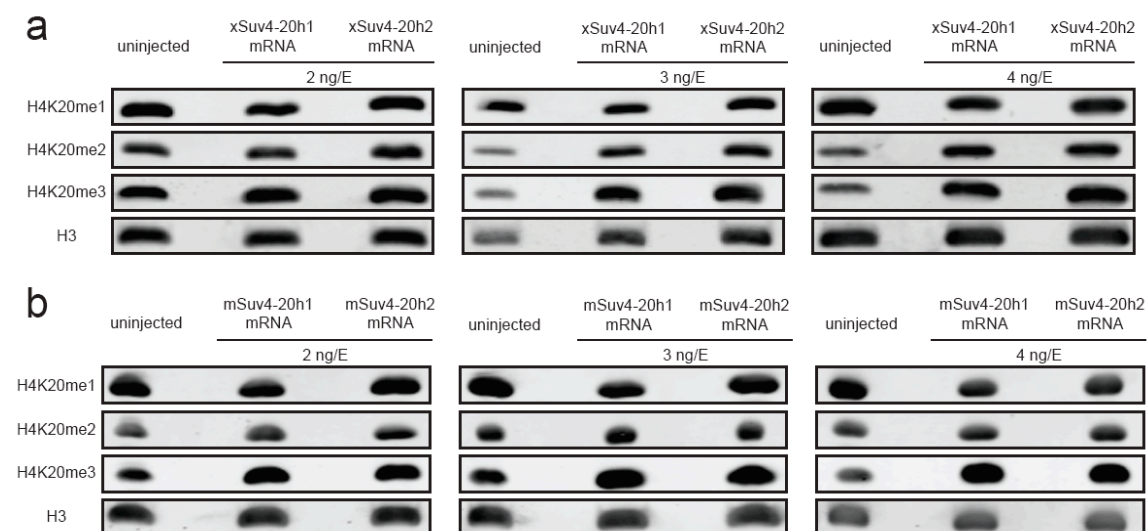


**Fig. 19: Suv4-20h enzymes gain-of-function experiments lead to a dose dependent upregulation of H4K20me2 and H4K20me3 in *Xenopus* embryos.** Western Blot analysis of uninjected embryos or embryos injected with *Xenopus laevis* (a) or *Mus musculus* (b) Suv4-20h1 or h2 mRNAs at different concentrations. Bulk histones from NF11.5 embryos were isolated and analyzed as described in Materials and Methods section. PanH3 staining was used as loading control.

The functional characterization of *Xenopus* Suv4-20h HMTases, by loss and gain of function experiments, showed that alterations in the amount of proteins in the embryo leads to opposite effects, with clear and specific modifications of the methylation profiles at H4K20. Moreover these experiments indicate that the bulk abundance of di- and trimethylated H4K20 can be manipulated over a wide range without compromising embryonic viability. Together these results identify the frog cDNAs as orthologs of mammalian Suv4-20h enzymes.

#### 4.4 Developmental functions of xSuv4-20h enzymes

We next tested whether alterations in xSuv4-20h HMTase expression affect embryonic development. In a first series of experiments, the phenotypic consequences, arising from depletion of xSuv4-20h enzymes, were investigated. For this purpose, we injected xSuv4-20h1 and h2 morpholinos in one of the two blastomeres in embryos at two-cell stage and scored any phenotypic alteration, comparing injected with uninjected side. In a second series of experiments we assessed the consequences of xSuv4-20h enzymes overexpression.

#### 4.4.1 Loss-of-function analysis

Upon morpholino injection, the process of patterning and morphogenesis of double-morphant embryos appeared largely normal. Gastrulation occurred properly and embryos showed regular antero-posterior and dorso-ventral axes. At the molecular level, the expression of Spemann's organizer genes, such as Chordin, Goosecoid and Xnr-3, appeared unaffected in control and double-morphant embryos (Fig. 20).

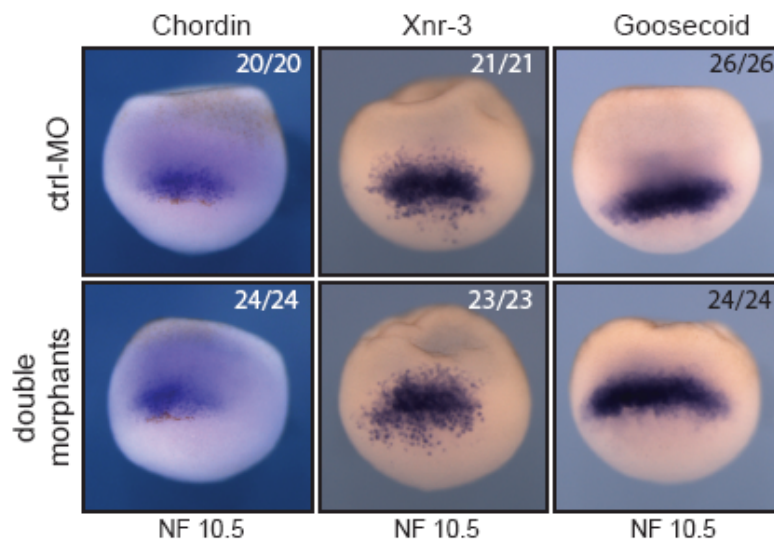


**Fig. 20: xSuv4-20h enzymes depletion have no effects on the expression of organizer genes.** RNA *in situ* hybridization analysis on NF10.5 ctrl-MO and double-morphant embryos using probes against Chordin, Xnr-3 and Goosecoid. The pictures show Spemann's organizer region stained with the three probes; animal pole is on the top, vegetal pole is on the bottom. For each condition, numbers refer to embryos showing the displayed staining, in comparison to the total number of analysed embryos (n= two independent experiments).

Similarly, the anteroposterior patterning of the central nervous system (CNS) appeared also to be normally established, as suggested by the wildtype-like expression patterns of Otx2 and Krox20, which demarcate the prospective forebrain or rhombomeres 3 and 5, respectively (Fig. 21).

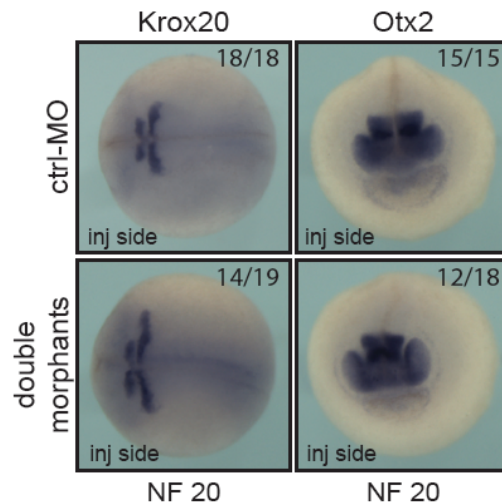


**Fig. 21: Krox20 and Otx2 expression is unaffected upon xSuv4-20h1, h2 morpholinos injection.** RNA *in situ* hybridization analysis on NF20 embryos using probes against Krox20 and Otx2. Krox20 expression: dorsal view of stained embryos with the anterior on the left. Otx2 expression: anterior view of stained embryos; dorsal is on the top, ventral is on the bottom. For each condition, numbers refer to embryos showing the displayed staining, in comparison to the total number of analysed embryos (n= two independent experiments).

Morphologically, from tailbud (NF30) stage on, two main phenotypes could be scored upon xSuv4-20h enzymes knockdown. First, as shown in Fig. 22, eye development was severely compromised in the injected side of double-morphant embryos. At NF33, control morpholino injected embryos showed the characteristic eye structure, with the lens placode surrounded by the pigmented retinal epithelium, partially open in its ventral-most portion (the so called choroid fissure, Fig. 22a). In the injected side of xSuv4-20h double morphants eye formation was strongly reduced: the eye rudiments contained no or little retinal pigment and most of them had no lens. Moreover the typical pattern of melanophores spread out over the dorsal part of the head and the lateral portion of the trunk was severely perturbed. The melanocyte number was reduced and in most of the cases completely lost from the injected side of double morphants (compare Fig. 22a, b and c). Both phenotypes were scored at high penetrance (80-90%;  $p < 0.0001$ , Fisher's exact test) in more than three independent experiments (Fig. 22). To test whether these phenotypes were specifically due to the downregulation of *Xenopus Suv4-20h* HMTases, rescue experiments were performed. Murine *Suv4-20h1* and *h2* mRNAs were coinjected, at increasing concentrations, together with *Xenopus Suv4-20h1* and *h2* morpholinos. In the rescue condition, the choroid pigmented layer appeared normally organized around the lens (Fig. 22c) and the typical pigmentation was properly re-established in number and sites in the injected embryos. 1ng of each mRNA was sufficient to rescue 2/3 of the embryos with eye and melanophores defects ( $p < 0.0001$ , Fisher's

exact test). The rescue efficiency did not increase upon injection of higher concentration of mouse mRNAs (Fig. 22).

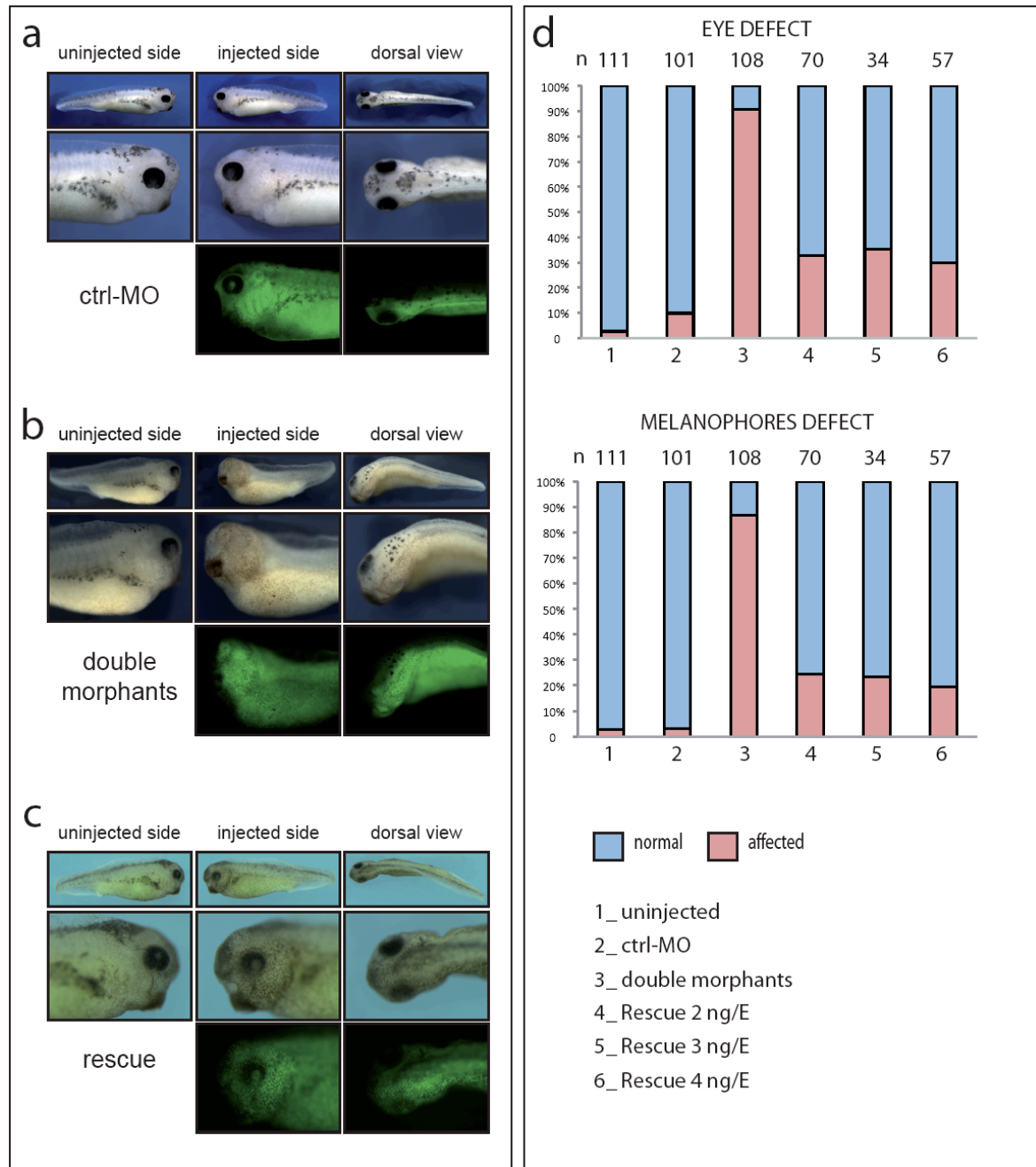


**Fig. 22: xSuv4-20h enzymes depletion represses eye and melanophores differentiation.** Morphological phenotypes of NF30-33 ctrl-MO (**a**), double morphants (**b**) and rescued embryos (**c**). Embryos were injected in one cell at two cells stage with morpholino (**a,b**) or morpholino and *Mus musculus* mRNAs (**c**) plus Alexa Fluor 488 Dextran as lineage tracer (green channel) to identify the injected side. (**d**) Penetrance of the eye and melanophores phenotypes in uninjected, ctrl-MO, double morphants and double-morphant embryos rescued with increasing concentration of *Mus musculus* Suv4-20h1 and h2 mRNAs. n= numbers of embryos analysed. The results from three to five independent experiments are presented.

The prominent eye defect and the high percentage of embryos affected by this phenotype encouraged us to further investigate this morphological alteration. On the genetic level, the expression patterns of the homeobox transcription factor Rx-1 and the paired box transcription factor Pax-6, two main genes involved in the cascade leading to eye development, were frequently reduced and sometimes even completely missing in double-morphant embryos. The missing expression of the eye regulatory genes was again restored to normal levels by mouse Suv4-20h mRNAs. Thus, knock-down of xSuv4-20h enzymes blocks eye development at the level of master regulatory genes Pax-6 and Rx-1.

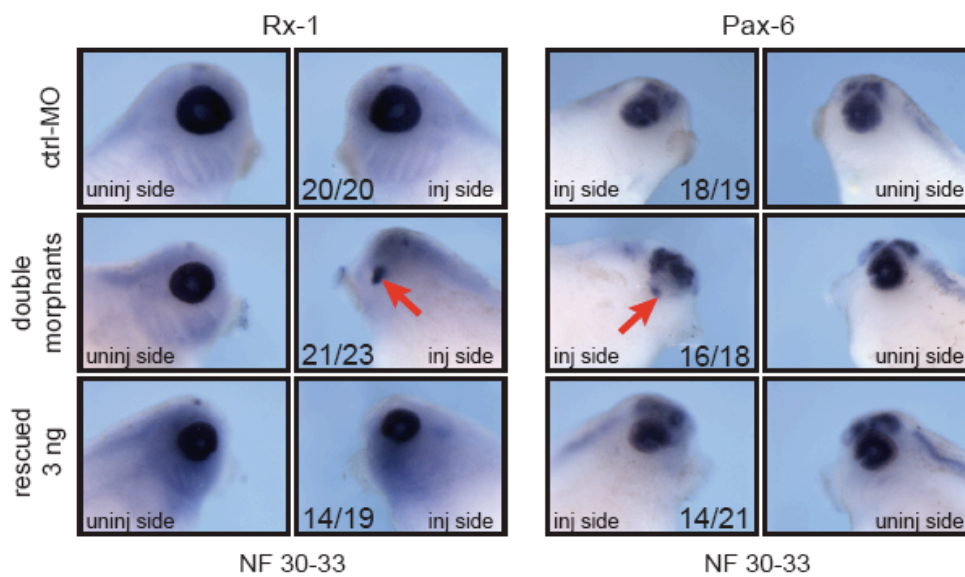


**Fig. 23: xSuv4-20h enzymes depletion compromises the normal eye development.** RNA *in situ* hybridization analysis of NF30-33 ctrl-MO, double morphants and rescued embryos using probes against Rx-1 and Pax-6. The pictures show the head of stained embryos. Upon xSuv4-20h enzymes depletion, the normal pattern of both the probes is deeply compromised (red arrows). mSuv4-20h enzymes mRNAs coinjection re-established the proper Rx-1 and Pax-6 expression. For each condition, numbers refer to embryos showing the displayed staining, in comparison to the total number of analysed embryos (n= three independent experiments).

#### 4.4.2 A functional SET domain is required for proper Suv4-20h enzymes function

To test whether this phenotypic rescue requires normal levels of Suv4-20h proteins or their enzymatic activities, mSuv4-20h HMTases carrying composite aminoacidic point mutations within the catalytic domain were created (Fig. 24). Protein sequence alignment of the SET domains (Dillon, Zhang et al. 2005), as well as crystal structures of SET-domain-containing HMTases (Kwon, Chang et al. 2003), highlighted conserved residues among several members of this superfamily, which

are important for S-adenosylmethionine (SAM) binding and catalytic activity. Two single mutations were introduced simultaneously in each enzyme, in the SAM binding pocket (Asp264Ala and Asp182Ala in mSuv4-20h1 and h2 respectively), and in the conserved catalytic Tyrosine residue (Tyr299Ala and Tyr217Ala in mSuv4-20 h1 and h2 respectively) (Fig. 24).

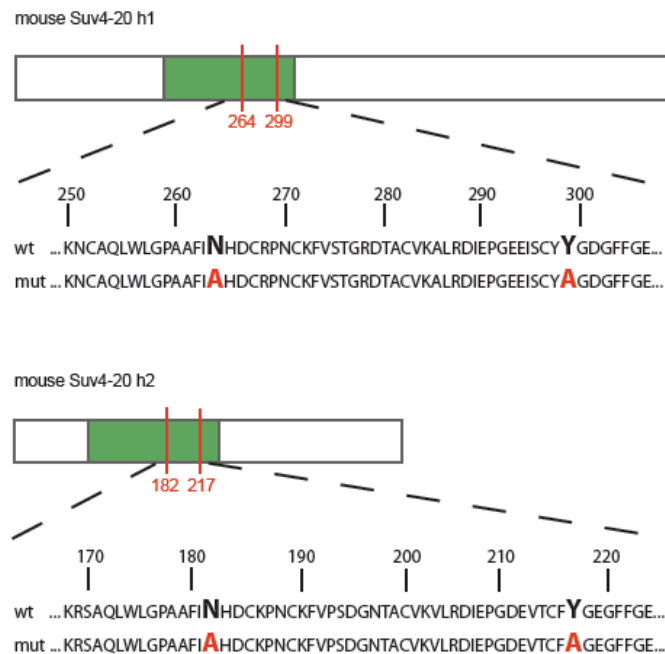


**Fig. 24: Schematic of *Mus musculus* Suv4-20h1 and h2 SET domain mutations.** The two single mutations Asp to Ala (N264A and N182A in mSuv4-20h1 and h2, respectively), and Tyr to Ala (Y299A and Y217A in mSuv4-20h1 and h2, respectively) are highlighted in red.

We tested the ability of the two mutated enzymes to rescue H4K20me3 state in Suv4-20h-double null primary MEFs. Both the variants were expressed and localized in the nuclei of transfected cells, as indicated by the eGFP signals. Nevertheless, unlike the wildtype proteins, neither variant restores the H4K20me3 mark at heterochromatic foci in Suv4-20h DKO MEFs (Fig. 25).

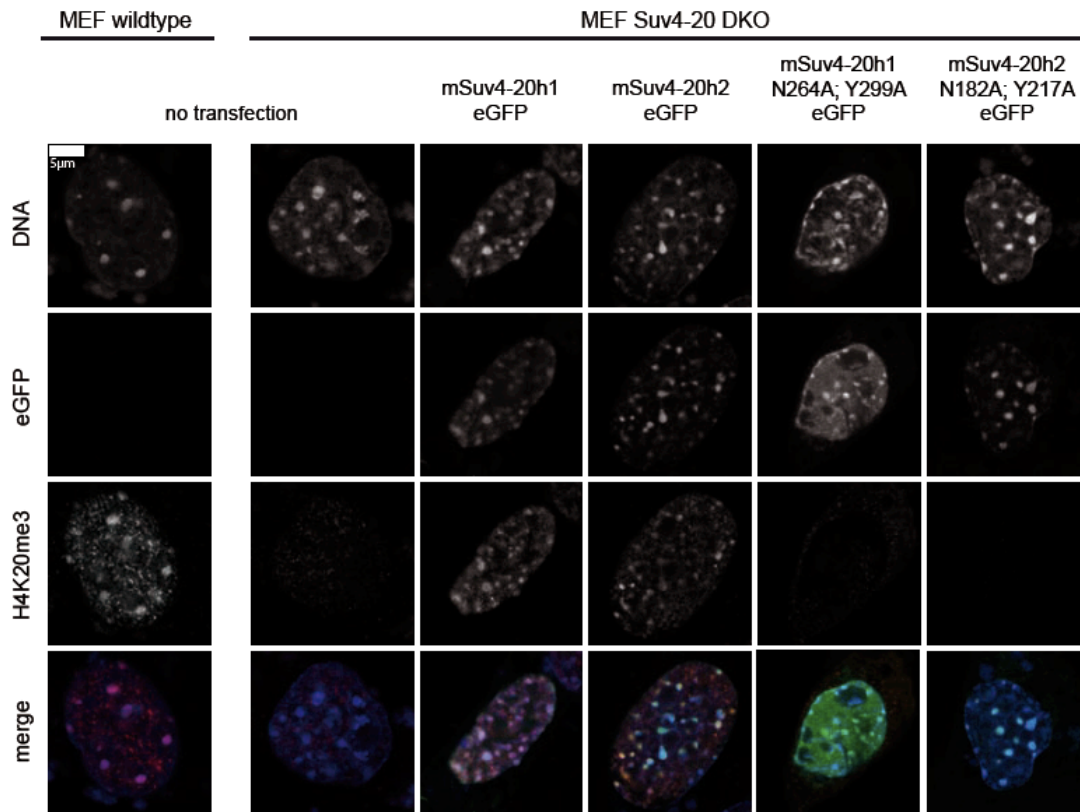


**Fig. 25: Mouse Suv4-20h double mutated enzymes are inactive.** Immunofluorescence of wildtype and Suv4-20h DKO MEFs transfected with eGFP-tagged indicated constructs. Untransfected Suv4-20h DKO MEFs show no H4K20me3 staining. The proper trimethylation pattern is re-established when wildtype, but not the double mutated, mouse HMTases are transfected. (Transfections were performed by Matthias Hahn, Laboratory of Professor Schotta, Department of Molecular Biology, Adolf Butenandt Institute, LMU, Munich).

To investigate whether the two variants possess dominant negative interference activity, we injected them into wt *Xenopus* embryos. As the western blot in figure 26a shows, forced expression of the mutated proteins triggered no changes in the methylation pattern of lysine 20 (compare lanes 1 and 5). Moreover, although the mutated variants accumulate to comparable levels as overexpressed wild-type proteins (Fig. 26b), they failed to re-established proper levels of H4K20me2 and H4K20me3 in xSuv4-20h double morphant embryos (compare lanes 2 and 6 with lane 4).

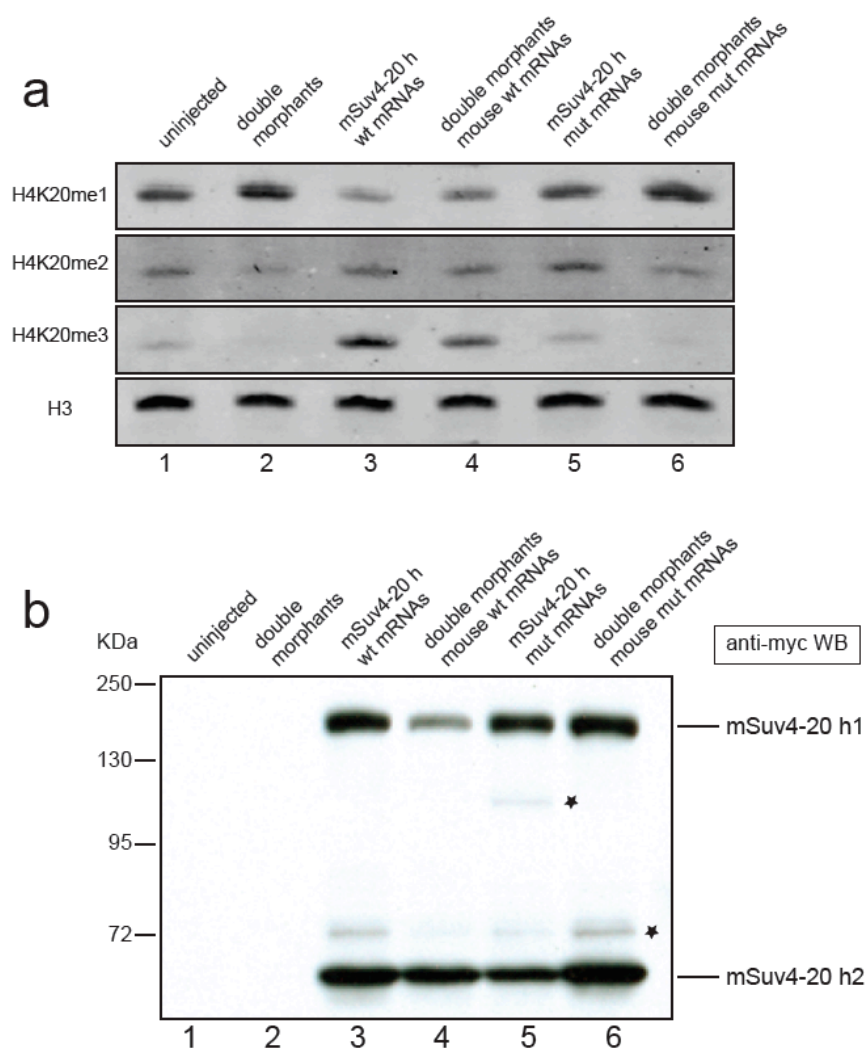


**Fig. 26: Functional SET domains are required for proper Suv4-20h HMTases activity.** (a) Western Blot analysis with antibodies against H4K20 mono-, di-, trimethylation and PanH3 (used as loading control) of uninjected embryos (lane 1), double-morphant embryos (lane 2), wt and mutant mSuv4-20h1, h2 mRNAs injected embryos (lane 3, 5 respectively), and double morphants coinjected either with wt or mutant mSuv4-20h1, h2 mRNAs (lane 4, 6 respectively). (b) Anti-myc western blot with the same samples used in a. Asterisks indicate unspecific bands. Comparable results were obtained in two additional independent experiments.

Morphologically, the proper eye structure, re-established upon coinjection of xSuv4-20h1 and h2 morpholinos plus wild type (active rescue) mSuv4-20h1, h2 mRNAs, was not developed when the mutated variants were expressed (inactive rescue; compare panels b and c of Fig. 27). The inability of the inactive mouse Suv4-20h enzymes to rescue the eye phenotype was detected in two independent experiments (Fig. 27d).

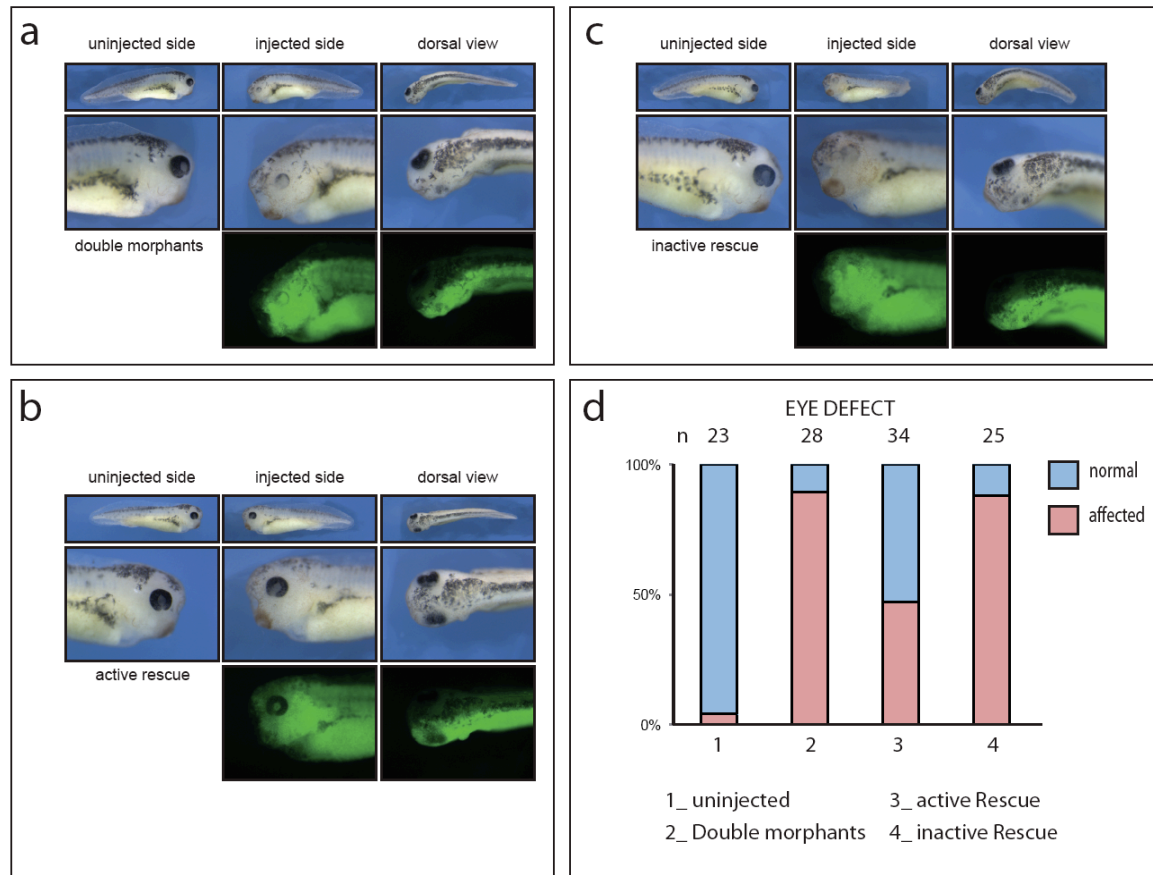


**Fig. 27: A functional SET domain is required for morphological rescue of double-morphant phenotypes.** (a-c) Morphological phenotypes of NF 30-33 double morphants (a), embryos injected with xSuv4-20h1, h2 morpholinos and active (active rescue, b), or inactive (inactive rescue, c) mSuv4-20h1, h2 mRNAs. Embryos were coinjected in one half at two-cell stage with Alexa Fluor 488 Dextran as lineage tracer (green channel) to identify the injected side and sort embryos. (d) Penetrance of the eye phenotype in the indicated samples. n= numbers of embryos analysed. The results from two independent experiments are presented.

These results clearly prove that single point mutations in key residues within the SET domain compromise the enzymatic activity of the two HMTases. The two variants failed to rescue the major developmental phenotypes in xSuv4-20h morphants. Therefore, the described phenotypes represent a direct consequence of the absence of normal H4K20me2 and me3 levels, rather than the absence of the enzymes themselves. It is remarkable that the two inactive enzymes do not exert any dominant interference activity when overexpressed alone in wild-type embryos, as it has been observed for other chromatin modifying enzymes, in particular ATP-dependent chromatin remodelling machine (Seo, Richardson et al. 2005). The implications of these findings will be discussed later.

#### 4.4.3 Gain-of-function analysis

To complement the Loss-of-Function analysis we next overexpressed Suv4-20h HMTases. Considering the comparable alteration of H4K20 methylation profile upon injection of single mRNAs (Fig. 19), Suv4-20h enzymes were overexpressed independently. Neither *Xenopus* nor mouse Suv4-20h mRNA injected embryos developed any morphological aberrations (Fig. 28a, b, d, e). Specifically, the size and the structure of the eye, as well as the number and the position of the melanocytes, which were strongly reduced upon protein knockdown, were indistinguishable between injected and uninjected sides. On the molecular level, Rx-1 and Pax-6 expression was also unaffected (Fig. 28c and f).

Taken together, these results demonstrate that an increase in H4K20me2/me3 levels is not sufficient to cause developmental defects in the embryo. This finding is in contrast to embryos in which Suv4-20h enzymes have been knocked down. The difference between loss- and gain-of-function analyses suggests that a certain minimal amount of H4K20me2 and me3 is required for proper eye and melanocyte formation, but experimentally increased levels of these modifications can either be tolerated or compensated.

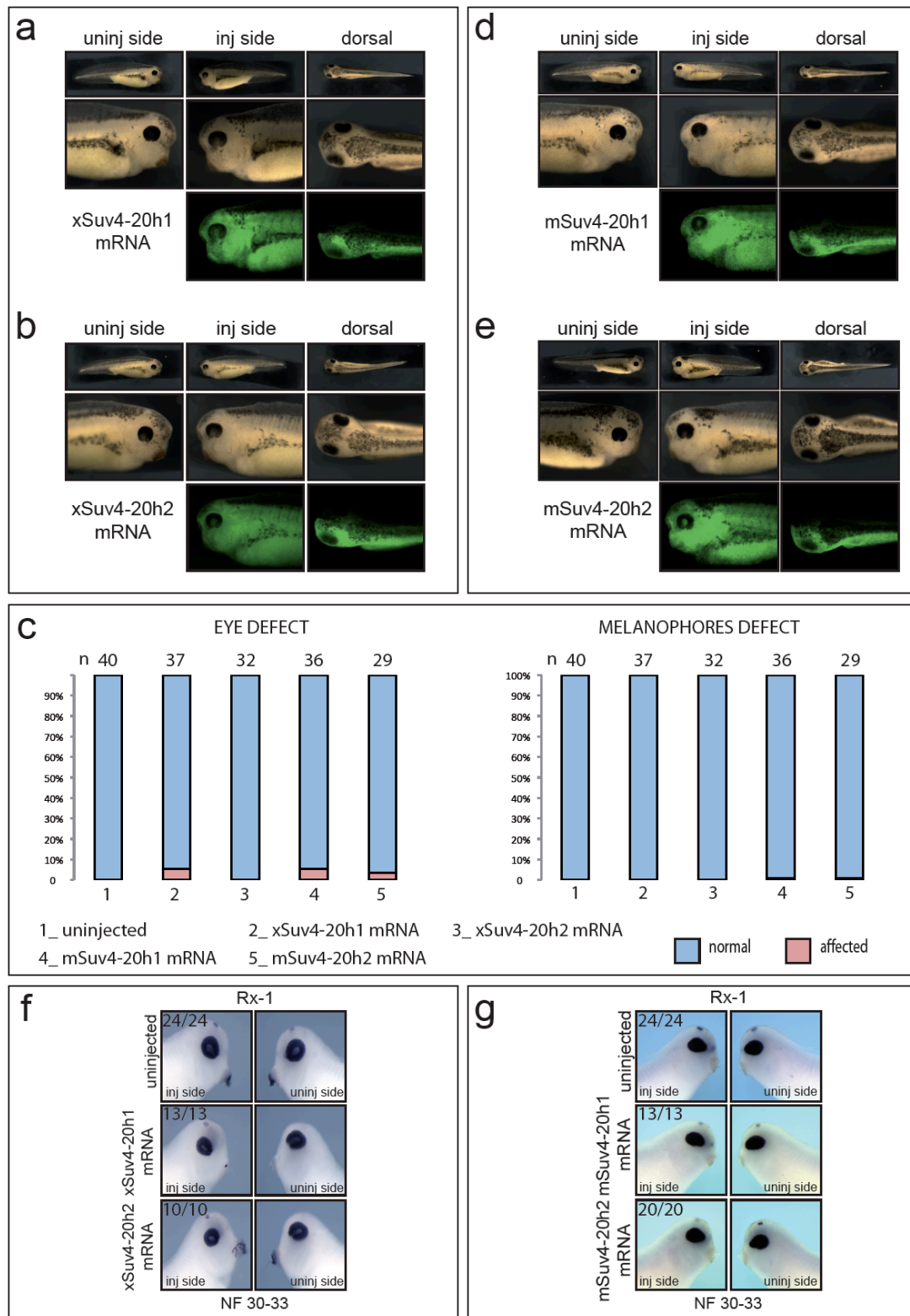


**Fig. 28: *Xenopus laevis* and *Mus musculus* Suv4-20h1 or h2 mRNA overexpression.** Morphological phenotypes of NF 30-33 embryos injected with xSuv4-20h1 (a) or h2 (b) and mSuv4-20h1 (d) or h2 (e) mRNAs as described in Material and Methods section. (c) Penetrance of the eye and melanophores phenotypes in embryos overexpressing *Xenopus* or mouse Suv4-20h1 or h2. n= numbers of embryos analysed. (f, g) *In situ* hybridization of NF30-33 uninjected embryos (top row) and embryos injected with Suv4-20h1 (middle row) or h2 (bottom row) mRNA using probes against Rx-1. The results from two to three independent experiments are presented.

#### 4.4.4 XSuv4-20h depletion misregulates a small group of genes

The morpholino-mediated morphological and molecular phenotypes described so far relate to ectodermal genes and tissues. To obtain a broader overview of the molecular deregulation caused by xSuv4-20h depletion, the transcriptomes of ctrl-MO and xSuv4-20h double-morphant embryos were compared. It is frequently observed that embryo cohorts develop in slight asynchrony as a non-specific consequence of morpholino injection, possibly obscuring transcriptional responses. Moreover, weakly and strongly affected embryos are mixed within the same injected population, potentially averaging out some gene deregulation. Finally, embryos injected radially with xSuv4-20h morpholinos show gastrulation problems, which prevents a proper analysis at neurula stage (data not shown). To bypass these complications, the microarray analysis was performed on half-injected embryos, which were dissected (based on Alexa448 fluorescence) into pairs of injected and uninjected sides. This approach allowed to minimize the non-specific developmental asynchrony that characterizes embryos cohorts injected with different morpholino, and to correlate injected versus uninjected sides within one morphant population. Control and xSuv4-20h morpholinos injected embryos were collected at NF15 and subsequently cut in two halves along the midline. The extracted mRNA was then used to perform the microarray analysis (Fig. 29) using the Affymetrix GeneChip® *Xenopus laevis* Genome 2.0 Array. Only 6% of the annotated 11639 probe sets present in the microarray were significantly altered in their expression, about equally split into up- (n=319) and downregulated (n=404) (Fig. 29b; for a complete list of the responding probesets see Appendix 2). On main caveat of this analysis is represented by incomplete gene annotation of the *Xenopus laevis* genome. This problem precludes a global and accurate analysis of the overall effects coupled to xSuv4-20h HMTases depletion. As a consequence, no clear developmental pathway or gene cohorts could be deduced from the data. Nevertheless analysis of gene ontology (GO) groups revealed that xSuv4-20h deletion leads to preferential downregulation of genes involved in DNA replication (data not shown). This very likely represents an indirect effect, given that H4K20me3 is considered a repressive histone mark. In general, the described results suggest that the observed phenotypes in double-morphant embryos originate from the misregulation of a small number of genes, rather than from global, pleiotropic effects.

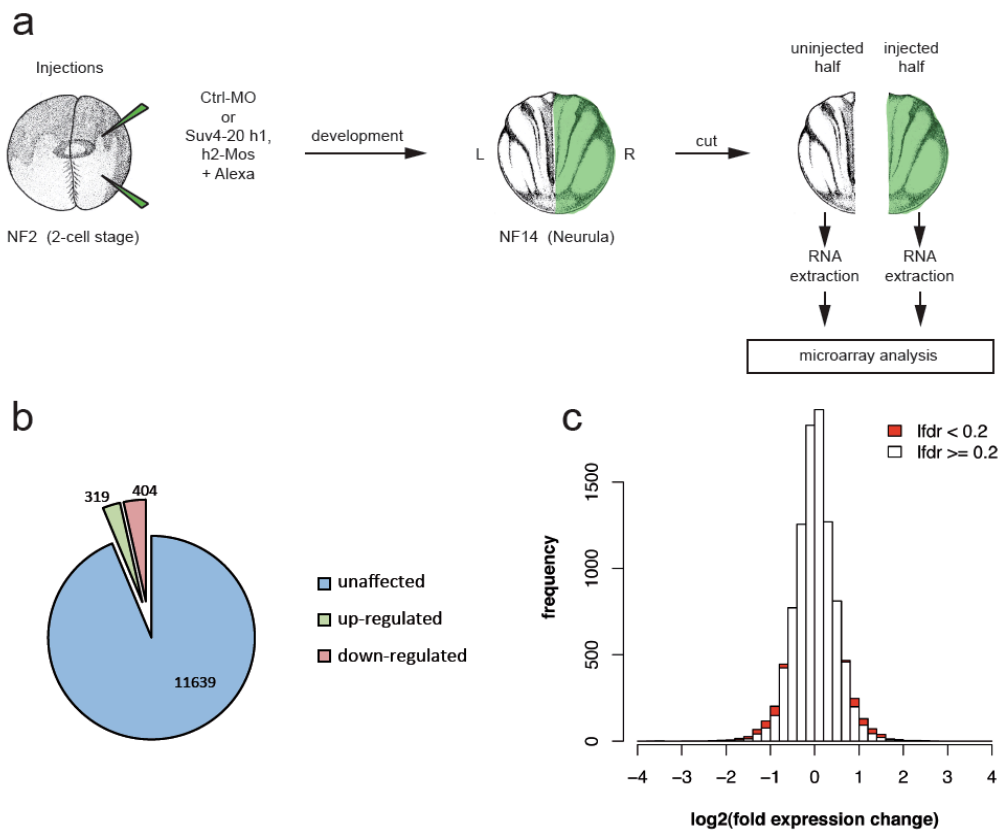


**Fig. 29: Microarray analysis.** (a) Schematic representing mRNA purification from NF14-15 embryos for global profiling experiments. (b) Pie chart showing the number of up- (green) and down- (red) regulated genes among the annotated probe sets. (c) Histogram summarizing the fold expression change of the analysed 9752 active genes. Indicated in red are responder genes (153 up, 169 down). LfdR, local fold discovery rate.

#### 4.4.5 XSuv4-20h enzymes are required for ectoderm formation

The broad expression of the two enzymes in the embryo (Fig. 10 and 11) and their apparent functional selectivity (Fig. 16) encouraged us to test, whether xSuv4-20h HMTases downregulation would affect the expression of genes involved in the specification of the three embryonic layers. Unfortunately microarray data were not strongly informative to detail the cause of the phenotypic perturbations in xSuv4-20h morphants. Therefore an extended analysis of candidate marker genes were carried out. We performed whole-mount RNA *in situ* hybridization with germ layer specific markers, comparing their expression in uni-laterally injected control morphants *versus* xSuv4-20h double morphants. Considering the clear downregulation of the anterior neural markers Rx-1 and Pax-6 in tailbud embryos we first examined several neuroectodermal genes at early stages of development. Injection of xSuv4-20h1 and h2 morpholinos suppressed the expression of the neural specific basic helix-loop-helix (bHLH) gene neurogenin (Ngnr 1a), Delta-like 1 and the neural differentiation

marker N-tubulin (Fig. 30): the lateral, intermediate and medial stripes of primary neurons, normally detected in a symmetric pattern on either side of the dorsal midline and positive for all the three genes during early to mid neurulation, were strongly reduced or completely absent from the injected side of double-morphant embryos. Coinjection of wt mSuv4-20h1 and h2 mRNAs effectively rescued the expression of the affected neuro-ectodermal markers while inactive mSuv4-20h HMTases were unable to re-establish the proper expression (Fig. 30, N-tubulin staining). Control morpholino injected embryos showed no effect on the expression of these marks. These phenotypes suggest that neurogenesis is inhibited from a very early stage on, i.e. determination of neuroblasts within the neuroectoderm.

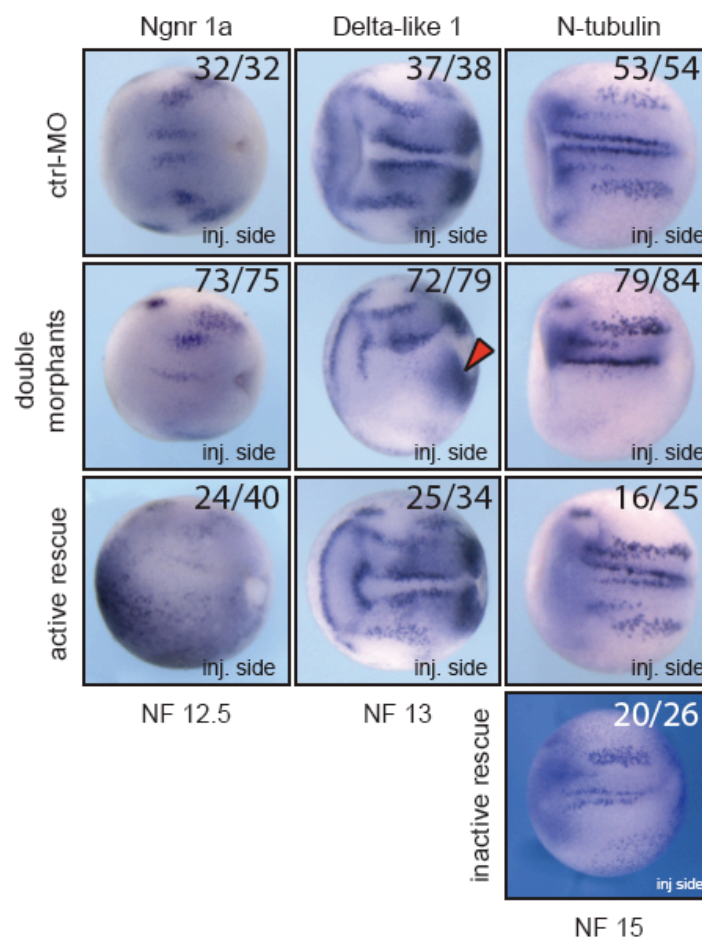


**Fig. 30: Neuroectodermal bHLH genes expression is compromised upon xSuv4-20h enzyme depletion.** RNA *in situ* hybridization analysis of ctrl-MO, double morphants and rescued embryos using probes against Ngnr 1a (NF 12.5), Delta-like 1 (NF 13) and N-tubulin (NF 15). Active/inactive rescue – embryos injected with xSuv4-20h1, h2 morpholinos and active or inactive mSuv4-20h1, h2 mRNAs, respectively. The pictures show dorsal view of stained embryos, anterior on the left. For N-tubulin, a representative picture of the rescue experiments performed with inactive mouse mRNAs is shown. The red arrowhead indicate unperturbed staining of the periblastoporal region for Delta-like 1, in double-morphant embryos. For each condition, numbers refer to embryos showing the displayed staining, in comparison to the total number of analysed embryos (n= three to six independent experiments).

#### 4.4.6 XSuv4-20h enzyme depletion affects epidermal ciliogenesis

The detailed observation of Delta-like 1 expression in late gastrula/early neurula morphant embryos revealed two important features: first, the typical mesodermal expression of this gene around the blastoporous was unaffected; second, and even more interesting, while Delta-like 1 expression in the neurogenic stripes of the forming brain was downregulated, its mRNA level in the epidermis was upregulated. Coinjection of xSuv4-20h enzymes morpholinos and wt mSuv4-20h enzymes mRNAs efficiently restored Delta-like 1 expression both in the neural plate (Fig.30) and in the non-neural ectoderm (Fig. 31).

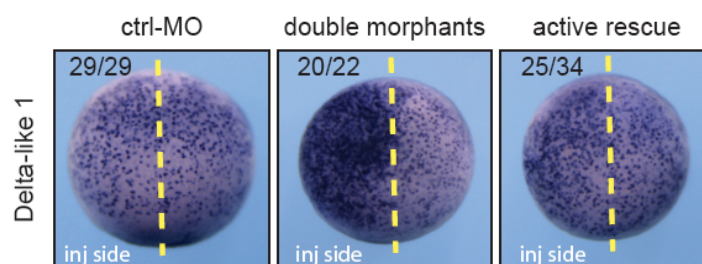


**Fig. 31: Non-neural Delta-like 1 expression is affected in morphants embryos.** Expression pattern of Delta-like 1 in the ventral side of ctrl-MO, double-morphant embryos and embryos rescued with wt mSuv4-20h mRNAs. Pictures show ventral views of NF 12.5 embryos. Anterior is on the top, posterior on the bottom. For each condition, numbers refer to embryos showing the displayed type of staining, in comparison to the total number of analysed embryos (n= two independent experiments).

Delta-like 1 expression in the non-neural ectoderm has been linked to the formation of ciliated cells in *Xenopus* embryonic skin (Deblandre, Wettstein et al. 1999), which can be recognized by the presence of acetylated alpha-tubulin on the extracellular cilia tuft. To further characterize the morphant embryos phenotype, immunocytochemistry was performed. As shown in figure 32, acetylated alpha-tubulin staining was less intense upon xSuv4-20h enzymes depletion; moreover, each spot, identifying a single ciliated cell, appeared smaller in morphant embryos compared to the control ones. Upon rescue, both these features were properly re-established (Fig. 32).

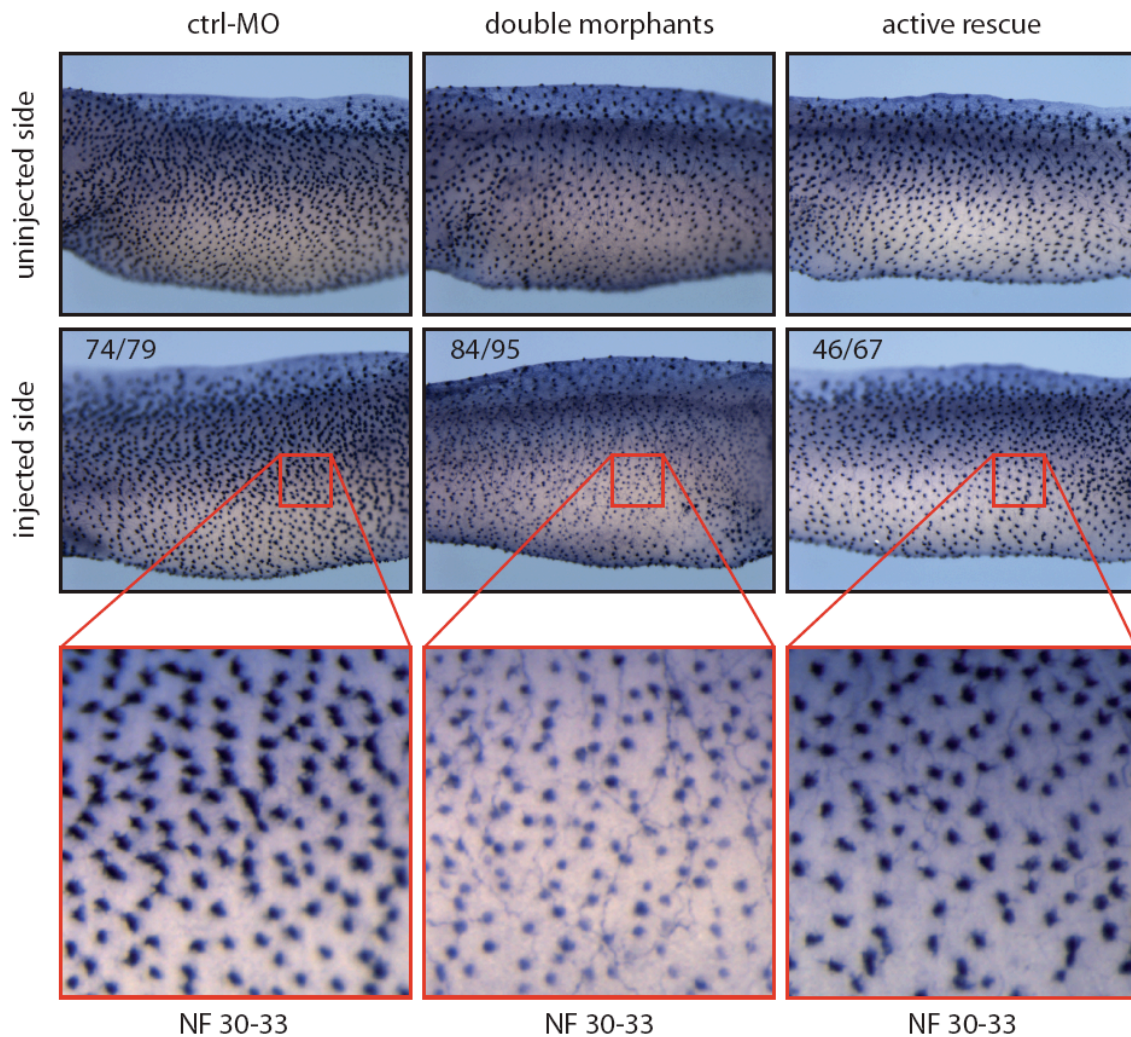


**Fig. 32: Acetylated alpha tubulin staining appeared reduced upon xSuv4-20h enzymes depletion.** Immunocytochemistry using an antibody against acetylated alpha tubulin in NF 30-33 embryos. The pictures show uninjected (top row, head on the left) and injected (middle row, head on the right) side of ctrl-MO, double morphants and rescued embryos. The bottom row represents a zoom of the areas indicated by the red square. For each condition, numbers refer to embryos showing the displayed staining, in comparison to the total number of analysed embryos (n= three to four independent experiments).

To confirm the ICC results, and to better visualize the ciliated cells in NF 30-33 embryos, confocal microscope analysis was performed (Fig. 33). Cilia in double-morphant embryos appeared less and shorter than on the control side. Moreover, upon rescue, although the number of cilia per cell increases and was comparable with that of control morpholino injected embryos, nevertheless the length of the cilia appeared not properly re-established, suggesting a partial rescue (Fig. 33).

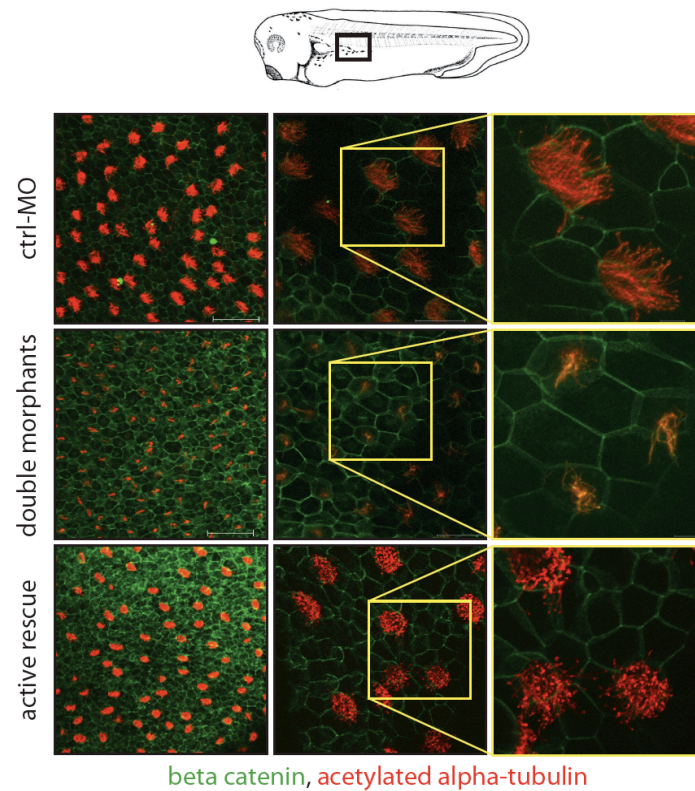


**Fig. 33: Confocal analysis of ciliated cells.** Confocal fluorescent microscope pictures of NF 30-33 ctrl-MO, double morphants and rescued embryos, using antibodies against acetylated alpha tubulin (red, for cilia identification) and beta catenin (green, to mark cells boundaries). For each condition, three to five embryos were analysed (n= one independent experiment).

Finally we used scanning electro-microscopy (SEM) to visualize ciliated cells on tadpole embryos (Fig. 34).

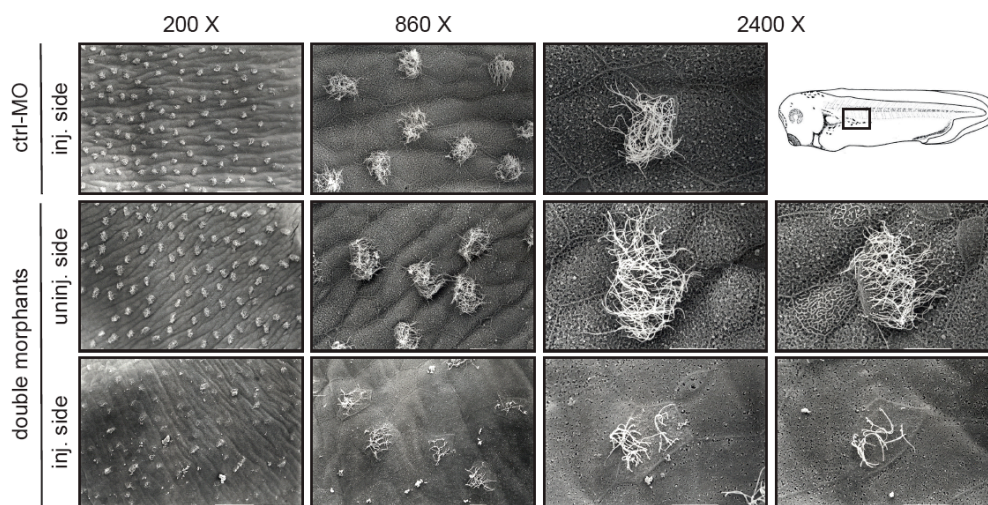


**Fig. 34: SEM analysis of ciliated cells.** Scanning electro-microscopy analysis pictures of NF 30-33 ctrl-MO and double-morphant embryos. For each condition, three to five embryos were analysed (n= one independent experiment).

Once again the analysis confirmed the previous results. The clear pictures obtained with SEM highlights that cilia formation was compromised both with regard to length and number, upon xSuv4-20h enzymes depletion. Taken together, these preliminary results suggest a molecular link between the H4K20me2/me3 marks and ciliogenesis in *Xenopus* development.

#### 4.4.7 XSuv4-20h enzymes are required for neurogenesis

The downregulation of key components of the proneural/neurogenic gene cascade (Fig. 30) clearly indicates an involvement of xSuv4-20h HMTases in neurogenesis. Therefore we analysed the expression of two neuronal markers implicated in the formation of the neural tube: Nrp1, ubiquitously expressed throughout the neural plate, and the neural cell adhesion molecule, N-CAM, associated with the central nervous system histogenesis (Kintner 1992). In double-morphant embryos both the genes were strongly reduced (Fig. 35). The proper expression pattern was re-established coinjecting xSuv4-20h morpholinos plus murine Suv4-20h wt mRNAs (active rescue).

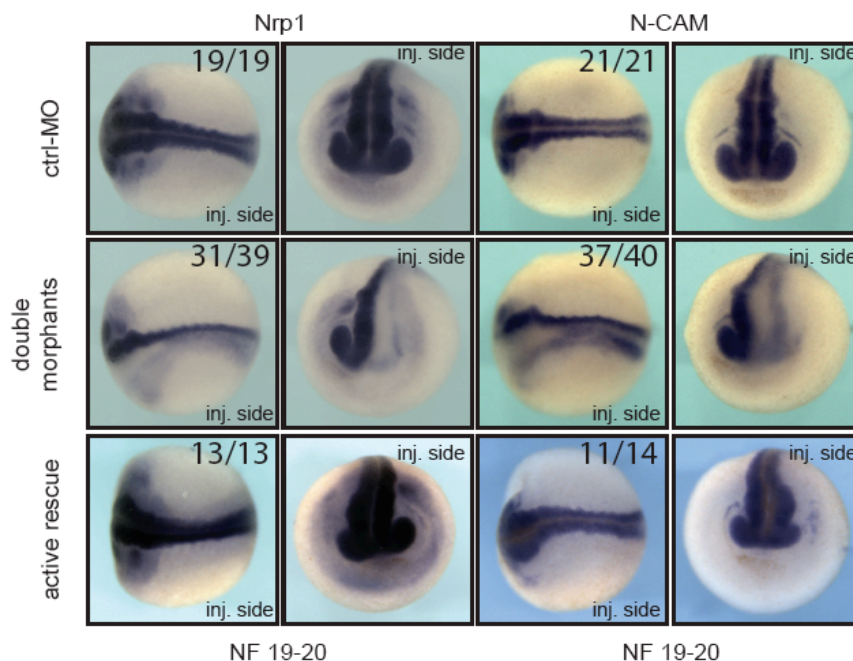


**Fig. 35: Nrp1 and N-CAM expression is reduced upon xSuv4-20h morpholinos injection.** RNA *in situ* hybridization analysis of ctrl-MO, double morphants and rescued embryos using probes against Nrp1 and N-CAM (NF 19-20). The pictures show dorsal view of stained embryos, anterior on the left. For each condition, numbers refer to embryos showing the displayed staining, in comparison to the total number of analysed embryos (n= two independent experiments).

At the same developmental stage, in which *Ngnr 1a*, *Delta-like 1* and *N-tubulin* were downregulated, the expression of the pan-neural transcription factors *Sox2*, *Sox3* and *Sox11* was unperturbed in the double morphants (Fig. 36). Moreover, the RNA in situ pattern of the epidermal keratin gene *XK81*, a non-neural ectodermal marker, was only mildly perturbed at the ectoderm-neuroectoderm border, which appeared fuzzy and not properly established upon *xSuv4-20h* depletion (Fig. 36). Interestingly, staining for both *XK81* as well as *Sox2* and *Sox3*, revealed that the closure of the neural tube was delayed on the injected side. This suggests an involvement of the two enzymes in the regulation of morphogenetic processes during neurulation. As a consequence of this effect, the *Sox2* and *Sox3* domains appear slightly broadened in the injected half. Nevertheless, the similar staining intensity of the two markers in injected versus uninjected side indicated rather normal expression levels for the two genes.

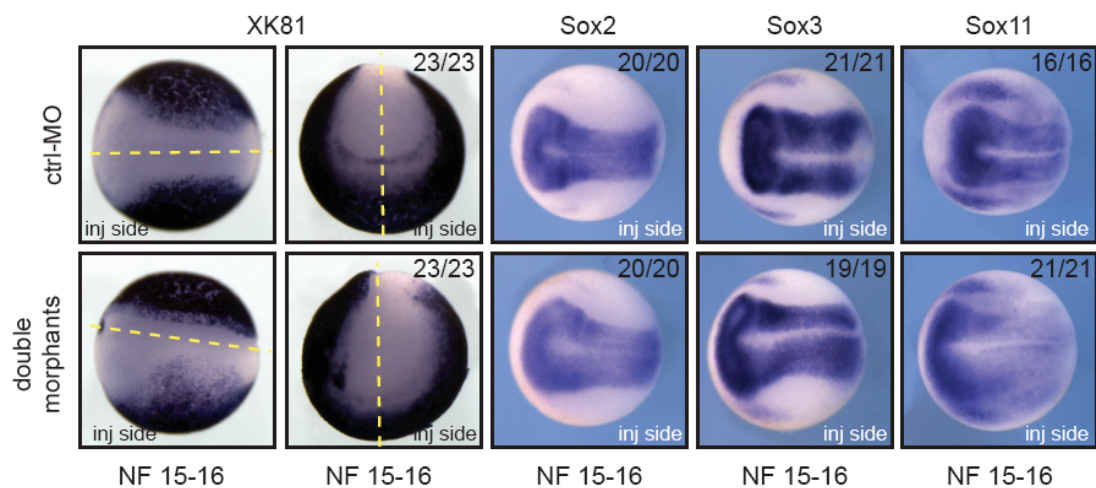


**Fig. 36: *XK81* and *Sox* genes expression are unaffected upon *xSuv4-20h* enzymes depletion.** Expression patterns of *XK81* and neuroectodermal *Sox2*, *Sox3* and *Sox11* genes in ctrl-MO and double-morphant embryos. Pictures show dorsal view of NF15-16 injected embryos, with the anterior on the left. Additional anterior views of embryos, with dorsal side on the top and ventral side on the bottom are shown for *XK81*. For each condition, numbers refer to embryos showing the displayed staining, in comparison to the total number of analysed embryos (n= two independent experiments).

Additionally, we tested the expression the mesodermal markers *Xbra*, *VegT*, *MyoD*, and the endodermal genes *Sox17  $\alpha$*  and *Endodermin*. Although the *xSuv4-20h* HMTases are expressed very broadly, including the prospective mesodermal germ layer (see Fig. 10 and 11), none of these genes was misregulated in double-morphant embryos (Fig. 37).

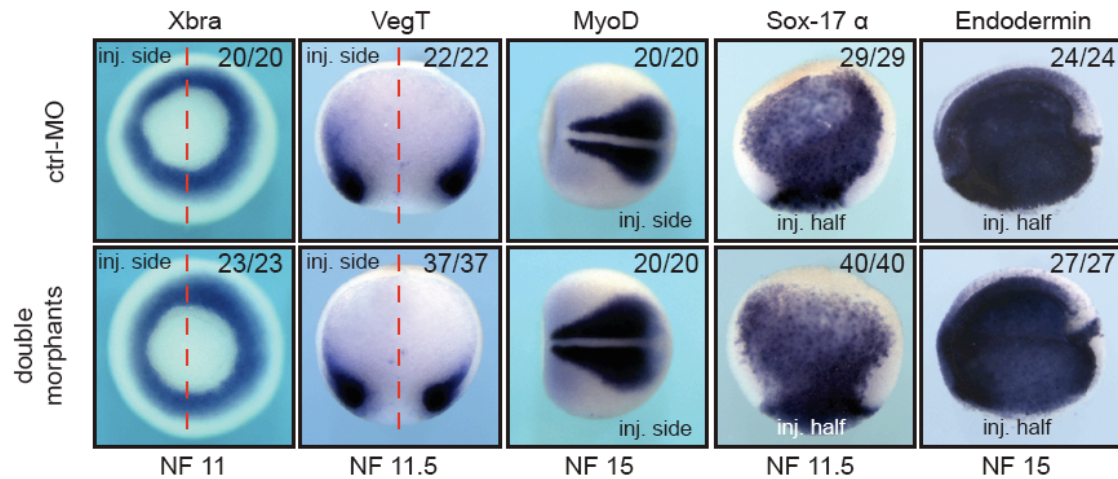


**Fig. 37: Mesodermal and endodermal markers are expressed normally in double-morphant embryos** RNA *in situ* hybridization analysis showing expression patterns of mesodermal (Xbra, Veg-T, MyoD) and endodermal (Sox-17  $\alpha$ , Endodermin) genes in ctrl-MO and double-morphant embryos. Xbra pictures show vegetal view of NF 11 embryos. MyoD pictures show dorsal view of NF 15 stained embryos, with the anterior on the left. For Veg-T and Sox-17  $\alpha$  expression, pictures show internal stain of NF11.5 embryos bisected along the animal-vegetal axis. For Endodermin detection, saggital sections of NF 15 embryos were created. Pictures show internal stain of the injected half of ctrl-MO and double-morphant embryos. The head is on the left. The closing blastopore is visible on the posterior most part of the embryos. For each condition, numbers refer to embryos showing the displayed staining, in comparison to the total number of analysed embryos (n= three independent experiments).

The loss of function analysis, which revealed a germ-layer specific requirement for xSuv4-20h activity in the ectoderm, was complemented by experiments in which either mouse or frog Suv4-20h mRNAs were microinjected. As we have shown before, this leads to a significant increase in H4K20me2 and –me3 levels (Fig. 19). Surprisingly, expression of the tested neuroectodermal, mesodermal and endodermal genes was completely normal (Fig. 38).

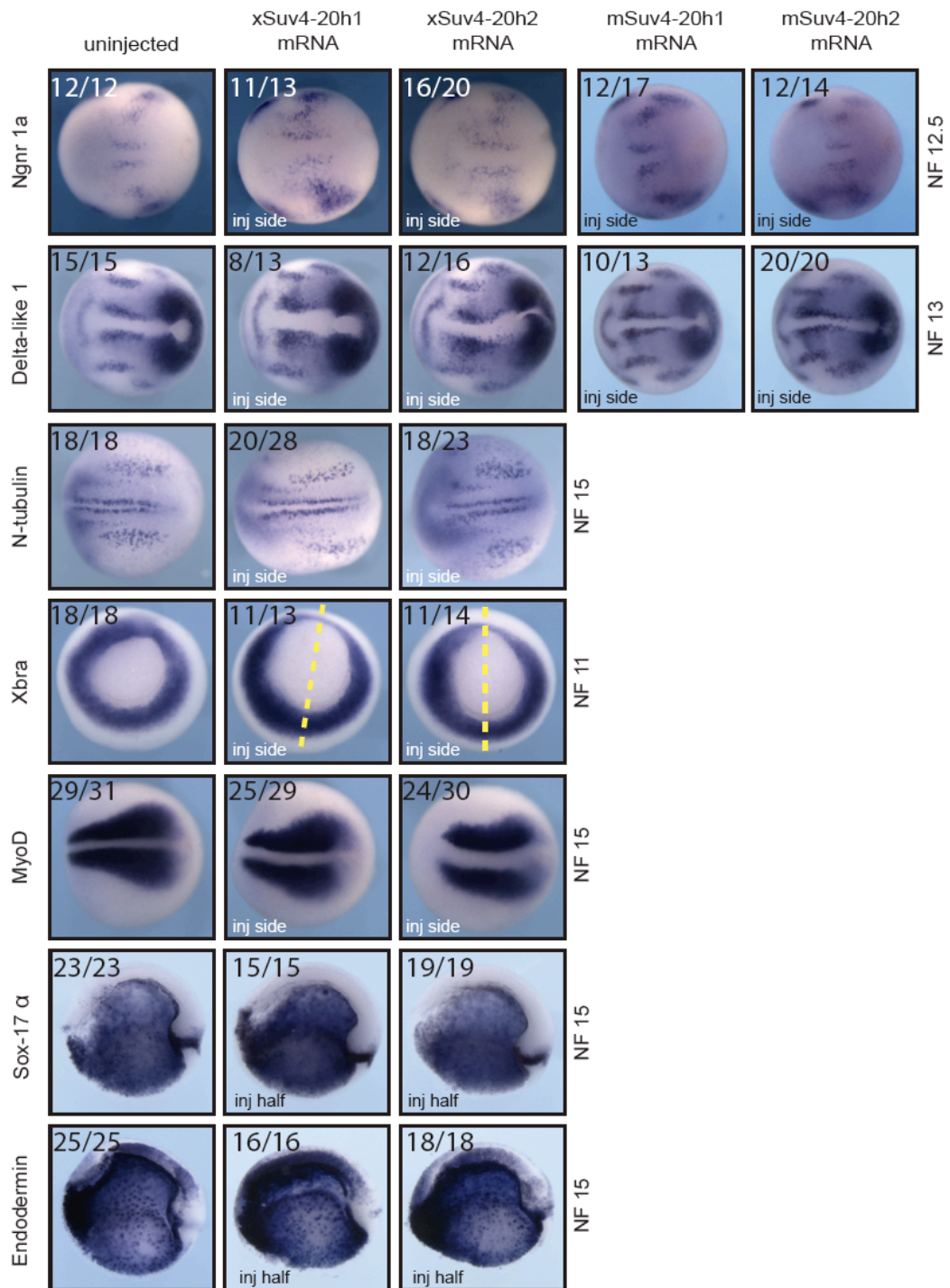


**Fig. 38: Overexpression of either *Xenopus* or mouse *Suv4-20h* mRNAs does not perturb germ layer-specific gene expression patterns.** RNA *in situ* hybridization analysis of uninjected embryos and embryos injected with *Xenopus* or mouse *Suv4-20h1* or *h2* mRNA, using probes against *Ngnr 1a*, *Delta-like 1*, *N-tubulin*, *Xbra*, *MyoD*, *Sox17  $\alpha$* , *Endodermin*. Pictures show dorsal view of stained embryos, anterior is on the left; *Xbra* pictures show vegetal view of NF11 embryos; *MyoD* pictures show dorsal view of NF 15 embryos, with the head on the left. For *Sox-17  $\alpha$*  and *Endodermin* sagittal sections of NF 15 embryos were created; pictures show internal view of the injected halves, with anterior on the left. For each condition, numbers refer to embryos showing the displayed staining, in comparison to the total number of analysed embryos (n= two independent experiments).

Considering the prominent absence of markers expressed in late stages of neuronal commitment from double-morphant embryos, we decided to investigate the neurogenic program in a broader manner, specifically in form of genes which act upstream of *Ngnr 1a*. At midgastrula *FoxD5*, *Geminin*, *Zic1*, *Zic2*, *Zic3* and *irx1* (*Xiro1*) transcripts are expressed in the prospective neuroectoderm. These genes – expressed in overlapping domains – exert pivotal role in the early neural plate establishment. While *FoxD5*, *Geminin* and *Zic2* maintain an undifferentiated neuroectoderm state, *Zic1*, *Zic3* and *Xiro1* have been shown promote the transition to neural differentiation (Rogers, Moody et al. 2009). At NF11, *FoxD5* and *Geminin* expression appeared unaffected upon morpholinos injections, while *Xiro1*, *Zic1*, *Zic2* and *Zic3* patterns were strongly reduced in the injected side of double-morphant embryos (Fig. 39).

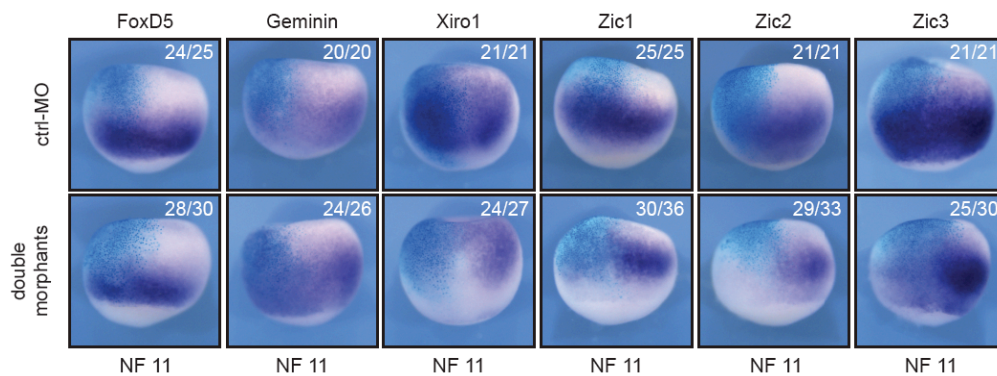


**Fig. 39: Early neuroectodermal genes expression in *xSuv4-20h* depleted embryos.** RNA *in situ* hybridization analysis showing expression patterns of the neuroectodermal genes *FoxD5*, *Geminin*, *Xiro1*, *Zic1*, *Zic2*, *Zic3*, at NF 11 in ctrl-MO and *xSuv4-20h* double-morphant embryos. Embryos were injected in one blastomere at two cells stage with morpholino (ctrl or *xSuv4-20h1/h2*) plus *LacZ* mRNA to detect the injected side (light blue stain). Pictures show dorsal views of representative embryos; the animal pole is on the top, the vegetal pole is on the bottom. For each condition, numbers refer to embryos showing the displayed staining, in comparison to the total number of analysed embryos (n= two to three independent experiments).

Taken together these results demonstrate that *xSuv4-20h* HMTases are critical for neural development, but dispensable for mesoderm and endoderm formation in *X. laevis*.

To further confirm the specific role of *Xenopus Suv4-20h* enzymes in neural development, we considered two different approaches. In a first series of experiments we performed injections at 8-cell stage in the animal or vegetal pole blastomeres, selectively depleting cells from *xSuv4-20h* activity that belong either to mesendoderm (vegetal injections Fig. 40) or ectoderm (animal injections Fig. 40).

Vegetal pole blastomere injections had no evident morphological and molecular phenotype (Fig. 40b and c), although differentiation of the proctodeum was delayed in double morphants (Fig. 40b dashed circle). Conversely, animal injections resembled the global injections at two-cell stage, with the eye and melanophores missing in double-morphant embryos, while mesodermal and endodermal structures normally developed (Fig. 40e). Consistent with these morphological results, Delta-like 1 expression was suppressed, while MyoD and Sox17  $\alpha$  appeared unaffected (Fig. 40f).

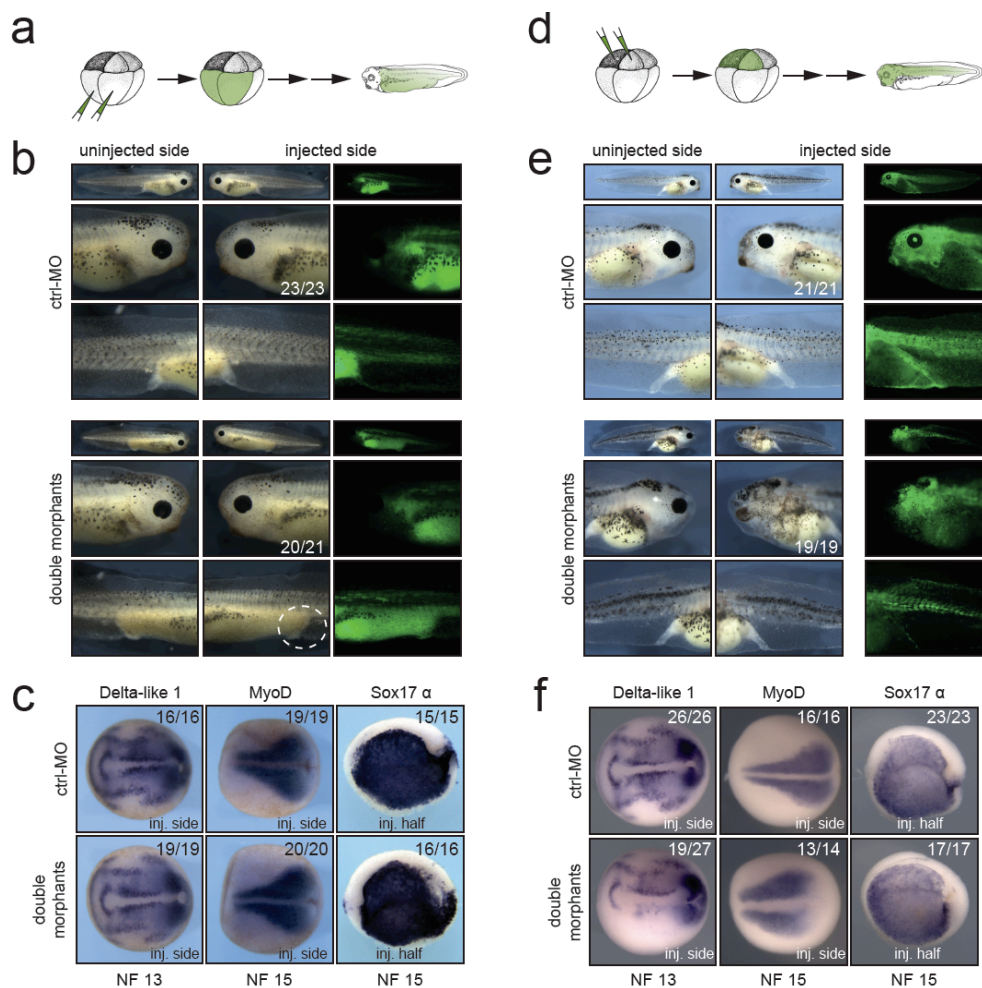


**Fig. 40: xSuv4-20h1/h2 enzymatic activity is required in the ectodermal germ layer.** (a) and (d) Schematic illustrations of targeting microinjections into mesendodermal or ectodermal territories at 8-cell stage, respectively. (b) Injecting xSuv4-20h MOs into the mesendoderm causes no apparent morphological phenotype in the embryo; the white dashed circle indicate proctodeum in double-morphant embryos; (c) neural, mesodermal and endodermal marker genes are expressed normally. (e) Xsuv4-20h MOs reduce eyes, cranial and trunk melanophores, when injected into the ectoderm; (f) expression of all tested markers in mesoderm and endoderm is normal, except for Delta-like 1, whose expression specifically in the open neural plate is strongly reduced on the injected side. Global morphology was assessed at hatching stage (NF 36), molecular markers at indicated stages during neurulation. Top row images in b and e depict whole embryos for overview. For each condition, numbers refer to embryos showing the displayed staining, in comparison to the total number of analysed embryos (n= two to three independent experiments).

These results unambiguously demonstrate, therefore, that the phenotypes in xSuv4-20h morphants arise in the ectoderm, and are not indirect consequence of perturbed mesoderm formation. Thus, accumulation of H4K20me3 is a prerequisite for differentiation of both regions of the ectoderm, i.e. epidermis and neuroectoderm.

To demonstrate the critical role of xSuv4-20h enzymes in ectodermal differentiation in complete absence of mesendoderm, we took advantage of the animal cap (AC) assay (Green 1999). In this technique, small animal pole explants are dissected from the embryos and cultured in isolation. These explants differentiate into epidermis by default, but can be forced to become neural by inducers such as Noggin (Lamb, Knecht et al. 1993). We exploited this effect to test, whether neural induction by Noggin occurs in the absence of xSuv4-20h enzymes.

Default differentiation was undistinguishable between control and double-morphant explants (Fig. 41): XK81 was expressed, while Nrp1 and Xbra expression (indicating absence of contaminating mesoderm) was not detected. Upon Noggin injection, control caps clearly upregulated Nrp1, while suppressing XK81, consistent with neural induction. Coinjection of Noggin mRNA plus xSuv4-20h HMTases morpholinos reduced Nrp1 induction, while XK81 expression was kept downregulated. Thus, double-morphant caps are both refractory to neural induction and restrained in epidermal differentiation.

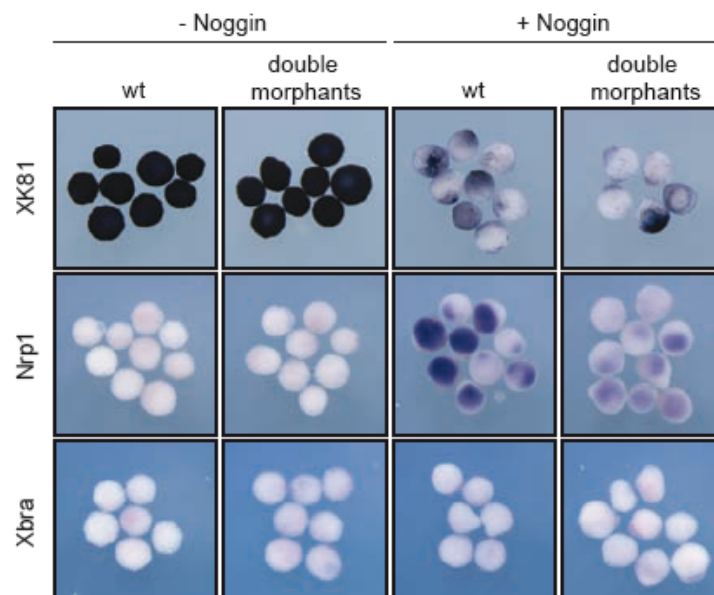


**Fig. 41: *In vitro* induction of xSuv4-20h double-morphant animal cap explants.** Noggin-dependent neuralisation. XK81, Nrp1 and Xbra expression is monitored in uninjected control caps and double-morphant caps with or without Noggin mRNA. Note that explants coinjected with xSuv4-20h MOs together with Noggin mRNA show reduced Nrp1 expression, but normal downregulation of XK81 mRNA. The figure shows one representative experiment (n= three independent experiments).

Notably, double-morphant animal caps responded normally to mesoderm induction. Caps cultured in medium containing the TGF-beta ligand Activin differentiated into skeletal muscle (Sokol, Wong et al. 1990), as shown by immunocytochemistry (ICC) against myosin heavy chain protein (MHC- $\alpha$ ). Both control and xSuv4-20h1 and h2 morpholino injected caps showed no difference as to MHC- $\alpha$  staining in presence of Activin (Fig. 42).

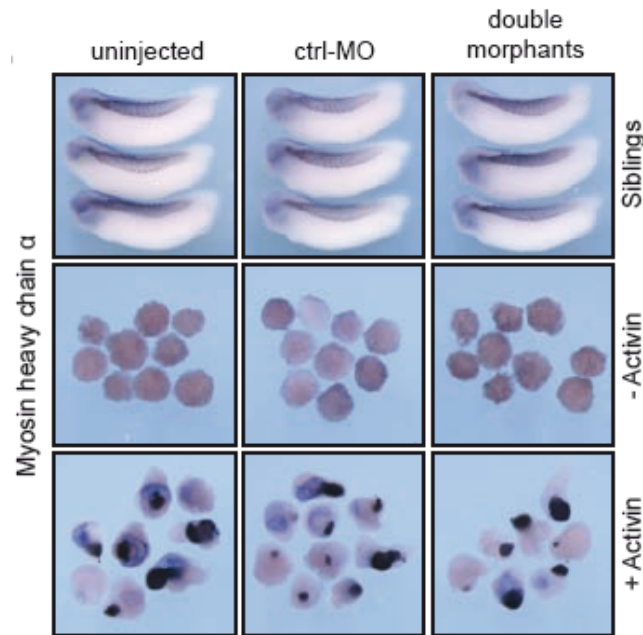


**Fig. 42: xSuv4-20h enzymes depletion has no effect on Activin-mediated mesoderm induction.** Muscle induction by Activin A in uninjected, ctrl-MO injected, and xSuv4-20h double-morphant animal caps. Top row demonstrates staining intensity of endogenous myosin heavy chain (MHC- $\alpha$ ) expression, in non-dissected sibling embryos, for comparison. The figure shows one representative experiment (n= two independent experiments).

These results confirm the crucial role of xSuv4-20h enzymes in coordinating the proper expression of neural markers genes, and show that in the absence of these two enzymes normal neural development is prevented. At the same time, mesoderm induction does not require xSuv4-20h activity, indicating a requirement for the function of the two enzymes that is restricted to the neuroectoderm. Considering the defects in ciliogenesis, previously described, this conclusion may be extended to the ectoderm.

#### 4.4.8 XSuv4-20h HMTases affect apoptosis and cell proliferation independently from the loss of primary neurons

The main characters of the double-morphant phenotypes described so far could be rooted in different scenarios. For instance, the loss of neurons could be due to a block in differentiation. Alternatively, prospective neuronal cells could be eliminated by apoptosis, or fail to be born due to an arrest in cell proliferation. We checked whether xSuv4-20h depletion activated apoptosis in embryos. Immunocytochemistry with an antibody against the active form of Caspase3 revealed a broad increase in the number of cells with activated Caspase3 on the injected side of double morphants. These embryos showed the described molecular phenotypes, as shown by Delta-like 1 and N-tubulin repression (Fig. 43). To clarify, whether the increase in apoptotic cells was responsible for the loss of the neuroblasts, we coinjected the potent anti-apoptotic factor xBcl-2 together with xSuv4-20h morpholinos. Under these conditions, the number of active Caspase3-positive cells was reduced to normal levels of control embryos; however, this did not restore the Delta-like 1 and N-tubulin positive neuronal cell population. This excludes selective death of neuronal cells as possible explanation for the xSuv4-20h morphants phenotype. Overexpression of xBcl-2 mRNA alone slightly reduced Caspase3 staining on the injected side of treated embryos, but had no effect on the expression of the tested probes by in situ hybridization (Fig. 43).

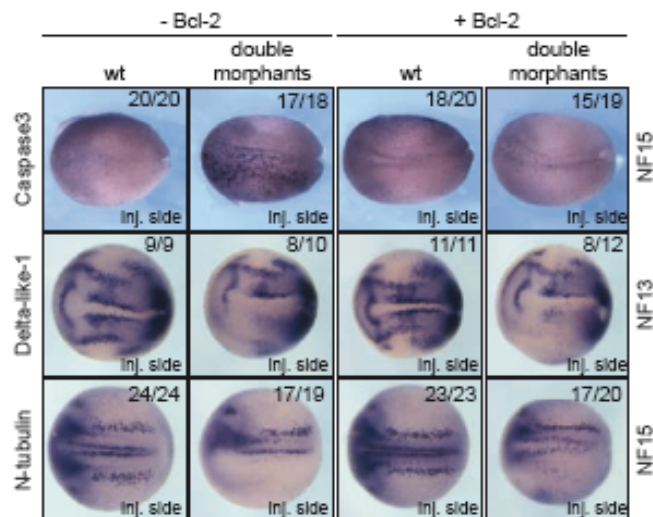


**Fig. 43: xSuv4-20h double-morphant embryos show increased apoptosis.** Double morphants show increased number of apoptotic cells during neurulation. Top row – immunocytochemistry for active Caspase3 in unilaterally injected embryos (NF15). Middle and bottom rows - RNA *in situ* hybridisation for Delta-like 1 (NF13) and N-tubulin mRNAs (NF15). Pictures show dorsal views, with anterior to the left. For each condition, numbers refer to embryos showing the displayed staining, in comparison to the total number of analysed embryos (n= two independent experiments).

These results suggest that although the depletion of xSuv4-20h enzymes triggered an upregulation of apoptosis in the embryos, nevertheless neurogenesis appeared to be compromised by a cause other than cell death.

Suv4-20h double null murine embryonic fibroblasts, which lack H4K20me2 and me3 are known to be compromised at the G1/S phase transition, showing reduced cell proliferation capacity (Schotta et al. 2008). Therefore we decided to test, via immunocytochemistry, whether morpholinos injections reduced the number of H3S10P positive cells (Fig. 44). Proliferation was not affected upon control morpholino injection, while double-morphant embryos showed a two-fold reduction in the number of proliferating cells ( $p=0.0058$ ) (Fig. 44b).

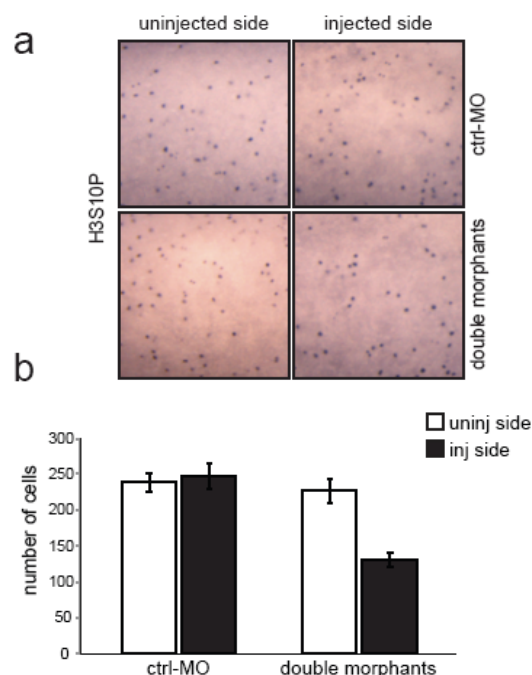


**Fig. 44: xSuv4-20h double-morphant embryos show reduced cell proliferation.** (a) Proliferation assay – immunocytochemistry for the mitotic histone modification H3S10P in ctrl-MO *versus* double-morphant embryos. (b) The chart shows a two-fold difference in the number of H3S10P positive cells on the injected side of double morphants. Data represent mean values of four embryos per condition from two independent experiments; error bars indicate SEM.

The mild reduction in cell proliferation is certainly influenced by the increased rate of apoptosis in double-morphant embryos. However, it is unlikely that the nearly complete loss of N-tubulin positive neurons is brought about by this mild effect, because one would expect much more neuronal cells, i.e. cells that are born and differentiate into neurons, than observed. In fact, neuronal differentiation is quite insensitive to cell cycle inhibition and occurs even in presence of Hydroxyurea and

Aphidicolin. (Harris and Hartenstein 1991). Thus, more likely, the described phenotype represents a block in neuroectodermal differentiation.

#### **4.4.9 XSuv4-20h enzyme depletion triggers the upregulation of the pluripotent gene Oct-25**

We finally considered the possibility that xSuv4-20h depleted cells from the animal hemisphere could be specifically impaired in their ability to undertake the neurogenic pathway. Neural competence requires several genes, including *Zic1* and *Xiro1*, which are involved in neural plate formation (Fig. 4 and 39). At the time when these genes are induced, embryonic cells in the animal hemisphere are still uncommitted and express members of the POU-V gene family (i.e. Oct-25, Oct-60 and Oct-91) that encode functional paralogs of the mammalian pluripotency regulator Oct4 (Hinkley, Martin et al. 1992; Morrison and Brickman 2006). In this line of argumentation, neural competence may not fully form in xSuv4-20h double-morphant embryos, if the H4K20me3 mark is involved in reducing or repressing pluripotency genes during development down to level compatible with germ layer differentiation. We therefore checked the expression of these factors (Fig. 45). At blastula, the three *Xenopus* genes are broadly expressed throughout the animal pole – i.e. in all naïve ectodermal cells – (data not shown). During gastrulation, Oct-25 and Oct-91 expression becomes restricted to the presumptive floor plate (notoplate) of the neuroectoderm, and in cells associated with the ventricular cavity in the anterior neural plate. Oct-60 expression, predominantly expressed during oogenesis, could not be detected at the same stage (NF 14-15). XSuv4-20h1 and h2 morpholinos injections caused a reproducible and readily detectable upregulation of Oct-25 on the injected side. Oct-91 mRNA was expressed normally in the majority of the embryos, although some showed a mild upregulation in the same domain as Oct-25 (Fig. 45). Interestingly, Oct-25 ectopic expression was detected exclusively in the deep/sensorial ectodermal layer, extending from the dorsal midline down to the ventral midline of the injected side. Cells in this layer are known to be precursor cells. Depending from their position along the dorso-ventral axis, they contribute to the formation of the different cells of the nervous system, from the neural plate, and to the differentiation of several epidermal cell types, originating from the non-neural ectoderm (Hartenstein 1989; Deblandre, Wettstein et al. 1999). It is possible that the described phenotypes in neuroectoderm and ectoderm share a common mechanism, i.e. the deregulation of Oct-25. Control morpholino injected embryos showed no

effect on the expression of the described markers. Interestingly, only wt mSuv4-20h enzymes restored the normal Oct-25 expression pattern (i.e. they repressed Oct-25 transcription in the ectoderm), while the overexpression of inactive mSuv4-20h HMTases mRNAs had no effect (Fig. 45, Oct-25 staining). A derepression of the Oct-25 gene was also observed in double-morphant AC explants, while Oct-60 and Oct-91 transcription remained normal (Fig. 46). Thus, the explant experiment indicates a selective response of the Oct-25 gene that occurs in isolated ectoderm, independent from mesendodermal signals.

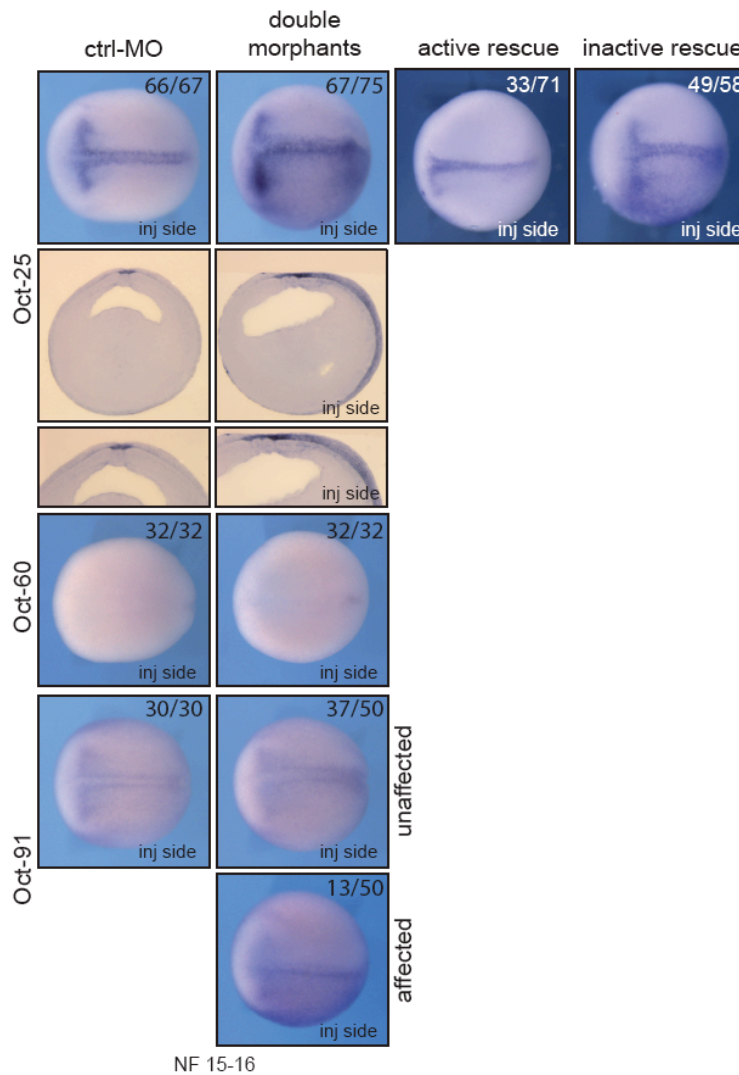


**Fig. 45: xSuv4-20h double morphants maintain Oct-25 expression in deep-layer ectoderm.** RNA *in situ* hybridization analysis for Oct-25, Oct-60 and Oct-91 in embryos injected with ctrl or xSuv4-20h1 and h2 morpholinos. Embryos were injected unilaterally at two-cell stage and fixed at midneurula stage (NF 15). Injected sides were defined by coinjected Alexa-fluorescence prior to *in situ* hybridisation. The figure shows dorsal views of stained embryos with anterior to the left. For Oct-25 Vibratome cross-sections of ctrl-MO and double-morphant embryos are shown. For Oct-91 a representative picture of one of the rare embryos exhibiting Oct-91 upregulation is shown (affected). For each condition, numbers refer to embryos showing the displayed staining, in comparison to the total number of analysed embryos (n= four independent experiments).

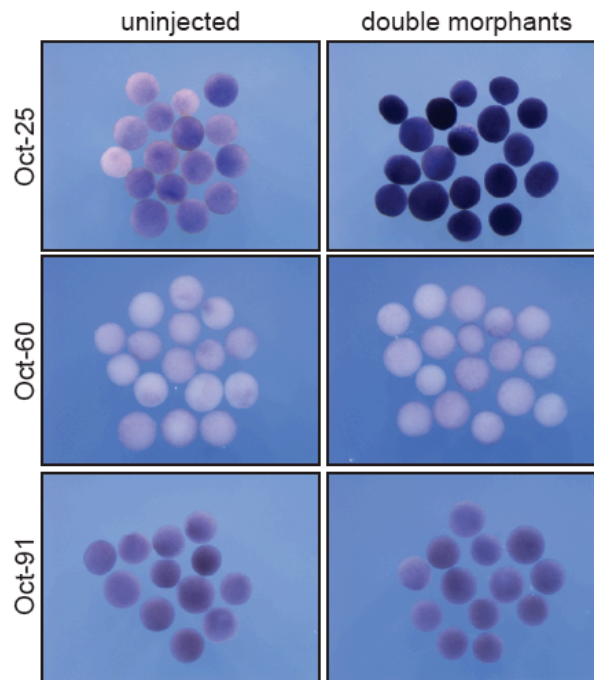


**Fig. 46: xSuv4-20h double morphants derepress Oct-25 expression in double-morphant animal cap explants.** RNA *in situ* hybridization analysis for Oct-25, Oct-60 and Oct-91 in animal cap explants for ctrl-morphants or xSuv4-20h double-morphant samples. Embryos were injected radially at two-cell stage; cap were cut at NF 9 and fixed at midneurula stage (NF 15). The figure shows one representative experiment (n= two independent experiments).

The selective, derepressed state of Oct-25 was finally confirmed via qRT-PCR. RNA was extracted from unilaterally injected embryos, using the same strategy applied for microarray sample preparation (Fig. 47a). As shown in figure 47b, Oct-25 mRNA was about three-fold higher in xSuv4-20h double-morphant halves ( $p=0.0123$ ), while being similar between control morphant and uninjected halves. In the same samples, Oct-91 was unaffected. The same assay was used to confirm the diminished expression of neural plate marker genes. With the exception of Ngnr 1a, whose levels appeared unaffected upon suvar depletion, the overall pattern strongly recapitulates the gene expression profiles obtained via RNA *in situ* hybridization. In particular, Nrp1 and N-tubulin mRNA levels were clearly reduced in the morphant halves ( $p=0.0122$  and  $0.0163$ , respectively). These results confirm the key role of xSuv4-20h1 and h2 HMTases during neurogenesis (Fig. 47b).

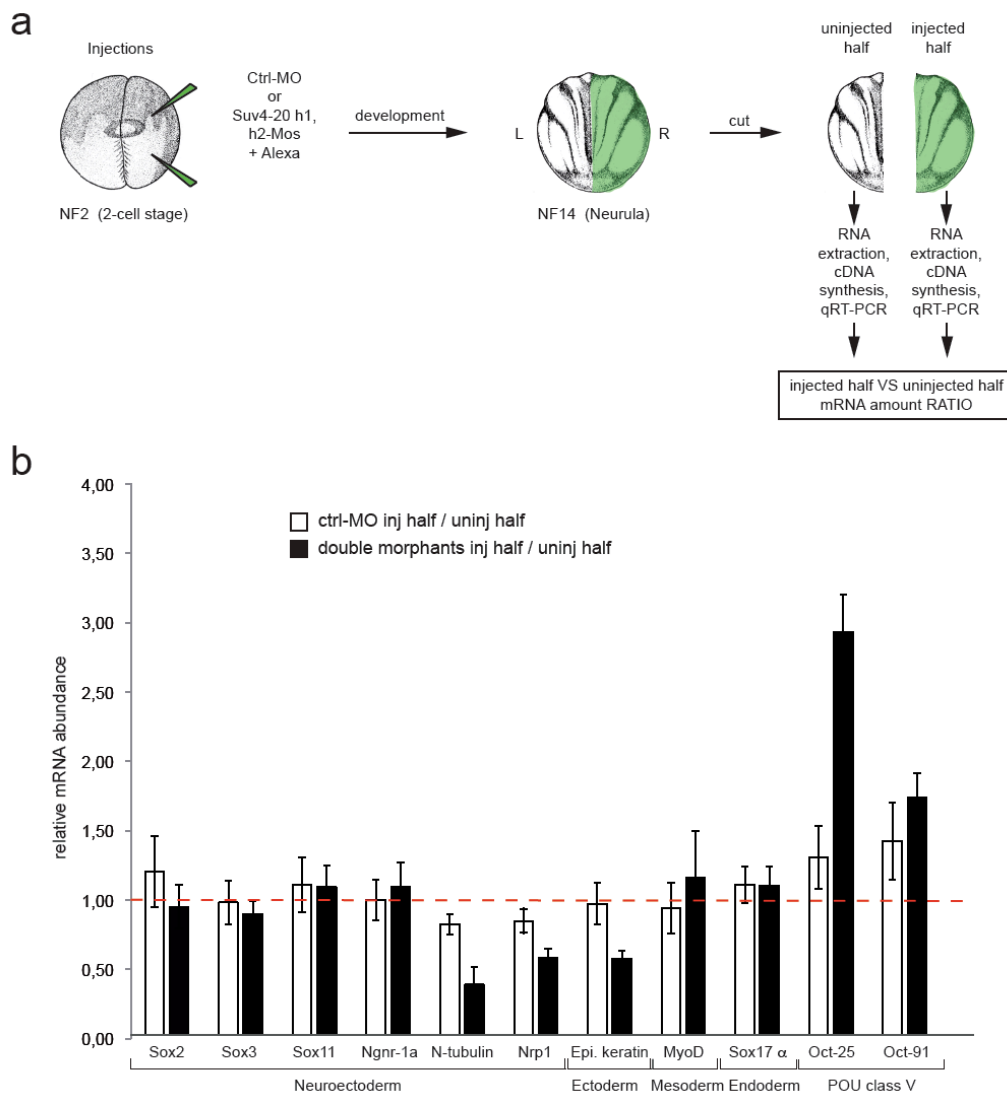


**Fig. 47: qRT-PCR experiments on ctrl- or xSuv4-20h double morphants. (a)** Schematic representing qRT-PCR experiments. **(b)** qRT-PCR profiles for the indicated genes in ctrl-MO and xSuv4-20h double-morphant embryos (NF 14-15). Oct-25 expression was three-fold higher in the injected side of double-morphant embryos, while Nrp1 and N-tubulin levels were two-fold reduced. Data represent normalized ratios of mRNA levels as means of four independent experiments, error bars indicate SEM.

#### 4.4.10 H4K20me3 levels are enriched in the 5'-UTR region of the Oct-25 gene

Trimethylation of H4K20 is known to be a repressive mark (Schotta, Lachner et al. 2004). Therefore, genes that are decorated by the H4K20me3 mark are expected to become derepressed in the absence of it. Based on this assumption, Oct-25 might be a direct target of xSuv4-20h enzymes, while the other neural markers – downregulated in double morphants – would be considered indirect targets. To test this assumption, chromatin immunoprecipitation (ChIP) experiments with H4K20me3-specific antibodies were performed at the neurula stage (NF 15-16). The access to the genomic information provided by the sequenced *Xenopus tropicalis* genome (Hellsten, Harland et al. 2010) allowed us to identify the pericentromeric major satellite repeat sequence (MSAT3) as positive control amplicon for the experiment. As negative controls we considered three genes: 1) GAPDH, a constitutively expressed housekeeping gene; 2) *thra*, a gene whose expression can be detected at neurula and 3) *thibz*, a gene expressed under *thra* activity, from metamorphosis on. H4K20me3 presence at these genomic regions, set as “background enrichment”, was compared to the enrichment at several amplicons spread out over the Oct-25 gene (Fig. 48a). In five independent experiments H4K20me3 levels were clearly enriched at pericentromeric MSAT3 repeat region, as expected from the analysis in murine cells (Schotta, Lachner et al. 2004). Interestingly, at the 5'-UTR region of Oct-25 (Fig. 48b), H4K20me3 was significantly enriched compared to the control gene GAPDH ( $p=0.0155$ ), *thra* ( $p=0.0103$ ) and *thibz* ( $p=0.0128$ ). The other Oct-25 amplicons showed no enrichment, when compared to the control genes (Fig. 48b). This result suggests a possible direct role for H4K20me3 in regulating Oct-25 expression.

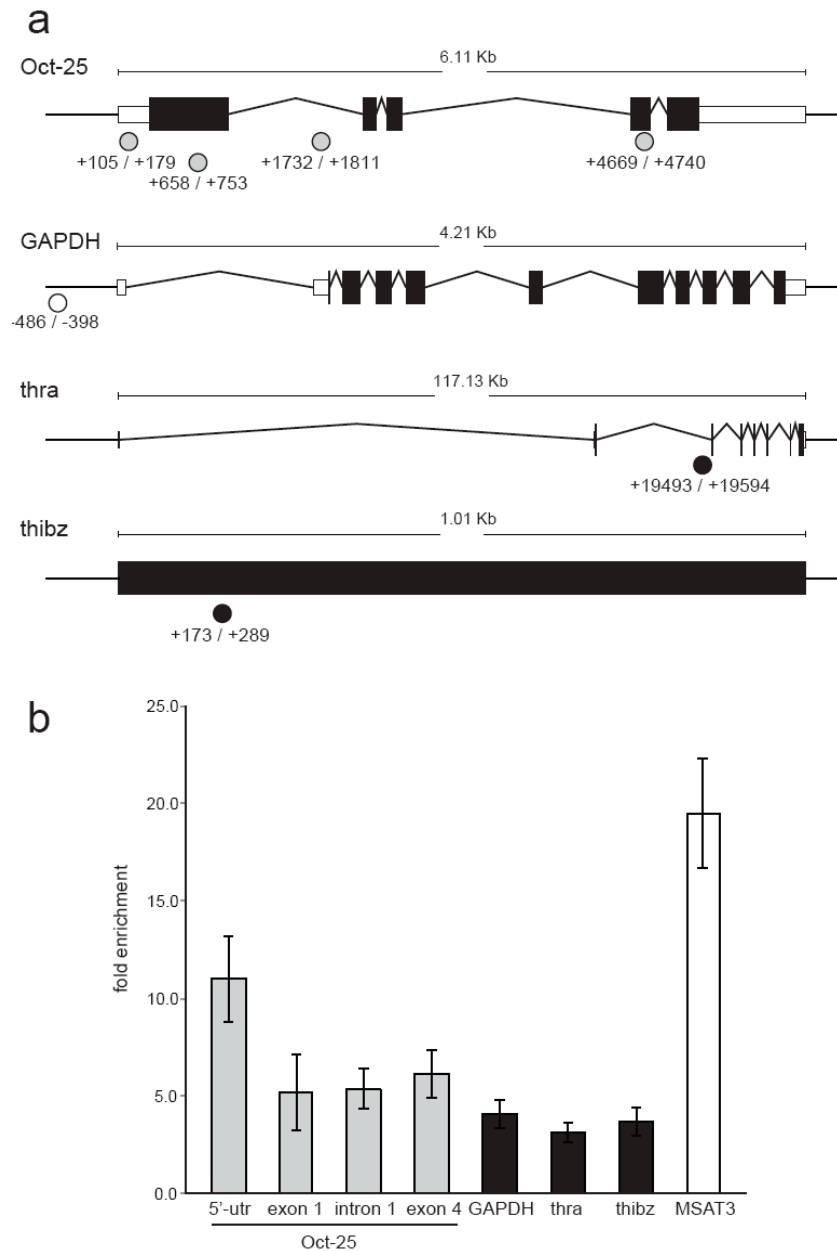


**Fig. 48: Oct-25 5'-UTR is enriched in H4K20me3 in ChIP-PCR experiments. (a)** Schematic representing amplicons position (circles) in each of the indicated genes. **(b)** Fold enrichment of H4K20me3 ChIP-PCR for the indicated amplicons. H4K20me3 is enriched at Oct-25 5'-UTR. Data represent mean values of five independent experiments, error bars indicate SEM.

Injection of *Xenopus tropicalis* specific morpholinos against xSuv4-20h enzymes revealed a clear reduction in H4K20me3 enrichment on Oct-25 5'-UTR (compared to uninjected embryos,  $p=0.004$ ) as well as on the MSAT3 amplicon (Fig. 49). Enrichment of the modification was reduced to a level comparable with the control gene. Surprisingly, a mild, non-significant ( $p=0.084$ ), reduction in H4K20me3 was observed for thibz, reflecting high variability between independent samples.

Together, these results strongly suggest that xSuv4-20h enzymes regulate Oct-25 expression via deposition of H4K20me3 on the first exon.

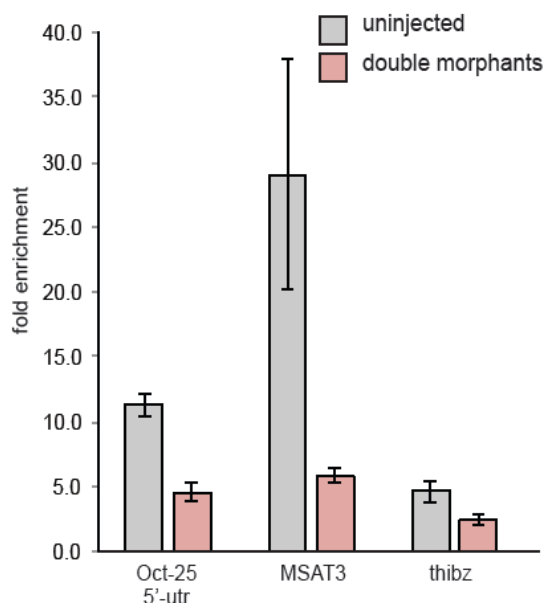


**Fig. 49: xSuv4-20h double-morphant embryos show reduce enrichment on Oct-25 5'-UTR in ChIP-PCR experiments.** Fold enrichment of H4K20me3 ChIP-PCR for the indicated amplicons in uninjected *versus* double-morphant embryos. H4K20me3 is more than 2.5-fold reduced at Oct-25 5'-UTR. Data represent mean values of three independent experiments, error bars indicate SEM.

#### 4.4.11 Regulation of early neural marker genes by Oct-25

Xenopus Oct-25 has been implicated in germ layer formation, by preventing cells to prematurely respond to differentiation signals (Takebayashi-Suzuki, Arita et al. 2007; Cao, Siegel et al. 2008). We thus decided to test whether the sustained expression of Oct-25 in xSuv4-20h morphants could cause the observed downregulation of early neural plate and neural differentiation markers. This question is difficult to address, since the role of Oct-25 in neural induction is ambiguous – both overexpression and morpholino knockdown inhibit neural differentiation (Takebayashi-Suzuki, Arita et al. 2007; Cao, Siegel et al. 2008). In a previous report (Boyer, Lee et al. 2005), Oct4 was reported to bind to promoters of early neural markers, including Zic and Sox genes, in undifferentiated human ES cells. In the absence of ChIP-grade Oct-25 antibodies, the epistatic relationships between Oct-25 and these neural genes were probed by overexpression of dominant activating or repressing Oct-25 protein variants in animal caps (Fig. 50a). Zic1, Zic3 and Sox2 responded to the Oct-25 variants in a manner that supports a direct regulator/target gene interaction, i.e. they were hyperactivated by Oct-25-VP16 ( $p= 0.0143$ ;  $0.0456$ ;

0.01622, respectively) and suppressed by Oct-25-EnR ( $p= 0.0236; 0.0167; 0.0231$ , respectively) compared to the uninjected sample. This qualitative combination of response is compatible with a direct regulation of the neural markers by Oct-25, or by indirect regulation via a positive mechanism. In light of the finding that Oct4 is bound to the neural genes in human ES cells, we assume this epistasis to reflect a direct interaction. For the two *Zic* genes, which are misregulated in the forming neural plate of morphant embryos (Fig. 39), we confirmed the misregulation by Oct-25 variants via RNA *in situ* hybridisation (Fig. 50b). The remaining genes tested either failed to respond to one of the two Oct-25 protein variants (*Zic2*, *Xiro1*), or did not respond (*Ngnr 1a*, *N-tubulin*).

These responses suggest an indirect effect. While it is possible that additional factors that are misregulated in *xSuv4-20h* morphants contribute to the neural phenotype, the combined results from ChIP experiments and Oct-25 variants define a pathway, in which *xSuv4-20h* dependent repression of Oct-25 is needed during gastrulation for proper neuroectoderm differentiation.

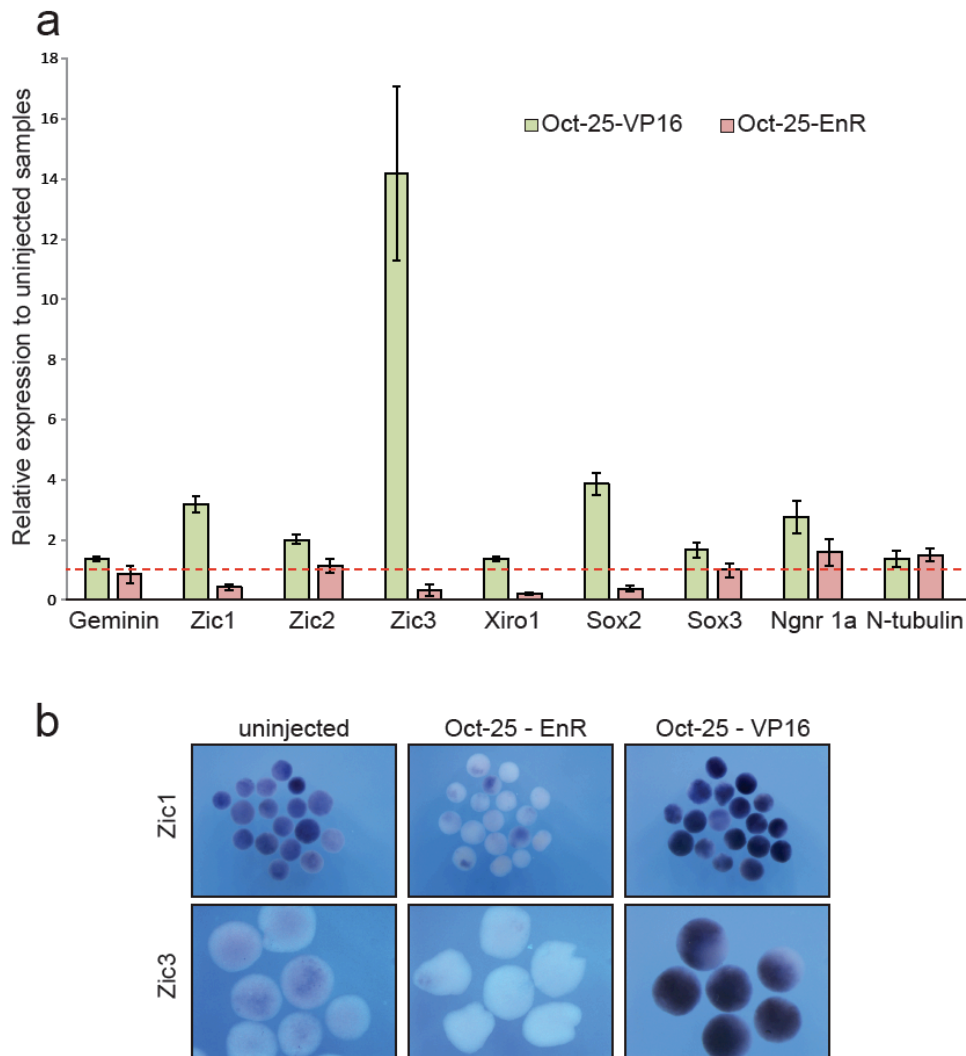


**Fig. 50: Regulation of early neural marker genes by Oct-25-VP16 and Oct-25-EnR fusion proteins.** (a) qRT-PCR on animal cap (AC) explants cut from uninjected embryos and embryos overexpressing Oct-25-VP16/EnR mRNAs. The chart shows the relative expression of the indicated genes compared to H4 gene levels. Data represent normalized ratios of mRNA levels as means of three or four independent experiments; error bars indicate SEM. (b) RNA *In situ* hybridization on uninjected AC or explants overexpressing Oct-25-VP16/EnR for Zic1 (upper row, 20X magnification) and Zic3 genes (lower row, 50X magnification).

#### 4.4.12 Downregulation of Oct-25 rescues double-morphant phenotypes

To further analyse the mechanistic interaction between xSuv4-20h enzymes and Oct-25, we performed epistasis experiments. In a first series of analysis we injected A1 blastomere at 32-cell stage, selectively labelling cells that predominantly contribute to the retina and brain development in the neuroectoderm. Morphologically, the eye of double-morphant embryos appeared strongly affected (Fig. 51a). 71% of the injected embryos showed a clear reduction of the retinal pigment, which often was found only in the dorsal-most portion of the eyecup. The

majority of the eyes contained no lens (Fig. 51b). When the downregulation of xSuv4-20 enzymes was coupled to the concomitant knockdown of Oct-25 (triple morphants), the percentage of embryo affected was reduced to 49% ( $p=0.0188$ , Fisher's exact test). Notably, triple-morphant embryos, in which retinal pigment was restored in Alexa-positive areas (i.e. progeny of the injected blastomere), also regained a lens of normal size (Fig. 51b).

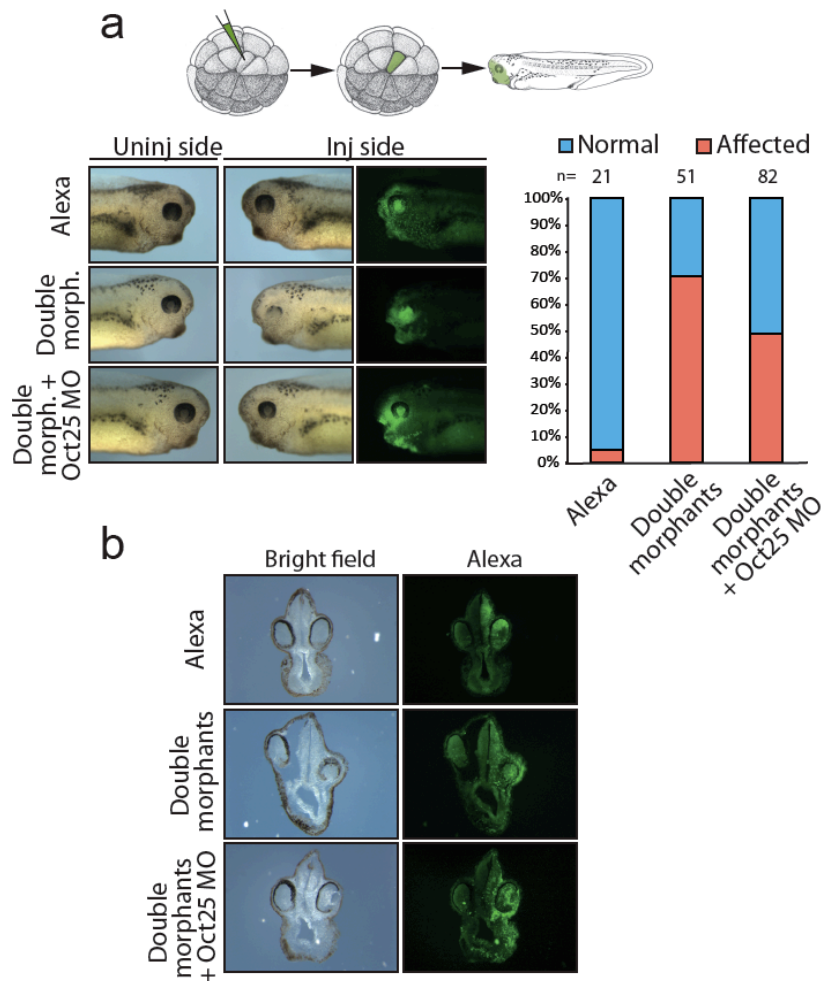


**Fig. 51: Morphological rescue of double-morphant phenotypes upon Oct-25 knockdown** (a) Schematic illustration of targeting microinjections of tadpoles injected into the A1 blastomere at 32-cell stage, and morphological phenotypes of representative embryos (NF 35-37) from cohorts injected with Alexa, xSuv4-20h MOs (double morphants) and double morphants plus Oct-25 MO. The chart shows penetrance of the eye phenotype. The results from three independent experiments are presented; n=total number of embryos scored. (b) Vibratome cross-sections of representative embryos injected as in panel (a).

This morphological rescue was confirmed molecularly in AC assay. Expression of a subset of genes involved in the establishment of the neural plate state (Zic1, Zic2, Xiro1, Sox2 and Sox3) was strongly reduced upon downregulation

of xSuv4-20 enzymes in NF 14-15 explants, when compared to uninjected animal caps ( $p=0.0068$ ;  $p=0.0127$ ;  $p=0.0113$ ;  $p=0.0321$ ;  $p=0.0037$ , respectively). With the exception of Sox2, the simultaneous downregulation of xSuv4-20h enzymes and Oct-25, restored the expression of these genes, actually leading to a 2-to-2.5-fold increase in their expression, compared to uninjected samples (Fig, 52).

This latter finding further supports the notion that some neural genes of the Zic/Sox/Xiro group repressed by Oct-25, when they become induced at the gastrula stage.

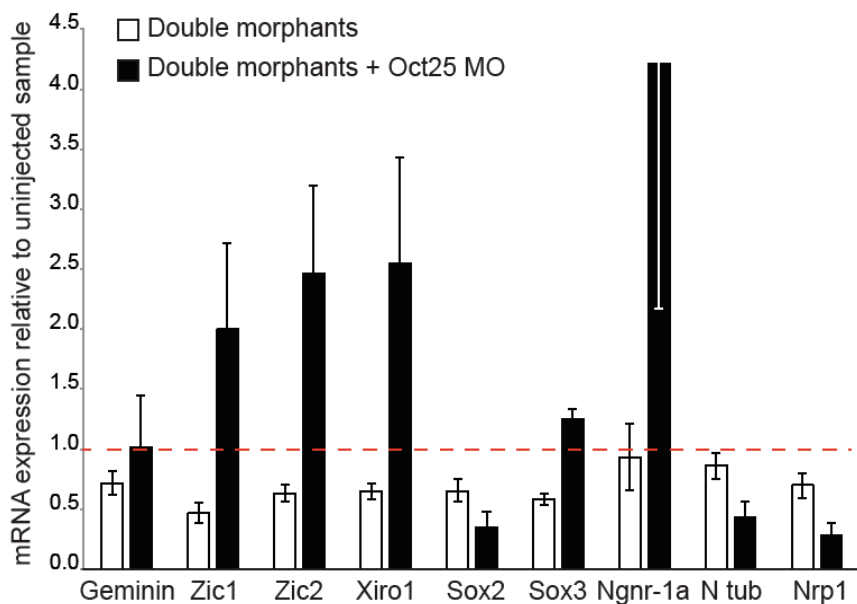


**Fig. 52: Molecular rescue of xSuv4-20h double-morphant phenotypes upon Oct-25 knockdown.** qRT-PCR profiles for the indicated genes in xSuv4-20h MOs (double morphants) and double morphants plus Oct-25 MO animal cap explants at NF 14-15. Data represent normalized mRNA levels as mean of three to four independent experiments; error bars indicate SEM.

The combined results of the morphological and molecular epistasis rescue experiments strongly suggest that derepression of Oct-25 is the major cause of the neural phenotype in xSuv4-20h double-morphant embryos. Since H4K20me3 decorates the 5'-UTR of the Oct-25 gene, it is concluded that xSuv4-20h enzymes control Oct-25 transcription as a prerequisite for neuronal induction

#### 4.4.13 Suv4-20h enzymes regulate murine Oct-4 expression

The mammalian Oct4 protein represents a master regulator of pluripotency in early embryos and ES cells. Recently, it has been shown that Oct4 antagonizes ectodermal differentiation as soon as ES cells exit pluripotency (Teo, Arnold et al. 2011; Thomson, Liu et al. 2011), reminiscent of the observations in *Xenopus*. This similarity led us to investigate Oct4 expression in wildtype and composite Suv4-20h1/h2 double- knockout (DKO) ES cells. We tested two independently derived DKO cell lines (B4-2 and B7-1) and compared them with two wildtype controls (wt26, an isogenic ES cell line, and GSES-1 cell line). All the four cell lines form typical ES cell-like colonies in LIF-containing medium. Upon aggregation, the two DKO lines formed clearly smaller embryoid bodies than the wild-type lines, both at day 2 and at day 6 of differentiation (Appendix 1, Fig. 55). Interestingly, after re-plating the embryoid bodies for one day, Suv4-20h DKO lines showed a lower extent of differentiation, appreciable by an ES-like morphology of the colonies (Appendix 1, Fig. 55, day7).

We then decided to quantify the Oct4 protein expression by FACS analysis. FACS profiles revealed a similar amount of Oct4 between wt26 and GSES-1 lines, as well as between the two DKO lines. Remarkably, both B4-2 and B7-1 signals were clearly shifted towards higher values, indicative of increase Oct4 expression in DKO ES cells (Appendix 1, Fig. 56a). Based on normalized median fluorescence intensity, the two DKO lines contained approximately three-fold higher Oct4 protein than the wildtype at day 0 ( $p=0.00604$ ), and still two-fold more at day 6 ( $p=0.01266$ ) (Appendix 1, Fig. 56b).

We conclude that Oct4 expression is being reduced during differentiation in Suv4-20h DKO cells. However these cells have a higher Oct4 level while undifferentiated and maintained higher levels during differentiation in comparison to wild-type cells. These findings implicate Suv4-20h HMTases as novel regulators of Oct4, even directly, as for Oct-25 in *Xenopus*, or indirectly.

To further characterize the differentiation process in wildtype and Suv4-20h DKO cell lines, we stained day 0 and day 6 cells for the chemokine receptor 4 (CXCR4) protein, whose expression indicates mesendoderm induction. At day 6 of differentiation wildtype cell lines showed a robust increase in CXCR4 expression (approx. 38% of CXCR4 positive cells) compared to day 0 (Appendix 1, Fig. 57). In contrast, both Suv4-20h DKO embryoid bodies contained a clear lower percentage of CXCR4 positive cells (approx. 8%) at day 6 when compared to the wildtype cell lines

( $p=0.03255$ ) (Appendix Fig. 56c). We then tested the ability of wildtype and Suv4-20h DKO cell lines for cardiomyocyte differentiation, which is easily detectable by autonomous contraction of representing pace-maker cells at differentiation day 14. While wt cultures contained multiple foci that beat autonomously at day 14, no contraction was observed in DKO cells (data not shown, four independent experiments). Finally, qRT-PCR analysis indicate a reproducible and statistically significant change in mesoderm gene expression in the DKO ES cells, which showed enhanced induction of FoxA2 ( $p=0.00706$ ) and reduced levels on Gata4 ( $p=0.00037$ ) (Appendix Fig. 57).

Together, these results reveal a compromised and biased differentiation capacity for Suv4-20h DKO ES cells. Importantly, Oct4 protein levels are enhanced in H4K20me3 depleted cells, both under non-differentiating and differentiating conditions, which suggests that repression of POU-V genes through Suv4-20h enzymes during exit from pluripotency, might be an evolutionary conserved function.

## 5 DISCUSSION

Understanding the processes leading the single-cell zygote to a mature organism represents the main challenge of developmental biology. Early embryonic development involves a tightly regulated series of lineage specification events, which progressively restrict cell fate and drive different cells, carrying the same genetic information, to acquire their own identity. Therefore, cell fate choice relies, on one hand, on the establishment of specific gene expression patterns, and on the other hand, on a properly organized cell memory system to precisely transmit the gene expression patterns during replication and cell division (Heasman 2006; Bogdanovic, van Heeringen et al. 2011). Epigenetic mechanisms play a pivotal role, in close connection with transcription factor networks, in the establishment and maintenance of cell-type-specific gene expression patterns.

In this study, the role of *Xenopus* Suv4-20h enzymes has been characterized during embryonic development. Both the functional and the biological analysis produced three main results: first of all, xSuv4-20h enzymes are specifically and selectively required for neuroectoderm specification and neurogenesis. H4K20me2 and me3 depleted morphant embryos are characterized by an intrinsic block in neuroectodermal differentiation, caused by the selective deregulation of genes required for the establishment of neural plate, and neuronal differentiation. This scenario seems to be true also for the epidermis, in particular for ciliogenesis, although more experiments have to be performed to properly understand the role of the two enzymes in this tissue. In contrast, mesendodermal gene expression was remarkably normal in morphant embryos. Secondly, xSuv4-20h enzymes directly regulate the pluripotent gene Oct-25 (and possibly also Oct-91, but not Oct-60), via H4K20me3 deposition. This epigenetic mark ensures the proper spatio-temporal downregulation of Oct-25 (Cao, Knochel et al. 2004). This process, occurring at a time when pluripotent embryonic cells of the animal pole region differentiate, probably involves the contribution of other factors. Finally, we showed that murine Suv4-20h DKO ES cell lines have elevated Oct4 levels both in undifferentiated and differentiating conditions, compared to wildtype ES cell line (Appendix 1). This study describes a pivotal role of xSuv4-20h enzymes in promoting a proper differentiation process. In other words, H4K20me2 and H4K20me3 represent key epigenetic marks, that shape regulatory networks which controll cellular differentiation.

## 5.1 Pluripotent features of single animal pole blastomeres

The ability of cells to undertake a specific differentiation pathway is restricted to early stages. In a series of experiments, Heasman and colleagues transplanted single labelled animal pole or vegetal pole derived cells into the blastocoels of host embryos (Heasman, Wylie et al. 1984; Snape, Wylie et al. 1987; Wylie, Snape et al. 1987) and followed their progeny into the three germ layers. These experiments led them to conclude that cells become determined by the beginning of gastrulation, while morula or blastula transplanted cells could differentiate into all the three germ layers. In a similar approach, we investigated whether animal pole cells show comparable pluripotent behaviour. Confocal microscopy analysis of host embryos allowed a precise evaluation of whole-mount transplanted embryos. The results were in agreement with those proposed by Heasman and colleagues: transplanted cells from blastula stage were able to differentiate into all the three germ layers; in particular early blastula cells (NF 7-8) gave rise to descendants of the three germ layers in a higher percentage (56%) compared to the late blastula transplanted blastomeres (NF 9; 41%). Moreover, by late blastula, 9% of the transplanted cells selectively colonized the ectoderm germ layer, following their “default” differentiation pathway and differentiating only into ectodermal cells. Finally, transplanted early gastrula (NF 10.5) blastomeres showed no pluripotent behaviour, and mainly differentiated as ectodermal cells (23% against 0% of NF 7-8 cells), suggesting that determination already took place. These results led us to the following conclusions. First, a main difference of the transplanted blastomeres is represented by the cell size. NF 7-8 cells were bigger than NF 9, while NF 10.5 cells were the smallest cells taken from donor embryos. Moreover the ability of NF 7-8 blastomeres to populate the three germ layers at highest percentage reflects the capacity of these cells to divide faster than NF 10.5 cells (Newport and Kirschner 1982). Second, the different cell fates can be determined in accordance to the cell position into the host blastocoel. The inversion experiments performed by Snape et al., whereby host embryos were turned upside down after being transplanted (in order to allow contact between the transplanted cell and the roof of the blastocoel), suggest a possible mechanism by which cells in contact with the blastocoel floor are subjected to a vegetalizing effect of the vegetal mass. Cells that attached to the blastocoel roof will escape such an influence and become ectoderm (Snape, Wylie et al. 1987). Although in our experiments the majority of the transplanted cells ended up on the blastocoel floor (data not shown), their close proximity to either dorsal or ventral regions of the blastocoel might affect the differentiation process. It would require a

much higher number of transplanted embryos to average out the effects and, thus, to evaluate differentiation potential independently from these biases. From a technical point of view the imaging of host transplanted embryos by confocal microscopy represents just a superficial analysis. The classification of labelled descendents into the three germ layers is based on the microscope analysis of the whole embryos, and limited by the frequent inability to discriminate particular cell types (e.g. derma cells *versus* epidermal cells) which results into misleading classification and incorrect statistical analysis. This “first-layer” analysis should be coupled to more detailed confirmatory experiments (e.g. ICC analysis with antibodies against epitopes of cell belonging to the different germ layers) in order to better classify the different cells. Although all these problems affect the overall output, the assay recapitulated previous results and indicated a progressive loss of pluripotency in animal pole blastomeres during development, which reflects the molecular changes associated with cell determination.

## **5.2 *Xenopus laevis* Suv4-20h HMTases**

The main part of the presented study concerned the characterization of *Xenopus laevis* Suv4-20h HMTases during development. Histone lysine methylation represents a complex and dynamic process, that is pivotal for genome stability, repair and transcriptional regulation (Dambacher, Hahn et al. 2010; Bogdanovic, van Heeringen et al. 2011). In particular, Suv4-20h1 and h2 HMTases are responsible for the establishment of the H4K20me2 and H4K20me3 (Schotta, Lachner et al. 2004; Schotta, Sengupta et al. 2008). Our experiments, based mainly on morpholino-mediated knockdown of the two enzymes, identified a specific and selective role of xSuv4-20h HMTases in ectoderm differentiation. In particular, we have shown that the enzymes are required for neurogenesis to occur, while having little effect on overall mesoderm and endoderm differentiation. It is important to note that little is known about Suv4-20h involvement in gene regulation. Studies in mouse describe a role for H4K20me2 and me3, and thereby for the enzymes responsible for their deposition, during development (Biron, McManus et al. 2004; Schotta, Sengupta et al. 2008). Nevertheless, both analysis have not addressed any specific function of Suv4-20h HMTases in activation or repression of target genes. In order to investigate this aspect, we performed gene expression profiling. Unfortunately, our microarray analysis provided only partial overview of the gene misregulation in *Xenopus* double-morphant embryos, due mainly to technical limitations (the microarray

experiment will be further discussed later in this section). Still, the molecular analysis revealed that xSuv4-20h enzymes are required for restricting the expression of the pluripotent gene Oct-25 to the floor plate of the neuroectoderm, preventing its ectopic expansion in the ectodermal sensorial layer. Consistent with this result, murine Suv4-20h1 and h2 DKO ES cells exhibit reduced and delayed Oct4 gene silencing upon *in vitro* differentiation (Appendix 1). In summary these results suggest that the appropriate function of Suv4-20h HMTases are needed for silencing pluripotency-associated POU-V genes within the sensorial cell layer of the ectoderm. In *Xenopus*, this role allows Oct-25 positive neuroectodermal cells to exit the undifferentiated state and undergo neuronal differentiation. Moreover, Oct-25 upregulation in the entire ectodermal sensorial layer (Fig.45, vibratome sections) suggests that the missregulation of this gene could be responsible also for the epidermal phenotype.

### 5.2.1 Functional analysis of xSuv4-20h HMTases

The functional analysis of xSuv4-20h enzymes led us to properly identify the frog paralogs of the mouse enzymes (as shown by Suv4-20dn MEFs transfection with *Xenopus* wt enzymes). Moreover it allowed us to characterize their function by altering the enzymes' concentration through morpholinos or mRNA injection. *Xenopus* versus mouse protein sequence analysis revealed a high conservation throughout the entire length, particularly within the SET domains that display at least 88% identity between mouse and frogs enzymes. Interestingly, xSuv4-20h2 amino acid sequence appears remarkably longer than the mouse homolog. RNA *in situ* hybridization analysis, as well as semiquantitative PCR assay, revealed a ubiquitous expression of *Xenopus laevis* HMTases in the embryo, at different developmental stages, and in different embryonic territories. Messenger RNA quantification via qRT-PCR highlighted the different expression profiles of the two enzymes: the maternal xSuv4-20h1 mRNA pool is progressively degraded and replaced by the zygotic mRNA. In contrast, xSuv4-20h2 mRNA is progressively reduced during development, suggesting a possible involvement of the h2 enzyme activity mainly in early developmental processes.

Western blot analysis performed with specific antibodies against the three H4K20 methyl states and quantitative mass spectrometry analysis allowed to identify coherent alterations of H4K20 methylation profiles, triggered by Gain- or Loss-of-function experiments. These alterations did not affect other repressive – H3K27me and H3K9me – methylation profiles, as shown by Mass Spectrometry and Western

blot analysis. On one hand overexpression of xSuv4-20h enzymes caused a clear upregulation of H4K20me2 and H4K20me3. Bulk chromatin H4K20me1 enrichment was mildly altered, probably due to the constant activity of Pr-Set7. On the other hand xSuv4-20h depletion led to a strong downregulation of H4K20me2 and H4K20me3, coupled to a concomitant increase of H4K20me1 as previously described in mouse (Schotta, Sengupta et al. 2008).

The conserved aminoacidic sequences of the SET domains between frog and mouse Suv4-20h enzymes represent another interesting aspect. Western blot analysis of rescue experiments highlighted the importance of functional HMTases to properly re-establish H4K20 methylation patterns in embryos injected with xSuv4-20h enzymes morpholinos. Overexpression of mSuv4-20h HMTases carrying key aminoacidic mutations in the SET domain at particular residues (Kwon, Chang et al. 2003; Dillon, Zhang et al. 2005) did not affect the levels of H4K20 mono-, di- and trimethylation compared to the uninjected situation. This result highlights two key points: first, the lack of H4K20me3 deposition prevents normal development, suggesting that this modification is crucial for the proper differentiation process. Second, the two mutated isoforms were inactive but did not show any dominant negative behaviour. As expected, while wt mSuv4-20h HMTases properly rescued the methylation profiles triggered by the morpholino injections, the inactive variants were not able to re-established H4K20me2 and H4K20me3 at normal levels. Similar results were achieved upon transfection of wt and mutated mSuv4-20h enzymes in Suv4-20dn MEFs cells. It is possible that the Asp to Ala mutation in both the enzymes compromised the binding of the substrate AdoMet (Dillon, Zhang et al. 2005), in a manner that prevents the binding of the mutated proteins to the histones. This finding suggests that these enzymes operate by a “hit and run” mechanism rather than by stable interactions with chromatin. These two features could explain the lack of dominant interference activity of the mutated mSuv4-20h variants.

Another interesting point concerns the biological alterations associated only to the morpholino-mediated knockdown approach: while xSuv4-20h enzymes depletion led to highly reproducible morphological and molecular phenotypes, mRNA-mediated overexpression of either *Xenopus* or mouse variants did not overtly perturb development, despite significantly increased levels of H4K20me2 and me3 states. This result might be explained considering *in primis* the higher stability of the knockdown compared to the transient protein upregulation by mRNA injection. Another explanation could be that demethylation of the higher methyl states might occur rather rapidly through H4K20me2 and me3 demethylases at specific sites,

where H4K20me1 is required, e.g. Wnt/ $\beta$ -Catenin inducible genes (Li, Nie et al. 2011). The observed increase in H4K20me2 and -me3 states may thus occur at non-functional sites on the genome. This could be investigated in future by ChIP-Seq analysis of wild-type and mRNA-injected embryos. In a similar approach, Barski and colleagues identified approx. 1800 H3K9me3 sites in ES cells, with the vast majority also showing H4K20me3 (Barski, Cuddapah et al. 2007). Since mono- and dimethylated H4K20 states are quite abundant modifications in *Xenopus* embryos (Schneider, Arteaga-Salas et al. 2011), most likely it is the loss of H4K20 trimethylation that interferes with normal development. Provided that in *Xenopus* H4K20me1, me2 and me3 states are interconverted by Suv4-20h enzymes, as suggested from knock-out studies in mice, it seems that these HMTases are used predominantly to repress genes via H4K20me3 than to antagonize H4K20me1-dependent transcriptional activation.

### **5.2.2 Biological analysis of xSuv4-20h HMTases**

Despite the presence of the two HMTases in the entire embryo, loss-of-function experiments led to a specific block in differentiation of neuroectoderm. This germ-layer selectivity requirement emerges both at morphological and molecular levels. Molecularly, xSuv4-20h enzymes knockdown did not interfere with the proper establishment of anterior-posterior and dorso-ventral axes, as confirmed by the unaffected expression patterns of the organizer genes Chordin, Xnr-3 and Goosecoid in double-morphant embryos. From tailbud stage on, two main phenotypes, concerning ectodermal structures could be scored upon morpholino injections: about 90% of double-morphant embryos displayed strongly reduced differentiation of the eye cup and a severely compromised melanophore pattern in the dorsal part of the head and in the lateral portion of the trunk. Approximately 2/3 of the affected populations restored normal eye structure and melanophore pattern upon coinjection of xSuv4-20h morpholinos and wt mSuv4-20h mRNAs enzymes. This result suggests that the two morphological changes were caused by xSuv4-20h HMTases depletion.

### **5.2.3 XSuv4-20h enzymes contribution to ciliogenesis**

The notable Delta-like 1 upregulation in non-neural ectoderm of double-morphant embryos suggests an involvement of xSuv4-20h enzymes in the formation

of motile cilia, as previously described by Deblandre et al. (Deblandre, Wettstein et al. 1999). According to this model lateral inhibition takes place in the inner ectodermal layer at gastrula stage, driven by a subset of cells that express high levels of Delta-like 1. These cells inhibit neighbouring cells from taking on the ciliated cell fate. At neurula stage,  $\alpha$ -tubulin positive cells intercalate into the outer cell layer where they finally differentiate by forming an atypical tuft of motile cilia. Immunohistochemistry and SEM analysis confirmed that ciliogenesis is affected in double-morphant embryos: upon xSuv4-20h enzyme depletion, the tadpole skin was characterized by a higher number of ciliated cells, comprising less and shorter cilia, in comparison to control embryos. Rescued embryos showed a comparable number of cilia per cell to the one of controls; however, the length of the cilia was apparently not fully re-established. Further experiments are required to elucidate the pathway by which xSuv4-20h enzymes regulate cilia formation.

An important link might be represented by the Oct-25 upregulation, which is detectable throughout the sensorial layer of the ectoderm in double-morphant embryos. Coinjection of xSuv4-20h and Oct-25 morpholinos presents a possibility to test, whether the persistent expression of Oct-25 is responsible for the upregulation of Delta-like 1 mRNA in the epidermis and/or for the compromised function of cilia. At the same time, we cannot exclude that other key ciliogenesis factors and multiple signalling pathways are affected (Stubbs, Davidson et al. 2006; Stubbs, Oishi et al. 2008; Yu, Ng et al. 2008; Mitchell, Stubbs et al. 2009). Ohnmar Hsam, from our laboratory, has found that the expression of Foxj1, a precursor of ciliogenesis, and Dnah9, a ciliogenesis marker, is significantly reduced upon xSuv4-20h enzymes depletion in AC (personal communication). Moreover, some microRNAs play pivotal roles during ciliogenesis: in a recent study, Marcet and colleagues identified miR-449 as a key repressor of the Delta/Notch pathway (Marcet, Chevalier et al. 2011). In particular, blocking of miR-449 function led to an increase number of Delta-like 1 expressing cells and a consequent expansion of multiciliogenesis, which can be rescued by Delta-like 1 morpholino injection (Marcet, Chevalier et al. 2011). In collaborations with Laurent Kodjabachian's laboratory in Marseille, Ohnmar Hsam has demonstrated that miR-449 expression is reduced in xSuv4-20h1 and h2 morphant embryos. This hypothesis is currently under investigation; nevertheless, if confirmed, it would connect a microRNA pathway to the H4K20me3 repressive histone. By repressing miR-449, xSuv4-20h enzyme might control whole gene batteries in a positive manner.

#### 5.2.4 A glimpse on the global role xSuv4-20h HMTases in gene regulation

Gene expression profiling has enabled the analysis of thousands of genes from a single RNA sample, providing a powerful tool for understanding gene regulation at a genomic level (Schena, Shalon et al. 1995). In this study, the Affimetrix GeneChip® *Xenopus laevis* Genome 2.0 Array has been used to study genome-wide transcriptional alterations caused by depletion of xSuv4-20h HMTase. The strategy described in figure 29 not only allowed us to compare the mRNA profiles between ctrl-MO injected embryos and double-morphant embryos, but also precisely enabled us to correlate injected *versus* uninjected sides within the same morphant population. This aspect represents a prerequisite to quantify mRNA changes in the dynamic and complex *Xenopus* system. Some important aspects have to be considered for this profiling experiment: first of all, the genome of *Xenopus laevis* is only partially annotated; this fact clearly represents an obstacle in understanding the global effect triggered by a specific gene alteration. Secondly, due to limited funding resources, the experiment included only two independent biological samples. Nevertheless, qRT-PCR analysis performed in parallel on key genes confirmed the results of the microarray analysis. Finally, the analysis was performed on NF 14-15 morphant embryos, because the neural differentiation defect is manifest at this stage. The result, in other words, represents only a snapshot of a particular developmental stage. It follows that the expression profiles of genes affected in stages earlier or later to the one analysed can be different. Although these aspects undoubtedly affected the overall result of the microarray, the analysis has pointed out some interesting details. First, gene expression profiling revealed a rather selective effect on the embryonic transcriptome, with approximate 6% of probe set being either up (~3%) or downregulated (~3%) in xSuv4-20h enzymes morphants. This is in accordance with the *in situ* experiments, which highlighted a selective impairment of genes expressed in the ectodermal germ layer. Interestingly, many of the transcripts present in both the up- and downregulated groups are genes involved in metabolic processes. Second, considering the annotated genes that were upregulated, Oct-25 is among the top ten affected genes. The significance of Oct-25 deregulation has been demonstrated by the epistasis rescue experiments at least with regard to neurogenesis. Morpholino-mediated knockdown of Oct-25 rescue morphological and molecular phenotypes of xSuv4-20h double-morphant embryos. Together, these results, observed using a variety of different approaches, establish a specific mechanistic link between xSuv4-20h enzymes and Oct-25.

### 5.2.5 A germ-layer specific function for xSuv4-20h HMTases

The two phenotypes scored in Loss-of-function experiments (i.e. deficiency in eye and cilia tuft differentiation) already showed the selective effects of xSuv4-20h enzyme depletion: only ectodermally derived structures were affected, while mesodermal and endodermal tissues appeared normal. This selectivity extends to the molecular level: the expression analysis of a broad number of markers required for the specification of the three germ layers, revealed a specific involvement of xSuv4-20h HMTases in ectodermal genes, mostly required for neurogenesis. Figure 53 shows a summary of all the markers tested via RNA *in situ* hybridization and ICC, upon suvars depletion.

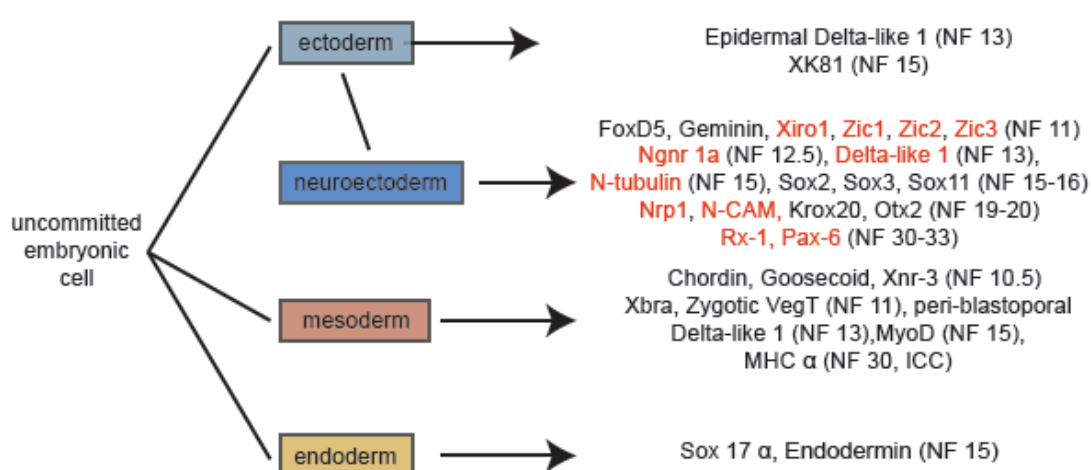


**Fig. 53: Schematic illustration of analysed markers of the different germ layers.** Genes downregulated and upregulated upon xSuv4-20h HMTase depletion are labelled in red and green, respectively. The developmental stages at which the analysis has been carried are indicated in brackets.

The neural differentiation pathway appears affected from the prospective neuroectoderm specification stage on (NF 10.5-11). While FoxD5 and Geminin, two key players in defining the neural ectodermal fate (Kroll, Salic et al. 1998; Yan, Neilson et al. 2009), were normally expressed in xSuv4-20h morphants, the neural inducing zinc-finger transcription factors Zic1, Zic3 and Xiro1 were strongly downregulated. Surprisingly, also Zic2, that has been characterized as an anti-neurogenic and crest-inducing factor (Brewster, Lee et al. 1998), was downregulated. This situation is contrasted by the normal mRNA levels of several neural genes. These include Sox11, which is involved in the neuronal maturation (Bergsland, Werme et al. 2006), as well as of the other two analysed HMG-box transcription

factors, Sox2 and Sox3, which keep neural cells undifferentiated by counteracting the activity of pro-neural bHLH proteins (Bylund, Andersson et al. 2003; Graham, Khudyakov et al. 2003; Pevny and Placzek 2005; Rogers, Moody et al. 2009). FoxD5, Geminin, and Zic2 are thought to create a regulatory network that maintains neural ectodermal cells in an immature stem-like state (Rogers, Moody et al. 2009), by inhibiting the neural inducing factors, which conversely stimulate bHLH pro-neural genes expression. In this context, Sox genes on the one hand prefigure the ability of neuroectodermal cells to adopt a neural fate, and on the other hand sustain neural cells in a progenitor/stem cell mode, maintaining their ability to proliferate and differentiate (Pevny and Placzek 2005). Subsequently, the pro-neural bHLH proteins restrict the number of neuronal cells within the neural plate (see Introduction chapter 2.1.3). Notably, Ngnr 1a expression was strongly reduced in double-morphant embryos probably as a consequence of the diminished expression of the upstream activators such as Zic1, Zic3 and Xiro1 factors. This in turn would also explain the absence of N-tubulin positive cells from the xSuv4-20h1 and h2 deficient neural plate. In contrast, Delta-like 1 expression is probably modulated by additional inputs, given that it is downregulated in the neural plate, upregulated in the epidermis and normal in the mesoderm (Revinski, Paganelli et al. 2010). In this context, it is possible that Oct-25 persistence in the neural plate compromises the appearance of the neural inducing factor. In other words, neuroectodermal cells initially follow the normal neurogenic pathway, but due to the missing silencing of Oct-25 expression, they become trapped in an undifferentiated progenitor state, which finally results in a loss of neurons.

While ectodermal and neuroectodermal structures appeared compromised upon xSuv4-20h depletion, mesoderm and endoderm differentiation was overtly unaffected. This statement is based on the large panel of marker genes investigated by RNA *in situ* hybridization, as well as on morphological features (i.e. properly structured skeletal musculature and externally observed heart beating). In addition, the length of the tail in morphants embryos was comparable to controls. Along this line, our results showed that morphant animal cap explants were refractory to Noggin-dependent neural induction, but were not compromised in mesoderm differentiation, as shown by Activin-driven induction of a terminal muscle marker (Fig. 42). Furthermore, targeted morpholinos injections into animal or vegetal blastomeres of 8-cell stage embryos clearly demonstrate that depletion of xSuv4-20h enzymes has little, if any, effect on mesoderm and endoderm specification. At the same time this confirms the importance of the two enzymes in the early step of neurogenesis.

Together these results suggest that a major function of xSuv4-20h HMTases lies in the transcriptional control of genes that coordinate and execute neuroectodermal differentiation. We can speculate that the observed selectivity might rely on two main processes. As discussed below, the first one is linked to a special cell fate determination mechanism operating in the neuroectoderm; the second process is related to the peculiar Oct-25 overexpression in morphant embryos.

After fertilization, maternal regulators drive the initial steps of embryonic patterning and body axis formation; subsequently, inductive events specify endoderm, mesoderm and finally the primitive ectoderm (Heasman 2006), whose determination is differentially achieved: while epidermis is specified via BMP signalling, neural induction is thought to occur by default, i.e. without requiring a specific TGF-ligand, as needed for mesendoderm. In fact, neural cell fate is established by inhibition of BMP signalling, by molecules secreted by the organizer (Munoz-Sanjuan and Brivanlou 2002; De Robertis and Kuroda 2004; Heasman 2006). Moreover, Oct-25 ectopic expression in double-morphant embryos, restricted to the sensorial layer of the ectoderm, might contribute to the selectively compromised neurogenesis in the neuroectoderm. As mentioned before, it might affect also the differentiation of ciliated epidermal cells in the non-neural ectoderm. Specifically, the different processes that characterize the neuroectoderm, could explain the absence of markers involved in neural differentiation in double-morphant embryos. The data presented in this thesis collectively suggest a model in which xSuv4-20h HMTases exert a key role in neurogenesis, by suppressing Oct-25 expression, through the proper establishment of H4K20me3 (and probably of H4K20me2) pattern. Immunofluorescence analysis of H4K20me1 and H4K20me3 distribution in mouse differentiating neurons and during skeletal and cardiac myogenesis suggested a model, in which H4K20me3 contributes to changes in chromatin structure that are required for cell differentiation (Biron, McManus et al. 2004). According to this model, H4K20me3 is needed to stably silence genes during development. This scenario is in agreement with the findings that this modification progressively accumulates during frog development (Schneider, Arteaga-Salas et al. 2011). The strong downregulation of neuroectodermal markers, from early specification (Zic1, Zic3, Xiro1) to neuronal commitment (N-tubulin), coupled to Oct-25 upregulation indicates that as soon as H4K20me3 is missing, cells of the neuroectoderm do not enter the normal differentiation pathway, and are kept in the undifferentiated state. With the exception of a previous study characterizing H4K20me3-chromatin-mediated gene silencing mechanism (Magklara, Yen et al.

2011), the analysis presented in this Ph.D. thesis describes, for the first time, a gene-regulatory function for xSuv4-20h enzymes during vertebrate development. It is tempting to speculate that RNA Polymerase elongation is impeded by H4K20me3 deposition to higher extent in older than younger embryos, possibly by a mechanism similar to the one suggested by Kapoor-Vazirani and colleagues (Kapoor-Vazirani, Kagey et al. 2011). This process might be involved in shutting down transcription of certain genes upon development.

### **5.2.6 Apoptosis and proliferation defects in xSuv4-20h morphant embryos**

While the molecular results explain the observed morphological phenotypes in a consistent manner, it has to be noted that these HMTases are involved in additional cellular aspects. Our analysis of the effects triggered by the downregulation of xSuv4-20h enzymes showed a significant increase of Caspase3 positive cells, and a milder reduction of H3P10-positive proliferating cells in double-morphant embryos. Significantly, the apoptotic phenotype was not responsible for the absent neuronal structures. When apoptosis was blocked by expression of xBcl-2, morphant embryos still lacked Delta-like 1 and N-tubulin expressing neurons. However, whether xSuv4-20h enzymes directly modulate the apoptotic machinery remains to be investigated.

The observed increase in cell death might be partially linked to the proliferation defects observed upon Suv4-20h depletion. It is known that H4K20 methylation is cell cycle regulated (Pesavento, Yang et al. 2008; Yang and Mizzen 2009), and that modulation of H4K20 methylation levels affect cell cycle-related mechanisms. Pr-Set7/Set8 dependent H4K20me1 plays an important role in cell proliferation. Downregulation of Pr-Set7/Set8 coupled to the consequent decrease in H4K20me1 activates the DNA damage checkpoint and compromise genome replication and stability (Sakaguchi and Steward 2007; Tardat, Murr et al. 2007; Beck, Oda et al. 2012). At the same time, increased levels of H4K20me1 (as a consequence of the downregulation of histone H4K20/H3K9 demethylase PHF8) decreased proliferation activity by delaying G1-S transition (Liu, Tanasa et al. 2010; Qi, Sarkissian et al. 2010). Unfortunately, many of these studies focused on the H4K20me1 state and the corresponding enzyme. It is therefore difficult to define whether depletion of xSuv4-20h HMTases has a direct effect on the cell cycle or whether the H4K20me1 increase, resulting from the decrease in H4K20me2 and H4K20me3 levels in double-morphant embryos, represents the main cause of cell

cycle defects. It is important to note that the described mild proliferation defect is very unlikely to explain the loss of neuronal structures. In a series of studies, Hartenstein demonstrated that cell division is neither critical for neural induction nor for early morphogenetic events in the central nervous system of *Xenopus laevis*. According to his data, neuronal cell determination depends predominantly on inductive cell-cell interactions, and not on successive rounds of mitosis (Hartenstein 1989; Harris and Hartenstein 1991).

The results observed in this study underline a link between apoptosis, cell proliferation and deregulation of xSuv4-20h HMTases; however the direct or indirect involvement of the two enzymes, as well as the role of H4K20me2 and H4K20me3 in these processes, require further investigation.

### **5.2.7 Neurogenesis is controlled by a Suv4-20h/Oct-25 regulatory module**

Different approaches identified Oct-25 as a direct target of xSuv4-20h enzymes. RNA *in situ* hybridization, qRT-PCR and microarray analysis consistently demonstrated that depletion of *Xenopus* Suv4-20h HMTases triggers an upregulation of this POU-V gene. At late blastula, uncommitted embryonic cells express in overlapping domains the three Oct3/4 homologs Oct-25, Oct-60 and Oct-91 (Hinkley, Martin et al. 1992). The pleiotropic roles of the Oct factors during vertebrate development have been intensely investigated in the last decades. Morrison and Brickman reported that the abovementioned POU-V genes from *X. laevis* can substitute for Oct4 to maintain pluripotency in ES cell, although to variable extent (Morrison and Brickman 2006). Oct-91 shows the highest activity to maintain murine ES cells in the absence of Oct4, while Oct-25, but not Oct-60, has some capacity to rescue ES cell self-renewal, suggesting a scenario in which these factors are required to maintain the multipotent uncommitted cell population in the embryo. This idea is supported by other experiments aimed to link *Xenopus* POU-V genes to the molecular mechanisms governing cell determination: Oct factors inhibit activin/nodal signalling (Cao, Siegel et al. 2006; Cao, Siegel et al. 2008) and BMP-mediated induction (Takebayashi-Suzuki, Arita et al. 2007), regulate transitions from mesoderm to neural cell fates (Snir, Ofir et al. 2006), and prevent cell from entering terminal differentiation pathways (Cao, Knochel et al. 2004). All these functions of *Xenopus* POU class V factors during development have been inferred from microinjection experiments with Oct-specific morpholinos or mRNAs all at 2-4 cell stage (i.e. pre-MBT). Our results differ from these studies: we describe a specific and

selective endogenous upregulation of Oct-25 expression, caused by H4K20me3 reduction, which prevents determination of neuroectodermal cells. Moreover, our observations are compatible with a recent model for ES cells differentiation by Thomson and colleagues, in which the differential activation of Oct4 and Sox2 regulate cell fate choices (Thomson, Liu et al. 2011). Studies in ES cell demonstrated that Oct4, Sox2 and Nanog constitute the pluripotency core transcriptional regulatory network (Boyer, Lee et al. 2005). These genes form an autoregulatory loop to sustain their own expression, and bind to target genes activating or repressing their expression. Overall, the pluripotent circuit inhibits germ layer differentiation, promoting the uncommitted state. In particular, Oct4 specifically represses neuroectoderm lineage, while Sox2 inhibits mesendodermal lineage (Thomson, Liu et al. 2011). The selective Oct-25 expression maintenance in the ectodermal sensorial layer and the impairment in the expression of neural markers suggest that a similar mechanism is present also in *Xenopus*.

ChIP experiments in uninjected and morphant embryos imply that Oct-25 is epigenetically regulated during development, by the progressive acquisition of H4K20me3 at its 5'-UTR; moreover, the persistent Oct-25 expression is linked with the loss of the mark upon xSuv4-20h depletion. Our analysis was restricted only to Oct-25 gene, but we cannot exclude that Oct-91, whose expression was upregulated in a small fraction of embryos upon suvar depletion, is regulated similarly to Oct-25. *Xenopus tropicalis* Oct genes are chromosomally linked in the genome; it is possible that H4K20me3 is assymmetrically distributed on Oct-25. Further ChIP-Seq analysis would elucidate this aspect and would allow a more complete overview of the Oct genes' epigenetic regulation.

As shown in our model (Fig. 54), we consider Oct-25 a major candidate to elicit the phenotypic consequences of xSuv4-20h enzyme depletion in frogs. First of all, its ectopic expression in the sensorial cell layer of the neuroectoderm in morphant embryos is in the right place to interfere with neuroblast determination by bHLH genes and lateral inhibition (Chitnis 1995; Lee, Hollenberg et al. 1995; Ma, Kintner et al. 1996). Furthermore, overexpression of Oct-25 in *Xenopus* embryos results in a very similar phenotype (i.e. repression of Ngnr 1a, N-tubulin and N-CAM, while leaving Chordin and MyoD expression untouched) (Cao, Siegel et al. 2006; Takebayashi-Suzuki, Arita et al. 2007).

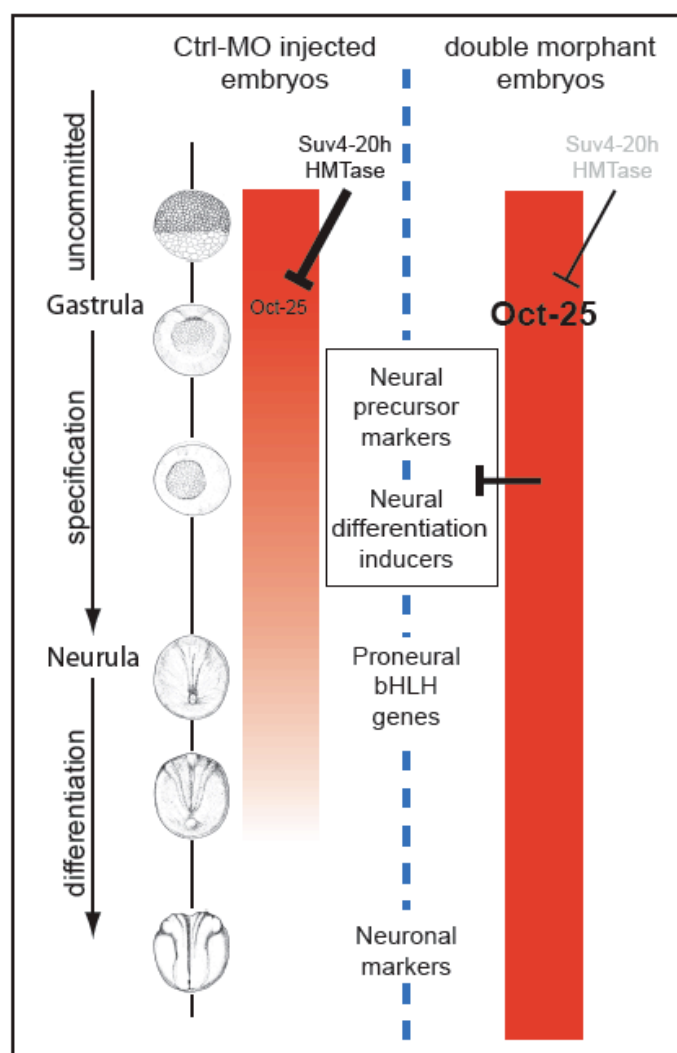


**Fig. 54: Model for *Xenopus* Suv4-20h enzyme function during neuroectoderm formation.** A global increase in H4K20me3 reduces widespread of Oct-25 expression in uncommitted cells during gastrulation as a prerequisite for neural induction. In H4K20me3 depleted morphant embryos, Oct-25 expression persists in the ectodermal stem cell compartment (sensorial cell layer), interfering with the transcriptional activation or activities of key regulators of the neural plate state and neurogenesis. Additional genes, that are like Oct-25 deregulated in xSuv4-20 morphant embryos, may also contribute to impaired ectoderm differentiation.

Another important aspect of this model concerns the misregulation of groups of genes functionally annotated as neural differentiation inducers, proneural genes and neuronal markers, respectively. RNA *in situ* hybridization experiments and qRT-PCR profiling in animal cap explants indicate that neural inducing markers like Zic1, Zic3 and Xiro factors (Xiro1) are suppressed in morphant embryos at gastrula stage. Subsequently, at early neurula, the proneural bHLH protein Ngnr 1a expression is compromised; this finally affects the normal levels of Delta-like 1 and N-tubulin in the neural plate. Genome scale location analysis in undifferentiated embryonic stem (ES)

cells identified several genes bound by the core transcriptional regulatory factors Oct4, Nanog and Sox2 (Boyer, Lee et al. 2005). Among these genes, Zic1, Zic2, Zic3 and IRX2 (homolog of *Xenopus* Xiro2) were described as “bound and expressed genes”, possibly indicating a positive regulation of these factors by Oct4 (Boyer, Lee et al. 2005). On the other hand, the Neurogenin2 (the homolog of *Xenopus* Ngnr 1a) gene locus is also bound by the pluripotency factors, but is not expressed, suggesting a repressive function exerted by the core pluripotency factors to this gene. Besides showing both the active and repressive role of Oct4 (and of Nanog and Sox2) in regulating gene expression in ES cells, as previously described by Ben-Shushan and colleagues (Ben-Shushan, Thompson et al. 1998), these results indicate a direct role of Oct4 on these neural differentiation inducers. The results from misexpression of constitutively active or repressive Oct-25 variants in *Xenopus*, are compatible with Zic1 and Zic3 as direct Oct-25 targets also in *Xenopus*. This result provides an entry point for future work to address the epistasis within this pathway and its interaction with the early neural gene network. Interestingly, the transcriptional repressor REST (RE1-silencing transcription factor), whose expression in ES cells is regulated by the pluripotency factors Oct4, Nanog and Sox2 (Boyer, Lee et al. 2005), has been shown to play a key role in ES cells and neural precursor cells (Hirabayashi and Gotoh 2010). REST abundance in pluripotent cells has been suggested to regulate genes involved in the neuronal differentiation, in a two-step process. In the transition from pluripotent to neural progenitor cell, REST binds to neuronal genes and keeps them in a poised state. As progenitors differentiate into neurons, REST dissociates from the RE1 sites of neuronal genes, triggering their activation. At the same time, it represses neuronal programmes in non-neural cells, by recruiting histone modifiers (e.g. H3K9-histone methyltransferases G9a and Suv39h1) and chromatin-binding proteins (Ballas, Grunseich et al. 2005; Hirabayashi and Gotoh 2010). The importance of chromatin changes upon differentiation (and more in general during development) is not only restricted to neurogenesis; it rather represents a complex layer of gene regulation, strongly connected to the transcriptional factors network, which is involved in the fate choice for cells of the different germ layers (Xu, Cole et al. 2011). These particular examples underline the intimate connections between transcription factor networks and the epigenetic machinery that regulates cell differentiation during development (Gaspar-Maia, Alajem et al. 2011; Young 2011).

The work presented here describes a similar scenario. *Xenopus* Suv4-20h HMTases and the modifications they establish exert a fundamental role in

determining neuroectodermal fate allocation by controlling Oct-25, a functional Oct3/4 homolog. The results from the epistasis experiments, whereby Oct-25 morpholino injections rescued double-morphant phenotypes, confirm and support the connection between the epigenetic machinery and the transcription factor circuitry. Moreover, Oct-25 upregulation in the sensorial layer of the epidermis in xSuv4-20h double morphants suggests that this POU-V protein exerts an additional role in the epidermal differentiation, possibly connected to the ciliogenic phenotype observed in xSuv4-20h enzymes depleted embryos.

### **5.2.8 Suv4-20h enzymes regulate Oct4 expression in murine ES cells**

The observed derepression of Oct-25 in the sensorial cell layer of the ectoderm implies a very intriguing role for Suv4-20h enzymes. This domain contains not only the uncommitted precursors of neuronal and epidermal cell types, but with regard to the involuting marginal zone also the mesodermal and endodermal precursors. Oct-25 deregulation may thus reflect a common mechanism by which Suv4-20h HMTases control pluripotency in the embryo. In agreement with this hypothesis we found elevated Oct4 protein levels in two independent Suv4-20h DKO ES cell lines both before and during differentiation, in comparison with two wildtype ES cell lines. Recent reports suggest that the pluripotency regulators Sox2 and Oct4 drive ES cells towards specific germ layer differentiation programs, as soon as the cells leave the pluripotent state (Teo, Arnold et al. 2011; Thomson, Liu et al. 2011). Our findings are in agreement with Thomson and colleagues, who describe Oct4 to antagonize ectodermal specification and to promote mesendodermal fate.

It is known that during ES cells differentiation, the mammalian Oct4 is repressed by a series of epigenetic mechanisms including DNA methylation, incorporation of somatic linker histones and repressive histone PTMs (e.g. H3K9me3, H3K27me3). Our findings that Oct4 protein levels are increased in the DKO ES cells both before and during differentiation suggest that Suv4-20h HMTases might regulate Oct4 transcription in a way that is at least partially independent from other repressive mechanisms targeting this locus. Further experiments are needed to extend our observation, e.g. to demonstrate H4K20me3 modification on the Oct4 gene. It would be interesting to test whether REST expression is different in Suv4-20h DKO and wildtype ES cells, and whether the misregulation of Oct4 affects the differentiation potential of Suv4-20h DKO ES cells along the neural lineage. It is important to note that the presented study, although describing in details the direct

regulation of Oct-25 in *Xenopus*, does not rule out contributions from additional factors and pathways possibly involved in blocking the exiting from pluripotency of murine ES cells.

### 5.3 Conclusion and future directions

Significant new insights have been obtained to further support the key role of epigenetic mechanisms during development. Active and repressive marks, as well as histone variants and ATP-dependent remodelling complexes, modulate gene expression both in pluripotent and terminally differentiated cells. One main challenge is to understand how the different epigenetic regulatory processes interact one another and cooperate with the transcription factor networks to ensure proper gene expression during embryonic development.

In this regard, the roles of *Xenopus* Suv4-20h HMTases have been investigated. The data shown here identifies a germ-layer specific function for H4K20me2 and -me3 states in the neuroectoderm. This function is achieved via the negative regulation of the pluripotency-related gene Oct-25 in frogs. Additionally, Suv4-20 DKO ES cells show an enhanced Oct4 expression, suggesting a conserved regulatory mechanism in which Suv4-20h enzymes regulate the transition from epiblast to ectoderm through transcriptional repression of POU-V genes in mice and frogs.

In my project, loss- and gain-of-function approaches have been used to characterize the functions of *Xenopus* Suv4-20h HMTases. The analysis, based mainly on RNA *in situ* hybridization and qRT-PCR assays, showed changes in the expression pattern of a small set of markers. Microarray analysis, performed in *Xenopus laevis*, confirmed and extended the RNA *in situ* hybridization results. It would be interesting to analyze the global gene expression profiling in *Xenopus tropicalis*, to gain a broader overview of the role of xSuv420h enzymes, during neurogenesis. Furthermore performing microarray analysis, or RNA-Seq experiments, at different developmental stages would give the chance to evaluate gene expression changes during development.

The presented ChIP experiments confirmed the presence of H4K20me3 at repetitive genomic regions, but at the same time highlighted a reproducible and significant enrichment on the Oct-25 gene locus. ChIP-seq analysis for trimethyl

H4K20 and for the two enzymes would help to understand the global enrichment of the mark and the proteins on the genome. This could lead to the identification of other direct target genes of the studied HMTases, proving that H4K20me3 regulates gene expression, besides the assumed role in pericentromeric heterochromatin formation (Schotta, Lachner et al. 2004).

Another important aspect of future experiments concerns the generation of specific antibodies against xSuv4-20h1 and h2. Besides being a fundamental tool for a variety of molecular approaches, antibodies would allow to understand possible interactions with other proteins. Mass Spectrometry analysis of xSuv4-20h HMTases IP samples could be the proper method to detect a complete set of interacting partners. In a comparable scenario, antibodies against Oct-25 would allow to carry out similar experiments (e.g. Mass Spectrometry and CHIP analysis), aimed to understand Oct-25 target genes during development and upon xSuv4-20h enzyme depletion.

The aforementioned approaches could be applied also to Suv4-20h DKO ES cells, in order to identify and elucidate the molecular mechanisms responsible for their elevated Oct4 levels. Moreover, differentiation of wildtype and Suv4-20h DKO ES cells into neuroectoderm would help to understand whether mechanisms similar to the ones described in *Xenopus* operate also in murine cells.

## 6 ABBREVIATIONS

<b>5' or 3'-UTR</b>	5' or 3' untranslated region
<b>53BP1</b>	p53 binding protein 1
<b>ACN</b>	acetonitrile
<b>ADP</b>	adenosine diphosphate
<b>AP</b>	alkaline phosphatase
<b>Approx.</b>	approximately
<b>ATP</b>	adenosine triphosphate
<b>BCIP</b>	5-bromo-4-chloro-3-indolyl-phosphate
<b>BCNE center</b>	blastula Chordin, Noggin expression center
<b>bHLH</b>	basic helix-loop-helix
<b>BMP</b>	bone morphogenetic proteins
<b>bp</b>	base pairs
<b>BSA</b>	bovine serum albumin
<b>CAF1</b>	chromatin assembly factor 1
<b>cDNA</b>	complementary DNA
<b>ChIP</b>	chromatin immunoprecipitation
<b>ChIP-seq</b>	chromatin immunoprecipitation sequencing
<b>CMFM</b>	calcium and magnesium free medium
<b>CNS</b>	central nervous system
<b>CpG</b>	cytosine-phosphate-guanine dinucleotide
<b>CTP</b>	cytosine triphosphate
<b>DEPC</b>	diethylpyrocarbonate
<b>DIG</b>	digoxigenin
<b>DKO</b>	double knockout
<b>DNA</b>	deoxyribonucleic acid
<b>e.g.</b>	exempli gratia, for example
<b>ESC</b>	embryonic stem cells
<b>et al.</b>	et alii, and others

<b>EtOH</b>	ethanol
<b>FGF</b>	fibroblast growth factor
<b>GFP</b>	green fluorescence protein
<b>GTP</b>	guanine triphosphate
<b>h</b>	hour
<b>HAT</b>	histone acetyltransferase
<b>HCG</b>	human chorionic gonadotropin
<b>HDAC</b>	histone deacetylase
<b>HMTase</b>	histone methyltransferase
<b>HP1</b>	heterochromatin protein 1
<b>hpf</b>	hour post fertilization
<b>ICC</b>	immunocytochemistry
<b>ICM</b>	inner cell mass
<b>i.e.</b>	id est
<b>IF</b>	immunofluorescence
<b>IP</b>	immunoprecipitation
<b>IR</b>	infrared
<b>KDa</b>	Kilodaltons
<b>M</b>	molar
<b>MAB</b>	maleic acid buffer
<b>MALDI-TOF</b>	matrix assisted laser desorption ionization-time of flight
<b>MBS</b>	modified Barth's saline
<b>MBT</b>	mid blastula transition
<b>MEF</b>	mouse embryonic fibroblast
<b>MeOH</b>	methanol
<b>miRNA</b>	micro RNA
<b>min</b>	minutes
<b>mRNA</b>	messenger RNA
<b>NBT</b>	nitro blue tetrazolium
<b>ncRNA</b>	non coding RNA
<b>NF</b>	Nieuwkoop Faber (Xenopus developmental stages)

<b>nm</b>	nanometer
<b>NTP</b>	nucleotide triphosphate
<b>o/n</b>	over-night
<b>PBS</b>	phosphate buffered saline
<b>PcG</b>	polycomb group
<b>PCP</b>	planar cell polarity
<b>PCR</b>	polymerase chain reaction
<b>PHF8</b>	PHD finger protein 8
<b>POU-V</b>	Pit-1, Oct1-2, Unc-86
<b>PRC1</b>	polycomb repressive complex 1
<b>PRC2</b>	polycomb repressive complex 2
<b>PRMT</b>	protein arginine N-methyltransferases
<b>PTM</b>	post translational modification
<b>qRT-PCR</b>	quantitative real time polymerase chain reaction
<b>Rb</b>	retinoblastoma
<b>RNA</b>	ribonucleic acid
<b>RNA-Seq</b>	RNA sequencing
<b>rpm</b>	revolutions per minute
<b>RT</b>	room temperature
<b>SDS-PAGE</b>	sodium dodecyl sulphate - polyacrylamide gel electrophoresis
<b>Sec</b>	seconds
<b>SET domain</b>	Suv39, E(z), Trx protein domain
<b>SS</b>	Steinberg's saline
<b>SUMO</b>	small ubiquitin-like modifier
<b>TE</b>	trophoectoderm
<b>TFA</b>	trifluoroacetic acid
<b>TGF beta</b>	transform growth factor beta
<b>TS cell</b>	trophoblast stem cell
<b>Ubx</b>	ultrabithorax
<b>UTP</b>	uridine triphosphate
<b>UV</b>	ultraviolet

<b>WB</b>	western blot
<b>XEN</b>	extraembryonic endoderm

## 7 REFERENCES

- Ahn, S. H., K. A. Henderson, et al. (2005). "H2B (Ser10) phosphorylation is induced during apoptosis and meiosis in *S. cerevisiae*." *Cell Cycle* **4**(6): 780-783.
- Akkers, R. C., S. J. van Heeringen, et al. (2009). "A hierarchy of H3K4me3 and H3K27me3 acquisition in spatial gene regulation in *Xenopus* embryos." *Dev Cell* **17**(3): 425-434.
- Azuara, V., P. Perry, et al. (2006). "Chromatin signatures of pluripotent cell lines." *Nat Cell Biol* **8**(5): 532-538.
- Ballas, N., C. Grunseich, et al. (2005). "REST and its corepressors mediate plasticity of neuronal gene chromatin throughout neurogenesis." *Cell* **121**(4): 645-657.
- Barski, A., S. Cuddapah, et al. (2007). "High-resolution profiling of histone methylations in the human genome." *Cell* **129**(4): 823-837.
- Beck, D. B., H. Oda, et al. (2012). "PR-Set7 and H4K20me1: at the crossroads of genome integrity, cell cycle, chromosome condensation, and transcription." *Genes Dev* **26**(4): 325-337.
- Ben-Shushan, E., J. R. Thompson, et al. (1998). "Rex-1, a gene encoding a transcription factor expressed in the early embryo, is regulated via Oct-3/4 and Oct-6 binding to an octamer site and a novel protein, Rox-1, binding to an adjacent site." *Mol Cell Biol* **18**(4): 1866-1878.
- Berger, S. L., T. Kouzarides, et al. (2009). "An operational definition of epigenetics." *Genes Dev* **23**(7): 781-783.
- Bergsland, M., M. Werme, et al. (2006). "The establishment of neuronal properties is controlled by Sox4 and Sox11." *Genes Dev* **20**(24): 3475-3486.
- Bhaumik, S. R., E. Smith, et al. (2007). "Covalent modifications of histones during development and disease pathogenesis." *Nat Struct Mol Biol* **14**(11): 1008-1016.
- Biron, V. L., K. J. McManus, et al. (2004). "Distinct dynamics and distribution of histone methyl-lysine derivatives in mouse development." *Dev Biol* **276**(2): 337-351.
- Blythe, S. A., C. D. Reid, et al. (2009). "Chromatin immunoprecipitation in early *Xenopus laevis* embryos." *Dev Dyn* **238**(6): 1422-1432.
- Bogdanovic, O., S. J. van Heeringen, et al. (2011). "The epigenome in early vertebrate development." *Genesis*.
- Bonasio, R., S. Tu, et al. (2010). "Molecular signals of epigenetic states." *Science* **330**(6004): 612-616.
- Bonisch, C., S. M. Nieratschker, et al. (2008). "Chromatin proteomics and epigenetic regulatory circuits." *Expert Rev Proteomics* **5**(1): 105-119.
- Boyer, L. A., T. I. Lee, et al. (2005). "Core transcriptional regulatory circuitry in human embryonic stem cells." *Cell* **122**(6): 947-956.
- Brewster, R., J. Lee, et al. (1998). "Gli/Zic factors pattern the neural plate by defining domains of cell differentiation." *Nature* **393**(6685): 579-583.
- Bylund, M., E. Andersson, et al. (2003). "Vertebrate neurogenesis is counteracted by Sox1-3 activity." *Nat Neurosci* **6**(11): 1162-1168.

- Cao, Y., S. Knochel, et al. (2004). "The POU factor Oct-25 regulates the Xvent-2B gene and counteracts terminal differentiation in *Xenopus* embryos." *J Biol Chem* **279**(42): 43735-43743.
- Cao, Y., D. Siegel, et al. (2007). "POU-V factors antagonize maternal VegT activity and beta-Catenin signaling in *Xenopus* embryos." *EMBO J* **26**(12): 2942-2954.
- Cao, Y., D. Siegel, et al. (2006). "Xenopus POU factors of subclass V inhibit activin/nodal signaling during gastrulation." *Mech Dev* **123**(8): 614-625.
- Cao, Y., D. Siegel, et al. (2008). "Oct25 represses transcription of nodal/activin target genes by interaction with signal transducers during *Xenopus* gastrulation." *J Biol Chem* **283**(49): 34168-34177.
- Cao, Y., D. Siegel, et al. (2008). "Oct25 represses transcription of nodal/activin target genes by interaction with signal transducers during *Xenopus* gastrulation." *The Journal of biological chemistry* **283**(49): 34168-34177.
- Chitnis, A. B. (1995). "The role of Notch in lateral inhibition and cell fate specification." *Mol Cell Neurosci* **6**(4): 311-321.
- Dambacher, S., M. Hahn, et al. (2010). "Epigenetic regulation of development by histone lysine methylation." *Heredity* **105**(1): 24-37.
- De Robertis, E. M. and H. Kuroda (2004). "Dorsal-ventral patterning and neural induction in *Xenopus* embryos." *Annu Rev Cell Dev Biol* **20**: 285-308.
- Deblandre, G. A., D. A. Wettstein, et al. (1999). "A two-step mechanism generates the spacing pattern of the ciliated cells in the skin of *Xenopus* embryos." *Development* **126**(21): 4715-4728.
- Diez del Corral, R. and K. G. Storey (2001). "Markers in vertebrate neurogenesis." *Nat Rev Neurosci* **2**(11): 835-839.
- Dillon, S. C., X. Zhang, et al. (2005). "The SET-domain protein superfamily: protein lysine methyltransferases." *Genome Biol* **6**(8): 227.
- Dupont, S., L. Zacchigna, et al. (2005). "Germ-layer specification and control of cell growth by Ectodermin, a Smad4 ubiquitin ligase." *Cell* **121**(1): 87-99.
- Dworkin-Rastl, E., H. Kandolf, et al. (1994). "The maternal histone H1 variant, H1M (B4 protein), is the predominant H1 histone in *Xenopus* pregastrula embryos." *Dev Biol* **161**(2): 425-439.
- Filion, G. J., J. G. van Bemmelen, et al. (2010). "Systematic protein location mapping reveals five principal chromatin types in *Drosophila* cells." *Cell* **143**(2): 212-224.
- Fussner, E., R. W. Ching, et al. (2011). "Living without 30nm chromatin fibers." *Trends Biochem Sci* **36**(1): 1-6.
- Gaspar-Maia, A., A. Alajem, et al. (2011). "Open chromatin in pluripotency and reprogramming." *Nat Rev Mol Cell Biol* **12**(1): 36-47.
- Gomez-Skarmeta, J., E. de La Calle-Mustienes, et al. (2001). "The Wnt-activated Xiro1 gene encodes a repressor that is essential for neural development and downregulates Bmp4." *Development* **128**(4): 551-560.
- Graham, V., J. Khudyakov, et al. (2003). "SOX2 functions to maintain neural progenitor identity." *Neuron* **39**(5): 749-765.
- Gray, R. S., P. B. Abitua, et al. (2009). "The planar cell polarity effector Fuz is essential for targeted membrane trafficking, ciliogenesis and mouse embryonic development." *Nat Cell Biol* **11**(10): 1225-1232.
- Green, J. (1999). "The animal cap assay." *Methods Mol Biol* **127**: 1-13.

- Grunz, H. and L. Tacke (1989). "Neural differentiation of *Xenopus laevis* ectoderm takes place after disaggregation and delayed reaggregation without inducer." *Cell Differ Dev* **28**(3): 211-217.
- Hansen, J. C. (2012). "Human mitotic chromosome structure: what happened to the 30-nm fibre?" *EMBO J* **31**(7): 1621-1623.
- Harland, R. (2000). "Neural induction." *Curr Opin Genet Dev* **10**(4): 357-362.
- Harris, W. A. and V. Hartenstein (1991). "Neuronal determination without cell division in *Xenopus* embryos." *Neuron* **6**(4): 499-515.
- Hartenstein, V. (1989). "Early neurogenesis in *Xenopus*: the spatio-temporal pattern of proliferation and cell lineages in the embryonic spinal cord." *Neuron* **3**(4): 399-411.
- Hayes, J. M., S. K. Kim, et al. (2007). "Identification of novel ciliogenesis factors using a new in vivo model for mucociliary epithelial development." *Dev Biol* **312**(1): 115-130.
- Heasman, J. (2006). "Patterning the early *Xenopus* embryo." *Development* **133**(7): 1205-1217.
- Heasman, J., C. C. Wylie, et al. (1984). "Fates and states of determination of single vegetal pole blastomeres of *X. laevis*." *Cell* **37**(1): 185-194.
- Hellsten, U., R. M. Harland, et al. (2010). "The genome of the Western clawed frog *Xenopus tropicalis*." *Science* **328**(5978): 633-636.
- Hemberger, M., W. Dean, et al. (2009). "Epigenetic dynamics of stem cells and cell lineage commitment: digging Waddington's canal." *Nat Rev Mol Cell Biol* **10**(8): 526-537.
- Hemmati-Brivanlou, A. and D. Melton (1997). "Vertebrate neural induction." *Annu Rev Neurosci* **20**: 43-60.
- Henikoff, S. (2000). "Heterochromatin function in complex genomes." *Biochim Biophys Acta* **1470**(1): 01-8.
- Hinkley, C. S., J. F. Martin, et al. (1992). "Sequential expression of multiple POU proteins during amphibian early development." *Mol Cell Biol* **12**(2): 638-649.
- Hirabayashi, Y. and Y. Gotoh (2010). "Epigenetic control of neural precursor cell fate during development." *Nat Rev Neurosci* **11**(6): 377-388.
- Kapoor-Vazirani, P., J. D. Kagey, et al. (2011). "SUV420H2-mediated H4K20 trimethylation enforces RNA polymerase II promoter-proximal pausing by blocking hMOF-dependent H4K16 acetylation." *Mol Cell Biol* **31**(8): 1594-1609.
- Kimelman, D. and K. J. Griffin (2000). "Vertebrate mesendoderm induction and patterning." *Curr Opin Genet Dev* **10**(4): 350-356.
- Kintner, C. (1992). "Molecular bases of early neural development in *Xenopus* embryos." *Annu Rev Neurosci* **15**: 251-284.
- Kohlmaier, A., F. Savarese, et al. (2004). "A chromosomal memory triggered by Xist regulates histone methylation in X inactivation." *PLoS Biol* **2**(7): E171.
- Kornberg, R. D. (1974). "Chromatin structure: a repeating unit of histones and DNA." *Science* **184**(139): 868-871.
- Kroll, K. L., A. N. Salic, et al. (1998). "Geminin, a neuralizing molecule that demarcates the future neural plate at the onset of gastrulation." *Development* **125**(16): 3247-3258.

- Kuroda, H., O. Wessely, et al. (2004). "Neural induction in *Xenopus*: requirement for ectodermal and endomesodermal signals via Chordin, Noggin, beta-Catenin, and Cerberus." *PLoS Biol* **2**(5): E92.
- Kwon, T., J. H. Chang, et al. (2003). "Mechanism of histone lysine methyl transfer revealed by the structure of SET7/9-AdoMet." *EMBO J* **22**(2): 292-303.
- Lamb, T. M., A. K. Knecht, et al. (1993). "Neural induction by the secreted polypeptide noggin." *Science* **262**(5134): 713-718.
- Latham, J. A. and S. Y. Dent (2007). "Cross-regulation of histone modifications." *Nat Struct Mol Biol* **14**(11): 1017-1024.
- Lee, B. M. and L. C. Mahadevan (2009). "Stability of histone modifications across mammalian genomes: implications for 'epigenetic' marking." *J Cell Biochem* **108**(1): 22-34.
- Lee, J. E., S. M. Hollenberg, et al. (1995). "Conversion of *Xenopus* ectoderm into neurons by NeuroD, a basic helix-loop-helix protein." *Science* **268**(5212): 836-844.
- Li, Z., F. Nie, et al. (2011). "Histone H4 Lys 20 monomethylation by histone methylase SET8 mediates Wnt target gene activation." *Proc Natl Acad Sci USA* **108**(8): 3116-3123.
- Liu, W., B. Tanasa, et al. (2010). "PHF8 mediates histone H4 lysine 20 demethylation events involved in cell cycle progression." *Nature* **466**(7305): 508-512.
- Luger, K., A. W. Mader, et al. (1997). "Crystal structure of the nucleosome core particle at 2.8 Å resolution." *Nature* **389**(6648): 251-260.
- Ma, Q., C. Kintner, et al. (1996). "Identification of neurogenin, a vertebrate neuronal determination gene." *Cell* **87**(1): 43-52.
- Maeshima, K., S. Hihara, et al. (2010). "Chromatin structure: does the 30-nm fibre exist in vivo?" *Curr Opin Cell Biol* **22**(3): 291-297.
- Magklara, A., A. Yen, et al. (2011). "An epigenetic signature for monoallelic olfactory receptor expression." *Cell* **145**(4): 555-570.
- Marcet, B., B. Chevalier, et al. (2011). "Control of vertebrate multiciliogenesis by miR-449 through direct repression of the Delta/Notch pathway." *Nat Cell Biol* **13**(10): 1280.
- Marks, H., T. Kalkan, et al. (2012). "The transcriptional and epigenomic foundations of ground state pluripotency." *Cell* **149**(3): 590-604.
- Martin, C. and Y. Zhang (2005). "The diverse functions of histone lysine methylation." *Nat Rev Mol Cell Biol* **6**(11): 838-849.
- Mikkelsen, T. S., M. Ku, et al. (2007). "Genome-wide maps of chromatin state in pluripotent and lineage-committed cells." *Nature* **448**(7153): 553-560.
- Mitchell, B., J. L. Stubbs, et al. (2009). "The PCP pathway instructs the planar orientation of ciliated cells in the *Xenopus* larval skin." *Curr Biol* **19**(11): 924-929.
- Mohammad, H. P. and S. B. Baylin (2010). "Linking cell signaling and the epigenetic machinery." *Nat Biotechnol* **28**(10): 1033-1038.
- Morrison, G. M. and J. M. Brickman (2006). "Conserved roles for Oct4 homologues in maintaining multipotency during early vertebrate development." *Development* **133**(10): 2011-2022.
- Munoz-Sanjuan, I. and A. H. Brivanlou (2002). "Neural induction, the default model and embryonic stem cells." *Nat Rev Neurosci* **3**(4): 271-280.

- Newport, J. and M. Kirschner (1982). "A major developmental transition in early *Xenopus* embryos: I. characterization and timing of cellular changes at the midblastula stage." *Cell* **30**(3): 675-686.
- Nishino, Y., M. Eltsov, et al. (2012). "Human mitotic chromosomes consist predominantly of irregularly folded nucleosome fibres without a 30-nm chromatin structure." *EMBO J* **31**(7): 1644-1653.
- Nishioka, K., J. C. Rice, et al. (2002). "PR-Set7 is a nucleosome-specific methyltransferase that modifies lysine 20 of histone H4 and is associated with silent chromatin." *Mol Cell* **9**(6): 1201-1213.
- Papp, B. and J. Muller (2006). "Histone trimethylation and the maintenance of transcriptional ON and OFF states by trxG and PcG proteins." *Genes Dev* **20**(15): 2041-2054.
- Park, T. J., S. L. Haigo, et al. (2006). "Ciliogenesis defects in embryos lacking inturned or fuzzy function are associated with failure of planar cell polarity and Hedgehog signaling." *Nat Genet* **38**(3): 303-311.
- Pesavento, J. J., H. Yang, et al. (2008). "Certain and progressive methylation of histone H4 at lysine 20 during the cell cycle." *Mol Cell Biol* **28**(1): 468-486.
- Pevny, L. and M. Placzek (2005). "SOX genes and neural progenitor identity." *Curr Opin Neurobiol* **15**(1): 7-13.
- Qi, H. H., M. Sarkissian, et al. (2010). "Histone H4K20/H3K9 demethylase PHF8 regulates zebrafish brain and craniofacial development." *Nature* **466**(7305): 503-507.
- Rea, S., F. Eisenhaber, et al. (2000). "Regulation of chromatin structure by site-specific histone H3 methyltransferases." *Nature* **406**(6796): 593-599.
- Revinski, D. R., A. R. Paganelli, et al. (2010). "Delta-Notch signaling is involved in the segregation of the three germ layers in *Xenopus laevis*." *Dev Biol* **339**(2): 477-492.
- Rogers, C. D., S. A. Moody, et al. (2009). "Neural induction and factors that stabilize a neural fate." *Birth Defects Res C Embryo Today* **87**(3): 249-262.
- Rugg-Gunn, P. J., B. J. Cox, et al. (2010). "Distinct histone modifications in stem cell lines and tissue lineages from the early mouse embryo." *Proc Natl Acad Sci U S A* **107**(24): 10783-10790.
- Sakaguchi, A. and R. Steward (2007). "Aberrant monomethylation of histone H4 lysine 20 activates the DNA damage checkpoint in *Drosophila melanogaster*." *J Cell Biol* **176**(2): 155-162.
- Sanders, S. L., M. Portoso, et al. (2004). "Methylation of histone H4 lysine 20 controls recruitment of Crb2 to sites of DNA damage." *Cell* **119**(5): 603-614.
- Santos, J., C. F. Pereira, et al. (2010). "Differences in the epigenetic and reprogramming properties of pluripotent and extra-embryonic stem cells implicate chromatin remodelling as an important early event in the developing mouse embryo." *Epigenetics Chromatin* **3**: 1.
- Sasai, N. and P. A. Defossez (2009). "Many paths to one goal? The proteins that recognize methylated DNA in eukaryotes." *Int J Dev Biol* **53**(2-3): 323-334.

- Sasai, Y. (1998). "Identifying the missing links: genes that connect neural induction and primary neurogenesis in vertebrate embryos." *Neuron* **21**(3): 455-458.
- Schena, M., D. Shalon, et al. (1995). "Quantitative monitoring of gene expression patterns with a complementary DNA microarray." *Science* **270**(5235): 467-470.
- Schneider, T. D., J. M. Arteaga-Salas, et al. (2011). "Stage-specific histone modification profiles reveal global transitions in the *Xenopus* embryonic epigenome." *PLoS One* **6**(7): e22548.
- Schotta, G., M. Lachner, et al. (2004). "A silencing pathway to induce H3-K9 and H4-K20 trimethylation at constitutive heterochromatin." *Genes Dev* **18**(11): 1251-1262.
- Schotta, G., R. Sengupta, et al. (2008). "A chromatin-wide transition to H4K20 monomethylation impairs genome integrity and programmed DNA rearrangements in the mouse." *Genes Dev* **22**(15): 2048-2061.
- Seo, S., G. A. Richardson, et al. (2005). "The SWI/SNF chromatin remodeling protein Brg1 is required for vertebrate neurogenesis and mediates transactivation of *Ngn* and *NeuroD*." *Development* **132**(1): 105-115.
- Slack, J. M. (2002). "Conrad Hal Waddington: the last Renaissance biologist?" *Nat Rev Genet* **3**(11): 889-895.
- Snape, A., C. C. Wylie, et al. (1987). "Changes in states of commitment of single animal pole blastomeres of *Xenopus laevis*." *Dev Biol* **119**(2): 503-510.
- Snir, M., R. Ofir, et al. (2006). "*Xenopus laevis* POU91 protein, an Oct3/4 homologue, regulates competence transitions from mesoderm to neural cell fates." *EMBO J* **25**(15): 3664-3674.
- Sokol, S., G. G. Wong, et al. (1990). "A mouse macrophage factor induces head structures and organizes a body axis in *Xenopus*." *Science* **249**(4968): 561-564.
- Spemann, H. and H. Mangold (2001). "Induction of embryonic primordia by implantation of organizers from a different species. 1923." *Int J Dev Biol* **45**(1): 13-38.
- Strahl, B. D. and C. D. Allis (2000). "The language of covalent histone modifications." *Nature* **403**(6765): 41-45.
- Stubbs, J. L., L. Davidson, et al. (2006). "Radial intercalation of ciliated cells during *Xenopus* skin development." *Development* **133**(13): 2507-2515.
- Stubbs, J. L., I. Oishi, et al. (2008). "The forkhead protein *Foxj1* specifies node-like cilia in *Xenopus* and zebrafish embryos." *Nat Genet* **40**(12): 1454-1460.
- Surani, M. A., K. Hayashi, et al. (2007). "Genetic and epigenetic regulators of pluripotency." *Cell* **128**(4): 747-762.
- Takebayashi-Suzuki, K., N. Arita, et al. (2007). "The *Xenopus* POU class V transcription factor XOct-25 inhibits ectodermal competence to respond to bone morphogenetic protein-mediated embryonic induction." *Mechanisms of development* **124**(11-12): 840-855.
- Takebayashi-Suzuki, K., N. Arita, et al. (2007). "The *Xenopus* POU class V transcription factor XOct-25 inhibits ectodermal competence to respond to bone morphogenetic protein-mediated embryonic induction." *Mech Dev* **124**(11-12): 840-855.

- Tardat, M., R. Murr, et al. (2007). "PR-Set7-dependent lysine methylation ensures genome replication and stability through S phase." *J Cell Biol* **179**(7): 1413-1426.
- Teo, A. K., S. J. Arnold, et al. (2011). "Pluripotency factors regulate definitive endoderm specification through eomesodermin." *Genes Dev* **25**(3): 238-250.
- Thomson, M., S. J. Liu, et al. (2011). "Pluripotency factors in embryonic stem cells regulate differentiation into germ layers." *Cell* **145**(6): 875-889.
- Trojer, P., G. Li, et al. (2007). "L3MBTL1, a histone-methylation-dependent chromatin lock." *Cell* **129**(5): 915-928.
- Turner, B. M. (2002). "Cellular memory and the histone code." *Cell* **111**(3): 285-291.
- van Steensel, B. (2011). "Chromatin: constructing the big picture." *EMBO J* **30**(10): 1885-1895.
- Varga-Weisz, P. D. and P. B. Becker (2006). "Regulation of higher-order chromatin structures by nucleosome-remodelling factors." *Curr Opin Genet Dev* **16**(2): 151-156.
- Vastenhouw, N. L., Y. Zhang, et al. (2010). "Chromatin signature of embryonic pluripotency is established during genome activation." *Nature* **464**(7290): 922-926.
- Wallingford, J. B. (2010). "Planar cell polarity signaling, cilia and polarized ciliary beating." *Curr Opin Cell Biol* **22**(5): 597-604.
- Weake, V. M. and J. L. Workman (2008). "Histone ubiquitination: triggering gene activity." *Mol Cell* **29**(6): 653-663.
- Wilson, S. I. and T. Edlund (2001). "Neural induction: toward a unifying mechanism." *Nat Neurosci* **4 Suppl**: 1161-1168.
- Wylie, C. C., A. Snape, et al. (1987). "Vegetal pole cells and commitment to form endoderm in *Xenopus laevis*." *Dev Biol* **119**(2): 496-502.
- Xu, C. R., P. A. Cole, et al. (2011). "Chromatin "prepattern" and histone modifiers in a fate choice for liver and pancreas." *Science* **332**(6032): 963-966.
- Yan, B., K. M. Neilson, et al. (2009). "foxD5 plays a critical upstream role in regulating neural ectodermal fate and the onset of neural differentiation." *Dev Biol* **329**(1): 80-95.
- Yang, H. and C. A. Mizzen (2009). "The multiple facets of histone H4-lysine 20 methylation." *Biochem Cell Biol* **87**(1): 151-161.
- Young, R. A. (2011). "Control of the embryonic stem cell state." *Cell* **144**(6): 940-954.
- Yu, X., C. P. Ng, et al. (2008). "Foxj1 transcription factors are master regulators of the motile ciliogenic program." *Nat Genet* **40**(12): 1445-1453.
- Zhang, Y. and D. Reinberg (2001). "Transcription regulation by histone methylation: interplay between different covalent modifications of the core histone tails." *Genes Dev* **15**(18): 2343-2360.
- Zhou, H., H. Hu, et al. (2010). "Non-coding RNAs and their epigenetic regulatory mechanisms." *Biol Cell* **102**(12): 645-655.

## 8 APPENDICES

### 8.1 Suv4-20h enzymes regulate murine Oct-4 expression

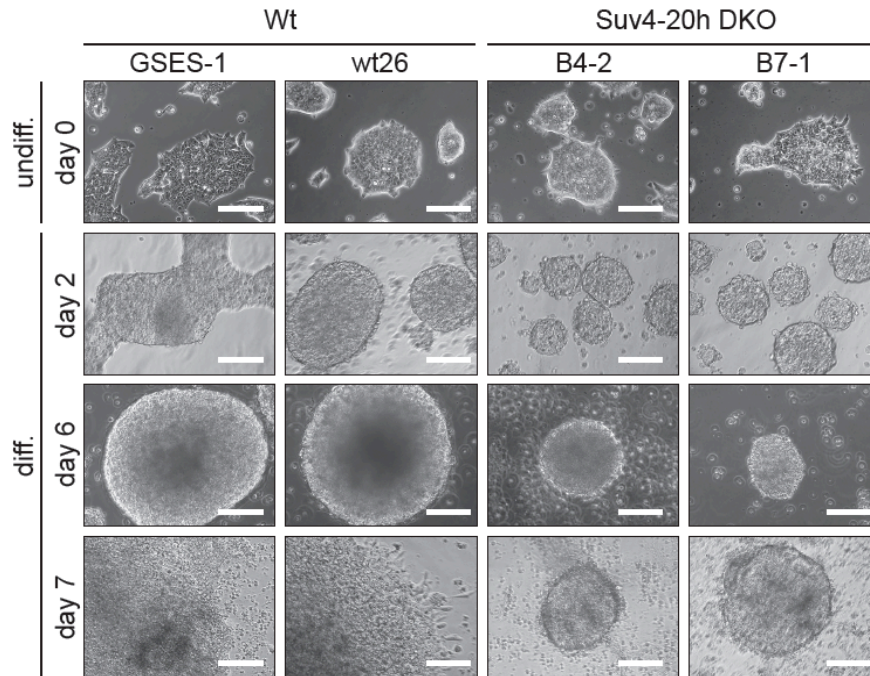


**Fig. 55: Morphology of wild-type and Suv4-20h DKO cell lines upon differentiation.** Wildtype (wt26, GSES) and Suv4-20h DKO (B4, B7) cell lines were differentiated *in vitro* by embryoid bodies formation. Top row: undifferentiated ES cells (day 0). Middle rows: embryoid bodies at day 2 and day 6, respectively. Note the smaller Suv4-20h DKO bodies compared to the wildtype. Bottom row: cells from disaggregated embryoid bodies, replated for 24h. Scale bar: 100  $\mu$ m.

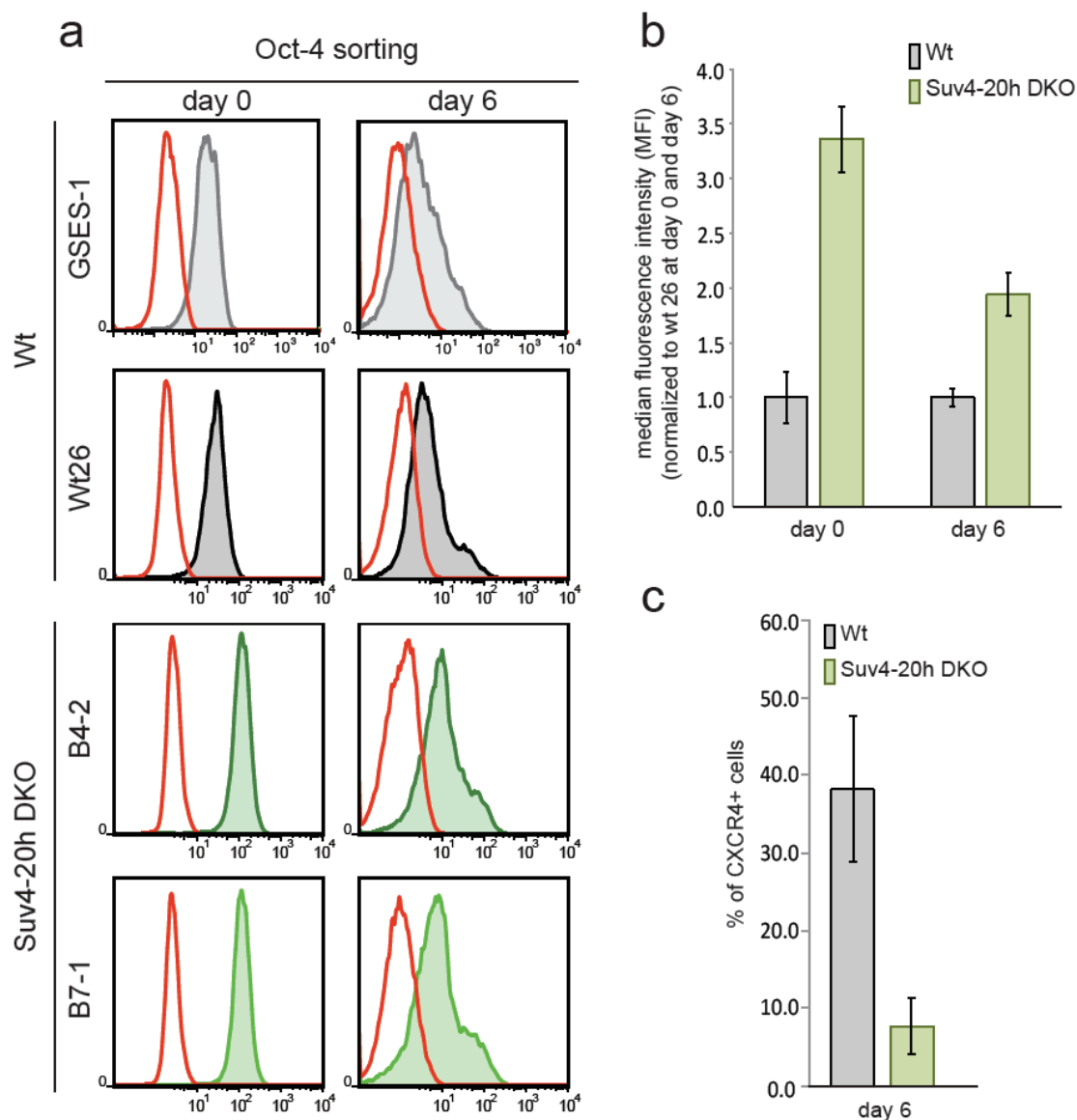


**Fig. 56: FACS analysis of wild-type and Suv4-20h DKO cell lines stained for Oct4 and CXCR4 protein, before and after differentiation. (a)** At day 0 and day 6 cell lines were stained for Oct-4 protein and subjected to FACS analysis. Red graph: fluorescence of non-specific isotype control; black and green graphs: Oct-4 protein levels in wild-type and Suv4-20h DKO ES cell lines. **(b)** Suv4-20h DKO cells have a higher Oct-4 protein levels compared to wild-type ES cells both at day 0 and at day 6. Median fluorescence intensity was calculated from data in panel a. Data represent mean values from two to three independent experiments, error bars indicate SEM. **(c)** Suv4-20h DKO cells show a reduction in the percentage of CXCR4+ cells at differentiation day 6. Data represent normalized values of percentage of CXCR4+ cells as means of three independent experiments, error bars indicate SEM

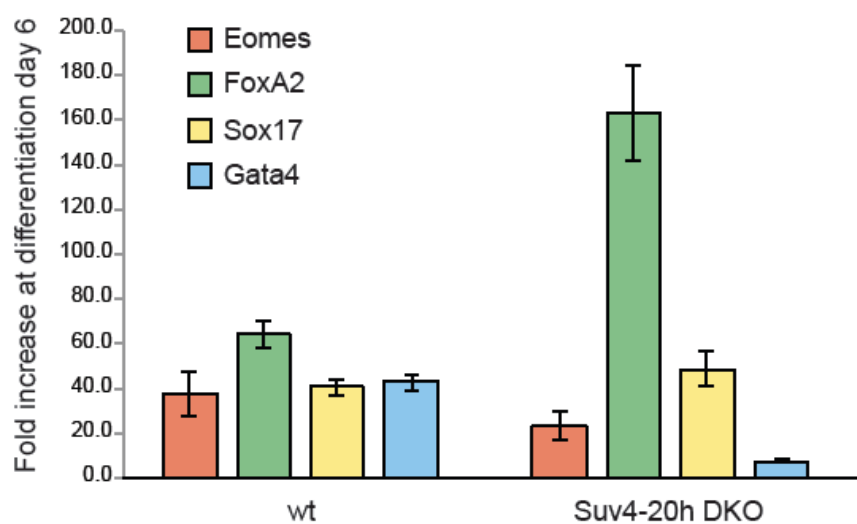


**Fig. 57: qRT-PCR profiles in wt and DKO cells at differentiation day 6.** qRT-PCR profiles for the indicated genes in wildtype (wt) and Suv4-20h DKO cell lines at differentiation day 6. FoxA2 and Gata4 expression levels are misregulated in Suv4-20 DKO cells upon differentiation.

## 8.2 Microarray gene lists

List of upregulated genes upon xSuv4-20h enzymes depletion (microarray data ordered by Log2 fold change).

Set-probes Number	Log2 fold change	Gene Name
XI.56179.1.S1_at	3,51	---
XI.51774.1.S1_at	2,88	---
XI.47853.1.A1_at	2,76	---
XI.25416.1.A1_at	2,69	---
XI.1193.1.S1_at	2,68	gck
XI.18439.1.S1_at	2,53	rilp
XI.47940.1.A1_at	2,49	---
XI.53476.1.S1_at	2,47	---
XI.1064.1.S1_at	2,42	trim7
XI.25774.1.S1_at	2,4	MGC81526
XI.40798.1.S1_at	2,39	---
XI.51372.1.S1_a_at	2,39	---
XI.52460.1.S1_at	2,38	---
XI.19172.1.A1_at	2,3	---
XI.34722.1.S1_s_at	2,3	---
XI.19376.1.S1_at	2,29	---
XI.31997.1.S1_at	2,25	---
XI.48728.1.S1_at	2,23	fitm2
XI.1289.1.S1_at	2,22	tdgf1
XI.53127.1.S1_at	2,22	---
XI.4750.1.S1_at	2,13	cdc42se2-c
XI.10927.1.S1_at	2,12	---
XI.2530.1.S1_at	2,1	creb1
XI.3179.1.A1_at	2,04	---
XI.23963.3.S1_a_at	2,04	LOC100137667
XI.28973.3.A1_at	2,03	---
XI.29712.1.A1_at	2,02	---
XI.42733.1.S1_x_at	1,99	---
XI.48266.2.A1_x_at	1,98	---
XI.4957.1.S1_at	1,97	pou5f1.1
XI.11656.1.S1_at	1,96	stk35
XI.19397.1.A1_at	1,94	---
XI.46630.2.S1_at	1,94	---
XI.16875.1.S1_at	1,94	LOC100137681
XI.373.1.S1_at	1,93	eomes
XI.11269.1.A1_at	1,92	---

XI.16230.1.A1_at	1,92	---
XI.7399.1.S1_at	1,92	amfr
XI.11611.1.A1_at	1,89	---
XI.32326.1.S1_at	1,87	etv3
XI.51799.1.S1_at	1,83	---
XI.51850.1.A1_at	1,83	---
XI.25849.1.S1_at	1,83	zar1
XI.42733.1.S1_at	1,81	---
XI.15360.2.S1_at	1,8	---
XI.16008.1.A1_at	1,79	---
XI.1047.1.S1_a_at	1,78	lhx5
XI.56327.1.S1_at	1,78	---
XI.51227.1.S1_at	1,75	peci
XI.41032.1.S1_at	1,74	---
XI.54965.1.A1_at	1,74	---
XI.6315.2.S1_at	1,74	c1orf124
XI.16322.1.A1_at	1,73	ccnb3-a
XI.41974.1.S1_at	1,72	---
XI.55152.1.A1_at	1,71	---
XI.7399.1.S2_at	1,71	amfr
XI.15207.1.S1_at	1,71	---
XI.53435.1.S1_at	1,7	ska3
XI.7160.1.S1_at	1,69	c3orf64
XI.9584.1.A1_at	1,69	---
XI.55449.1.S1_at	1,67	zfyve27
XI.32657.2.S1_at	1,66	---
XI.30041.1.S1_at	1,65	---
XI.47766.1.A1_at	1,62	---
XI.54072.1.S1_at	1,62	---
XI.47946.1.A1_at	1,61	---
XI.31059.1.S1_at	1,6	---
XI.23456.1.S1_at	1,6	ncdn
XI.34091.1.A1_at	1,6	---
XI.11388.1.A1_at	1,6	---
XI.12020.2.A1_at	1,59	---
XI.50620.1.S1_at	1,59	---
XI.42689.1.S1_at	1,58	---
XI.15360.1.A1_at	1,58	---
XI.32139.2.S1_at	1,57	hsd17b14
XI.6244.1.S1_at	1,57	plin3
XI.2314.1.S1_at	1,56	ccdc3
XI.30112.2.S1_at	1,56	---
XI.28979.1.S1_at	1,55	oraov1

XI.12093.1.S1_at	1,55	tdrd6
XI.52566.1.S1_at	1,55	---
XI.25710.1.S1_at	1,54	MGC68595
XI.14872.1.A1_at	1,54	---
XI.54908.1.A1_at	1,54	---
XI.4281.1.A1_s_at	1,53	rdh9
XI.2922.1.S1_at	1,53	LOC100137665
XI.19293.1.S1_at	1,53	kctd5
XI.2986.1.S1_at	1,53	---
XI.51384.1.S1_at	1,53	---
XI.34532.1.S1_at	1,53	---
XI.46177.1.S1_at	1,51	---
XI.49986.1.S1_at	1,51	pnpla4
XI.5163.1.A1_at	1,5	---
XI.9123.1.A1_at	1,5	---
XI.55112.1.A1_at	1,49	ska3
XI.8031.1.S1_at	1,49	hist1h2aj
XI.9393.1.S1_at	1,47	---
XI.51398.1.S1_at	1,46	---
XI.1775.1.S1_at	1,46	vegt-a
XI.50033.1.S1_at	1,46	dnajc27-b
XI.9887.1.S1_at	1,45	cyp4v2
XI.12880.1.A1_at	1,45	---
XI.22487.1.S1_at	1,44	tor1b
XI.2428.1.S1_at	1,44	LOC733412
XI.32657.1.A1_at	1,44	---
XI.2852.1.S1_at	1,44	---
XI.24032.1.S1_at	1,43	jak1
XI.14329.1.A1_at	1,43	---
XI.1406.1.S1_a_at	1,43	---
XI.18363.1.A1_at	1,43	---
XI.55247.1.A1_at	1,43	---
XI.17947.1.S1_at	1,42	sort1
XI.25413.1.A1_at	1,42	---
XI.44533.1.S1_at	1,41	---
XI.52576.1.S1_at	1,41	LOC733198
XI.13021.1.A1_at	1,41	---
XI.21562.1.S1_at	1,41	rasd1
XI.21151.1.S1_at	1,41	---
XI.46588.1.S1_at	1,41	atp6v0b
XI.13064.1.S1_at	1,41	---
XI.48206.1.S1_at	1,4	oat

XI.7191.1.S1_at	1,39	EIF4E3-A
XI.25872.1.S1_at	1,39	---
XI.46947.1.S1_at	1,39	---
XI.1765.1.S1_at	1,39	---
XI.30010.1.S1_at	1,39	---
XI.32139.1.S1_at	1,39	HSd17b14
XI.52844.1.S1_at	1,39	---
XI.32532.1.A1_at	1,38	---
XI.46054.1.A1_at	1,38	---
XI.21562.2.S1_at	1,38	RASD1
XI.6315.1.A1_at	1,38	C1orf124
XI.55777.1.A1_at	1,38	---
XI.45598.1.S1_at	1,38	---
XI.31412.1.S1_at	1,37	---
XI.11925.1.A1_at	1,37	---
XI.44851.2.S1_at	1,37	---
XI.13136.1.S1_a_at	1,36	DAP
XI.51793.1.S1_at	1,36	---
XI.47078.1.S1_at	1,36	PTP4A3
XI.32061.1.S1_at	1,35	MFAP3L
XI.21150.1.S1_at	1,35	Hpgdsa
XI.17503.3.S1_at	1,34	---
XI.50699.1.S1_at	1,34	---
XI.33175.1.S2_at	1,34	RPS6KA3
XI.24496.1.S1_at	1,34	---
XI.18858.1.A1_at	1,33	---
XI.53809.1.A1_at	1,33	SPop
XI.24085.1.S1_at	1,33	ST3Gal3
XI.33937.1.S1_at	1,33	Rab11fip2
XI.29614.1.S1_a_at	1,32	PLIN2
XI.33403.1.S1_at	1,32	FAM83D
XI.6470.1.S1_at	1,32	---
XI.34601.1.S1_a_at	1,32	ACSL3
XI.37859.1.S1_at	1,31	LOC100037047
XI.44959.1.S1_at	1,31	---
XI.37539.1.S1_at	1,31	GS17
XI.32570.1.S1_s_at	1,31	DEGS2 /// MGC83232
XI.10102.1.A1_at	1,31	LOC100174804
XI.12973.1.S1_a_at	1,3	---
XI.2522.1.S1_at	1,3	---
XI.54994.1.A1_at	1,3	---

XI.56049.1.S1_at	1,3	---
XI.33477.2.A1_at	1,29	---
XI.11887.1.S1_at	1,29	MGC115675
XI.44851.2.S1_x_at	1,29	---
XI.16251.1.S1_at	1,29	---
XI.53905.1.S1_at	1,28	---
XI.8187.1.S1_at	1,28	dctn2
XI.21326.1.S1_at	1,28	klhdc10
XI.3735.1.S1_at	1,28	MGC81429
XI.14713.1.S1_at	1,27	---
XI.21359.1.S1_at	1,27	---
XI.1697.1.A1_at	1,27	---
XI.16855.1.S1_at	1,27	---
XI.46698.1.S1_at	1,27	wbscr27
XI.7479.2.S1_at	1,26	---
XI.45992.1.A1_at	1,26	---
XI.9874.1.A1_at	1,26	---
XI.30468.1.S1_at	1,26	ergic1
XI.18727.1.A1_at	1,26	---
XI.4078.1.A1_at	1,25	---
XI.1838.1.S1_at	1,25	afg3l2
XI.17281.1.S1_at	1,25	---
XI.48153.1.A1_at	1,25	---
XI.29045.1.A1_at	1,24	---
XI.7812.1.S1_at	1,24	---
XI.47379.1.S1_at	1,24	rnf219
XI.34176.1.A1_at	1,24	---
XI.11925.1.A1_x_at	1,24	---
XI.17470.1.S1_at	1,24	dctn1
XI.2893.2.A1_a_at	1,24	faf1
XI.517.1.S1_at	1,24	rnd1
XI.47381.1.S1_at	1,24	gtf2i
XI.30271.1.S1_at	1,23	---
XI.48567.3.S1_at	1,23	LOC100127246
XI.10226.1.S1_at	1,23	ube3c
XI.4601.1.S1_at	1,22	incenp-a
XI.10739.1.S1_at	1,22	---
XI.34772.1.S1_at	1,22	p4ha2
XI.7722.1.S1_at	1,22	sccpdh.2
XI.24771.1.S1_at	1,22	lpin2
XI.25957.1.S1_at	1,22	mrpl53
XI.49054.1.S1_at	1,22	ing5

XI.512.1.S1_s_at	1,22	kif22
XI.44918.1.S1_at	1,21	---
XI.46997.1.S1_at	1,21	kctd2
XI.52319.1.S1_at	1,21	---
XI.2519.1.S1_at	1,21	---
XI.14166.1.A1_at	1,21	---
XI.17848.2.S1_at	1,21	---
XI.19520.1.A1_at	1,21	MGC115523
XI.806.1.S1_at	1,21	hist1h1t
XI.49096.1.S1_at	1,21	LOC100037099
XI.4940.1.S1_at	1,2	ivns1abp
XI.28973.1.S1_at	1,2	---
XI.13437.1.S1_at	1,2	LOC398263
XI.12155.1.S1_at	1,2	---
XI.5394.1.S1_at	1,2	rnf34
XI.55930.1.S1_at	1,2	---
XI.46797.1.S1_at	1,2	LOC779088
XI.33550.1.S1_at	1,19	LOC443647
XI.53201.1.S1_at	1,19	---
XI.23948.1.S1_at	1,19	murc
XI.6342.1.S1_at	1,19	pcmt1
XI.4195.1.S1_at	1,18	irf5
XI.56006.1.S1_at	1,18	---
XI.48349.1.S1_at	1,18	dcaf6
XI.53491.1.S1_at	1,18	---
XI.10025.1.A1_at	1,18	LOC414703
XI.52581.1.S1_at	1,18	---
XI.31159.1.A1_at	1,18	---
XI.1164.1.S1_at	1,17	d7
XI.7714.1.A1_at	1,17	---
XI.54204.1.A1_at	1,17	---
XI.3305.1.S1_s_at	1,17	sip1
XI.48196.1.A1_at	1,17	sip1
XI.47669.1.S1_at	1,17	MGC80990
XI.34601.1.S1_at	1,17	acsl3
XI.33707.1.S1_at	1,17	---
XI.9337.1.A1_at	1,17	---
XI.7880.1.A1_at	1,17	---
XI.16058.1.S1_at	1,16	---
XI.17454.1.A1_at	1,16	sec23ip
XI.32379.1.S1_at	1,16	LOC443674
XI.7045.1.S1_x_at	1,16	---

XI.53498.2.S1_at	1,16	---
XI.31154.1.S1_at	1,16	---
XI.49719.1.S1_s_at	1,15	LOC494743
XI.10630.1.S1_at	1,15	dph1
XI.47958.1.A1_at	1,15	---
XI.641.1.S1_at	1,15	bicc1-a
XI.11330.1.S1_at	1,15	---
XI.49481.1.S1_at	1,14	LOC495441
XI.25688.1.S1_at	1,14	baf-l
XI.9218.1.S1_at	1,14	---
XI.49741.1.S1_at	1,14	rwdd2a
XI.47366.1.S1_at	1,13	MGC80983
XI.13850.2.S1_at	1,13	---
XI.52319.2.A1_x_at	1,13	---
XI.25810.1.S1_at	1,13	LOC443658
XI.5697.1.S1_at	1,13	c-raf
XI.54870.1.S1_at	1,13	---
XI.34475.1.S1_at	1,13	trappc9
XI.41313.1.A1_at	1,13	---
XI.5968.1.S1_at	1,13	ube2j2
XI.50438.1.S2_at	1,12	anp32c
XI.9002.1.A1_at	1,12	---
XI.33749.1.S1_at	1,12	---
XI.5479.1.S1_at	1,12	---
XI.54080.1.S1_at	1,12	---
XI.11612.1.A1_at	1,12	---
XI.7094.1.S1_a_at	1,12	---
XI.32000.1.A1_at	1,12	---
XI.13567.1.A1_at	1,12	---
XI.51014.1.S1_at	1,11	---
XI.10854.1.S1_at	1,11	c18orf55
XI.30614.1.S1_s_at	1,11	acadsb
XI.34974.1.S1_at	1,11	MGC68531
XIAffx.98.1.S1_x_at	1,11	NA
XI.25997.1.S1_at	1,11	coq5
XI.34650.1.S2_at	1,11	Ufd1l
XI.20994.1.S1_at	1,11	---
XI.41265.1.A1_at	1,11	---
XI.56986.1.A1_at	1,11	---
XI.50400.1.S1_a_at	1,11	nipa1
XI.21289.1.S1_at	1,1	---
XI.45732.1.S1_at	1,1	---
XI.11330.2.S1_a_at	1,1	---

XI.5042.3.S1_at	1,1	---
XI.23517.1.S1_a_at	1,09	LOC398493
XI.50629.1.S1_at	1,09	---
XI.48605.1.S1_at	1,09	MGC86493
XI.23364.1.S1_at	1,09	---
XI.25927.1.A1_at	1,09	---
XI.42146.1.S1_at	1,09	LOC494706
XI.15260.1.S1_at	1,09	---
XI.1201.1.S1_at	1,08	nr3c1
XI.8253.1.S1_at	1,08	snag1
XI.23902.1.S1_at	1,08	MGC82150
XIAffx.98.1.S1_at	1,08	NA
XI.8903.2.S1_at	1,08	---
XI.44533.1.S1_x_at	1,08	---
XI.26083.1.S1_at	1,08	mdh2a
XI.25786.1.S1_at	1,08	csnk1g2
XI.50087.1.S1_at	1,07	fam96a
XI.50891.2.A1_at	1,07	---
XI.7121.1.S2_at	1,07	acp1
XI.6339.1.A1_at	1,07	---
XI.32102.1.A1_at	1,07	---
XI.56382.1.S1_at	1,07	tmem45b
XI.45559.1.S1_at	1,07	tmod3
XI.26460.1.S1_at	1,06	---
XI.14983.2.S1_at	1,06	---
XI.31412.3.S1_at	1,06	---
XI.56301.1.S1_at	1,06	---
XI.14606.1.S1_at	1,06	---
XI.46199.1.S2_at	1,05	hs2st1
XI.51975.2.A1_at	1,05	---
XI.31693.1.S1_at	1,05	pex1
XI.13891.1.A1_at	1,05	---
XI.54959.1.S1_at	1,05	MGC154476
XI.15182.1.S2_at	1,05	dhdds
XI.56952.1.S1_at	1,04	---
XI.55197.2.S1_a_at	1,04	bnip3l
XI.11706.1.S1_x_at	1,04	pabpn1l-a
XI.48567.1.A1_at	1,04	LOC100127246
XI.20115.3.A1_a_at	1,04	trmu
XI.7706.1.S1_at	1,04	ybx2-b
XI.49744.1.S1_at	1,04	tp53inp1
XI.54850.1.S1_at	1,04	---

XI.10050.2.S1_at	1,04	---
XI.15119.2.S1_at	1,03	LOC100158450
XI.48515.1.S1_at	1,03	---
XI.53048.1.S1_at	1,03	---
XI.29225.1.S1_at	1,03	---
XI.12033.1.A1_at	1,03	---
XI.6936.1.A1_at	1,03	---
XI.42160.1.S2_at	1,03	otx5-A
XI.9389.2.S1_at	1,02	---
XI.28967.1.A1_at	1,02	---
XI.24002.1.S1_at	1,02	papss1
XI.13079.1.S1_at	1,02	cdkal1
XI.6999.1.S1_at	1,02	timmm50
XI.50575.1.S1_at	1,02	---
XI.23557.1.S1_at	1,02	epb4.1l3
XI.1430.2.S1_at	1,02	pik4ca
XI.49882.1.S1_at	1,02	LOC496018
XI.11915.1.A1_at	1,02	---
XI.48567.2.S1_at	1,02	LOC100127246
XI.5714.1.S1_at	1,01	rpn2
XI.52397.1.S1_at	1,01	---
XI.43573.1.S1_at	1,01	lrwd1
XI.11078.1.A1_at	1,01	---
XI.18279.1.S1_at	1,01	tbc1d4
XI.8543.1.S1_at	1,01	pitpnb.2
XI.20422.1.A1_at	1,01	---
XI.9460.1.S1_at	1,01	gtdc1
XI.47115.1.S1_at	1,01	LOC432186
XI.34771.1.S1_at	1,01	LOC496311
XI.24466.1.S1_at	1	---
XI.3594.1.S1_a_at	1	---
XI.29016.2.S1_a_at	1	metap1
XI.12099.1.S1_at	1	cla
XI.1132.1.S1_at	1	slc7a5b
XI.6630.2.S1_a_at	0,99	patl1
XI.18171.2.S1_at	0,99	---
XI.47976.1.A1_at	0,99	---
XI.5575.1.S1_at	0,99	gyg
XI.1015.1.S1_at	0,99	pole2
XI.25352.1.S1_at	0,99	---
XI.24173.1.S1_at	0,99	---
XI.34880.1.S1_at	0,99	---

XI.15195.1.A1_at	0,99	---
XI.7574.1.A1_at	0,99	---
XI.15428.1.A1_at	0,99	---
XI.10248.1.S1_at	0,99	atpbd4
XI.32258.1.S1_at	0,98	dbt
XI.19520.1.A1_s_at	0,98	ubr2
XI.30268.1.S1_at	0,98	---
XI.6990.1.S1_at	0,98	ap1g2
XI.19972.1.S1_a_at	0,98	---
XI.4568.1.S1_at	0,98	MGC115587
XI.14861.1.A1_at	0,98	---
XI.8401.2.S1_a_at	0,98	stx18
XI.13268.1.A1_at	0,98	cwc27
XI.13017.2.S1_at	0,97	LOC495838
XI.24432.1.S1_at	0,97	ubr2
XI.16399.1.S1_at	0,97	Imbrd2
XI.7199.1.S1_at	0,97	---
XI.55137.1.A1_at	0,97	---
XI.3542.1.A1_at	0,97	---
XI.19223.1.S1_at	0,97	os9
XI.50412.1.S1_at	0,97	chst13
XI.25597.1.S1_at	0,97	sfxn2
XI.46166.1.S1_at	0,97	slc30a2
XI.18250.1.S1_at	0,96	abr
XI.2704.1.A1_at	0,96	---
XI.9458.2.S1_at	0,96	---
XI.3714.1.A1_at	0,96	---
XI.17590.1.A1_at	0,96	---
XI.12020.1.S1_at	0,95	---
XI.32875.1.A1_at	0,95	---
XI.34699.1.A1_at	0,95	---
XI.14607.1.S1_at	0,95	---
XI.8273.1.A1_at	0,95	---
XI.57086.1.A1_at	0,95	---
XI.1132.1.S2_at	0,94	slc7a5b
XI.32522.1.S1_at	0,94	fkbp8
XI.52297.1.S1_at	0,94	---
XI.48996.1.S1_at	0,94	iyd
XI.43713.1.S1_at	0,94	LOC734170
XI.54485.1.S1_at	0,94	cstf3
XI.50390.1.S1_at	0,94	zdhhc15
XI.51644.1.S1_at	0,94	---
XI.52096.1.A1_at	0,94	---

XI.53168.1.S1_at	0,93	---
XI.55920.1.S1_at	0,93	---
XI.3104.1.S1_at	0,93	shkbp1
XI.6794.2.S1_at	0,93	---
XI.34901.1.S1_s_at	0,93	---
XI.55554.1.A1_at	0,93	---
XI.7563.3.S1_at	0,93	---
XI.50822.1.S1_at	0,93	---
XI.47932.1.S1_at	0,93	---
XI.24767.3.S1_at	0,93	---
XI.49562.1.S1_s_at	0,93	eps8l3
XI.46390.1.S1_at	0,92	scyl1
XI.24617.1.A1_at	0,92	---
XI.3594.2.S1_a_at	0,92	---
XI.13978.1.S1_at	0,92	arhgdia
XI.12701.1.S1_at	0,92	---
XI.19496.1.S1_at	0,92	MGC130950
XI.56798.1.S1_at	0,92	---
XI.19657.2.A1_at	0,92	---
XI.8212.1.S2_at	0,92	rtn3
XI.54755.1.S1_at	0,92	slc2a10
XI.2893.1.S1_at	0,91	faf1
XI.7574.2.S1_at	0,91	---
XI.15232.1.S1_at	0,91	---
XI.25888.1.S1_at	0,91	mrpl1
XI.54802.2.S1_at	0,9	zic3-A
XI.26421.1.S1_at	0,9	---
XI.29436.1.S1_at	0,9	slc25a24-b
XI.53513.1.S1_at	0,9	---
XI.41260.1.S1_at	0,9	---
XI.4149.1.A1_at	0,9	---
XI.5877.1.S1_at	0,9	map2k1
XI.51830.1.S1_at	0,9	---
XI.4738.2.S1_a_at	0,9	mark2
XI.3178.1.S1_at	0,89	psmd10
XI.19967.1.S1_at	0,89	---
XI.54363.1.S1_at	0,89	---
XI.57066.1.S1_a_at	0,89	---
XI.29003.1.S1_at	0,89	pnrc2
XI.13115.2.S1_a_at	0,89	hpgds
XI.33634.1.S1_at	0,89	haus1
XI.56824.1.S1_at	0,89	LOC100158303

XI.22321.1.S1_at	0,89	tulp3
XI.13803.1.A1_x_at	0,89	---
XI.787.1.S1_at	0,89	frgy2
XI.658.1.S1_at	0,89	tpx2-a
XI.21944.1.S2_at	0,88	slc35b1
XI.16074.1.S1_at	0,88	nup88B
XI.25909.1.S1_at	0,88	strn
XI.7557.1.S1_at	0,88	---
XI.14036.3.S1_at	0,88	---
XI.47844.1.A1_at	0,88	---
XI.45488.1.S1_at	0,88	---
XI.55167.1.A1_at	0,88	SUI1
XI.19769.1.S1_at	0,87	---
XI.14130.1.S1_at	0,87	myo1a
XI.1767.1.S2_at	0,87	ranbp9
XI.20494.1.S1_at	0,87	---
XI.1474.1.S1_at	0,87	smox
XI.51061.1.S1_at	0,87	MGC114992
XI.5376.1.S1_at	0,87	inpp5b
XI.3006.1.S1_at	0,87	LOC495281
XI.52800.1.S1_at	0,87	---
XI.42165.1.A1_at	0,87	---
XI.55528.1.A1_at	0,87	---
XI.47077.1.S1_at	0,87	ibtk
XI.46944.1.S1_at	0,87	set-06
XI.6415.1.S1_at	0,86	lap3
XI.12995.2.S1_at	0,86	c14orf126
XI.55199.1.A1_at	0,86	---
XI.612.1.S1_at	0,86	rngtt
XI.40.1.A1_at	0,86	X-beta 1-1b
XI.2832.1.S1_at	0,86	tk2
XI.32558.1.S1_at	0,86	ppapdc1b
XI.34435.1.A1_at	0,86	---
XI.51169.1.S1_at	0,86	---
XI.4773.1.S1_s_at	0,86	igl@ /// iglv5-48
XI.10234.1.S1_at	0,86	ogdhl
XI.151.1.S1_at	0,86	fscn1
XI.27918.2.S1_s_at	0,86	---
XI.19693.1.S1_at	0,86	tyrp1
XI.2437.1.A1_at	0,85	---
XI.3607.1.S1_at	0,85	coq9
XI.20787.1.S1_at	0,85	lrrc58

XI.19282.1.S1_at	0,85	gyg1
XI.16857.1.S1_at	0,85	pld6
XI.22512.1.S1_at	0,84	---
XI.9075.2.S1_at	0,84	---
XI.52395.1.S1_at	0,84	---
XI.21792.1.A1_at	0,84	---
XI.32418.1.S1_at	0,84	---
XI.14673.1.A1_at	0,84	---
XI.301.1.S1_at	0,84	orc3l
XI.4356.1.A1_at	0,84	---
XI.8914.3.S1_at	0,84	LOC100036904
XI.10691.1.A1_at	0,84	---
XI.40900.1.S1_at	0,83	---
XI.7156.1.S1_at	0,83	---
XI.14260.1.A1_at	0,83	---
XI.16261.2.S1_at	0,83	---
XI.8302.1.S1_at	0,83	---
XI.47011.1.S1_at	0,83	mccc1
XI.50573.1.S1_at	0,83	---
XI.15110.1.S1_at	0,83	ftcd
XI.12489.1.A1_s_at	0,83	gphn /// MGC83148
XI.23834.2.S1_at	0,83	---
XI.46430.1.S1_at	0,82	kiaa1109
XI.16220.1.S1_at	0,82	shmt1
XI.155.1.S1_at	0,82	irx2
XI.47781.1.A1_at	0,82	---
XI.15224.1.S1_at	0,82	pex19
XI.50891.1.S1_at	0,81	---
XI.14188.1.A1_x_at	0,81	---
XI.7489.1.A1_at	0,81	---
XI.52386.1.S1_at	0,81	---
XI.18302.1.A1_at	0,81	---
XI.11706.1.S1_at	0,81	pabpn1l-a
XI.50655.1.A1_at	0,81	LOC100101301
XI.52449.1.S1_at	0,81	---
XI.45623.2.S1_at	0,81	---
XI.52327.1.S1_at	0,81	---
XI.11016.1.S1_at	0,81	---
XI.18588.1.S1_at	0,8	---
XI.23896.1.S1_at	0,8	cox4i2
XI.12580.1.S1_at	0,8	sirt4

XI.536.1.S1_a_at	0,8	pam-b
XI.52733.1.S1_at	0,8	c17orf37
XI.25540.1.S3_at	0,8	khdrbs1
XI.4804.1.A1_at	0,8	---
XI.8239.1.S2_at	0,8	chst10
XI.10670.1.S1_at	0,79	cno
XI.53873.1.S1_s_at	0,79	slc3a1
XI.56983.1.S1_at	0,79	---
XI.47648.1.S1_at	0,79	gpr155
XI.48475.1.S1_at	0,79	MGC114707
XI.3703.1.A1_at	0,79	---
XI.51216.1.S1_at	0,79	---
XI.2414.1.S1_at	0,79	LOC495487
XI.28650.1.S2_at	0,79	MGC64541
XI.7664.2.A1_a_at	0,79	ggps1
XI.13460.2.S1_at	0,79	---
XI.14036.1.A1_at	0,79	---
XI.732.1.S2_at	0,79	gipc1
XI.14307.1.S1_at	0,79	---
XI.46827.1.S1_at	0,79	gphn
XI.55747.1.S1_at	0,78	---
XI.6097.1.A1_at	0,78	---
XI.10860.1.S1_at	0,78	mgat4b
XI.12697.1.S1_at	0,78	ube2f
XI.6642.1.A1_at	0,78	---
XI.151.1.S2_at	0,78	fscn1
XI.11046.1.S1_at	0,78	---
XI.9914.1.A1_at	0,77	---
XI.25300.1.A1_at	0,77	---
XI.5241.1.A1_at	0,77	---
XI.41650.1.S1_at	0,77	gpr137c
XI.9847.1.S1_at	0,77	naaa
XI.34677.1.S1_at	0,77	insrr
XI.14248.1.A1_at	0,77	---
XI.23969.1.A1_at	0,77	---
XI.14491.1.A1_at	0,76	---
XI.33902.3.S1_at	0,76	---
XI.4001.1.A1_at	0,76	---
XI.53925.1.S1_at	0,76	rbp2
XI.28906.1.A1_at	0,76	---
XI.52414.1.S1_at	0,76	---
XI.50656.2.S1_a_at	0,76	---
XI.55572.1.A1_at	0,76	---

XI.13217.1.A1_at	0,76	---
XI.21636.1.S1_at	0,76	lmnb2
XI.12468.1.S1_at	0,76	bub1b
XI.83.1.S1_s_at	0,76	rfng
XI.23844.1.A1_at	0,75	---
XI.55003.1.A1_at	0,75	---
XI.3996.1.S1_at	0,75	shpk
XI.15785.1.A1_at	0,75	---
XI.23075.1.S1_at	0,75	aca2
XI.1919.1.A1_at	0,75	---
XI.48862.1.S1_at	0,75	nup37
XI.53905.2.A1_at	0,75	---
XI.44824.1.S1_at	0,75	---
XI.8026.1.A1_at	0,75	---
XI.24045.1.A1_at	0,75	---
XI.18359.1.S1_at	0,74	MGC130928
XI.52538.1.S1_at	0,74	---
XI.34236.1.A1_at	0,74	---
XI.13025.1.S1_at	0,74	---
XI.4641.2.A1_x_at	0,74	---
XI.1796.1.S1_at	0,74	zic1
XI.29378.1.S1_at	0,74	pdia6
XI.1954.1.S1_at	0,74	nol10
XI.48847.1.S1_at	0,74	ppp1r14c
XI.12830.1.A1_at	0,74	---
XI.55621.1.A1_at	0,74	---
XI.50956.2.S1_at	0,74	---
XI.21229.1.A1_at	0,74	LOC100158361
XI.9629.1.A1_at	0,73	---
XI.8988.1.S1_at	0,73	---
XI.24002.1.S2_at	0,73	papss1
XI.48343.1.S1_at	0,73	vps13a
XI.15575.1.A1_at	0,73	---
XI.10743.1.S1_at	0,73	MGC68653
XI.54837.1.S1_at	0,73	smpd3
XI.53549.1.S1_at	0,73	---
XI.9136.1.S1_at	0,73	snx2
XI.52842.1.S1_at	0,73	---
XI.21718.1.S1_at	0,73	gpt2
XI.32039.1.S1_a_at	0,73	---
XI.13178.1.A1_at	0,72	eif2ak2
XI.7479.1.A1_at	0,72	---

XI.18873.1.A1_at	0,72	---
XI.6913.1.S1_at	0,72	gpnmb
XI.5942.1.S1_at	0,71	tmem56.2
XI.12605.1.S1_at	0,71	lims1a
XI.33670.1.A1_at	0,71	LOC495512
XI.15678.1.S1_at	0,71	LOC495295
XI.19141.1.S1_at	0,71	MGC130860
XI.4070.1.S1_s_at	0,71	camkk1
XI.40684.1.A1_at	0,71	---
XIAffx.133.1.S1_at	0,71	NA
XI.488.1.S1_at	0,71	mre11a
XI.12355.1.S1_at	0,71	agk
XI.624.2.S1_a_at	0,71	tp53bp1
XI.18074.1.S1_at	0,71	usp25
XI.33329.1.S1_at	0,71	ptgs2
XI.25752.1.S1_at	0,71	serpinb1
XI.13658.1.S1_at	0,7	snx31
XI.735.1.S1_at	0,7	p2rx4
XI.56469.1.S1_at	0,7	---
XI.16509.1.A1_x_at	0,7	---
XI.34473.1.S1_s_at	0,7	gnpda2
XI.11443.1.S1_a_at	0,7	ap3s1
XI.7620.1.S2_at	0,7	cg7197
XI.6656.1.A1_at	0,7	---
XI.3649.1.S1_at	0,7	c1orf144
XI.19375.1.S1_at	0,7	hacl1
XI.48888.1.S1_at	0,7	appl2
XI.3366.1.S1_at	0,7	---
XI.45062.1.S1_at	0,7	LOC495462
XI.33610.1.S1_at	0,7	hyou1
XI.23844.2.S1_at	0,69	---
XI.221.1.S1_a_at	0,69	mier1
XI.7322.1.S1_at	0,69	---
XI.53684.1.S1_at	0,69	---
XI.28904.1.S1_at	0,69	cnrip1
XI.47370.1.S1_at	0,69	MGC83648
XI.53391.1.S1_at	0,69	blcap-a
XI.34521.1.A1_at	0,69	---
XI.7373.2.S1_at	0,69	---
XI.7322.1.S1_x_at	0,69	---
XI.13013.1.S1_x_at	0,69	---
XI.34245.1.S1_at	0,69	tbc1d19
XI.25238.1.S1_at	0,69	MGC85124

XI.5377.1.S2_at	0,69	p4hb
XI.11480.1.S1_at	0,68	nom1
XI.12749.1.A1_at	0,68	---
XI.2079.1.S1_at	0,68	b3gnt7
XI.5351.1.S1_at	0,68	lpp
XI.3567.1.A1_a_at	0,68	---
XI.50551.1.S1_at	0,68	cul5
XI.12884.1.S1_at	0,68	---
XI.25187.1.S1_at	0,68	---
XI.21240.1.S1_at	0,68	---
XI.13791.1.A1_at	0,68	---
XI.3946.1.S1_at	0,68	nploc4
XI.13319.1.A1_at	0,68	---
XI.20116.1.A1_at	0,67	---
XI.9385.1.A1_at	0,67	---
XI.10922.1.A1_at	0,67	---
XI.6818.1.S1_at	0,67	slc30a9
XI.29432.1.A1_at	0,67	dnajc4
XI.14922.1.S1_s_at	0,67	coq9 /// coq9-b
XI.15877.1.S1_at	0,67	MGC64589
XI.12585.1.S1_at	0,67	sec1415
XI.16366.1.A1_at	0,67	---
XI.55990.2.S1_at	0,67	cdc25b
XI.23364.2.S1_at	0,66	---
XI.5241.1.A1_a_at	0,66	---
XI.23825.1.A1_x_at	0,66	---
XI.54215.2.A1_at	0,66	---
XI.25826.1.S2_at	0,66	sh3glb1
XI.50690.1.S1_at	0,65	nfxl1
XI.1009.1.S1_at	0,65	porcn
XI.4837.1.S1_at	0,65	nomo3
XI.27242.1.S1_at	0,65	snx6
XI.24470.1.A1_at	0,65	---
XI.8992.1.A1_at	0,65	---
XI.46801.1.S1_at	0,65	dynll1a
XI.728.1.S1_at	0,65	dync1li1
XI.56486.2.A1_x_at	0,64	---
XI.50365.1.S1_at	0,64	cyb5b
XI.53748.2.S1_at	0,64	cdc5l
XI.12059.1.S1_at	0,64	MGC68519
XI.56011.1.S1_at	0,64	---
XI.19231.1.S1_at	0,63	clpx

XI.49160.1.S1_at	0,63	dnajb5
XI.15747.1.A1_at	0,63	---
XI.27918.2.S1_at	0,63	---
XI.21175.1.S1_at	0,63	---
XI.13292.1.S1_at	0,63	MGC81394
XI.6679.1.S1_at	0,63	ppp1cc
XI.34095.1.S1_a_at	0,62	---
XI.16509.1.A1_at	0,62	---
XI.4257.1.A1_at	0,62	---
XI.55621.2.S1_at	0,62	---
XI.14526.1.A1_at	0,62	---
XI.1079.1.S1_at	0,62	fth1a
XI.2711.2.S1_at	0,62	---
XI.26172.1.S1_at	0,62	---
XI.52576.1.S1_s_at	0,62	trim33
XI.3786.1.S1_at	0,62	gins2
XI.52120.1.S1_at	0,62	---
XI.57029.1.S1_at	0,61	---
XI.7582.1.S1_at	0,61	rfc4
XI.25335.1.A1_at	0,61	rnf25
XI.53524.1.S1_at	0,61	---
XI.51208.1.S1_at	0,61	ccnc
XI.2832.2.A1_at	0,61	tk2
XI.55905.1.S1_at	0,61	LOC100037040
XI.27469.2.S1_s_at	0,6	MGC115288 /// stk17a
XI.23834.1.A1_at	0,6	---
XI.54321.1.S1_at	0,6	gtpbp2
XI.16501.1.S2_at	0,6	LOC495307
XI.45032.1.A1_at	0,6	ddt-b
XI.14308.1.A1_at	0,6	---
XI.18602.1.S1_at	0,59	kiaa0564
XI.7631.2.A2_at	0,59	yrdc
XI.22438.1.S1_at	0,59	---
XI.13760.1.S1_at	0,59	mapk11
XI.23802.2.S2_at	0,58	rap1a
XI.11921.1.S1_at	0,58	MGC64353
XI.23782.1.A1_at	0,58	---
XI.6907.1.S1_at	0,58	bre
XI.14062.1.A1_at	0,57	---
XI.15490.3.A1_at	0,57	---
XI.24115.1.A1_at	0,56	---
XI.50410.1.S1_at	0,56	MGC85151

XI.7653.1.S1_s_at	0,56	---
XI.24763.1.S1_at	0,56	dhx9
XI.20656.1.S1_at	0,56	---
XI.51246.2.S1_a_at	0,56	---

List of downregulated genes upon xSuv4-20h enzymes depletion (microarray data ordered by Log2 fold change).

Set-probes Number	Log2 Fold change	Gene Name
XI.1685.1.S1_at	-2,92	LOC398260
XI.16272.1.A1_at	-2,36	---
XI.22272.1.S1_at	-2,32	krt16
XI.16668.1.A1_at	-2,28	---
XI.533.1.S1_at	-2,26	six6
XI.23560.1.S1_at	-2,21	LOC779073
XI.15545.1.A1_at	-2,03	---
XI.25847.1.A1_at	-1,98	agr2
XI.50673.1.S1_at	-1,97	---
XI.47492.1.S1_at	-1,95	tcf21
XI.8908.1.S1_at	-1,93	aldh1a2
XI.33212.2.A1_at	-1,92	---
XI.15929.1.A1_at	-1,92	---
XI.29309.1.S1_at	-1,91	cxcl12
XI.29248.1.S1_at	-1,9	gtf2a1
XI.9476.1.S1_at	-1,88	cybb
XI.48053.1.A1_at	-1,87	---
XI.53618.1.A1_at	-1,86	---
XI.4294.1.S1_at	-1,83	---
XI.53156.1.S1_at	-1,8	---
XI.34512.1.A1_at	-1,76	---
XI.468.1.S1_at	-1,76	cdc7
XI.15008.1.A1_at	-1,75	---
XI.5100.1.A1_a_at	-1,74	krt19
XI.14730.1.A1_at	-1,73	vgl12
XI.50479.1.S1_at	-1,72	haus4
XI.6748.1.S2_at	-1,72	gfpt1
XI.33895.1.S1_at	-1,7	---
XI.8950.4.A1_at	-1,68	---
XI.48331.1.S1_at	-1,66	scn3b
XI.54767.1.A1_at	-1,65	---
XI.24839.1.S2_s_at	-1,64	mafb
XI.886.1.S1_s_at	-1,64	smad10 /// smad4.2
XI.279.2.S1_at	-1,63	mab21l2
XI.9671.1.S1_at	-1,63	capn8-a
XI.5100.2.S1_x_at	-1,62	krt19
XI.54877.1.S1_at	-1,62	ankrd10
XI.18216.1.S1_at	-1,59	pdlim1
XI.53716.1.A1_at	-1,58	---

XI.77.1.S1_at	-1,56	tmeff1
XI.53276.1.S1_at	-1,56	---
XI.54876.1.A1_at	-1,56	MGC131032
XI.10868.1.S1_at	-1,55	lgals4
XI.14209.1.S1_at	-1,55	MGC83762
XI.3143.1.A1_at	-1,54	---
XI.5100.2.S1_at	-1,52	krt19
XI.14807.1.A1_at	-1,51	---
XI.7195.1.S1_a_at	-1,51	zmcm6b
XI.24336.1.A1_at	-1,49	---
XI.2683.1.A1_at	-1,45	---
XI.16320.1.S1_at	-1,45	anxa9
XI.15182.1.S1_at	-1,44	dhdds
XI.22817.1.S1_at	-1,44	rspry1
XI.15545.2.S1_at	-1,43	---
XI.40993.1.S1_at	-1,42	nfatc1
XI.21776.1.S1_at	-1,42	---
XI.385.1.S1_at	-1,42	mcm4-a
XI.6748.1.S1_at	-1,42	gfpt1
XI.16421.1.A1_at	-1,41	---
XI.21707.1.S1_at	-1,41	crls1
XI.47608.2.S1_a_at	-1,41	LOC733330
XI.47639.1.S1_at	-1,41	MGC80632
XI.22601.1.S1_at	-1,4	LOC496239
XI.8559.1.A1_at	-1,4	---
XI.20488.1.S1_at	-1,39	---
XI.2424.1.S1_at	-1,39	---
XI.26537.2.S1_at	-1,39	rpl27a
XI.15047.1.S1_at	-1,39	MGC52968
XI.26342.1.S1_at	-1,38	gsr
XI.16867.1.A1_at	-1,38	---
XI.27093.1.S1_at	-1,37	---
XI.53432.1.S1_at	-1,37	---
XI.9896.1.S1_at	-1,36	---
XI.15669.1.S1_at	-1,36	dtx4
XI.24839.1.S2_x_at	-1,36	mafb
XI.56702.1.S1_at	-1,35	stim1
XI.54898.1.A1_at	-1,34	MGC69128
XI.16350.1.A1_at	-1,34	---
XI.52991.1.A1_at	-1,34	---
XI.15485.1.A1_at	-1,33	---
XI.16060.1.S1_at	-1,33	nubp1
XI.5139.1.A1_at	-1,32	---

XI.51705.2.A1_at	-1,32	---
XI.32400.1.S1_at	-1,31	MGC84091
XI.55810.1.S1_at	-1,31	ptcd2
XI.49002.1.S1_at	-1,31	dhrrsx
XI.279.1.S2_at	-1,31	mab21l2
XI.33187.1.S1_at	-1,31	---
XI.56432.1.S1_x_at	-1,31	LOC100036853
XI.5100.3.S1_x_at	-1,31	krt19
XI.1589.1.S2_at	-1,31	agr3
XI.4916.1.S1_at	-1,31	mettl13
XI.1360.1.S1_at	-1,3	---
XI.33397.1.S1_at	-1,3	dnlz
XI.34512.2.A1_at	-1,3	---
XI.7149.1.S1_at	-1,29	mcm6.2
XI.12494.1.S1_at	-1,29	---
XI.3371.1.S1_at	-1,29	gdi2
XI.7031.1.S2_at	-1,29	ccdc97
XI.1501.1.S1_at	-1,28	---
XI.16734.2.S1_at	-1,28	---
XI.6392.1.S1_a_at	-1,28	slc5a8
XI.3698.1.A1_at	-1,28	---
XI.12659.2.A1_at	-1,28	---
XI.322.1.S2_at	-1,28	mknk1
XI.48778.1.A1_at	-1,28	---
XI.13357.1.A1_at	-1,28	---
XI.13768.1.A1_at	-1,27	---
XI.2465.1.S1_at	-1,27	---
XI.10520.1.A1_at	-1,27	LOC100036853
XI.22853.1.A1_at	-1,26	---
XI.34370.1.S1_at	-1,26	MGC68807
XI.5251.1.S1_at	-1,26	prkaa1
XI.34945.1.S1_at	-1,26	pot1
XI.38632.1.A1_at	-1,26	---
XI.52008.2.A1_at	-1,26	---
XI.51705.1.S1_at	-1,26	---
XI.45691.1.A1_at	-1,25	---
XI.54961.1.S1_s_at	-1,25	---
XI.48224.1.S1_at	-1,25	---
XI.9392.1.A1_at	-1,24	---
XI.30142.1.A1_at	-1,24	---
XI.13724.1.A1_a_at	-1,24	---
XI.15345.1.A1_at	-1,24	---

XI.56334.2.S1_at	-1,24	---
XI.1589.1.S1_at	-1,23	agr3
XI.19708.1.A1_at	-1,23	---
XI.15137.1.S1_at	-1,23	atad3a-b
XI.18686.1.A1_at	-1,22	---
XI.24336.1.A1_a_at	-1,22	---
XI.44870.1.S1_at	-1,22	nrm
XI.19284.1.S1_at	-1,22	gchfr
XI.22667.1.S1_at	-1,22	---
XI.39449.1.A1_at	-1,22	---
XI.19836.1.A1_at	-1,21	---
XI.46928.1.A1_a_at	-1,21	---
XI.5987.1.S1_at	-1,21	cav-3
XI.48264.1.A1_at	-1,21	---
XI.10172.1.S1_at	-1,2	gja3
XI.6511.1.S1_at	-1,2	armc7
XI.21931.1.S1_at	-1,2	kcnj16
XI.50105.1.S1_at	-1,2	nkiras2
XI.19210.1.S1_at	-1,2	klhdc2
XI.27093.3.A1_at	-1,2	---
XI.9111.1.A1_at	-1,19	---
XI.24195.1.S1_at	-1,19	ak1-a
XI.11931.1.A1_at	-1,19	---
XI.17300.1.A1_at	-1,19	---
XI.51521.1.S1_at	-1,19	---
XI.11349.1.A1_at	-1,19	---
XI.15705.1.S1_at	-1,19	---
XI.2439.1.S1_s_at	-1,19	hppt1
XI.25217.1.S1_at	-1,19	prmt5
XI.7299.1.S1_at	-1,18	odf3
XI.55002.1.A1_at	-1,18	---
XI.47574.1.S1_at	-1,17	MGC84082
XI.16330.2.A1_at	-1,17	---
XI.21534.1.S1_at	-1,17	nr2c1-a
XI.4985.2.S1_at	-1,17	---
XI.24391.1.A1_at	-1,16	LOC100037072
XI.3048.1.A1_x_at	-1,16	---
XI.10639.1.S1_at	-1,16	dpysl4
XI.57098.1.A1_at	-1,16	---
XI.13496.1.A1_at	-1,16	---
XI.19278.1.S1_at	-1,16	bcdin3d
XI.8500.1.A1_at	-1,15	---

XI.6728.1.S1_at	-1,15	cep63
XI.6772.1.S1_at	-1,15	plxnb2
XI.1656.1.A1_at	-1,15	---
XI.8033.1.A1_at	-1,15	ankrd37
XI.23146.1.S1_at	-1,15	MGC68557
XI.18578.1.A1_at	-1,15	---
XI.47419.1.S1_at	-1,15	MGC84409
XI.1014.1.S1_at	-1,14	mcm4-b
XI.21349.1.S1_at	-1,14	wars
XI.13550.1.S1_at	-1,13	gnb1
XI.20487.1.S1_at	-1,13	---
XI.49172.1.S1_at	-1,13	rab3d
XI.2292.1.S1_at	-1,13	pmp22
XI.44846.1.S1_at	-1,13	add3
XI.19064.1.A1_at	-1,13	---
XI.15529.2.A1_at	-1,13	---
XI.15415.1.S1_at	-1,13	cdkn1a
XI.15894.2.S1_a_at	-1,12	---
XI.14407.1.A1_at	-1,12	---
XI.48348.1.S1_at	-1,12	hppt1
XI.13935.1.A1_x_at	-1,12	---
XI.53652.1.S1_a_at	-1,12	---
XI.48132.1.A1_at	-1,12	---
XI.19394.1.S1_at	-1,12	---
XI.51920.1.S1_at	-1,11	---
XI.12714.1.A1_at	-1,11	LOC100137680
XI.32202.1.S1_at	-1,11	---
XI.32305.1.S1_at	-1,11	---
XI.29104.1.S1_at	-1,1	nme3b
XI.8779.2.A1_at	-1,1	---
XI.11234.1.A1_at	-1,1	---
XI.18971.1.S1_at	-1,1	ppip5k2
XI.11190.1.S1_at	-1,09	lgals8
XI.16186.1.A1_at	-1,09	---
XI.14279.1.A1_at	-1,09	---
XI.12945.1.S1_at	-1,09	---
XI.29638.1.S1_at	-1,09	---
XI.17779.3.S1_at	-1,09	---
XI.6915.1.A1_x_at	-1,09	---
XI.7293.1.S1_at	-1,09	nr2c1
XI.53974.1.S1_at	-1,09	---
XI.92.1.S1_a_at	-1,09	drg1

XI.16508.1.S1_at	-1,08	rab3c
XI.16259.1.A1_at	-1,08	---
XI.19264.1.S1_at	-1,08	---
XI.35336.1.S1_at	-1,08	mpv17
XI.9261.1.A1_at	-1,08	---
XI.9694.1.A1_at	-1,07	---
XI.48513.1.S1_at	-1,07	psmc3ip
XI.528.1.S1_at	-1,07	nr2f1
XI.9023.1.A1_at	-1,07	---
XI.46789.1.S1_at	-1,07	inf2
XI.20029.2.S1_a_at	-1,06	pdgfra
XI.14868.1.A1_at	-1,06	---
XI.14120.2.A1_a_at	-1,06	---
XI.55575.1.S1_at	-1,06	---
XI.2134.1.S1_a_at	-1,06	---
XI.15831.1.S1_at	-1,06	c19orf40
XI.23540.1.S1_at	-1,06	pars2
XI.25084.1.A1_at	-1,06	---
XI.16379.1.S1_at	-1,05	impa1
XI.54520.1.S1_at	-1,05	---
XI.13414.1.S1_at	-1,05	LOC494708
XI.23575.1.S1_at	-1,04	psip1
XI.54876.3.A1_a_at	-1,04	MGC131032
XI.12351.1.A1_at	-1,04	---
XI.24089.1.A1_at	-1,04	---
XI.12097.1.S2_a_at	-1,04	pcdh1
XI.47910.1.A1_s_at	-1,04	---
XI.54238.1.S1_at	-1,04	---
XI.24005.1.S1_at	-1,04	c14orf129
XI.8630.1.S1_at	-1,04	MGC53542
XI.2662.1.A1_at	-1,04	---
XI.13659.1.S1_at	-1,04	LOC414714
XI.53693.1.S1_at	-1,03	MGC131091
XI.3048.1.A1_at	-1,03	---
XI.16891.1.A1_at	-1,03	e2f1
XI.7153.1.S1_at	-1,03	---
XI.5399.1.A1_at	-1,03	---
XI.24391.2.A1_at	-1,02	LOC100037072
XI.2581.1.S1_at	-1,02	---
XI.48824.1.S1_at	-1,02	fam101b
XI.11294.1.A1_at	-1,02	---
XI.14090.1.A1_at	-1,02	LOC100158420

XI.13160.2.S1_at	-1,02	---
XI.371.1.S1_at	-1,02	orc1l
XI.8236.1.S1_at	-1,01	gby
XI.11449.1.S1_at	-1,01	---
XI.52736.1.A1_at	-1,01	---
XI.15793.1.S1_at	-1,01	---
XI.9379.1.S1_at	-1,01	c3orf17
XI.434.1.S1_at	-1,01	mycn
XI.29333.1.S1_a_at	-1,01	MGC114697
XI.11445.1.S1_at	-1,01	bap1
XI.12400.1.A1_at	-1,01	fnta
XI.19745.1.S1_at	-1,01	cdbl2
XI.11267.1.A1_at	-1,01	---
XI.2885.1.S1_at	-1	alg5
XI.10215.1.A1_at	-1	---
XI.55700.1.A1_x_at	-1	---
XI.6261.1.S1_at	-1	LOC431836
XI.15990.1.S1_at	-1	---
XI.33599.1.A1_at	-1	---
XI.56407.2.A1_at	-1	---
XI.49822.1.S1_at	-1	ppap2a
XI.32778.2.S1_at	-1	---
XI.16777.1.A1_a_at	-1	---
XI.18648.1.A1_at	-1	---
XI.56796.1.A1_at	-1	---
XI.20029.1.S1_at	-1	pdgfra
XI.6007.1.A1_at	-1	---
XI.687.1.S1_at	-0,99	MGC131011
XI.7347.1.S1_at	-0,99	angel2
XI.444.1.S1_a_at	-0,99	nudt6
XI.14211.1.S1_at	-0,99	---
XI.6136.2.S1_at	-0,99	---
XI.15185.1.S1_at	-0,99	c3orf75
XI.57023.1.A1_at	-0,98	---
XI.17779.1.A1_at	-0,98	---
XI.9880.1.A1_at	-0,98	---
XI.54333.1.A1_at	-0,98	---
XI.28461.1.S1_a_at	-0,98	ssr4
XI.17880.1.A1_at	-0,98	---
XI.46937.1.A1_at	-0,98	---
XI.46873.1.S1_at	-0,97	ttc18
XI.15629.1.A1_at	-0,97	---
XI.50004.1.S1_at	-0,97	LOC496148

XI.10580.1.A1_at	-0,97	---
XI.11454.1.S1_at	-0,97	ikbkg
XI.13389.1.S1_at	-0,97	zdhhc6
XI.1475.1.A1_at	-0,97	pik3r2
XI.16193.1.S1_at	-0,97	---
XI.51861.1.S1_at	-0,97	---
XI.1881.1.S1_at	-0,97	emilin1
XI.10173.1.S1_at	-0,96	MGC64450
XI.53523.1.S1_at	-0,96	---
XI.20486.1.A1_at	-0,96	---
XI.16148.1.S1_at	-0,96	---
XI.52041.1.S1_a_at	-0,96	tmem115
XI.16060.2.S1_x_at	-0,96	nubp1
XI.11201.1.A1_at	-0,96	---
XI.55574.1.S1_s_at	-0,96	MGC68847 /// pfkp
XI.9381.1.A1_at	-0,96	---
XI.3931.1.S1_at	-0,95	sept8-b
XI.6181.1.S1_at	-0,95	tfc2l1
XI.45183.1.A1_at	-0,95	---
XI.23457.1.S1_at	-0,95	MGC53277
XI.28611.1.S2_x_at	-0,95	tfiaa/b-1
XI.55558.1.S1_at	-0,95	---
XI.11111.1.A1_at	-0,95	---
XI.7201.1.S1_at	-0,95	mrps12
XI.14126.1.A1_at	-0,95	LOC100137623
XI.16060.1.S1_a_at	-0,95	nubp1
XI.11199.1.A1_at	-0,95	---
XI.18884.1.A1_at	-0,94	---
XI.49847.1.S1_at	-0,94	LOC495954
XI.51624.1.S1_at	-0,94	---
XI.11147.2.S1_a_at	-0,94	gmps
XI.13324.1.A1_at	-0,94	---
XI.30004.2.S1_s_at	-0,94	---
XI.21558.1.S1_at	-0,94	lhx2
XI.17257.1.A1_at	-0,94	---
XI.56047.1.S1_at	-0,94	---
XI.2722.1.S1_at	-0,94	---
XI.34205.2.S1_at	-0,94	---
XI.1464.1.S2_at	-0,94	myh8
XI.14569.1.S1_at	-0,94	---
XI.57016.1.A1_s_at	-0,93	---
XI.21906.1.S1_at	-0,93	MGC53997

XI.2669.1.A1_at	-0,93	---
XI.23645.1.A1_at	-0,93	MGC53182
XI.33366.1.S1_at	-0,93	ppap2bb
XI.12825.1.A1_at	-0,93	---
XI.32778.1.A1_at	-0,93	---
XI.1399.1.A1_at	-0,92	arpc5l
XI.19374.1.S1_at	-0,92	---
XI.25797.1.S1_at	-0,92	---
XI.25662.1.S1_at	-0,92	snip1b
XI.16402.1.A1_at	-0,92	---
XI.33727.1.A1_at	-0,92	---
XI.12097.1.S1_a_at	-0,92	pcdh1
XI.26943.1.S1_at	-0,92	bicd2
XI.15263.1.A1_at	-0,92	---
XI.15070.1.S1_at	-0,92	MGC80314
XI.2220.1.S1_at	-0,91	c5orf44
XI.46552.1.S1_at	-0,91	tubb
XI.29525.1.A1_at	-0,91	---
XI.17667.1.A1_at	-0,91	---
XI.3957.1.S1_at	-0,91	rpa1
XI.14170.1.S1_at	-0,91	gigyf2
XI.11701.1.A1_at	-0,91	---
XI.53824.1.S1_at	-0,91	styx
XI.15560.2.A1_at	-0,91	---
XI.34612.1.S1_at	-0,91	atp6v1g3
XI.46910.1.A1_x_at	-0,9	---
XI.40556.1.S1_at	-0,9	---
XI.50317.1.A1_s_at	-0,9	---
XI.10817.1.S1_at	-0,9	zbtb12
XI.3515.1.A1_at	-0,9	---
XI.23328.1.S1_at	-0,9	impdh2
XI.32296.1.S1_at	-0,89	klh12
XI.153.1.S1_at	-0,89	cdh20
XI.5636.1.S1_at	-0,89	c21orf57
XI.2503.1.S2_at	-0,89	---
XI.4985.1.S1_a_at	-0,89	hells
XI.32225.1.S1_at	-0,88	med7
XI.54474.1.A1_s_at	-0,88	gmps
XI.9189.1.S1_at	-0,88	---
XI.25600.1.S1_at	-0,88	c14orf109
XI.10908.1.S1_at	-0,88	---
XI.10175.2.S1_at	-0,88	---
XI.6185.1.A1_at	-0,88	LOC733307

XI.23166.1.S1_at	-0,88	tmem53-b
XI.13469.1.A1_at	-0,88	---
XI.50317.1.A1_at	-0,88	---
XI.53987.1.S1_at	-0,87	dnai2
XI.22429.2.A1_at	-0,87	---
XI.5325.1.A1_at	-0,87	---
XI.23934.1.S1_at	-0,87	gins1
XI.12400.2.S1_at	-0,87	fnta
XI.3233.1.S1_at	-0,87	tbl3
XI.472.1.S1_at	-0,87	surf6
XI.18772.1.S1_at	-0,87	med8
XI.29075.1.S1_a_at	-0,87	---
XI.11428.1.A1_s_at	-0,87	---
XI.4093.1.A1_at	-0,87	---
XI.51211.1.S1_at	-0,87	trim62
XI.16790.2.A1_at	-0,86	---
XI.14801.1.A1_at	-0,86	---
XI.1099.1.S1_at	-0,86	ptprz1
XI.7611.1.S1_at	-0,86	MGC115443
XI.3751.1.A1_at	-0,86	---
XI.1030.1.S1_at	-0,86	orc2l
XI.13057.2.S1_at	-0,86	---
XI.32092.1.A1_at	-0,86	---
XI.35372.1.S1_at	-0,86	MGC99250
XI.53541.1.S1_at	-0,86	esco2
XI.45691.2.S1_at	-0,86	---
XI.24296.1.A1_at	-0,86	---
XI.43865.1.S1_at	-0,86	kif2c
XI.8908.3.A1_at	-0,86	---
XI.21032.1.S1_at	-0,85	LOC398406
XI.54741.1.A1_at	-0,85	---
XI.12135.1.A1_at	-0,85	---
XI.8299.1.A1_at	-0,85	---
XI.41105.1.S1_x_at	-0,85	rg9mtd1
XI.14528.1.S1_at	-0,85	MGC81115
XI.12248.1.A1_at	-0,85	---
XI.7396.1.S1_at	-0,85	alg13
XI.3508.1.S1_at	-0,85	---
XI.12385.1.A1_at	-0,85	---
XI.15221.1.S1_at	-0,85	slc27a2
XI.40191.1.A1_at	-0,85	---
XI.24823.2.S1_s_at	-0,85	---
XI.50703.1.A1_at	-0,84	---

XI.18558.1.S1_at	-0,84	c20orf11
XI.16670.1.S1_at	-0,84	dnajc17
XI.49820.1.S1_at	-0,84	ints6
XI.6583.1.S1_at	-0,84	---
XI.4484.1.A1_at	-0,84	---
XI.24755.1.S1_at	-0,84	LOC495362
XI.46851.1.A1_at	-0,84	c9orf21
XI.5092.1.A1_at	-0,84	eif4a2
XI.5880.1.A1_at	-0,84	---
XI.2361.1.S1_at	-0,84	pik3r5
XI.20609.1.S1_at	-0,83	tctex1d1-a
XI.12622.1.A1_at	-0,83	---
XI.2462.1.S1_at	-0,83	mrps30
XI.10096.1.A1_at	-0,83	c7orf25
XI.47982.1.A1_at	-0,83	---
XI.24390.1.A1_at	-0,83	---
XI.14462.1.A1_at	-0,83	---
XIAffx.81.1.S1_at	-0,83	NA
XI.6027.1.S1_at	-0,83	qars
XI.2160.1.A1_at	-0,83	---
XI.29087.1.S1_at	-0,83	---
XI.47149.1.S1_at	-0,83	dmrta1
XI.55700.1.A1_at	-0,83	---
XI.17890.1.A1_at	-0,83	---
XI.41350.3.A1_x_at	-0,83	---
XI.3639.1.S1_at	-0,83	ssb
XI.46699.1.S1_at	-0,83	rasgrp1
XI.20680.1.S1_at	-0,83	farsa-b
XI.1527.1.S1_at	-0,82	gpr107
XI.13646.1.S1_at	-0,82	tatdn1
XI.16726.2.A1_x_at	-0,82	---
XI.29694.1.S1_at	-0,82	traf6
XI.29532.1.S2_at	-0,82	flrt3
XI.11117.1.S1_at	-0,82	gsto1
XI.41102.1.S1_at	-0,82	---
XI.15729.1.A1_at	-0,81	---
XI.51756.2.S1_at	-0,81	---
XI.50709.1.S1_at	-0,81	---
XI.25544.1.A1_a_at	-0,81	tfdp2
XI.18894.2.A1_at	-0,81	---
XI.44805.1.S1_at	-0,81	---
XI.6945.1.S1_at	-0,81	---
XI.25124.1.A1_at	-0,81	---

XI.47925.2.A1_at	-0,81	---
XI.1424.1.S1_at	-0,81	LOC100127277
XI.9795.1.A1_at	-0,81	---
XI.34114.3.A1_a_at	-0,81	---
XI.1267.1.S1_at	-0,81	orc4l
XI.13049.1.A1_at	-0,81	---
XI.167.1.S1_at	-0,81	adar
XI.4300.1.S1_at	-0,8	brp44lb
XI.48190.1.A1_at	-0,8	---
XI.52523.2.A1_at	-0,8	---
XI.17438.1.S1_at	-0,8	rnf103
XI.54030.1.S1_at	-0,8	c11orf2
XI.52561.1.S1_at	-0,8	---
XI.18639.1.S1_at	-0,8	ccdc9
XI.28993.1.S1_at	-0,8	phactr4-b
XI.6266.1.S1_at	-0,8	itln1
XI.6468.1.S1_at	-0,79	ghitm
XI.7236.1.S1_at	-0,79	adss
XI.54470.1.A1_at	-0,79	---
XI.53741.2.A1_at	-0,79	hs3st3a1
XI.22766.1.A1_s_at	-0,79	---
XI.1827.1.S1_at	-0,79	ctsa
XI.22841.1.A1_at	-0,79	---
XI.30323.1.A1_at	-0,79	---
XI.40818.1.A1_at	-0,79	---
XI.7743.1.A1_at	-0,79	---
XI.17190.1.A1_at	-0,79	sft2d1
XI.25332.1.S1_at	-0,78	MGC115057
XI.46871.1.A1_at	-0,78	---
XI.13270.1.A1_at	-0,78	---
XI.48112.1.S1_at	-0,78	sdr39u1
XI.16517.1.S1_at	-0,78	znf830
XI.56432.1.S1_s_at	-0,78	LOC100036853 /// rpa2
XI.21884.1.S1_at	-0,78	LOC398447
XI.52535.1.S1_s_at	-0,78	usp12 /// usp12-b
XI.13378.1.S1_at	-0,77	---
XI.18910.1.A1_at	-0,77	---
XI.46958.1.S1_at	-0,77	---
XI.41763.1.S1_at	-0,77	---
XI.13012.1.S1_at	-0,77	---
XI.44313.1.A1_at	-0,77	---

XI.55683.1.A1_at	-0,77	---
XI.15826.1.A1_a_at	-0,77	LOC100037193
XI.21993.1.S1_at	-0,77	mak16
XI.10476.1.A1_at	-0,76	---
XI.16332.1.A1_at	-0,76	---
XI.28913.1.S1_at	-0,76	LOC446975
XI.15529.3.S1_at	-0,76	---
XI.1776.1.A1_at	-0,76	---
XI.22643.1.S1_at	-0,76	kiaa0494
XI.42753.1.S1_at	-0,76	---
XI.28611.2.S1_x_at	-0,76	TFIIAa/b-1
XI.11336.1.S1_at	-0,76	cxcr4-b
XI.48265.1.A1_at	-0,76	---
XI.1041.1.S1_at	-0,76	gli3
XI.3289.1.A1_at	-0,75	---
XI.10272.1.A1_at	-0,75	thg1l
XI.5228.1.S1_at	-0,75	LOC496082
XI.13362.1.A1_at	-0,75	---
XI.14664.1.S1_at	-0,75	mcm3
XI.14970.1.S1_at	-0,75	LOC100158385
XI.41105.1.S1_at	-0,75	rg9mtd1
XI.56932.1.S1_at	-0,75	junb
XI.13539.1.A1_at	-0,75	---
XI.16797.1.S1_at	-0,75	tmem208
XI.53898.1.S1_s_at	-0,75	hdac3
XI.8104.1.S1_at	-0,74	LOC446305
XI.12400.1.A1_a_at	-0,74	fnta
XI.47265.1.S1_a_at	-0,74	rrn3
XI.53706.1.A1_at	-0,74	---
XI.50024.1.S1_at	-0,74	hivep1
XI.7166.1.S1_at	-0,74	---
XI.47272.1.A1_at	-0,74	---
XI.56399.1.S1_at	-0,74	tmem120a
XI.928.1.S1_at	-0,74	smc2
XI.8873.1.S1_x_at	-0,74	mttfa-A
XI.24166.1.S2_at	-0,73	rarres1
XI.8266.1.S1_at	-0,73	rrm2.2
XI.47919.1.A1_s_at	-0,73	---
XI.19139.1.S1_at	-0,73	---
XI.16396.1.S1_at	-0,73	MGC52622
XI.2544.1.S1_at	-0,73	LOC495474
XI.10801.1.S1_at	-0,73	gpaa1

XI.55232.1.A1_at	-0,73	---
XI.14197.1.S1_at	-0,73	cdca7
XI.40756.1.A1_at	-0,73	---
XI.32988.1.S1_at	-0,73	---
XI.51877.1.S1_at	-0,73	---
XI.48672.1.S1_at	-0,73	syt14
XI.47777.1.A1_at	-0,73	---
XI.12966.1.A1_at	-0,73	LOC100049781
XI.6937.1.S1_at	-0,72	ndufb2
XI.4558.1.S1_at	-0,72	fmr1-A
XI.21744.1.S1_at	-0,72	dnajc21
XI.17309.1.S1_at	-0,72	MGC115064
XI.686.1.S2_s_at	-0,72	sox4 /// sox4-1 /// sox4-2
XI.5629.1.S1_at	-0,72	rpa2
XI.19016.1.A1_at	-0,72	---
XI.12755.1.A1_at	-0,72	---
XI.48494.1.S1_at	-0,72	wdr75
XI.16312.1.A1_at	-0,72	---
XI.7684.2.A1_at	-0,71	---
XI.9757.1.A1_at	-0,71	---
XI.53383.1.S1_at	-0,71	---
XI.9576.1.S1_at	-0,71	ca2
XI.55408.1.S1_s_at	-0,71	psen1
XI.15301.1.S1_at	-0,71	lars
XI.55493.1.S1_at	-0,71	cops7b
XI.1811.1.S1_at	-0,71	---
XI.13864.1.A1_at	-0,71	---
XI.13594.1.S1_a_at	-0,71	cyp4b1.2
XI.4419.1.S1_at	-0,71	atp6v0a1
XI.6201.1.S1_at	-0,71	phb2
XI.6522.1.S1_at	-0,71	sephs1
XI.14056.1.S1_at	-0,71	rangap1
XI.52845.1.S1_at	-0,71	---
XI.15462.1.S1_at	-0,71	---
XI.15843.1.S1_at	-0,71	LOC100127337
XI.5443.1.S1_at	-0,71	---
XI.25993.1.S1_s_at	-0,71	MGC132184 /// MGC84072
XI.47361.1.S1_at	-0,7	MGC80203

XI.1241.1.S1_at	-0,7	sox7
XI.7093.1.S2_at	-0,7	aatf
XI.9325.1.A1_at	-0,7	---
XI.54513.1.S1_at	-0,7	sec11c
XI.5255.1.S1_at	-0,7	n6amt2
XI.11050.1.S1_at	-0,7	gin1
XI.20302.1.S1_at	-0,7	c6orf125
XI.24409.1.S1_at	-0,7	LOC398639
XI.7267.1.S1_at	-0,69	det1
XI.46879.1.A1_at	-0,69	---
XI.10468.1.S1_at	-0,69	pfdn1
XI.22166.1.A1_at	-0,69	---
XI.52870.1.S1_at	-0,69	c10orf140
XI.55806.1.S1_at	-0,69	---
XI.23871.1.A1_at	-0,69	---
XI.56038.1.S1_at	-0,69	---
XI.19781.1.S1_at	-0,69	zufsp
XI.20552.1.S1_at	-0,69	---
XI.18637.1.S2_at	-0,69	---
XI.13513.1.A1_at	-0,68	---
XI.10336.1.S1_at	-0,68	MGC84775
XI.6226.1.S1_at	-0,68	mrpl24
XI.54397.1.A1_s_at	-0,68	mpv17
XI.11332.1.S1_at	-0,68	impdh1
XI.18307.1.S1_at	-0,68	hmgcl
XI.8284.1.S1_at	-0,68	---
XI.6438.1.S1_at	-0,68	tspan15
XI.52656.1.S1_at	-0,68	---
XI.7817.1.S2_at	-0,68	xcen
XI.6956.1.S1_at	-0,68	crpc
XI.5563.1.S1_at	-0,68	---
XI.25873.1.A1_at	-0,68	---
XI.46645.1.S1_at	-0,68	supt7l
XI.26192.1.A1_at	-0,68	---
XI.972.1.S1_at	-0,68	hes1
XI.21745.1.S1_at	-0,68	---
XI.32947.1.S1_at	-0,68	txn1
XI.516.1.S1_at	-0,67	tcp1
XI.12115.1.S1_s_at	-0,67	MGC53542 /// plk2
XI.8258.1.S1_at	-0,67	isot
XI.10574.1.S1_at	-0,67	lig4
XI.17664.3.A1_at	-0,67	---

XI.24117.1.A1_at	-0,67	---
XI.1654.1.A1_a_at	-0,66	---
XI.19491.1.S1_at	-0,66	nif3l1
XI.2758.1.A1_at	-0,66	---
XI.14682.1.S1_at	-0,66	traf6-a
XI.7254.1.S1_at	-0,66	c6orf136
XI.4175.1.S2_at	-0,66	sh3gl1
XI.47686.1.S1_at	-0,66	MGC80972
XI.18997.1.S1_at	-0,66	nek4
XI.4793.1.A1_at	-0,66	---
XI.2590.1.S1_at	-0,66	trappc1
XI.10803.1.A1_at	-0,66	anapc13.2
XI.48299.1.A1_at	-0,66	---
XI.13032.1.A1_at	-0,65	XFO 9-3
XI.34159.1.A1_at	-0,65	---
XI.27263.2.S1_s_at	-0,65	MGC154351
XI.2613.1.S1_s_at	-0,65	cct5
XI.24077.1.S1_at	-0,65	---
XI.43211.1.A1_at	-0,65	---
XI.30674.1.S1_at	-0,65	MGC84185
XI.49801.1.S1_s_at	-0,65	psma6
XI.25664.1.S1_at	-0,65	MGC79091
XI.5477.3.S1_at	-0,65	hnrnpm
XI.3013.1.A1_at	-0,65	---
XI.15852.1.S1_at	-0,65	abcf1
XI.17276.1.S1_at	-0,65	---
XI.32524.1.A1_a_at	-0,64	---
XI.50117.1.S1_at	-0,64	---
XI.33551.1.S1_at	-0,64	MGC115285
XI.53711.1.A1_at	-0,64	---
XI.26254.1.S1_x_at	-0,64	---
XI.7551.2.S1_a_at	-0,64	eef2.1
XI.10175.1.A1_at	-0,64	---
XI.7698.2.S1_a_at	-0,64	grb2-a
XI.34799.1.S1_at	-0,64	mrpl20
XI.48115.1.S1_at	-0,64	stk39
XI.46818.1.S1_at	-0,64	rps15
XI.56833.1.S1_at	-0,64	chchd10
XI.55681.2.A1_at	-0,64	---
XI.12494.3.A1_at	-0,63	---
XI.11493.1.S1_at	-0,63	---
XI.2757.1.S1_at	-0,63	---
XI.43094.2.S1_a_at	-0,63	---

XI.7893.1.S1_at	-0,63	fam192a
XI.16231.1.S1_at	-0,62	tim10-a
XI.53784.1.S1_at	-0,62	ints6-a
XI.13330.1.A1_at	-0,62	---
XI.25544.1.A1_at	-0,62	tfdp2
XI.3645.1.S1_at	-0,62	uqcrq
XI.46847.1.S1_at	-0,62	---
XI.17309.1.S1_s_at	-0,62	MGC115064 /// rad23b
XI.5891.2.S1_at	-0,62	---
XI.14540.1.A1_x_at	-0,62	---
XI.14386.1.A1_x_at	-0,61	---
XI.4504.1.A1_at	-0,61	---
XI.13195.1.S1_at	-0,61	etaa1
XI.48450.1.S1_at	-0,61	MGC83110
XI.55988.2.S1_at	-0,6	LOC100036878
XI.13720.1.S1_at	-0,6	gxylt2
XI.41921.1.S1_at	-0,6	LOC443600
XI.29008.1.S1_at	-0,6	ppat
XI.50182.1.A1_at	-0,6	---
XI.32510.1.A1_x_at	-0,6	---
XI.56209.1.A1_at	-0,59	---
XI.53948.1.S1_s_at	-0,59	klhl24
XI.16794.1.S1_at	-0,59	eap1-b
XI.21915.1.S1_at	-0,59	gins3
XI.57016.1.A1_at	-0,59	---
XI.18553.1.A1_at	-0,59	---
XI.16483.1.S1_at	-0,59	hiatl1
XI.21546.1.S1_at	-0,59	xG28K
XI.13354.1.A1_at	-0,58	---
XI.20087.1.S1_a_at	-0,58	---
XI.32324.2.S1_at	-0,58	---
XI.13799.1.A1_at	-0,57	---
XI.56743.1.A1_at	-0,57	---
XI.2.1.S1_at	-0,57	rpl18
XI.45316.1.S1_at	-0,57	ndufa13
XI.24716.1.A1_at	-0,57	---
XI.20506.1.S1_at	-0,57	---
XI.10320.1.A1_at	-0,56	---
XI.32732.1.A1_at	-0,55	---
XI.6299.1.S1_at	-0,55	paics
XI.33613.1.A1_at	-0,55	---
XI.46193.1.S1_at	-0,54	xrcc6bp1

XI.20189.1.S1_at	-0,54	lyrm4
XI.5614.1.S1_at	-0,54	meig1
XI.47835.1.A1_at	-0,54	---

## 9 ACKNOWLEDGEMENTS

*First of all, I would like to thank Professor Ralph Rupp, for providing me the opportunity to work in his group. I really appreciated his supervision, his advices, the way he encouraged and supported me during all these years, the many stimulating and inspiring discussions and the freedom he gave me in thinking and performing experiments.*

*I also thank Professor Peter Becker, for being a member of my thesis advisory committee, but most of all for providing an excellent, stimulating scientific environment and a nice department atmosphere.*

*I express my gratitude to Professor Gunnar Schotta, for being a member of my thesis advisory committee, for the fruitful collaboration on the Suv4-20h project and for the many stimulating discussions and critical advices.*

*I express my gratitude to Professor Herbert Steinbeisser and Professor Thomas Hollemann for critical reading of the Suv4-20h manuscript and for providing helpful protocols.*

*I also want to thank the whole Rupp's lab, specially Gabi, for useful discussions, advices and experimental contribution, and for being a very nice person; Edith and Babs for their help and support; all the past and present medical students – Markus, Laura, Sissi, Max, Steffi and Adrian – and specially Tobias and Ohnmar, for helping me with the Suv4-20h project.*

*I thank all the past and present colleagues in the Becker department I had the pleasure to work and party with. In particular, I also want to thank Matthias and Silvia, for the nice discussions, for sharing expertise and for creating a nice atmosphere in the 7<sup>th</sup> floor "Rupp-Schotta office". Moreover, I would like to thank the members of the "Team Excellence", and all the guys I had the pleasure to play football with. I enjoyed every single match!*

*I want to thank the lunch mates Viola and Alessandra, also for all the coffee we had together.*

*I thank my parents Daniela and Gianni, as well as my brother Mauro, for constantly supporting me.*

*I thank Mara, for being the person she is and for walking beside me.....*

## 10 CURRICULUM VITAE

### Personal Information

**Name:** Dario Nicetto  
**Date of Birth:** October 29, 1983  
**Place of Birth:** Padua  
**Nationality:** Italian

### Education

**10/2007 – 12/2012**      **Ludwig-Maximilians Univeristy**, Munich, Germany  
Adolf-Butenandt Insitut, Prof. Dr. Ralph Rupp  
Ph.D. studies  
  
Project: “On the way to differentiation: Xenopus Suv4-20h histone methyltrasnferases regulat the transition from the pluripotent to the ectoderm cell state”

**09/2005 – 07/2007**      **University of Padua**, Padova, Italy  
Master Degree in Molecular Biology

**09/2002 – 07/2005**      **University of Padua**, Padova, Itlay  
Bachelor Degree in Molecular Biology

**09/1997 – 07/2002**      **Liceo Scientifico “E. Fermi”**, Padova, Italy  
Secondary School Studies

### Publications

**Nicetto D**, Hahn M, Jung J, Schneider TD, Straub T, David R, Schotta G, Rupp RA (2012) Suv4-20h Histone Methyltransferases Promote Neuroectoderm Differentiation by Silencing the Pluripotency Associated Oct-25 Gene, PLoS Genetics, in press

Schneider TD, Arteaga-Salas JM, Mentele E, David R, **Nicetto D**, Imhof A, Rupp RA (2011) Stage-Specific Histone Modification Profiles Reveal Global Transitions in the Xenopus Embryonic Epigenome. PLoS ONE 6(7): e22548